Electronic Supplementary Material (ESI) for Chemical Science.

Supplementary Information

A Single Phosphorylation Mechanism In Early Metabolism– The Case of Phosphoenolpyruvate

Joris Zimmermann, Robert J. Mayer, and Joseph Moran

University of Strasbourg, CNRS, ISIS UMR 7006, 67000 Strasbourg, France

Contact: moran@unistra.fr

Table of Contents

General information

I. Materials

Unless otherwise noted, all reagents and solvents were purchased from Sigma-Aldrich, Fluka, TCI, Acros organics, or Carbosynth, and used without further purification. Water was obtained from a Milli-Q purification system (18.2 MΩcm). All reactions were carried out in 2 mL BRAND® microcentrifuge tubes with lids. Experiments were carried out in a Thermo Scientific™ Digital Heating Shaking Drybath without using stir bars. pH values were measured using a Mettler Toledo FiveGo F2 pH-meter equipped with a Mettler-Toledo InLab® Flex-micro pH electrode.

II. NMR and mass spectroscopy

A. NMR spectroscopy

^{1}H and ^{31}P NMR spectra were recorded on a Bruker Avance Neo-500 (500 MHz) or Bruker UltraShield Plus Avance III spectrometer (400 MHz) at ambient temperature (23 °C) in a H_2O:D_2O mixture (9:1) as solvent or D_2O. Dimethyl sulfone **DMS** (δ = 3.00 ppm in ^{1}H NMR) and phosphonoacetic acid (δ = 15.7 ppm in ^{31}P NMR) were used as internal standards.

Data are reported as: multiplicity (br = broad, s = singlet, d = doublet, t = triplet, q= quartet, m = multiplet), integration and coupling constant(s) in Hz.

Unless otherwise stated, the following parameters were used for the different NMR experiments:

Experiment	Pulse sequence	Pulse delay (d1)	Number of scans (ns)	Coupling constant (Hz)/ Mixing time (ms)
^{1}H	zg30	2 s	16	
^{1}H water suppression	noesygppr1d	2 s	16	
^{31}P (^{1}H coupled)	zgdc30	3 s	64	
^{31}P (^{1}H decoupled)	zgesfpgp	2 s	16	
qNMR (^{1}H)	zg30	45 or 60 s	8 or 16	
qNMR (^{31}P)	zgpg30	60 s	8	
HMQC (^{1}H –^{31}P)	hmbcgpndqf	1.5 s	4	8 Hz
^{13}C	zgdc30	2.5 s	8192 or 512	
HSQC (^{1}H –^{13}C)	hsqcedetgpsisp2.2	0.25	8	
HMBC (^{1}H –^{13}C)	hmbcetgpl2nd	0.3	14	
NOESY (^{1}H – ^{1}H)	noesygpph	0.3 s	16	800 ms
HOESY (^{1}H –^{31}P)	hoesyetgp.2	3 s	256	800 ms
HMBC (^{1}H –^{15}N)	hmqcgpqf	0.5 s	32	8 Hz

Integration was performed using MestReNova v14.3.1 software.

B. HRMS spectroscopy

High resolution mass spectrometry (HRMS) analysis was performed on a Thermo Scientific Exactive Plus EMR (ESI-Orbitrap) using electrospray ionization (ESI).

III. Analytical methods

General procedure I (GP-I) for NMR sample preparation: After the reaction, 800 µL of MQ water were added to the paste. After shaking for 30 min to 1 h, mixtures were completely dissolved, and NMR samples were prepared by taking 500 µL of the reaction mixture and adding 50 µL of a 23.6 mM stock solution of DMS (dimethyl sulfone in D_2O) and 50 µL of a 155.4 mM stock solution of phosphonoacetic acid as internal standards.

A. Product identification by ^{1}H and ^{31}P NMR

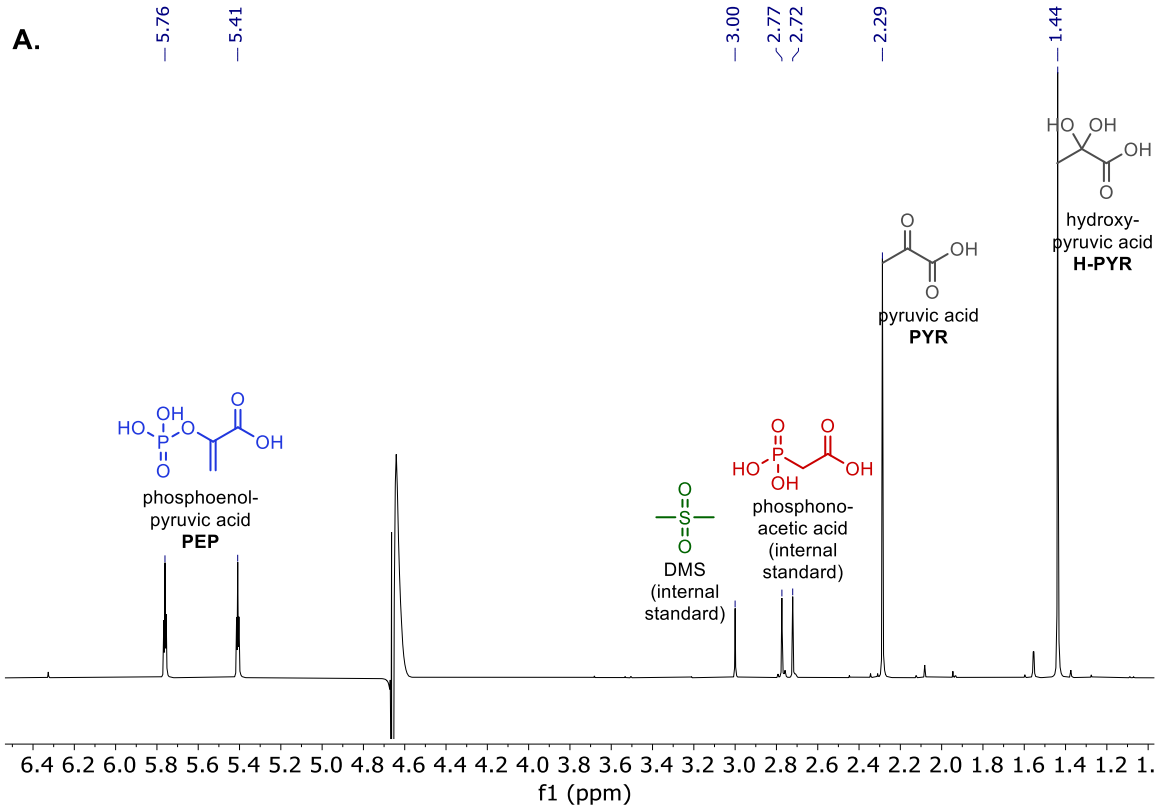

B.

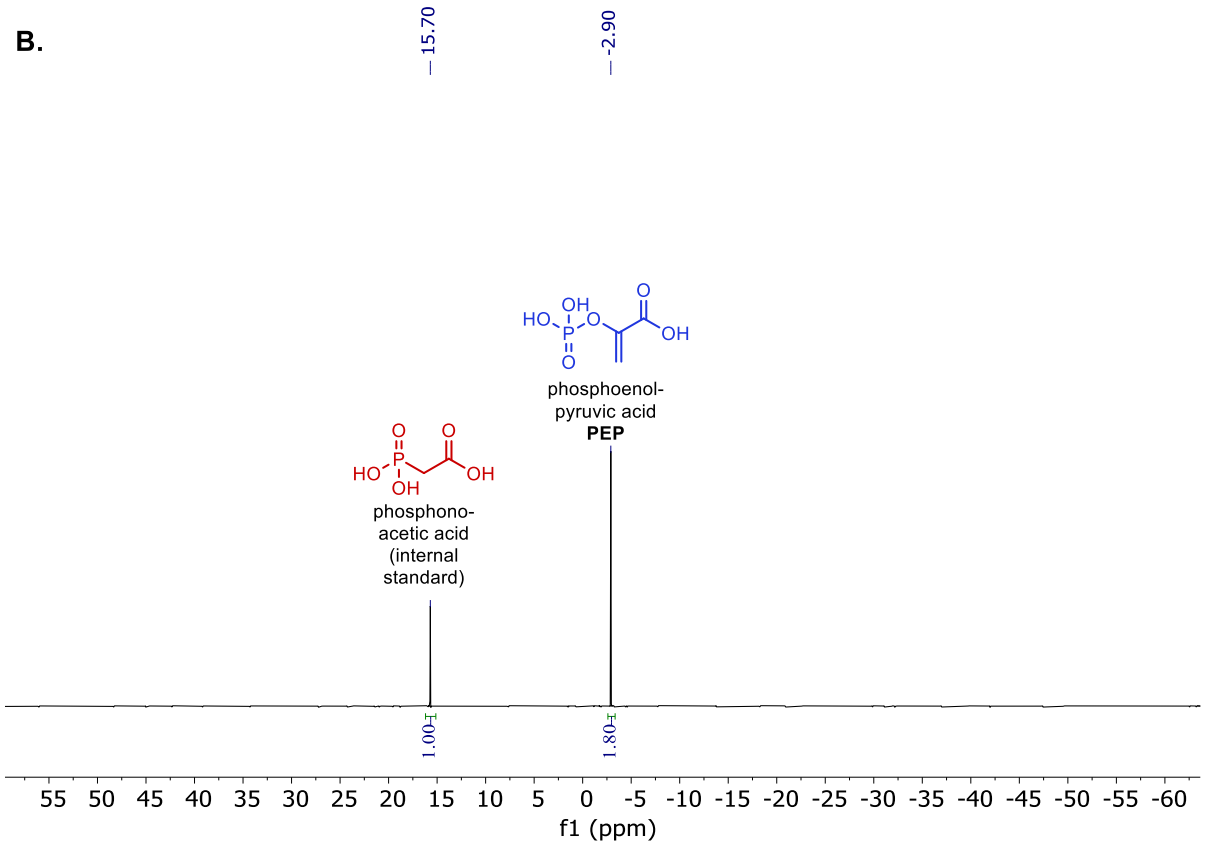

Figure S1. ^{1}H and ^{31}P NMR of the mixture of the starting material (pyruvic acid **PYR** and its hydrated form hydroxy-pyruvic acid **H-PYR** in gray), the product (phosphoenolpyruvate, **PEP** in blue), and the two internal standards (dimethyl sulfone, **DMS** in red and phosphonoacetic acid in green) used in this study. The mixture was prepared in H_2O:D_2O mixture (9:1) as solvent without adjustment of the pH (pH 1). **A.** ^{1}H NMR (400 MHz, ns = 16, d1 = 2s); **B.** ^{31}P NMR (400 MHz, ns = 16, d1 = 2s).

B. Stability of the product in highly acidic condition (in the presence of P_4O_{10}, pH 1)

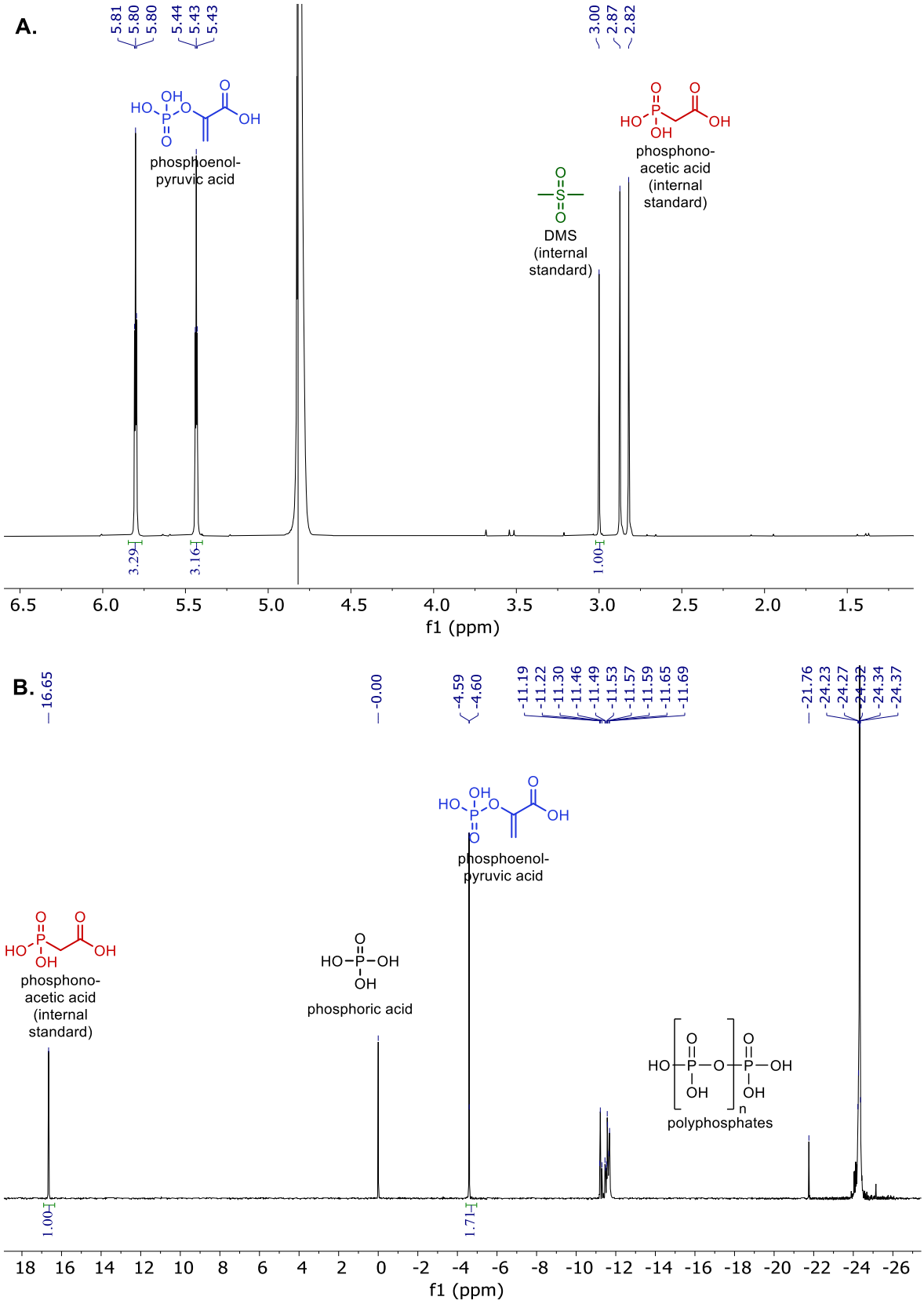
A.
5.81
5.80
5.80
5.44
5.43
5.43
3.00
2.87
2.82
phosphoenol-
pyruvic acid
phosphono-
acetic acid
(internal
standard)
DMS
(internal
standard)
3.29
3.16
1.00
6.5
6.0
5.5
5.0
4.5
4.0
3.5
3.0
2.5
2.0
1.5
f1 (ppm)
B.
16.65
-0.00
-4.59
-4.60
-11.19
-11.22
-11.30
-11.46
-11.49
-11.53
-11.57
-11.59
-11.65
-11.69
-21.76
-24.23
-24.27
-24.32
-24.34
-24.37
phosphoenol-
pyruvic acid
phosphono-
acetic acid
(internal
standard)
phosphoric acid
polyphosphates
n
1.00
1.71
18
16
14
12
10
8
6
4
2
0
-2
-4
-6
-8
-10
-12
-14
-16
-18
-20
-22
-24
-26
f1 (ppm)

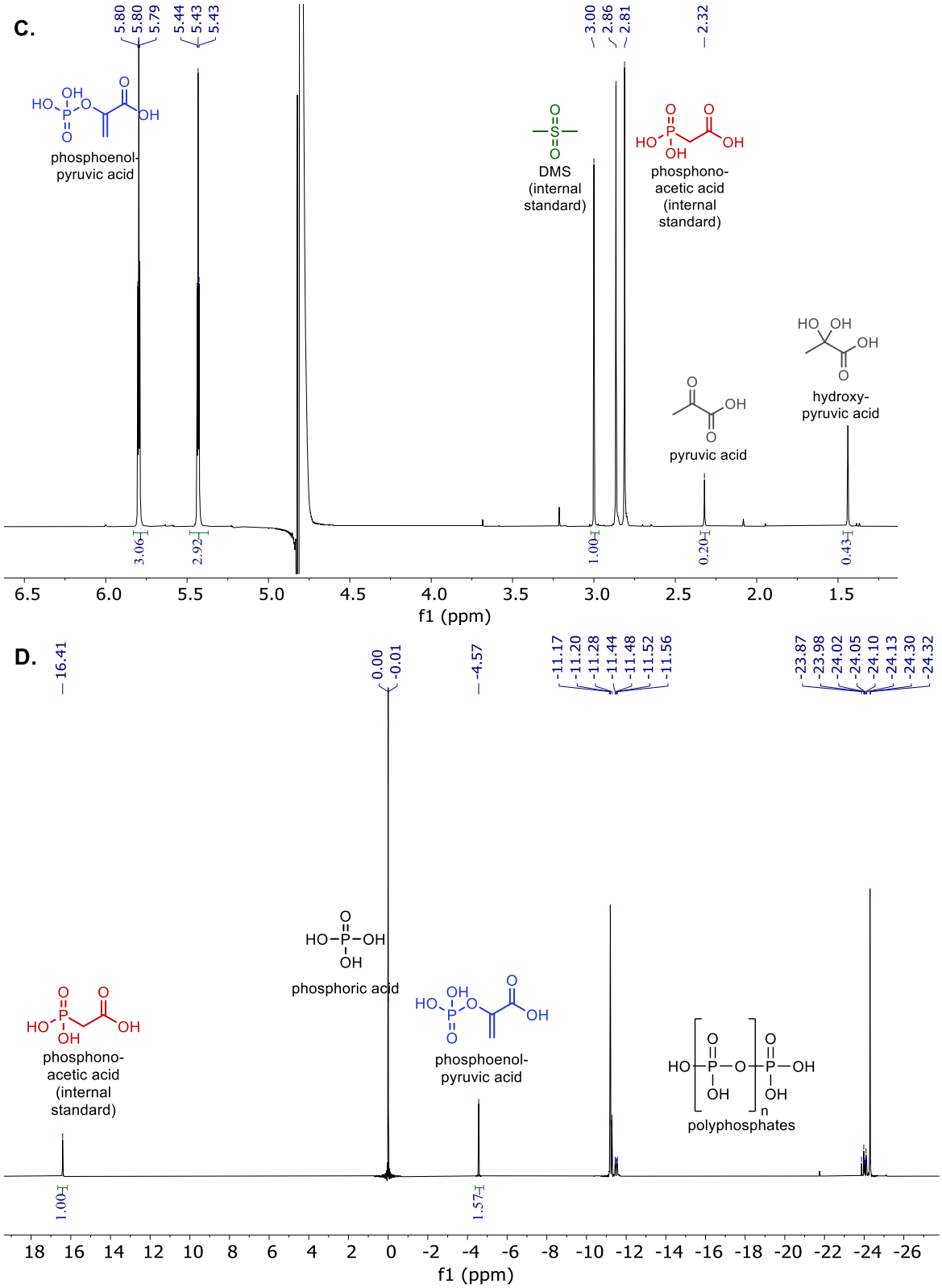

Figure S2. ^{1}H and ^{31}P NMR of the product (phosphoenolpyruvate, PEP in blue) in the presence of P_4O_{10} both dissolved in H_2O and the two internal standards (dimethylsulfone, DMS in red and phosphonoacetic acid in green). The mixture was prepared in a H_2O:D_2O mixture (9:1) as solvent at pH 1 without adjustment. A second measurement was performed after 24 h to evaluate the stability of PEP in these conditions. **A.** ^{1}H NMR (400 MHz, ns = 16, d1 = 2 s); **B.** ^{31}P NMR (400 MHz, ns = 16, d1 = 2 s) with calibration at 0 ppm for H_3PO_4. P_4O_{10} decomposes to phosphoric acid and other

polyphosphates.[1] **C.** ^{1}H NMR (400 MHz, ns = 16, d1 = 2 s) quantification of PEP hydrolysis after 24 h according to the internal standard (roughly 7%). **D.** ^{31}P NMR (400 MHz, ns = 16, d1 = 2 s) with reference at 0 ppm for H_3PO_4.

C. PEP quantification by ^{1}H or ^{31}P NMR

For ^{1}H NMR quantification, a calibration curve of **PEP** was made to compensate for the small errors induced by the water suppression method (the peaks of **PEP** are close to the water peak on ^{1}H NMR, which can affect their integration). A ^{31}P NMR quantification was independently performed to confirm the yield found with ^{1}H NMR quantification. ^{31}P quantification was done on a few samples to confirm the ^{1}H NMR quantification because of the higher limit of detection using ^{31}P NMR quantification (see below). Phosphonoacetic acid was used as an internal standard instead of H_3PO_4 because H_3PO_4 is a subproduct of the reaction.

The calibration curves were prepared as following: various solutions of phosphoenolpyruvic acid potassium salt **PEP** (0.05, 0.09, 0.19, 0.37, 0.74, 1.48, 2.96, 5.93, 11.85 mM) were prepared in MilliQ water. For quantification, NMR samples were prepared by taking 500 µL of the solution and adding 50 µL of a 23.6 mM stock solution of internal standard (DMS in D_2O) and 50 µL of a 155.4 mM stock solution of the second internal standard (phosphonoacetic acid in D_2O). Each of the standard calibration samples was subjected to ^{1}H and ^{31}P NMR spectroscopies using the water suppression technique at ambient temperature and the ^{31}P (^{1}H decoupled) method described in the **General information** section above. The data from these measurements for every concentration allowed us to obtain ten-point calibration plots for ^{1}H NMR quantification and seven-point calibration plots for ^{31}P NMR quantification (because of the limit of detection with the ^{31}P method, the 0.05, 0.09- and 0.19-mM concentrations were not considered in the calibration curve). The calibration curves were constructed by correlating the substrate-to-standard ratio peaks: δ = 5.76 ppm in ^{1}H NMR (the signal further away from the water resonance was chosen for the calibration to minimize the eventual loss of integration) and δ = -4.57 ppm in ^{31}P NMR for **PEP**, 3.00 ppm for the **DMS** standard and 15.7 ppm for the phosphonoacetic acid standard.
Reaction samples were prepared according to the general procedure described above (section III) using the same quantity of internal standards and were quantified using the calibration curve.

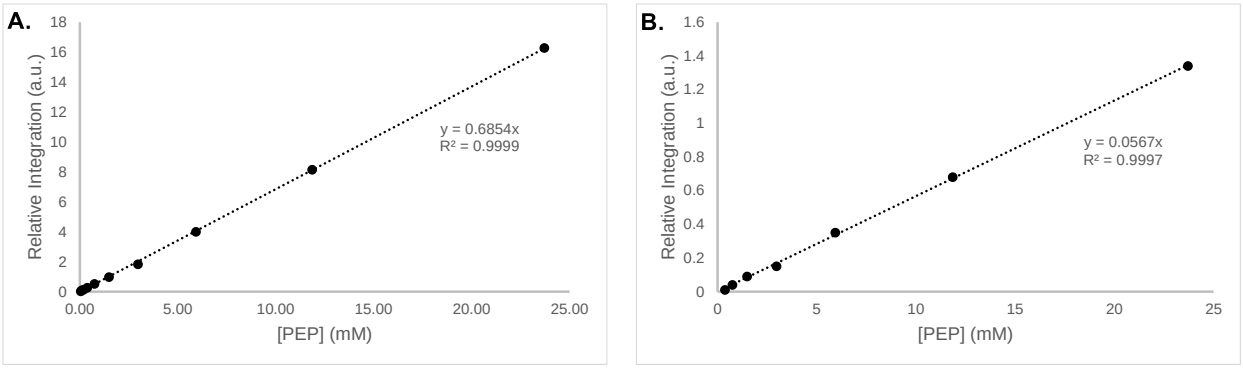

Figure S3. Correlation between the concentration of an aqueous solution of **PEP** and the measured ^{1}H (left, **A.**) and ^{31}P (right, **B.**) NMR integral relative to **DMS** (**A**.) which was set to 6.00 and relative to phosphonoacetic acid (**B**.) which was set to 1.00. Results were recorded on a 400 MHz spectrometer, at ambient temperature with ns = 16 and d1 = 2 s.

D. Product quantification by qNMR using ^{1}H or ^{31}P NMR for other substrates

The other organo-phosphorylated products were analyzed by quantitative ^{1}H and ^{31}P NMR (qNMR) using 500 µL of the reaction mixture, 50 µL of a 23.6 mM DMS stock solution in D_2O, and 50 µL of a 77.8 mM phosphonoacetic acid stock solution in D_2O (total volume of NMR sample: 600 µL). The parameters reported in the **General Information** part (NMR Spectroscopy) were d1 = 45 or 60 s and ns = 8 or 16. Yields were calculated by comparing the ^{1}H NMR and ^{31}P NMR integrals against the DMS and phosphonoacetic acid internal standard, respectively.

E. Product identification by HRMS (direct infusion)

LC Method:

Flow Gradient

Time	Flow [mL/min]	%B	%C	%D	Curve
Equilibration					
0	Run				
0	0.4	0	100	0	5
1	0.4	0	100	0	5
3	0.4	0	60	40	5
3.2	0.4	0	100	0	5
3.5	0.4	0	100	0	5
3.501	0.4	0	100	0	5
3.501	Stop Run				

- (C): MeOH
- (D): MeOH + 0.05% formic acid

Mass Spectrometry Mode:

Full MS:

- General
  - Run time: 0 to 3.5 min
  - Polarity: Positive (or Negative)
- Full MS
  - Resolution: 140000
  - QGC target: 3e6
  - Maximum IT: 200ms
  - Scan range: 50 to 750 m/z

Synthetic procedures and quantification

IV. Investigation and optimization of the phosphorylation of pyruvate to PEP

A. General procedure II (GP-II) for the phosphorylation reaction in paste conditions

Substrates (0.06 ± 0.005 mmol) and phosphates (2 equiv) were weighed together in a 2 mL microcentrifuge tube with a lid and the resulting heterogenous mixture (paste) was mixed for 20 s using a vortex. Then, the base was added, and the mixture was centrifuged for 2 min. The resulting paste was heated at 60 °C for the indicated time in a thermoshaker. Subsequently, the general procedure **GP-I** for the preparation of the NMR sample was applied.

B. Phosphorylating agent screening

The screening was performed according to the general procedure **GP-II**. The different phosphorylating agents which were tested are summarized in **Table S1** (see below). In this screening, $KHCO_3$ (2 equiv) was used as a base and H_2O (2 equiv) was added to make a paste.

Table S1. Phosphorylating agent screening with product quantification by ^1H NMR.

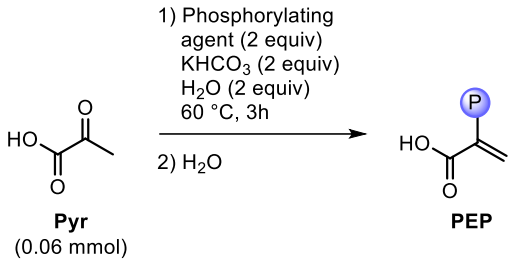

Pyr (0.06 mmol) → **PEP**

Entry	Phosphorylating agent	Integration	Yield of PEP (%)
1	Phosphorous pentoxide P_4O_{10} (1 equiv)	0.04	Traces
2	Linear triphosphate $Na_5P_3O_9$	0	0
3	Trimetaphosphate (TMP)	0	0
4	Hexametaphosphate (HMP)	0	0
5	Acetyl Phosphate	0	0
6	Diamidophosphate (DAP)	0	0

Table S1 Entry 1 - ^{1}H and ^{31}P spectra for the experiments where PEP was observed.

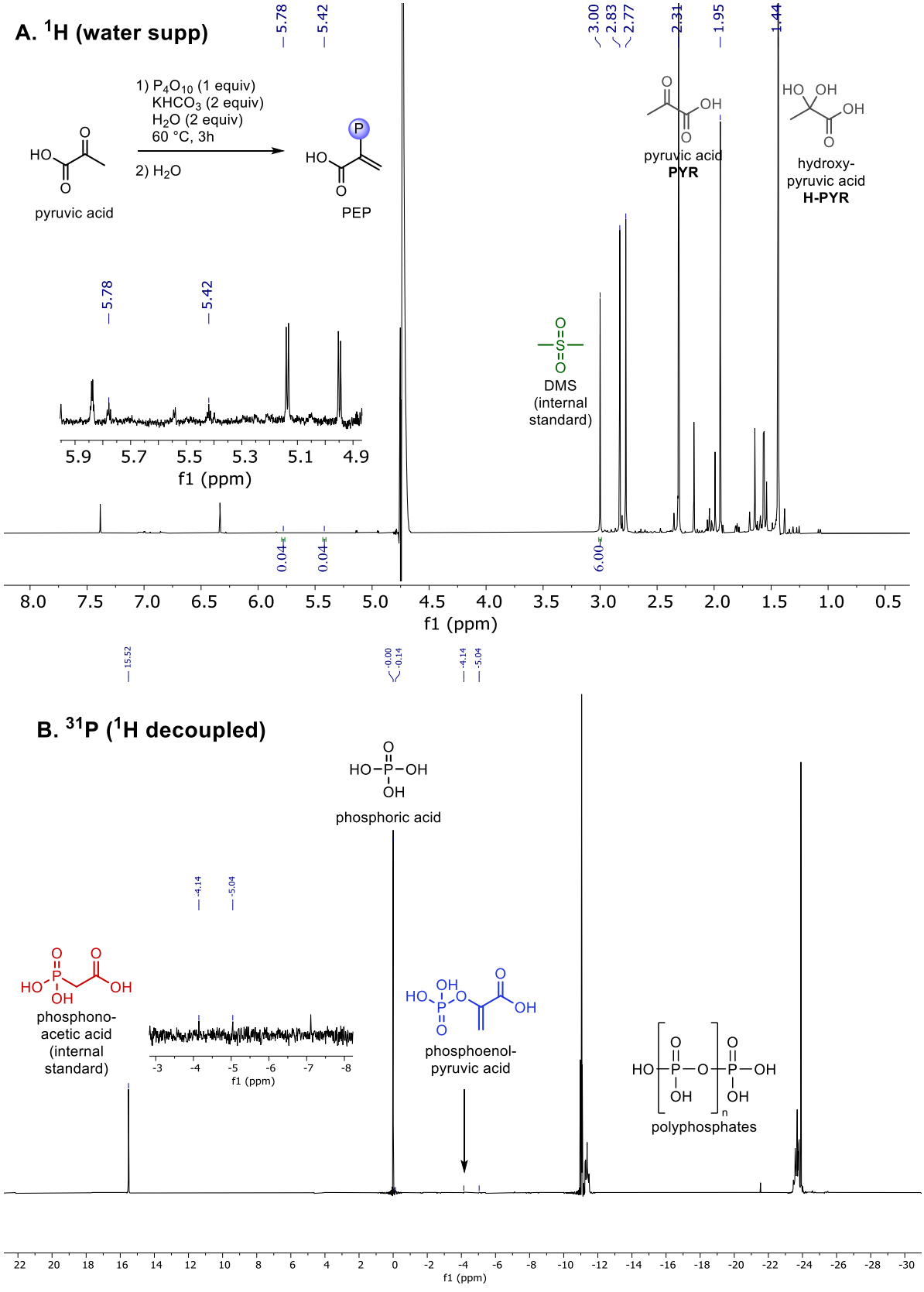

C. Base screening

The screening was performed according to the general procedure **GP-II**. In this screening, P_4O_{10} was used as phosphorylating agent and reactions were performed in neat conditions. The different bases which were tested are summarized in **Table S2** (see below). Pyruvic acid (0.06 mmol) was used as substrate in combination with nitrogenous bases that resulted in the formation of a paste without the need for the addition of water.

Table S2. Base screening with product quantification by ^{1}H NMR.

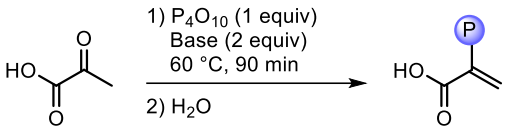

Pyr (0.06 mmol) **PEP**

Entry	Base	Mass substrate (mg)	Integration ^{1}H	Yield PEP (%)	Integration ^{31}P	Yield PEP (%)
1[a]	None		< 0.1	traces	0	0
2	Pyridine	5.6	3.76	6.9%	0.32	7.1%
3	Imidazole	5.4	0.12	0.2%	0.03	0.7%
4	1-methylimidazole	5.5	0.89	1.7%	0.06	1.4%
5	2,6-lutidine	5.3	0.73	1.4%	0.07	1.6%
6	Pyrimidine	5.5	1.71	3.2%	0.12	2.7%
7	Triethylamine	5.4	2.06	4.0%	0.22	5%
8	Collidine	5.9	0.27	0.5%	0.03	0.6%
9	Picoline	5.3	2.63	5.1%	0.22	5.1%
10	Quinoline	5.7	0.63	1.1%	0.05	1.1%

[a] Two equiv of water were added to make a paste.

^{1}H and ^{31}P spectra for the experiments where PEP was observed.
Table S2 Entry 2

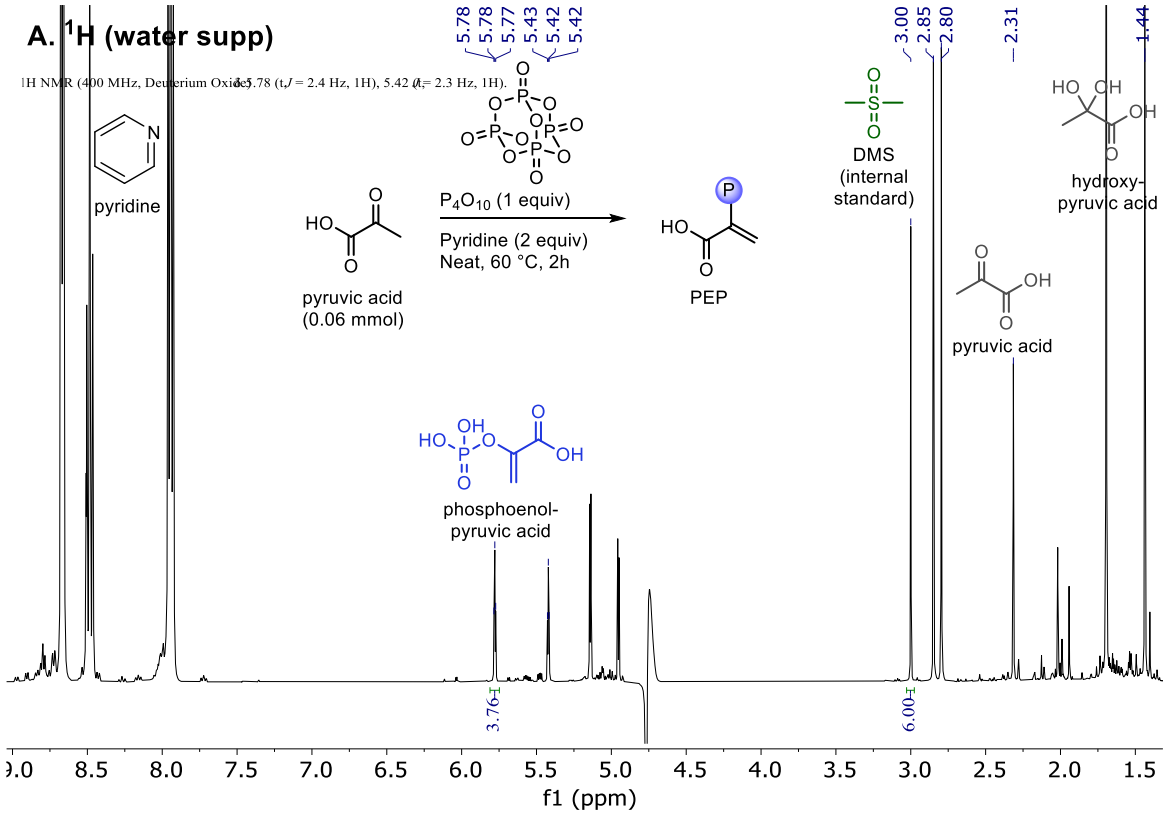

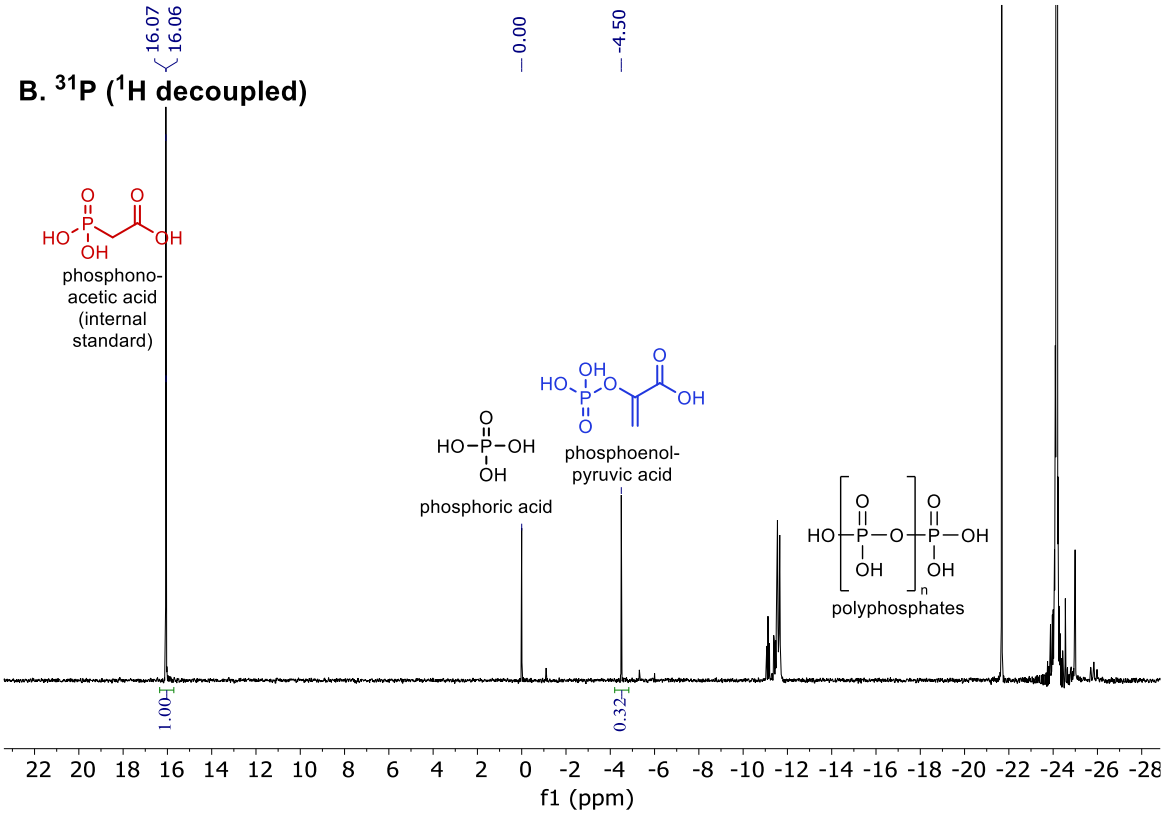

Table S2 Entry 3

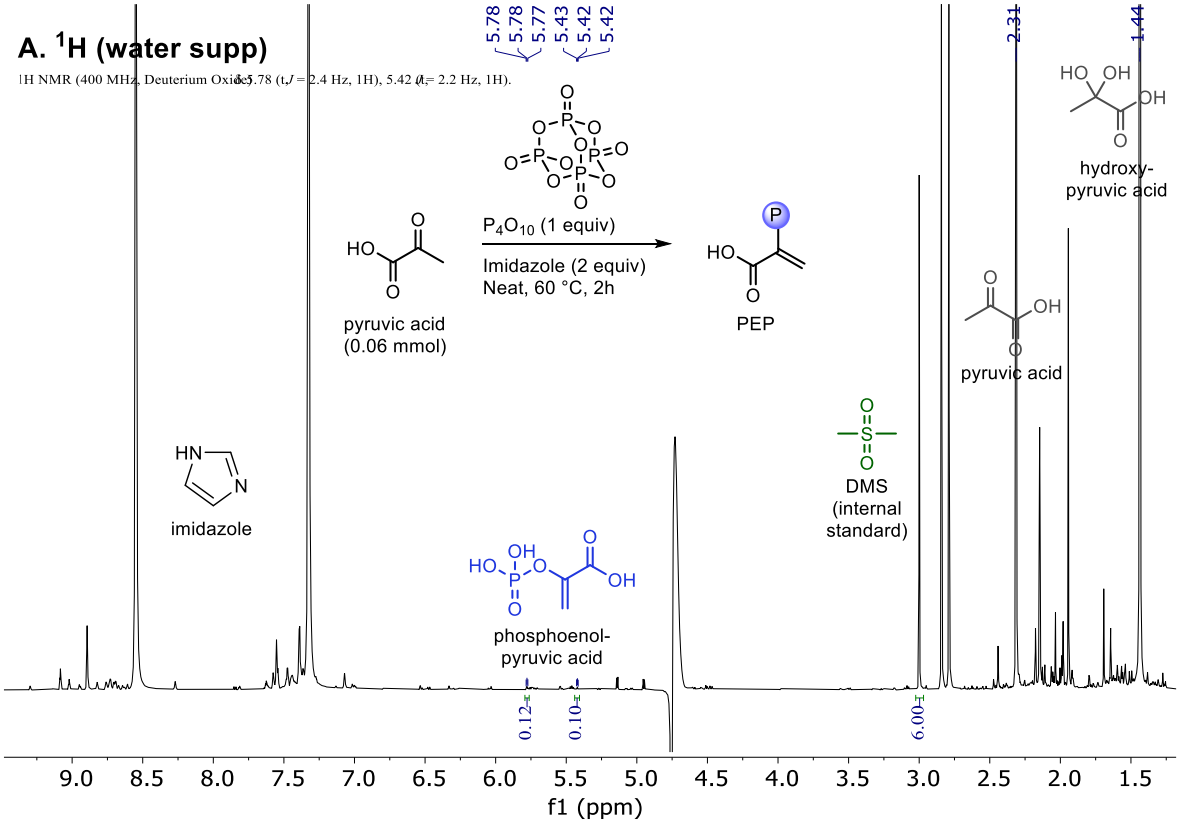

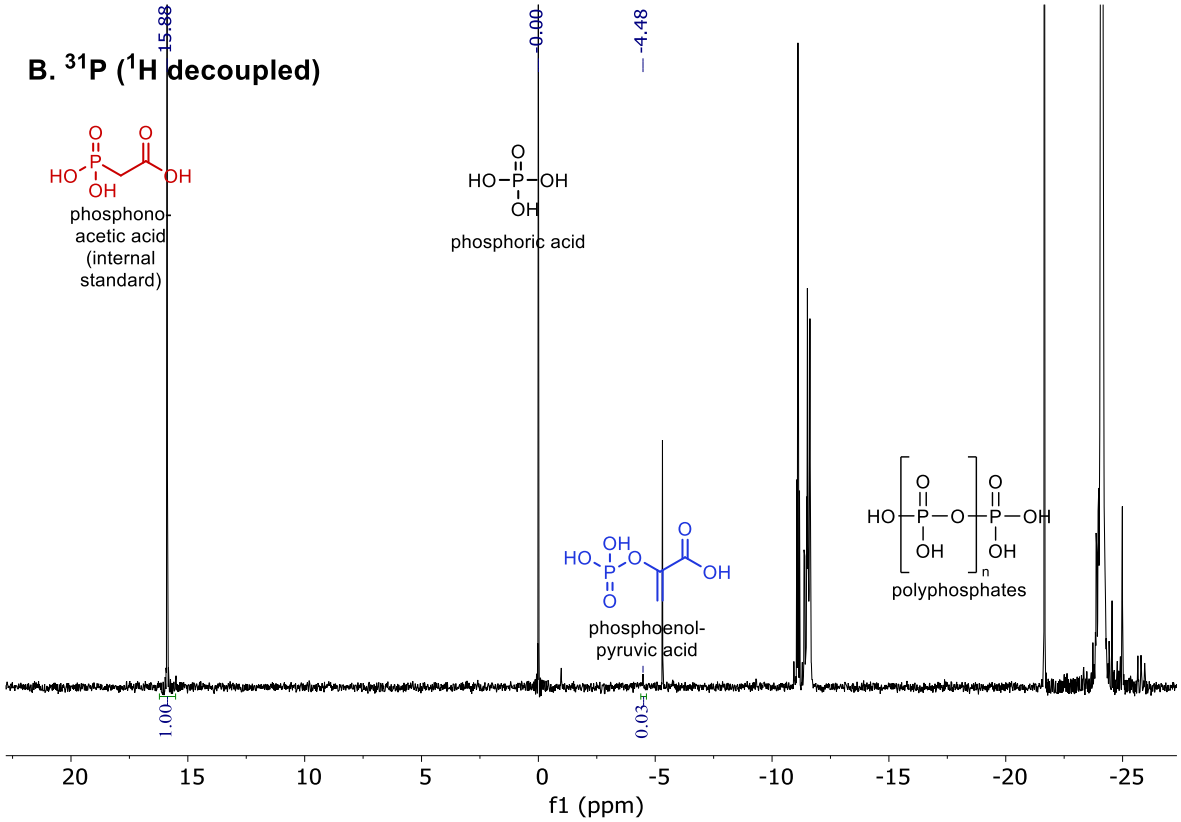

Table S2 Entry 4

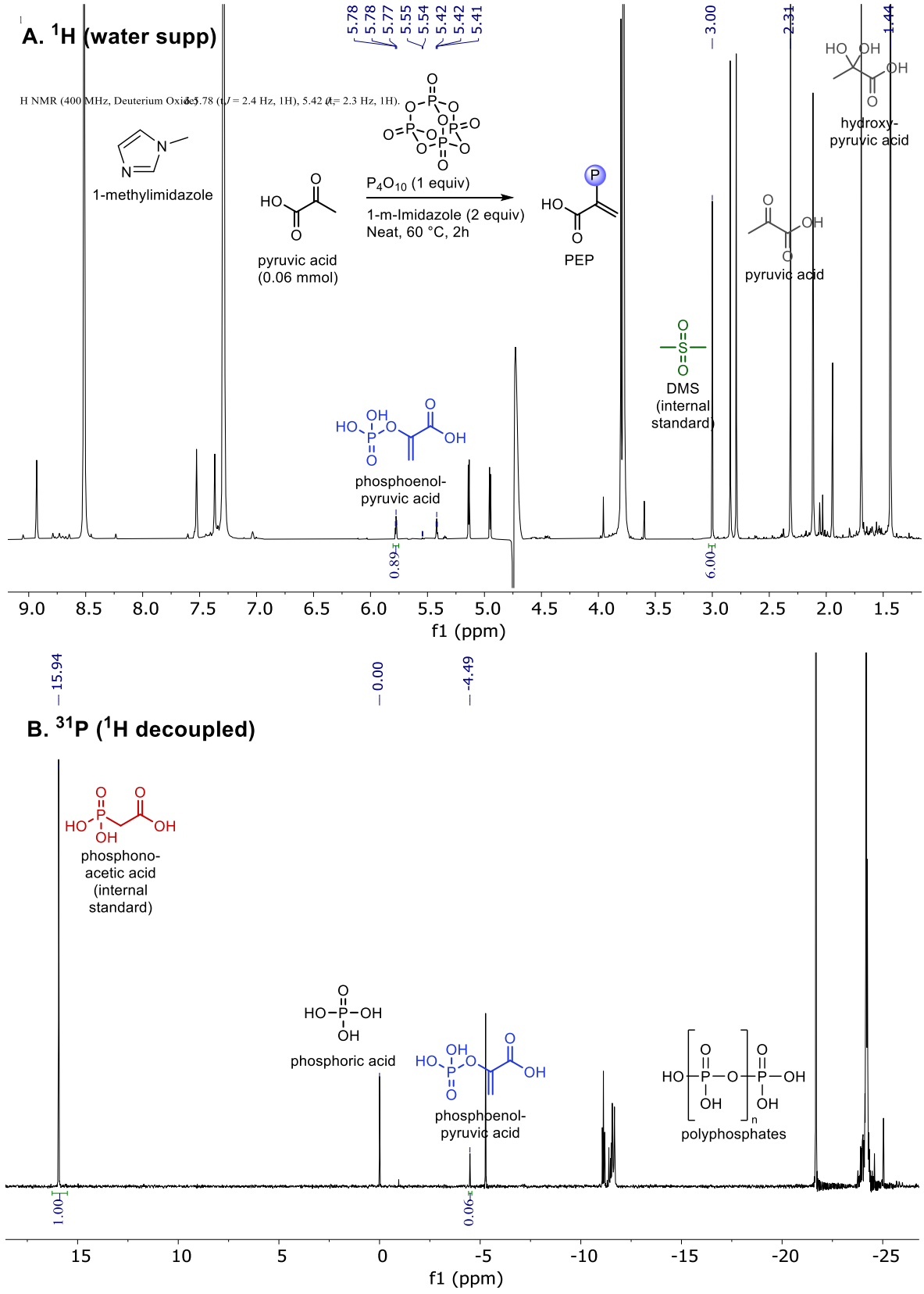

Table S2 Entry 5

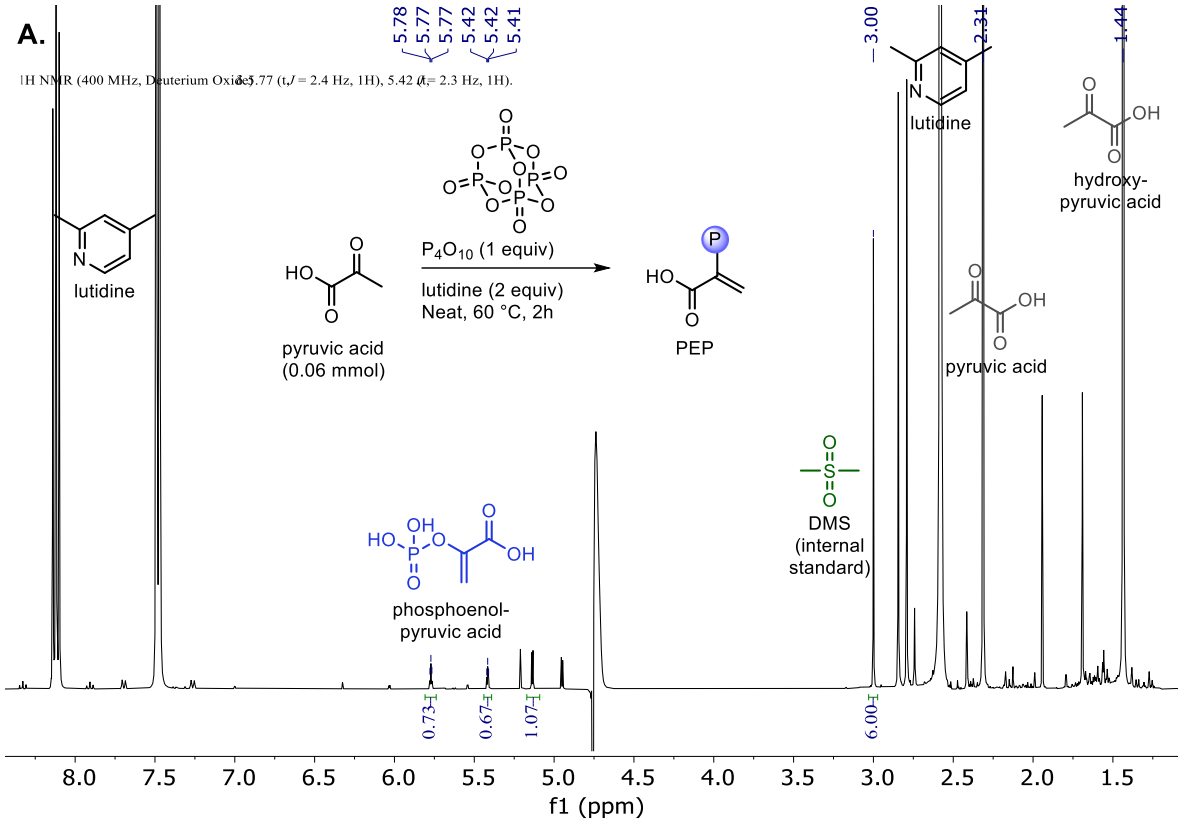

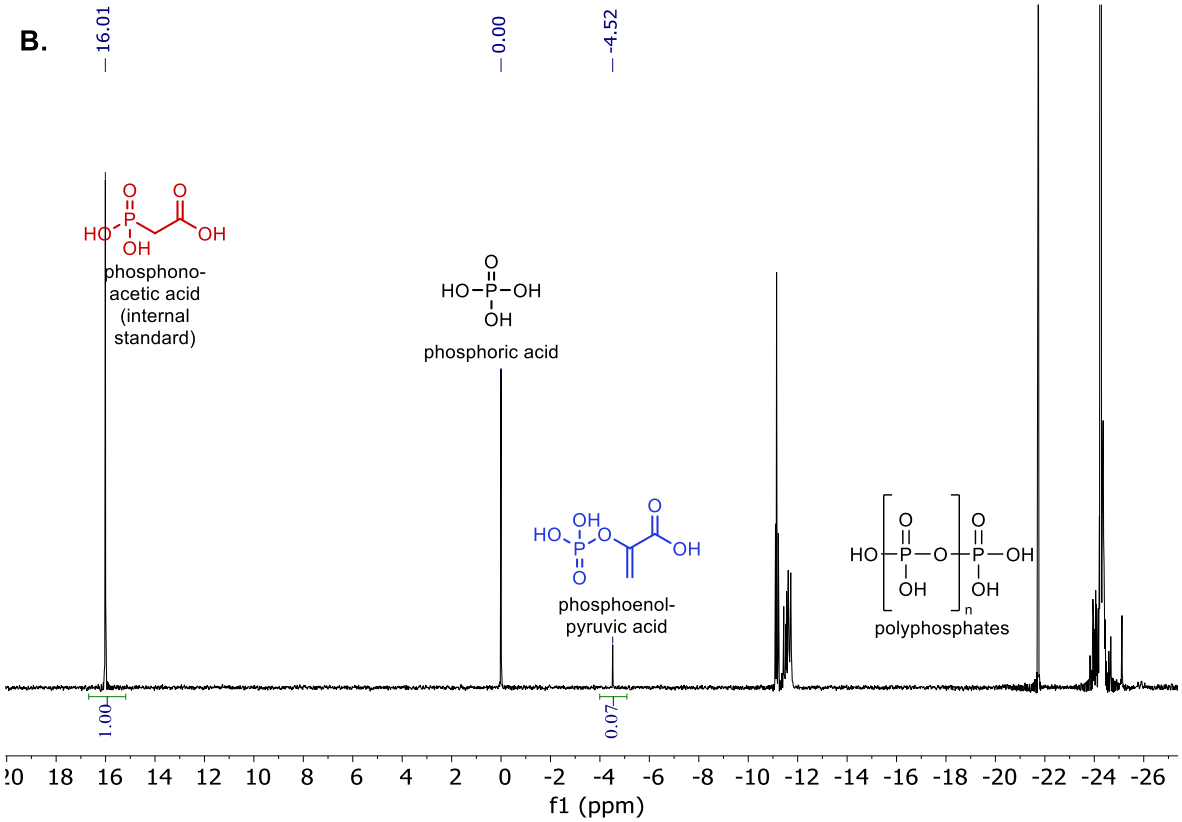

Table S2 Entry 6

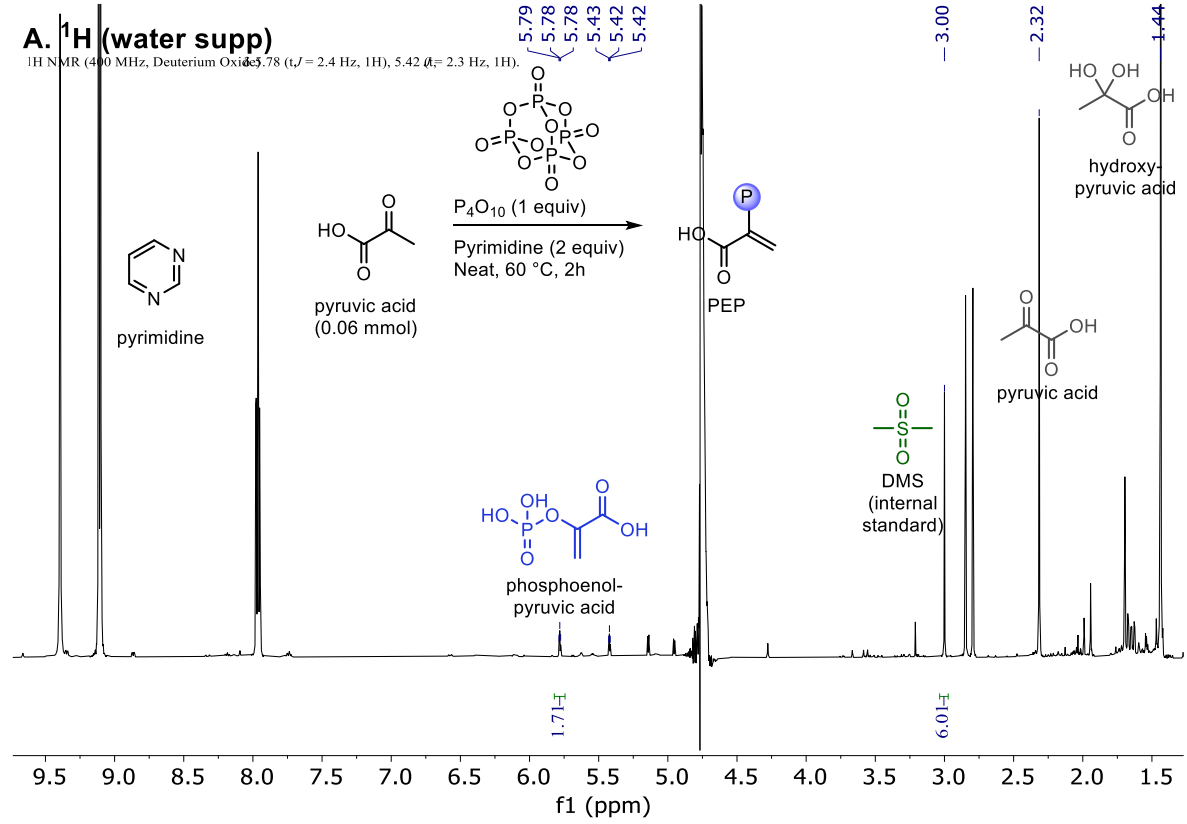

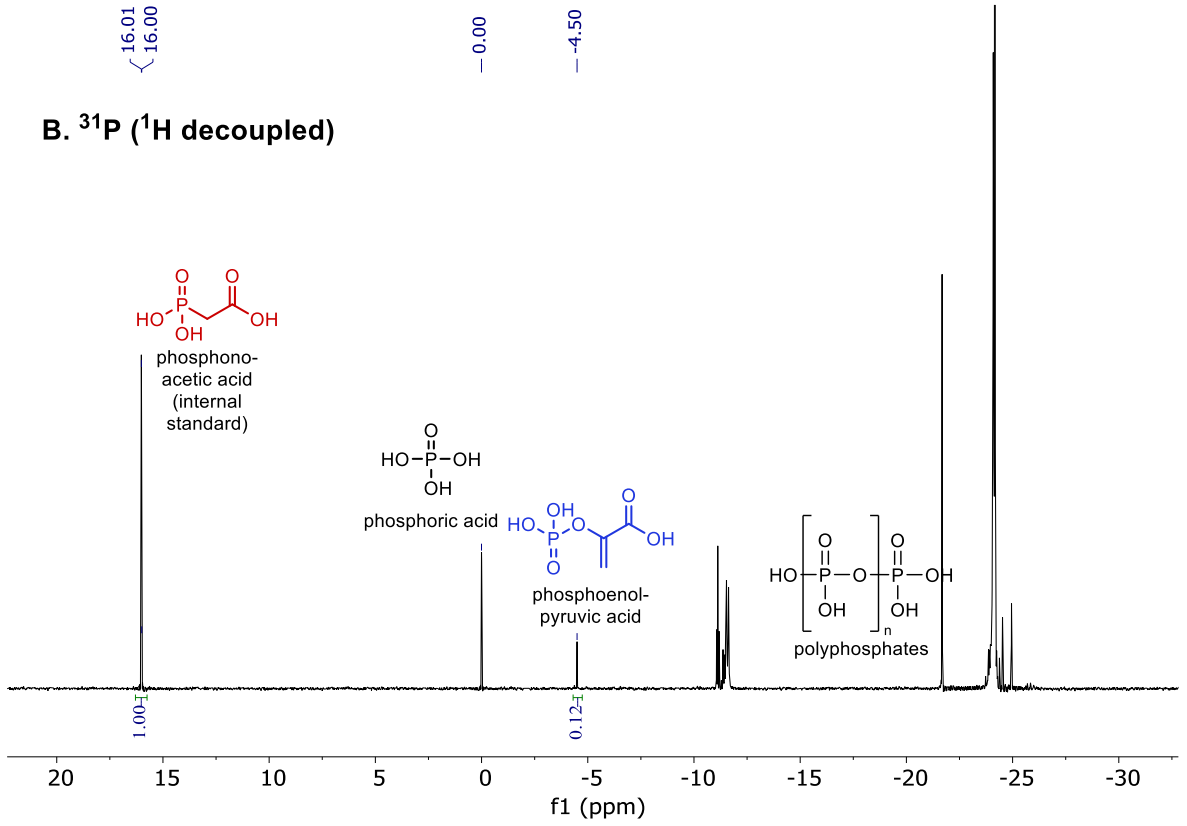

Table S2 Entry 7

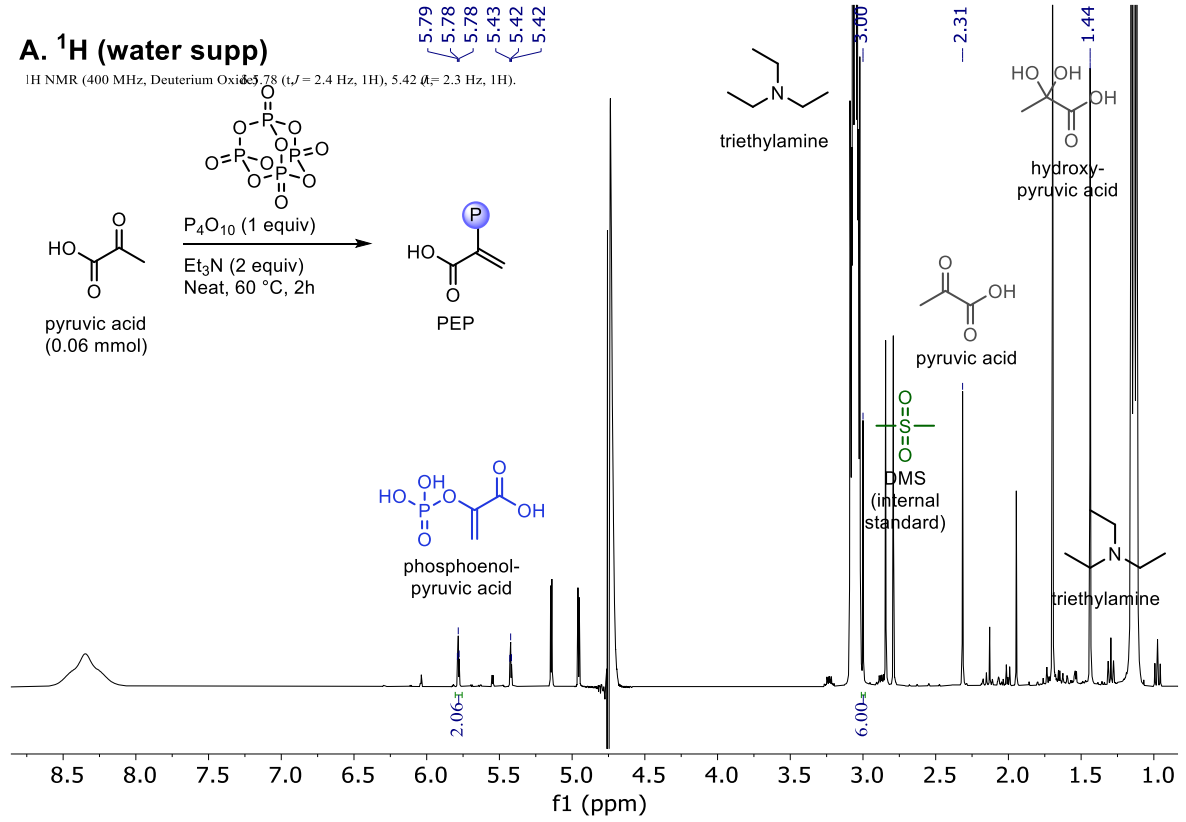

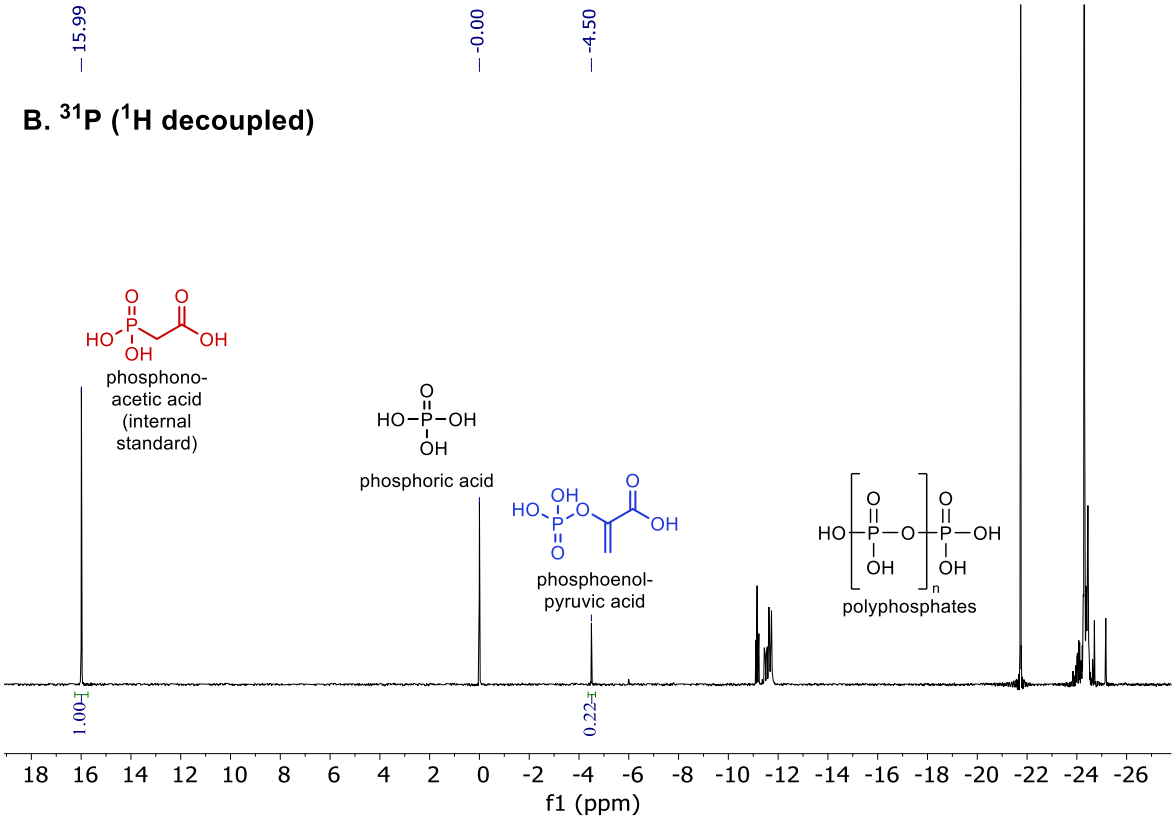

Table S2 Entry 8

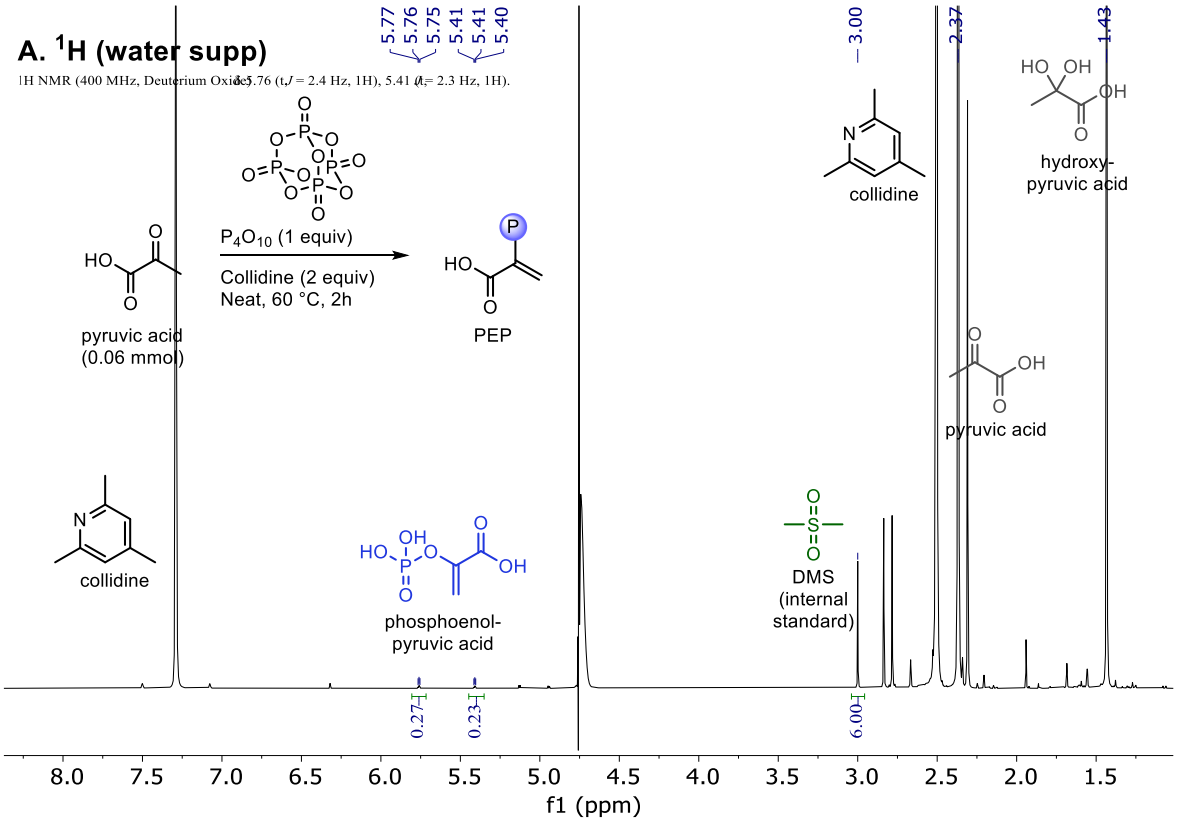

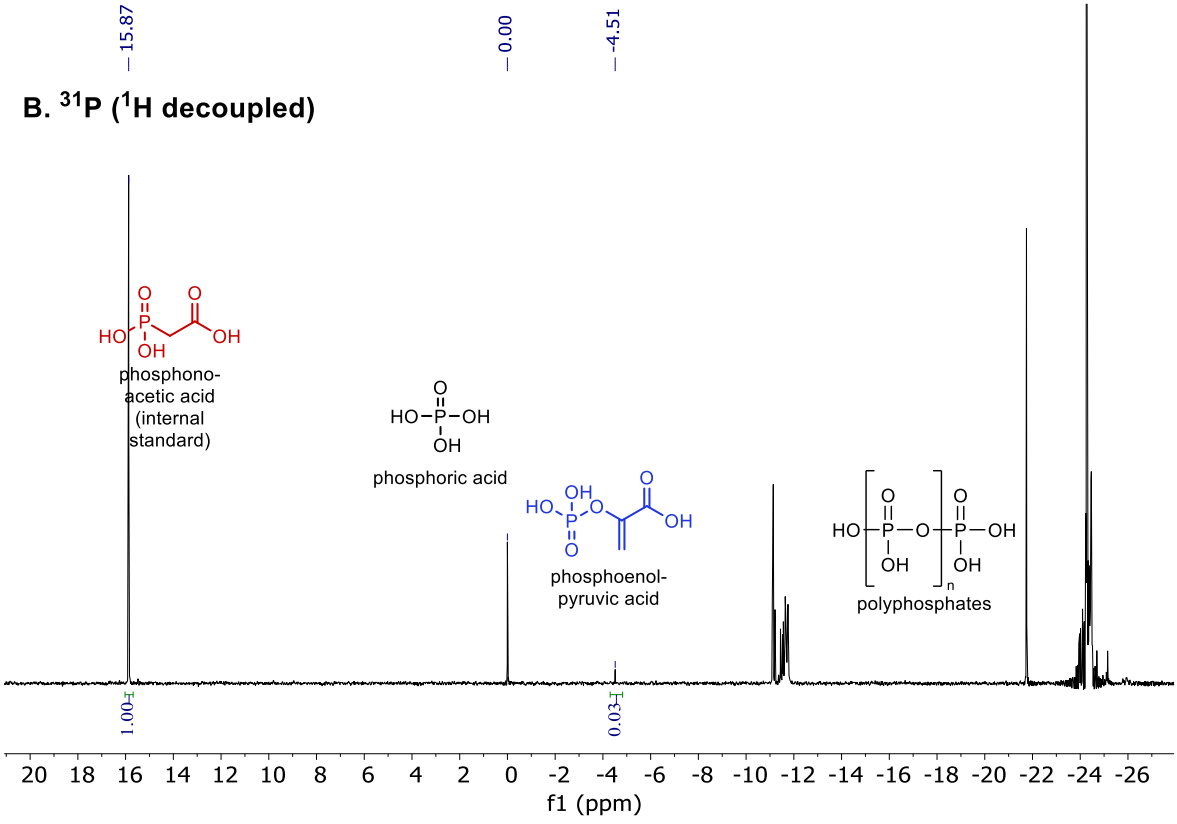

Table S2 Entry 9

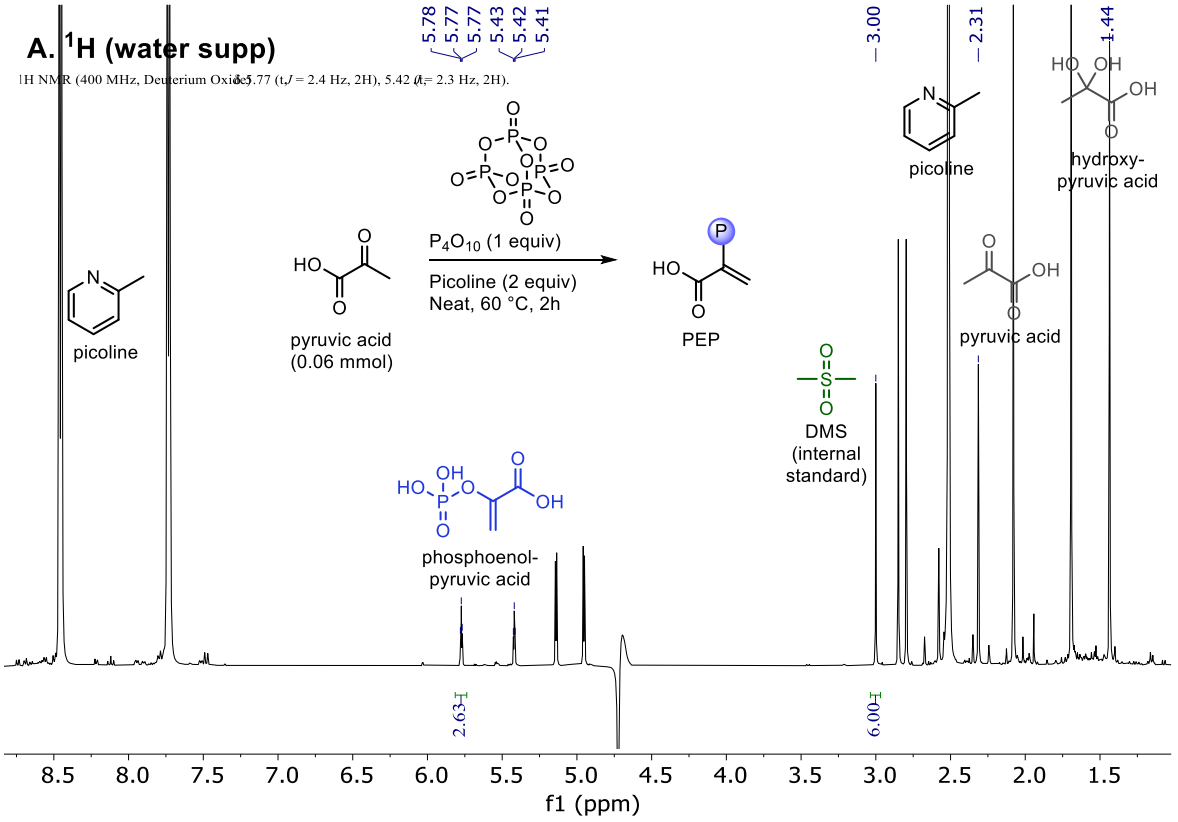

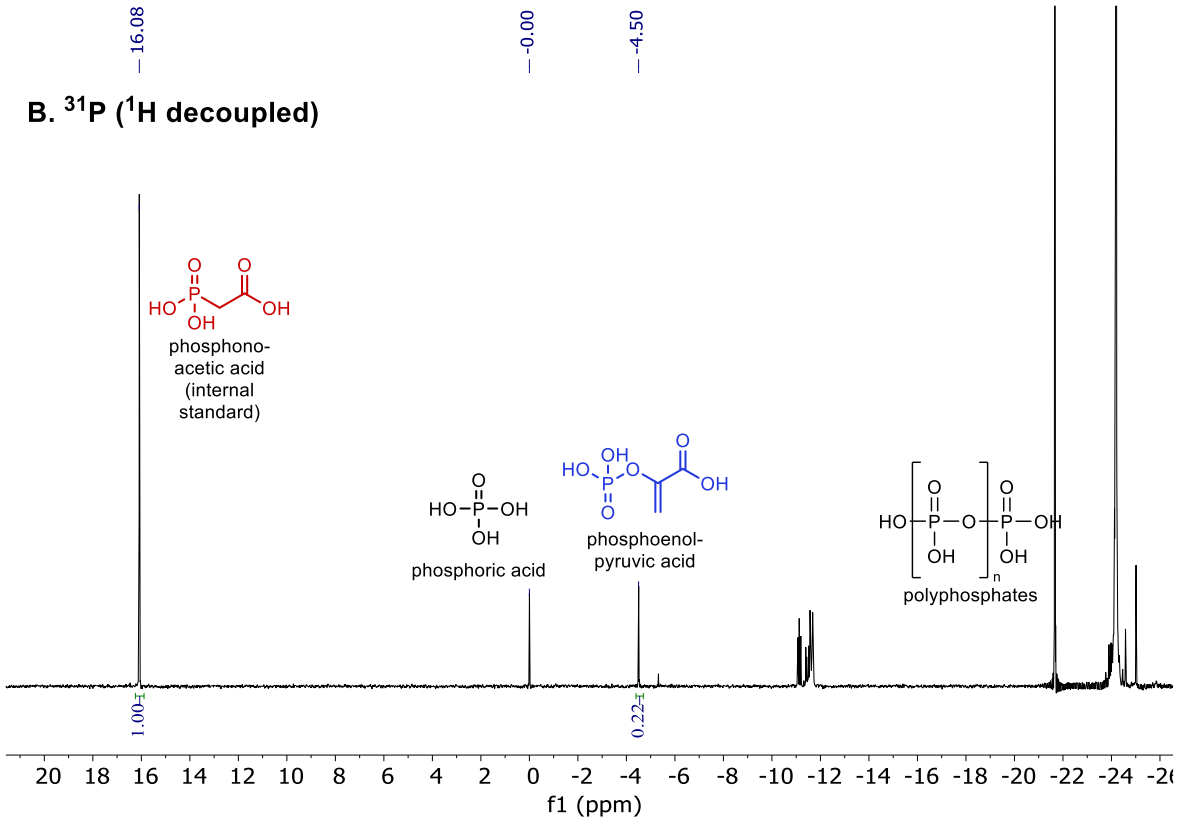

Table S2 Entry 10

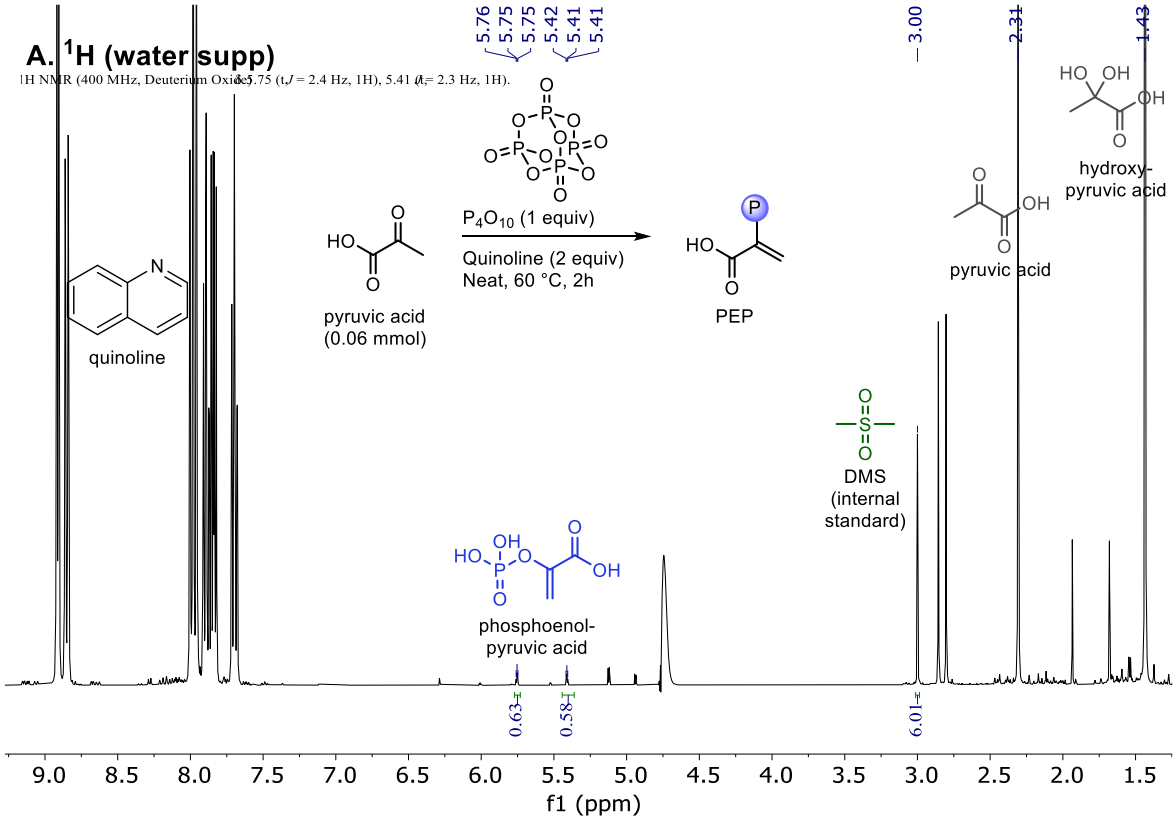

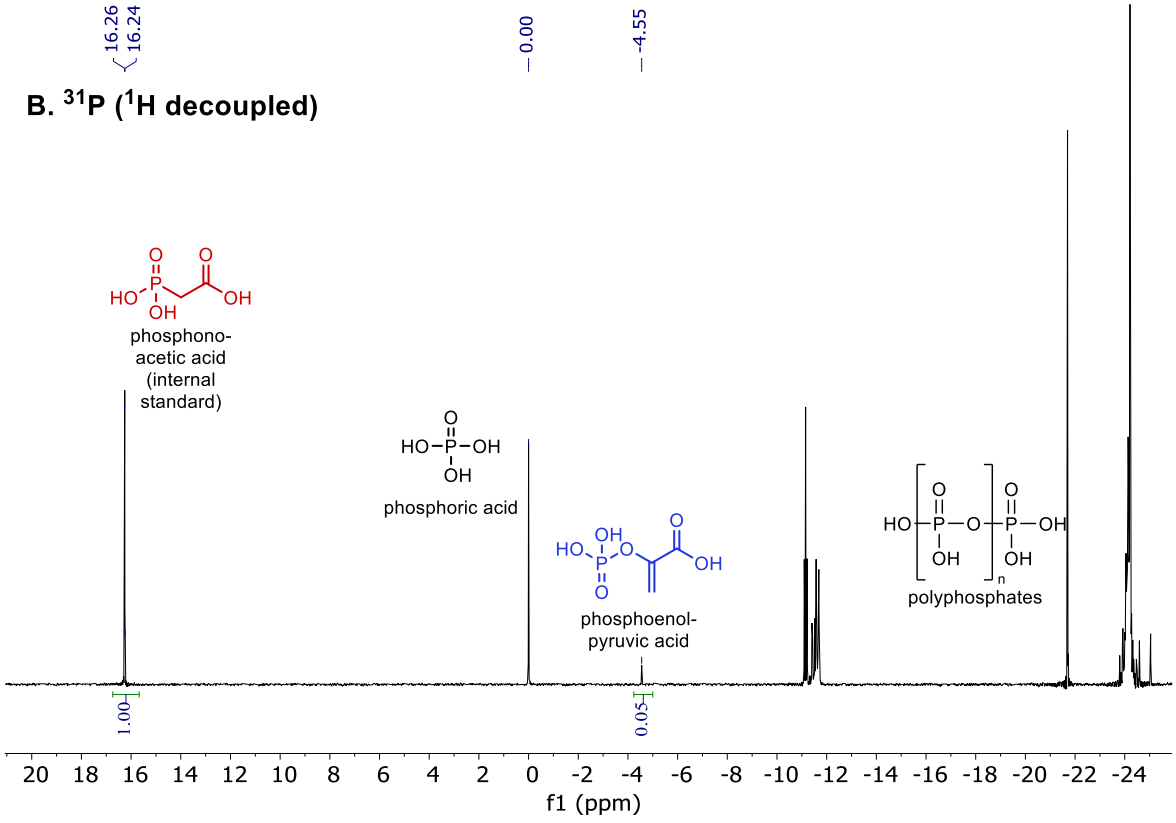

D. Optimization table

The screening was performed according to the general procedure **GP-II**. In this screening, P_4O_{10} was used as the phosphorylating agent, pyridine as the base and reactions were performed in neat conditions. The different parameters which were changed are summarized in **Table S3** (see below).

Table S3. Optimization table with product quantification by ^1H NMR.

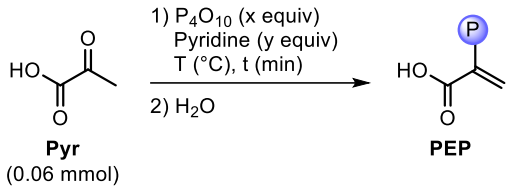

Pyr (0.06 mmol) **PEP**

Entry	Mass substrate (mg)	P_4O_{10} (x equiv)	Pyridine (y equiv)	Time	Temperature	Integration ^1H	Yield PEP (%)
1	5.5	0.5	2	90 min	60 °C	2.3	4.2%
2	5.7	1.0	2	90 min	60 °C	3.8	6.9%
3	5.3	1.5	2	90 min	60 °C	3.6	7.1%
4	5.6	2.5	2	90 min	60 °C	3.1	5.7%
5	5.6	1.0	1	90 min	60 °C	1.7	3.1%
6	5.3	1.0	3	90 min	60 °C	3.7	7.1%
7	5.26	1.0	5	90 min	60 °C	3.2	6.3%
8	5.4	1.0	10	90 min	60 °C	2.3	4.2%
9	5.4	1.0	2	15 min	60 °C	2.9	5.5%
10	5.3	1.0	2	30 min	60 °C	2.8	5.5%
11	5.4	1.0	2	1 h	60 °C	3.8	7.2%
12	5.3	1.0	2	2 h	60 °C	3.7	7.2%
13	5.4	1.0	2	4 h	60 °C	3.4	6.4%
14	5.5	1.0	2	6 h	60 °C	2.7	5.6%
15	5.5	1.0	2	16 h	60 °C	2.8	5.2%
16	5.7	1.0	2	24 h	60 °C	2.5	4.5%
17	5.5	1.0	2	48 h	60 °C	2.5	4.7%
18	6.2	1.0	2	16 h	-20 °C		Traces
19	6.0	1.0	2	16 h	2 °C		Traces
20	5.8	1.0	2	16 h	23 °C	0.9	1.6%
21	5.2	1.0	2	16 h	40 °C	3.4	6.6%
22	5.9	1.0	2	16 h	80 °C	0.8	1.5%

E. Screening of other phosphorylating agents

The screening was performed according to the general procedure **GP-II**. In this screening, the decomposition products of P_4O_{10} (H_3PO_4 and several polyphosphates) as well as other phosphates (2 equiv) were screened using pyridine as base. Reactions were performed in neat conditions at 60 °C for 60 min.

Table S4. Optimization table with product quantification by ^{1}H NMR.

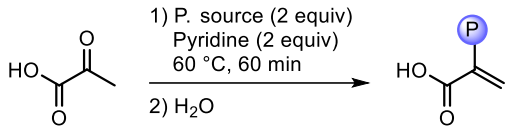

Pyr (0.06 mmol) **PEP**

Entry	Mass substrate (mg)	Phosphorylating agent	Integration	Yield PEP (%)
1	5.4	Phosphorous pentoxide P_4O_{10} (1 equiv)	3.8	7.2%
2	n.d	H_3PO_4	/	/
3	n.d	Sodium diphosphate ($Na_4O_7P_2$)	/	/
4	n.d	Sodium triphosphate ($Na_5O_{10}P_3$)	/	/
5	n.d	Sodium trimetaphosphate ($Na_3O_9P_3$)	/	/
6	n.d	Sodium hexametaphosphate ($Na_6O_{18}P_6$)	/	/
7	n.d	Acetyl-phosphate	/	/
8[a]	n.d	Polyphosphoric acid	< 0.1	traces
9	5.8	Bipyridinium phosphate ($P_2O_5L_2$ (L = pyridine))	1.9	3.3%

[a] 30 mg of polyphosphoric acid were used for the reaction

V. Investigating the mechanism of the non-enzymatic phosphorylation of pyruvate to PEP

A. Study of the reaction progress

As quantitative product analysis requires the quenching of the whole reaction mixtures, several identical reactions were prepared and run in parallel. They were then quenched and analyzed at the times stated in Table S5 following the general procedure **GP-II.** The qualitative evolution of each species of the reaction was calculated according to their relative integration compared to the internal standards (DMS for ^{1}H NMR and phosphonoacetic acid for ^{31}P NMR) using ^{1}H and ^{31}P NMRs. Importantly, the formation of **PEP** from the phosphate intermediate **P1** is only occurring in neat conditions, once in solution, there is no conversion of the intermediate into **PEP** (see Table S6, p. S27).

Table S5. Evolution of the different products during the reaction, integration by ^{1}H and ^{31}P NMR spectroscopy.

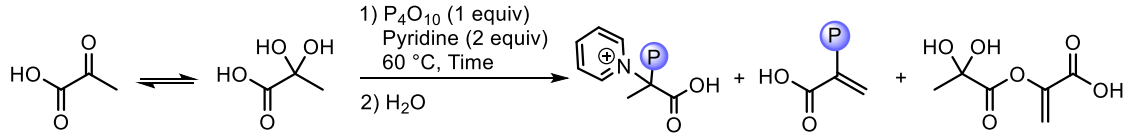

Pyr (0.06 mmol) **H-Pyr** (0.06 mmol) **P1-pyr-py** **P2-pyr (PEP)** **P3-pyr**

En-try	Time (min)	^{1}H Int. (Pyr, 2.31 ppm, 3H)	Approx. Conc. [a]Pyr (mM)	^{1}H Int. (H-Pyr, 1.44 ppm, 3H)	Approx. Conc. [a]H-Pyr (mM)	^{1}H Int. (P1, 2.28 ppm, 3H)	Approx. Conc. [a]P1 (mM)	^{1}H Int. (PEP, 5.7 ppm, 1H)	Approx. Conc. [a]PEP (mM)	^{1}H Int. (P3, 5.1 ppm, 1H)	Approx. Conc. [a]P3 (mM)	^{31}P Int. (P1, -5.3 ppm)	^{31}P Int. (P2, -4.5 ppm)
1	0	32.7	21.4	71.3	46.7	0	0.00	0	0.00	0.02	0.04	0	0
2	1	27.1	17.7	60.0	39.3	5.0	3.27	0.37	0.73	1.04	2.04	0.14	0.04
3	2	26.7	17.5	61.0	39.9	4.5	2.95	0.95	1.87	2.31	4.54	0.12	0.08
4	3	23.9	15.6	54.4	35.6	4.1	2.67	1.2	2.36	2.8	5.50	0.12	0.1
5	5	18.3	12.0	41.9	27.4	4.2	2.73	1.54	3.02	3.8	7.46	0.14	0.12
6	10	16.8	11.0	36.2	23.7	2.64	1.73	2.1	4.12	4.86	9.54	0.08	0.18

7	15	15.5	10.1	34.8	22.8	3.13	2.05	2.9	5.69	7	13.7	0.08	0.26
8	30	10.8	7.07	23.7	15.5	1.46	1.01	2.8	5.60	6.18	12.1	0.03	0.25
9	60	5.54	3.63	12.8	8.40	1.47	0.92	3.8	7.40	6.9	13.6	0.04	0.34
10	120	4.8	3.14	11.6	7.57	0.73	0.50	3.7	7.26	6.1	12.0	0.01	0.31
11	240	3.25	2.13	7.86	5.14	0.50	0.33	3.32	6.52	5	9.82	0	0.31
12	330	2.7	1.77	6.0	3.93	traces	traces	3.05	5.99	4.83	9.48	0	0.27
13	960	3.11	2.04	6.9	4.52	traces	traces	2.67	5.24	4.11	8.07	0	0.24

[a] The concentrations were determined relative to dimethyl sulfone used as an internal standard (integral set to 6 H, 1.9634 mM concentration inside the NMR tube). Concentrations are only qualitative as we did not correct for different relaxation times.

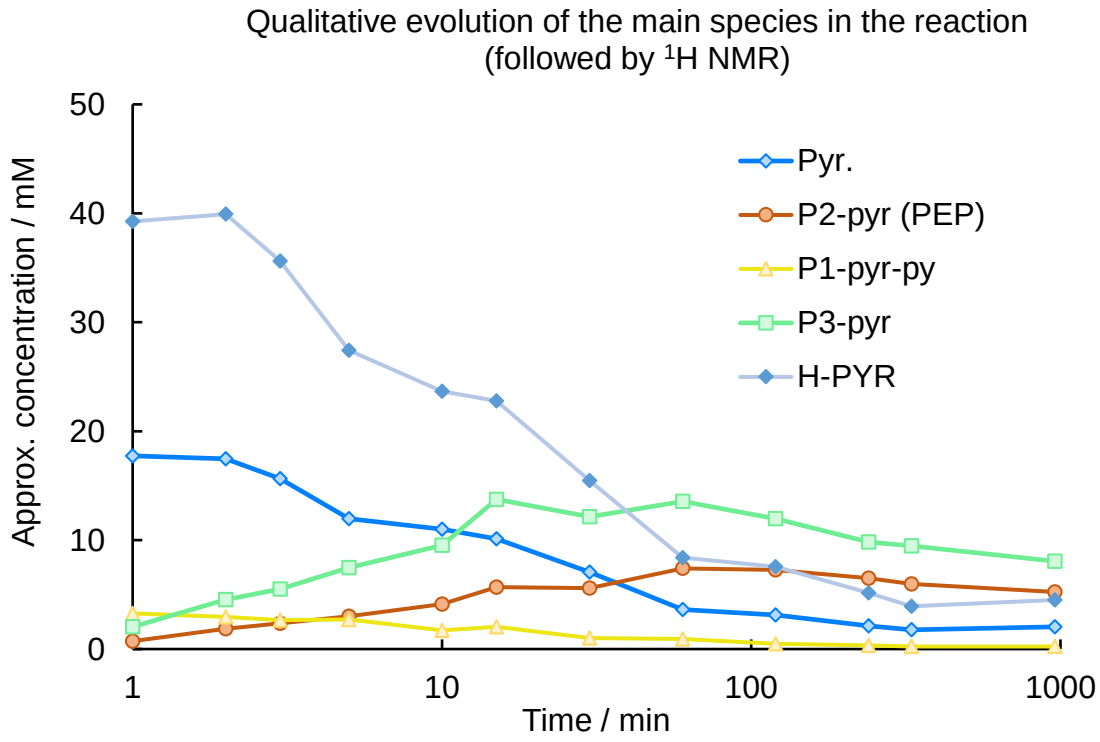

Representative ^{1}H and ^{31}P examples of a reaction mixture after heating the paste for 3 min at 60 °C.

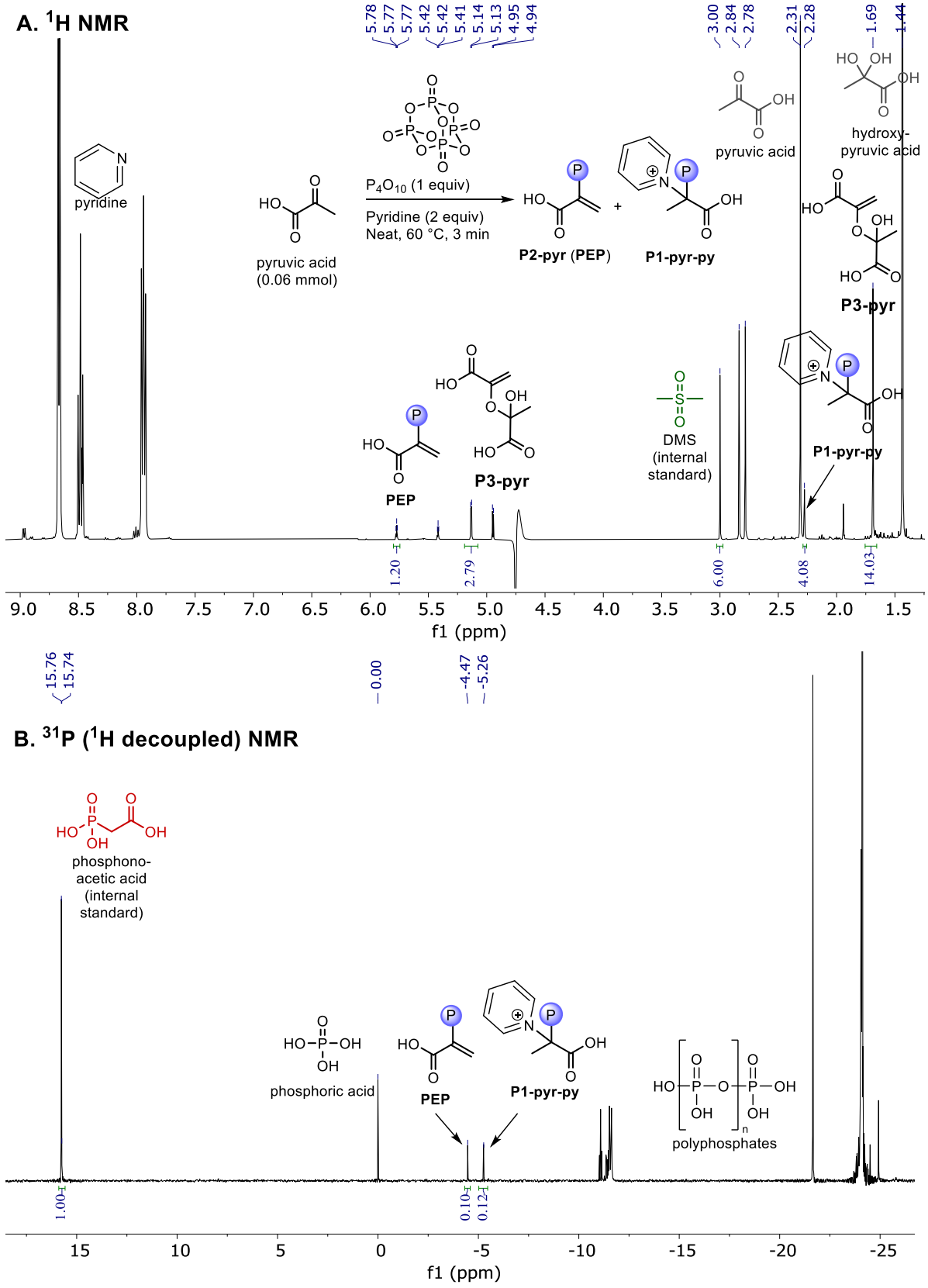

B. Stability of P1-type adducts and P3-pyr in solution and study of the conversion of P1 to PEP

1) Stability of the products and study of the conversion of P1 to PEP

To determine the stability of products in solution at different pHs, a scale-up reaction was prepared following the general procedure **GP-II** with the modification of the reaction scale (from 0.06 mmol to 0.6 mmol). The reaction was run for 5 min at 60 °C. Samples at different pHs (indicated in Table S6) were prepared by adjusting the pH using 1 M NaOH. To determine the stability of products in solution at different temperatures and to observe a potential conversion of **P1**-type products to **PEP,** the sample (with no pH adjustment) was studied by *in-situ* NMR. A stepwise temperature gradient was applied to the sample for the indicated time, and the relevant products were observed by ^{1}H and ^{31}P NMR. **P1** refers to the general structure of the hydroxy-phosphate intermediate (see below) **P1-pyr-py** and **P1-pyr-im** refer, respectively, to the phosphorylated intermediate containing pyridine (**Py**) and 1-methylimidazole (**Im**). No conversion of **P1**-type adducts to **PEP** was observed in solution.

Table S6. pH and temperature stability of reaction products with identification by ^{1}H and ^{31}P NMR spectroscopy.

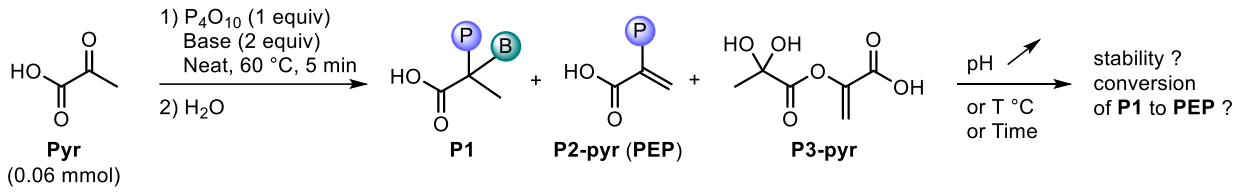

Entry	pH	Tempe-rature	Observation of P1-pyr-py	Observation of P1-pyr-im	Observation of PEP	Observation of P3-pyr	Conversion of P1-pyr-py to PEP[a]
1[a]	0-1	23 °C	Yes	Yes	Yes	Yes	No (after 8 days)
2	1-2	23 °C	Yes	Yes	Yes	Yes	/
3	2-3	23 °C	Yes	Yes	Yes	Yes	/
4	4	23 °C	Yes	Yes	Yes	Yes	/
5	5	23 °C	No	Yes	Yes	Yes	/
6	6-7	23 °C	No	Yes	Yes	Yes	/
7	7-8	23 °C	No	Yes	Yes	Yes	/
8	12	23 °C	No	Yes	Yes	Yes	/
9	0-1	40 °C	Yes	/	Yes	Yes	No
10	0-1	60 °C	Started to decompose	/	Yes	Yes	No (see below)
11	0-1	90 °C	No	/	Started to decompose	Started to decompose	/

[a] The same NMR sample was measured a second time after 8 days at RT, at pH 0-1: yield by qNMR (^{31}P); at t = 0: **P1-pyr-py** (integration 0.15) 1.5% / **PEP** (integration 0.24) 2.5%; after t = 8 days: **P1-pyr-py** (integration 0.13) 1.3% / **PEP** (int. 0.25) 2.6%.

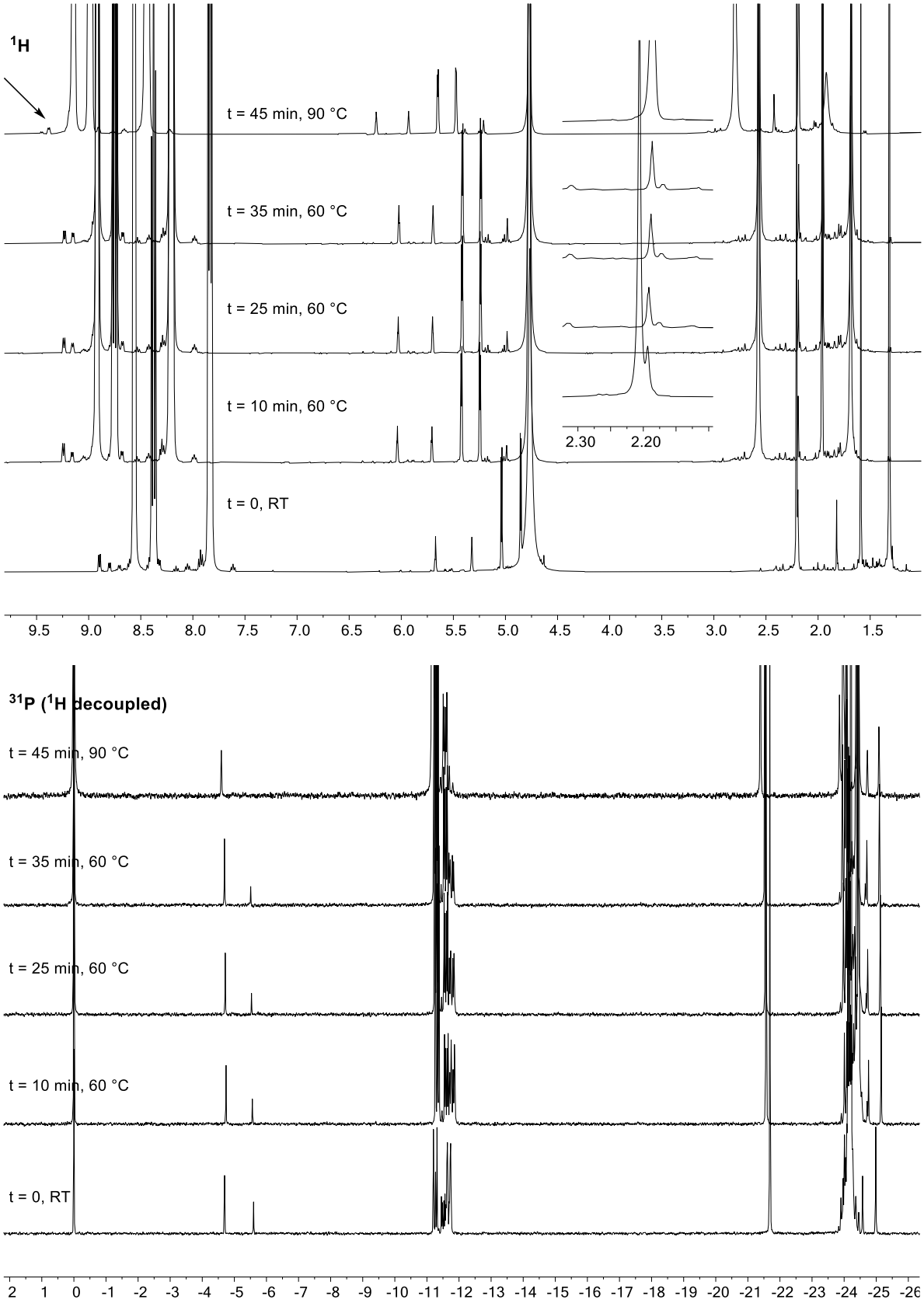
^{1}H
t = 45 min, 90 °C
t = 35 min, 60 °C
t = 25 min, 60 °C
t = 10 min, 60 °C
t = 0, RT
2.30
2.20
9.5 9.0 8.5 8.0 7.5 7.0 6.5 6.0 5.5 5.0 4.5 4.0 3.5 3.0 2.5 2.0 1.5
^{31}P (^{1}H decoupled)
t = 45 min, 90 °C
t = 35 min, 60 °C
t = 25 min, 60 °C
t = 10 min, 60 °C
t = 0, RT
2 1 0 -1 -2 -3 -4 -5 -6 -7 -8 -9 -10 -11 -12 -13 -14 -15 -16 -17 -18 -19 -20 -21 -22 -23 -24 -25 -26

2) Study of the formation of P1 and its conversion (through base elimination) to PEP with three different bases

Reactions were set up as described in the general procedure **GP-II**. The formation of **P1** and its conversion to **PEP** in the reaction was studied with three different bases: 1-methylimidazole **Im**, pyridine **Py** and triethylamine **TEA**. To do so, several reaction mixtures were prepared and stopped at different times (see Table S7). In some cases, more base was added during the reaction. NMR tubes were prepared according to the general procedure. The qualitative evolution of each species of the reaction was calculated according to their relative integration compared to the internal standards (DMS for ^{1}H NMR and phosphonoacetic acid for ^{31}P NMR) using ^{1}H and ^{31}P NMR spectroscopy.

Table S7. Comparison of three bases in the system with identification of products by ^{1}H and ^{31}P NMR spectroscopy.

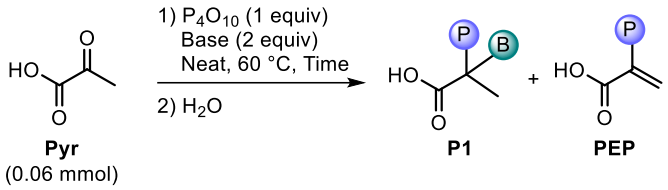

Entry	Base	Time (total)	Further addition of the base (2 equiv)	^{31}P Integration (P1-pyr-im, -5.3 ppm)	^{31}P Integration (P1-pyr-py, -5.3 ppm)	^{31}P Integration (PEP, -4.5 ppm)	Comment
1	**Im**	5 min	/	0.06	/	traces	**PEP** formation from **P1-pyr-im** (through the elimination of the base) is very low. Further addition of **Im** increased the relative concentration of **P1-pyr-im** and **PEP**. Further addition of a stronger base (e.i., **TEA**) to push the elimination of **Im** forming **PEP** from **P1-pyr-im** did not work. **Im = bad leaving group for the elimination step**
2	**Im**	10 min	/	0.21	/	0.02	
3	**Im**	20 min	/	0.31	/	0.08	
4	**Im**	20 min	**Im** (after 10 min of reaction)	1.59	/	0.16	
5	**Im**	20 min	**Im** (at the beginning of the reaction	1.8 qNMR: 13%	/	0.18 qNMR: 1.5%	
6	**Im**	60 min	/	0.4 qNMR: 4%	/	0.1 qNMR: 1%	
7	**Im**	2 h	/	0.31	/	0.11	
8	**Im**	2 h	**Im** (after 1 h of reaction)	1.1	/	0.21	
9	**Im**	16 h	/	0.20	/	0.09	
10	**Im**	20 min	**Py** (after 10 min of reaction)	0.42		0.03	
11	**Im**	20 min	**TEA** (after 10 min of reaction)	0.6	/	0.13	
12	**Py**	10 min	/	/	0.09	0.25	The further addition of **Py** is not improving the yield of **P1-pyr-py** neither of **PEP**. After 1-2h of reaction **P1-pyr-py** is completely converted to **PEP** (see Table S5). **Py = better leaving group for the elimination step**
13	**Py**	20 min	/	/	0.04	0.34	
14	**Py**	20 min	**Py** (after 10 min of reaction)	/	0.06	0.39	
15	**TEA**	3 min	/	No formation of **P1**-type adducts		0.03	No formation of **P1**-type adducts with **TEA.** **TEA = stronger base.** -> Different mechanism than **Py** and **Im**
16	**TEA**	5 min	/			0.06	
17	**TEA**	10 min	/			0.12	
18	**TEA**	60 min	/			0.6	

C. Investigating the reactivity, substrate scope

Reactions were set up as described in general procedure **GP-II**. The reaction was run for 5 min at 60 °C. Phosphorylated products were quantified by qNMR using ^{31}P NMR and confirmed by HRMS analyses.

Table S8. Scope table with product quantification by ^{31}P NMR.

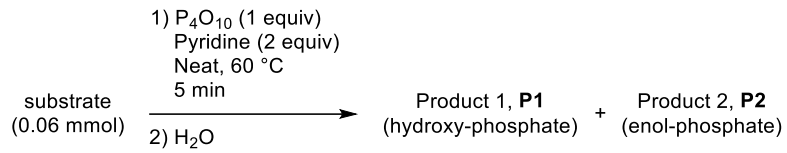

/	En-try	Substrate	P1 or expected P1 adducts	Int. ^{31}P / Yield P1 (%)	P2 or expected products	Int.^{31}P / Yield P2 (%)	Interest
Pyruvate derivatives	**1**	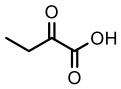	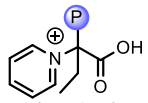 **P1-(pyr-1Me)-py** (presumed)	Int: 0.10 Yield: 1.0%	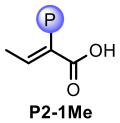 **P2-1Me**	Int.: 0.44 Yield: 4.6%	Influence of the R group of pyruvates (by adding some steric hindrance and by blocking the enol transfer). Influence of the stability of the enol tautomer substrate: Does the reaction work better when the keto-enol tautomer ratio is favored toward the enol tautomer?
	2	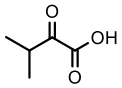	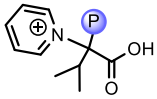 **P1-(pyr-2Me)-py** (expected)	✖	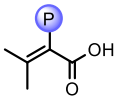 **P2-2Me**	Integration: 0.09 Yield: 0.9%	
	3[a]	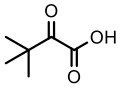	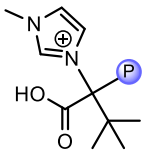 **P1-(pyr-3Me)-im**	Integration: 0.13 Yield: 1.3%	/	/	
	4	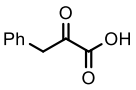	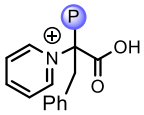 **P1-(pyr-Ph)-py** (presumed)	Traces	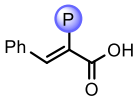 **P2-Ph**	Int.: 1.5 Yield: 14%	
Competitive experiment	**5**[b]	 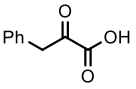	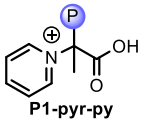 **P1-pyr-py** 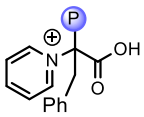 **P1-(pyr-Ph)-py** (presumed)	Int.: 0.05 Yield: 0.43% Int.: 0 Yield: 0%	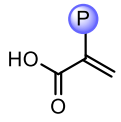 **P2-pyr (PEP)** 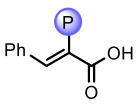 **P2-Ph**	Int.: 0.04 Yield:0.35 % Int.: 0.73 Yield: 7%	Which one is the more reactive? Ratio **P1-pyr-py**: **P2-Ph** 1: 16 Ratio **P2-pyr (PEP)**: **P2-Ph** 1: 20

Distance effect	**6**	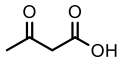	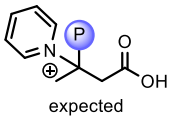 expected	✖	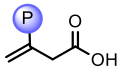	✖	Influence of the distance between the ketone and the carboxylate function. Can the phosphoryl group still be transferred (from the acyl-phosphate to the enol-phosphate) when we are increasing the distance?
	7[a, c]	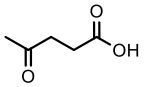	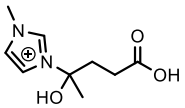	Observed (see VI.A8 for characterization)	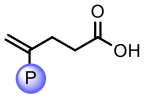	✖	
	8	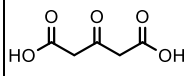	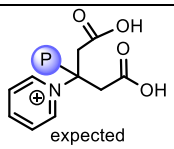 expected	✖	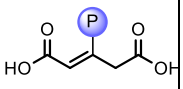	✖	
Alphaketoacids	**9[d]**	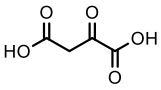	/	✖	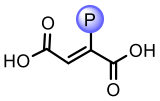 **P2-Ox**	Integration: 0.07 Yield: 0.7%	Is the phosphorylation reaction also working with other α-ketoacids leading to the formation of an enol-phosphate product?
	10	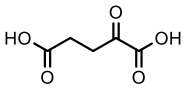	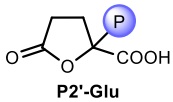 **P2'-Glu**	Integration: 0.32 Yield: 3.2%	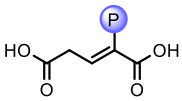 **P2-Glu**	Integration: 0.08 Yield: 0.8%	
Protected carboxylates	**11[e]**	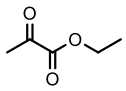	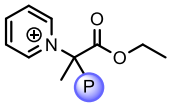	✖ **Traces of P1-pyr-py** (due to hydrolysis)	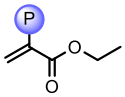	✖ **Traces of PEP** (due to hydrolysis)	Does the reaction go through carboxylate phosphorylation? The use of a protected carboxylate should prevent the formation of the acyl-phosphate intermediate without blocking a potential phosphorylation of the hydroxy group (generated in-situ by attack of the base on the ketone)
	12[e]	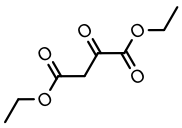	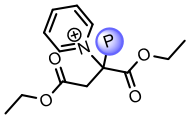	✖	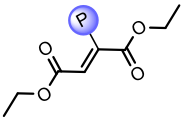	✖	
	13[e]	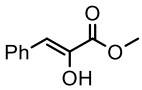	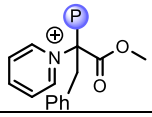	✖	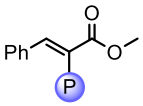	✖	
	14[e]	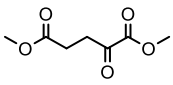	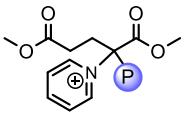	✖	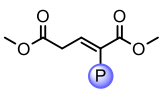	✖	

Separation of the two	15	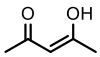	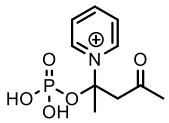	✖	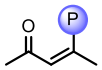	✖	Reactivity of the functions of the pyruvate toward phosphorylation: an enol function without an alpha carboxylate, a carboxylate function alone
	16[f]		 AcP	Integration: 0.03 Yield: 0.15%	Acetyl-polyphosphates (presumed)	Int.: 0.46 Yield: 2.3%	

[a] Both 1-methytlimidazole and pyridine were tried in this reaction. In the case of entry 3 and 7, the reported product was not detected using pyridine.
[b] Competitive experiment using 4 equiv of pyridine, otherwise the reaction is less efficient.
[c] The reaction was run for a longer reaction time (30 min) to detect the formation of the product.
[d] Without pyridine otherwise oxaloacetic acid is directly decarboxylated into pyruvate. Instead, 2 equiv of H_2O to make the paste.
[e] The reaction was also run for a longer reaction time (90 min), but the expected enol phosphate product was not observed.
[f] Substrate at 0.12 mmol scale.

Table S8 Entry 1

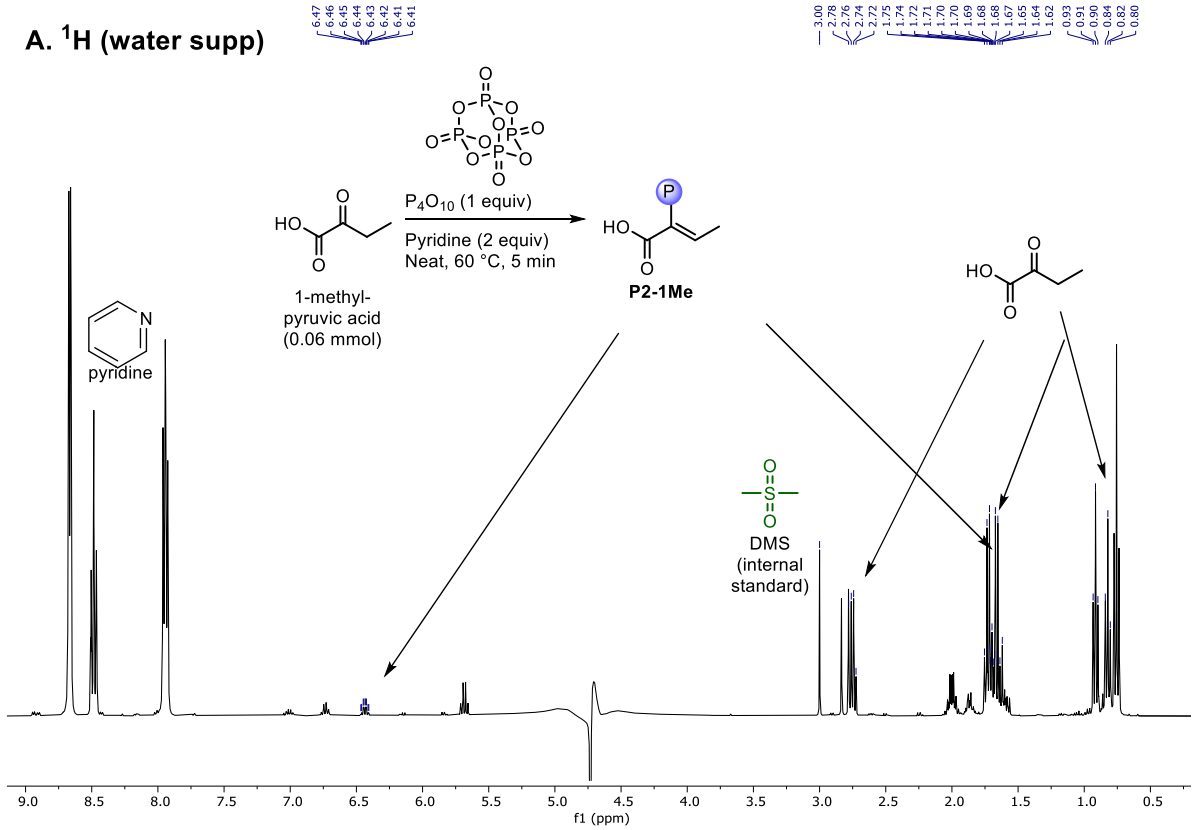

B. ^{31}P (^{1}H decoupled)

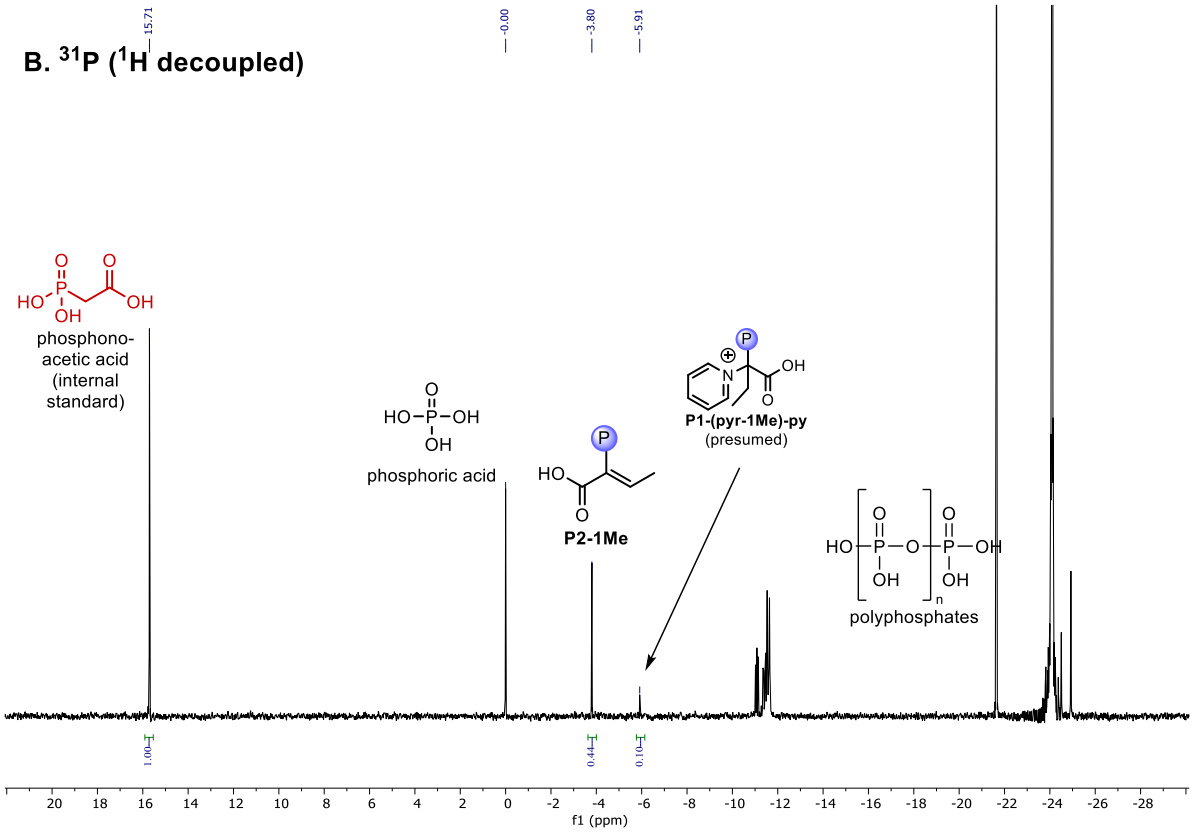

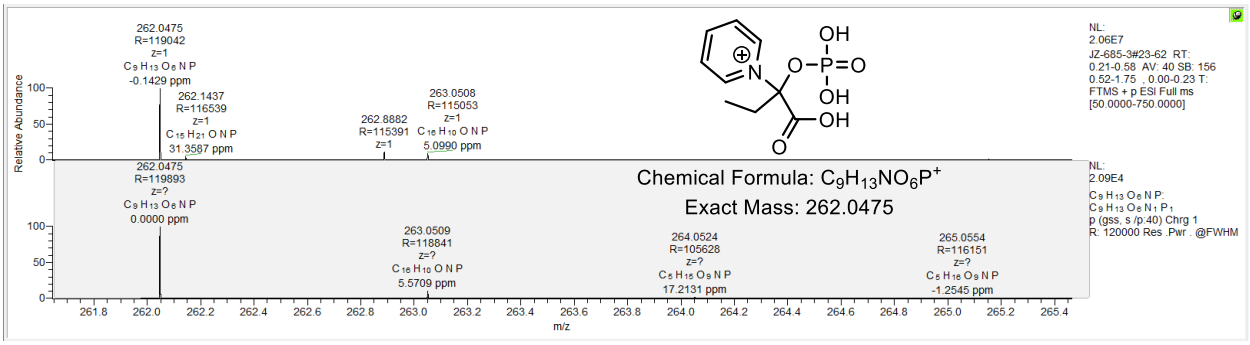

Table S8 Entry 2

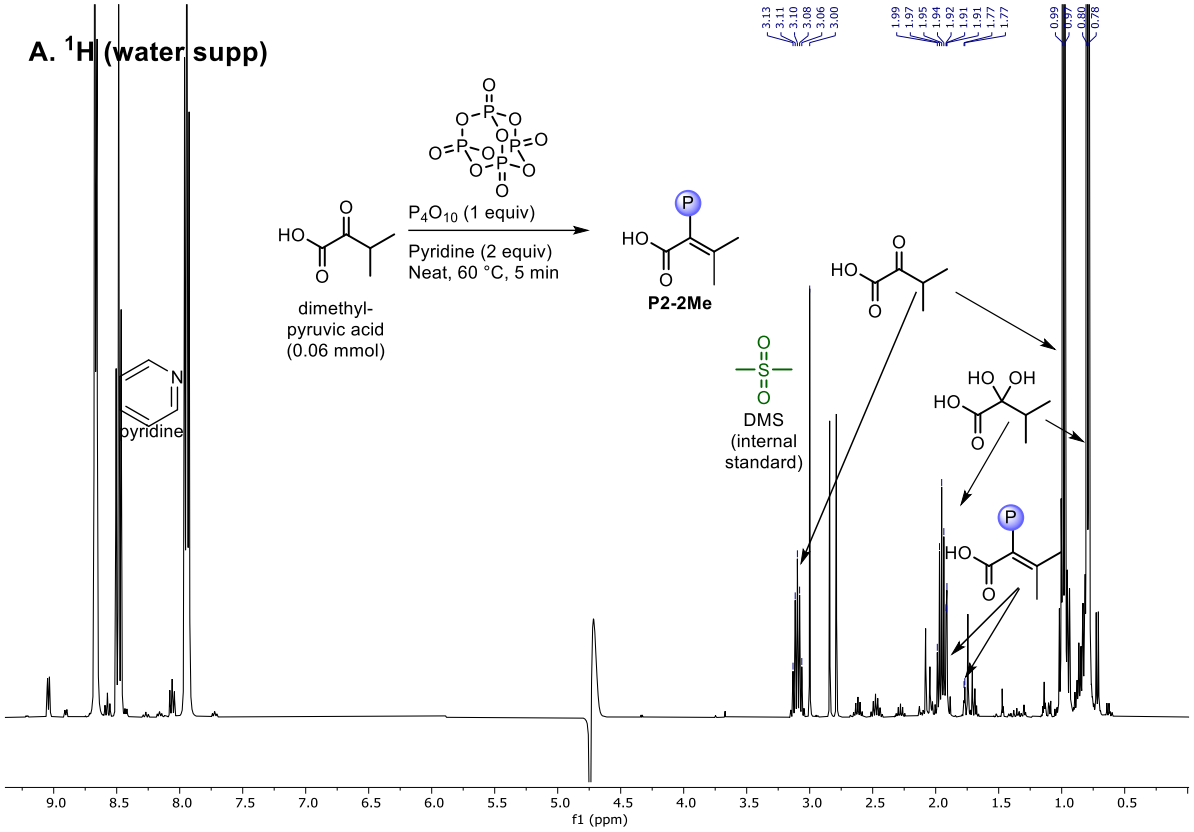

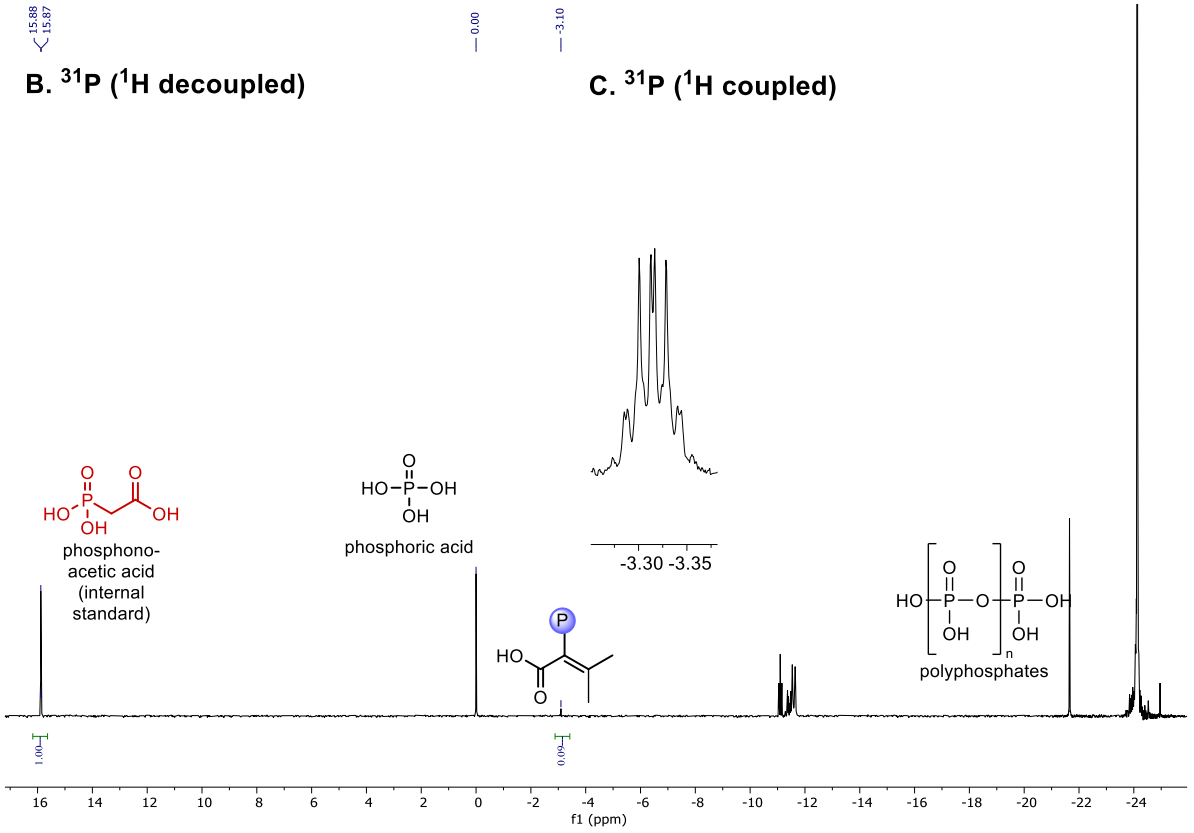

Table S8 Entry 3

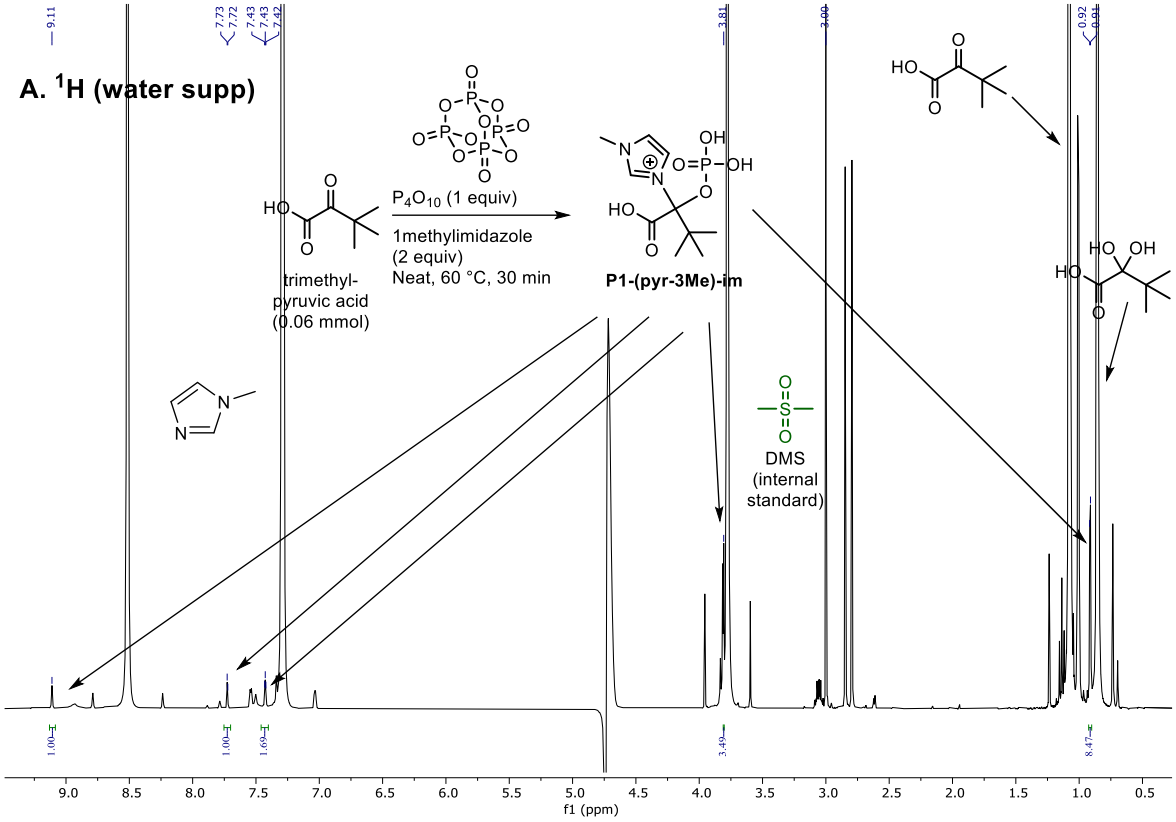

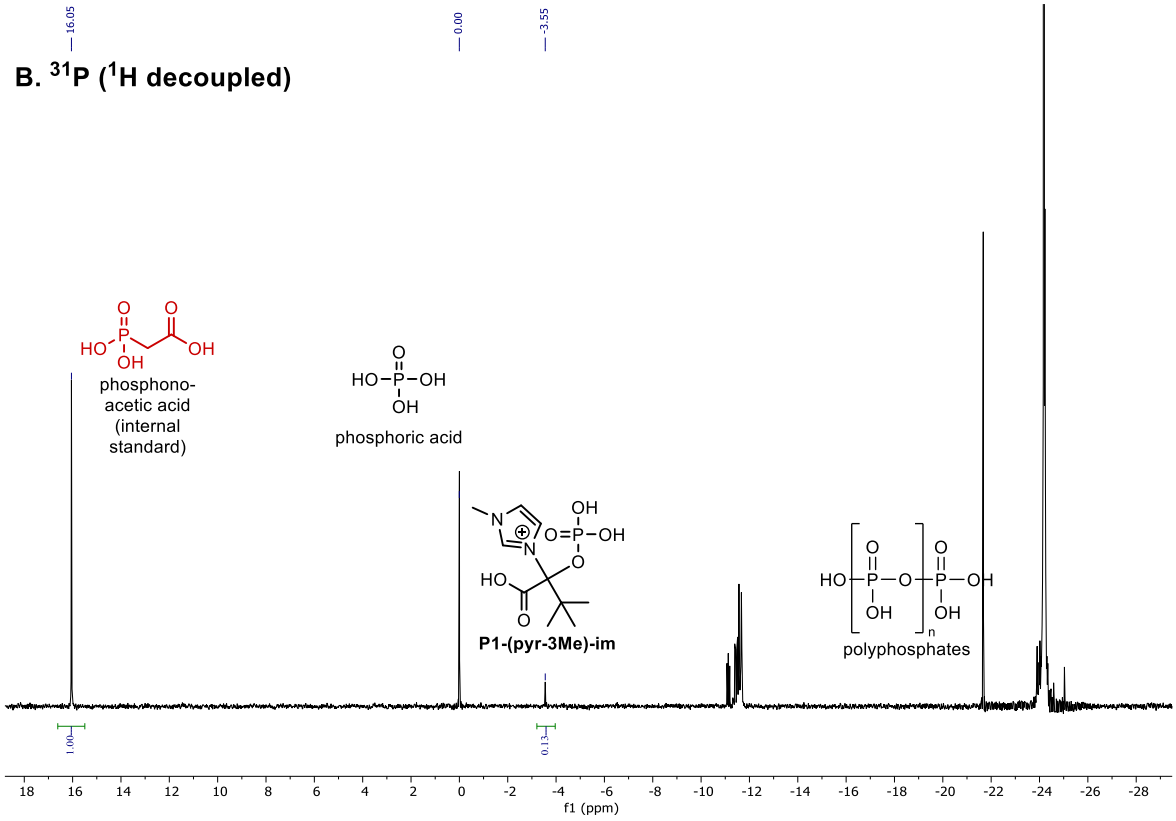

Table S8 Entry 4

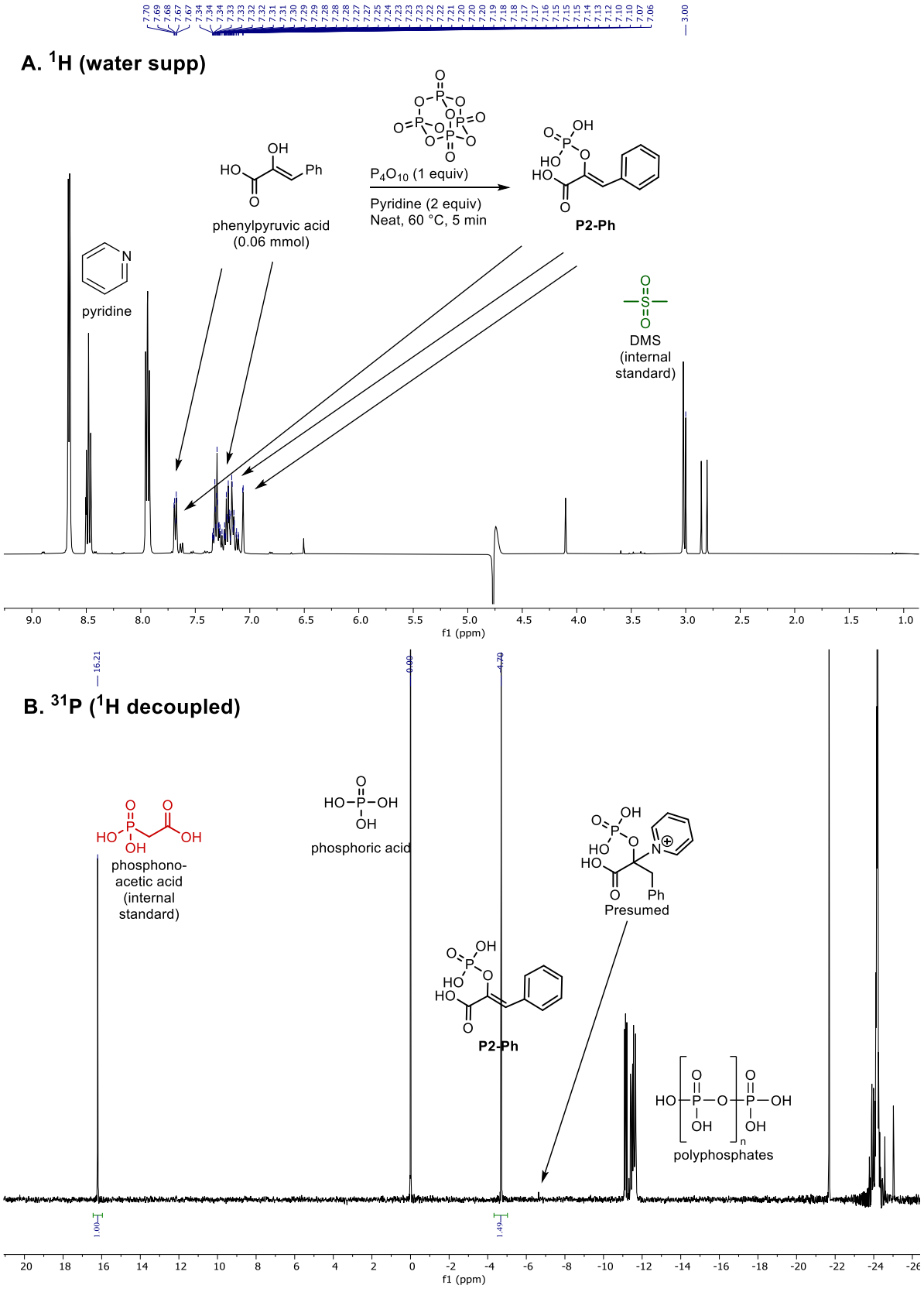

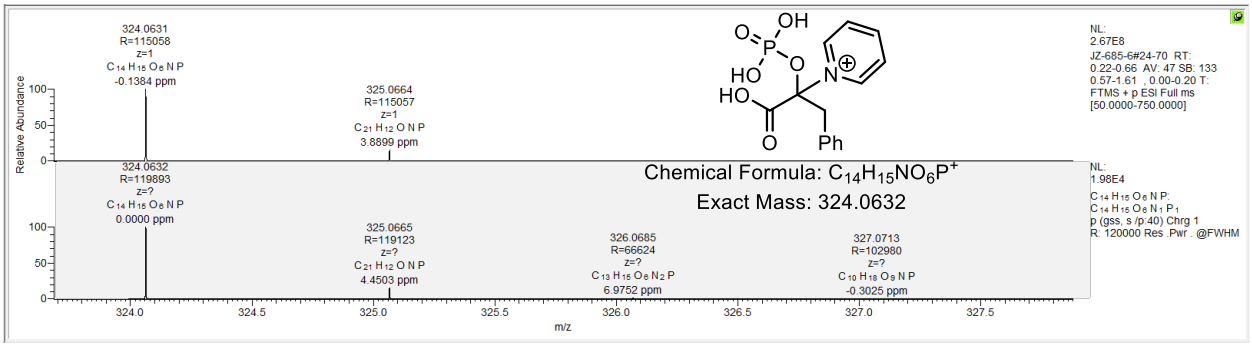

Table S8 Entry 5

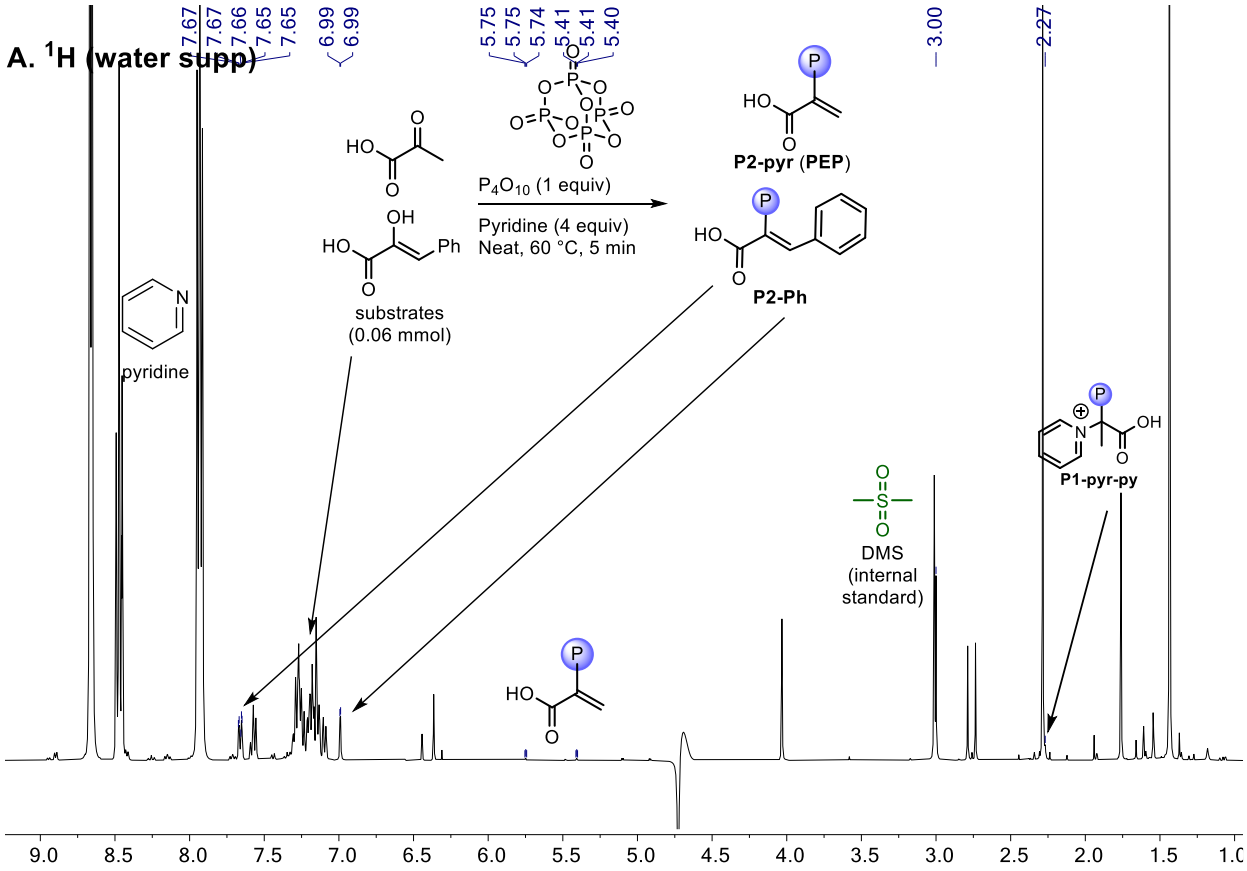

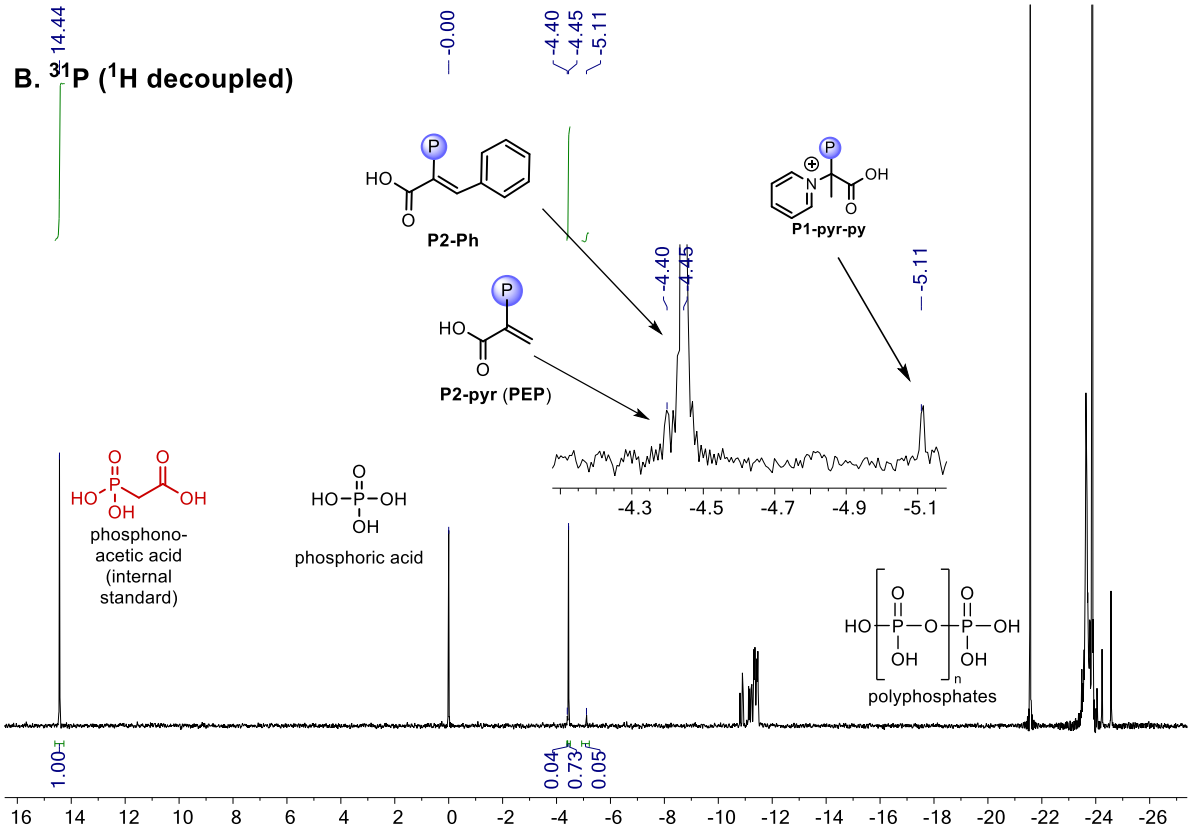
B. 31P (1H decoupled)
14.44
-0.00
-4.40
-4.45
-5.11
P2-Ph
P2-pyr (PEP)
P1-pyr-py
phosphono-
acetic acid
(internal
standard)
phosphoric acid
polyphosphates
1.00
0.04
0.73
0.05
16 14 12 10 8 6 4 2 0 -2 -4 -6 -8 -10 -12 -14 -16 -18 -20 -22 -24 -26

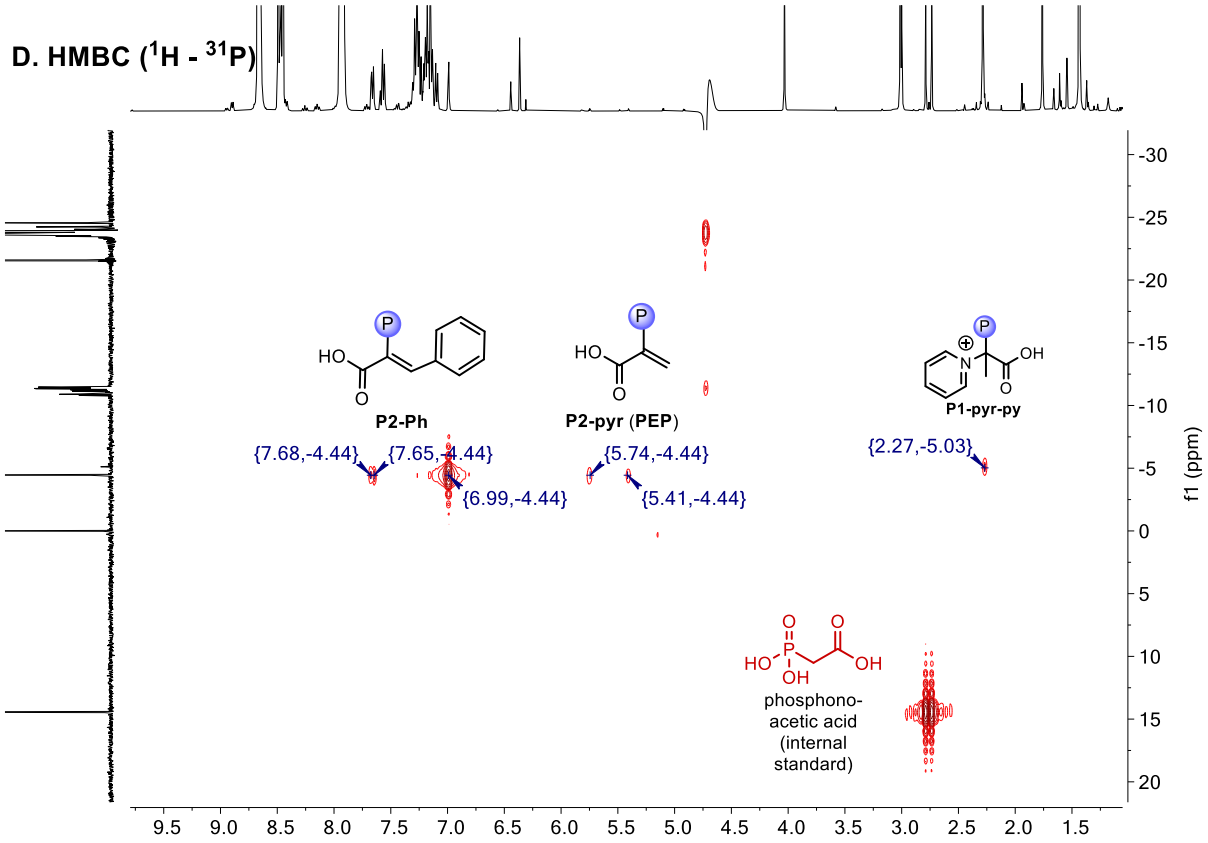
D. HMBC (1H - 31P)
P2-Ph
P2-pyr (PEP)
P1-pyr-py
{7.68,-4.44}
{7.65,-4.44}
{6.99,-4.44}
{5.74,-4.44}
{5.41,-4.44}
{2.27,-5.03}
phosphono-
acetic acid
(internal
standard)
f1 (ppm)
-30 -25 -20 -15 -10 -5 0 5 10 15 20
9.5 9.0 8.5 8.0 7.5 7.0 6.5 6.0 5.5 5.0 4.5 4.0 3.5 3.0 2.5 2.0 1.5

Table S8 Entry 9

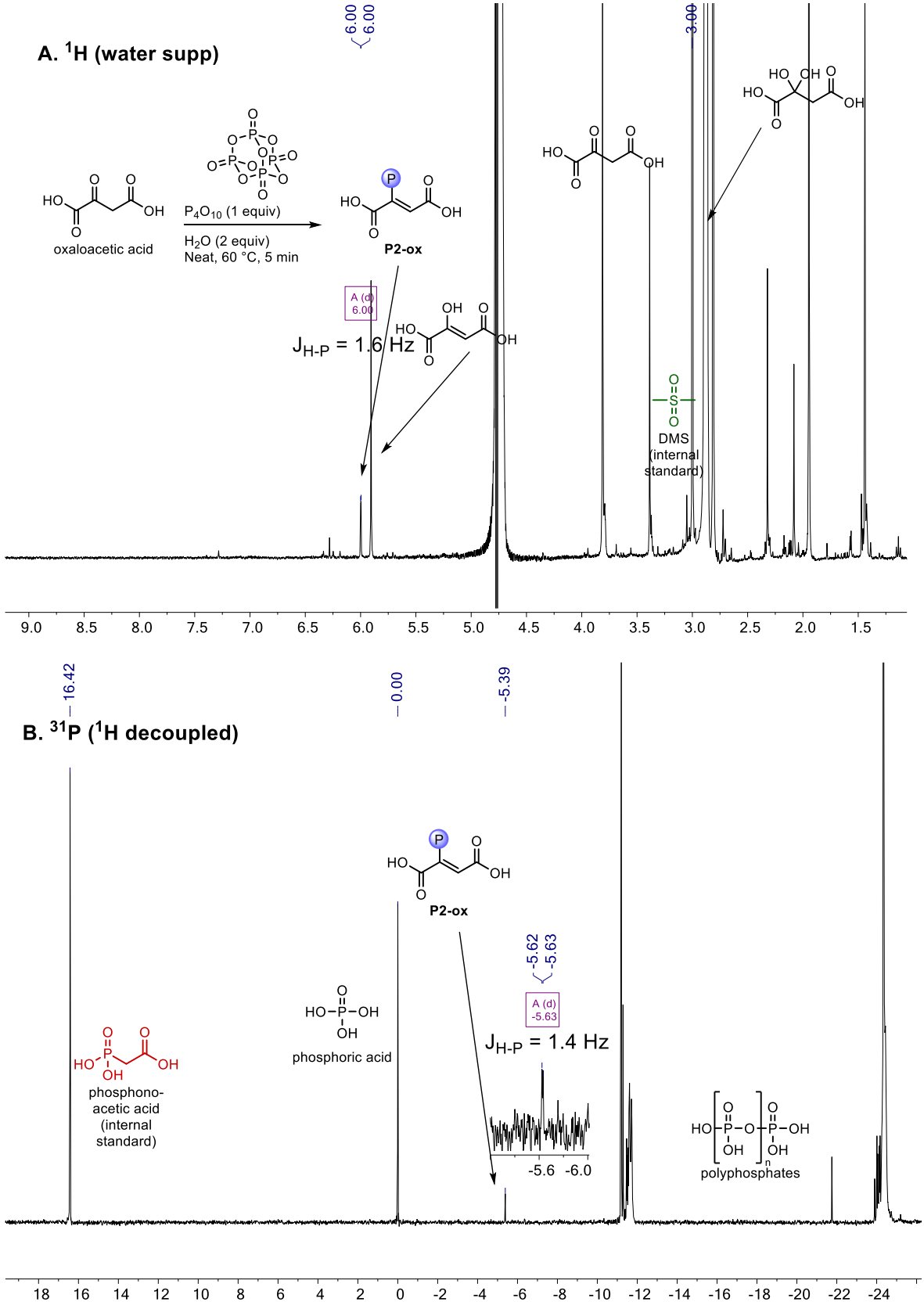

Table S8 Entry 10

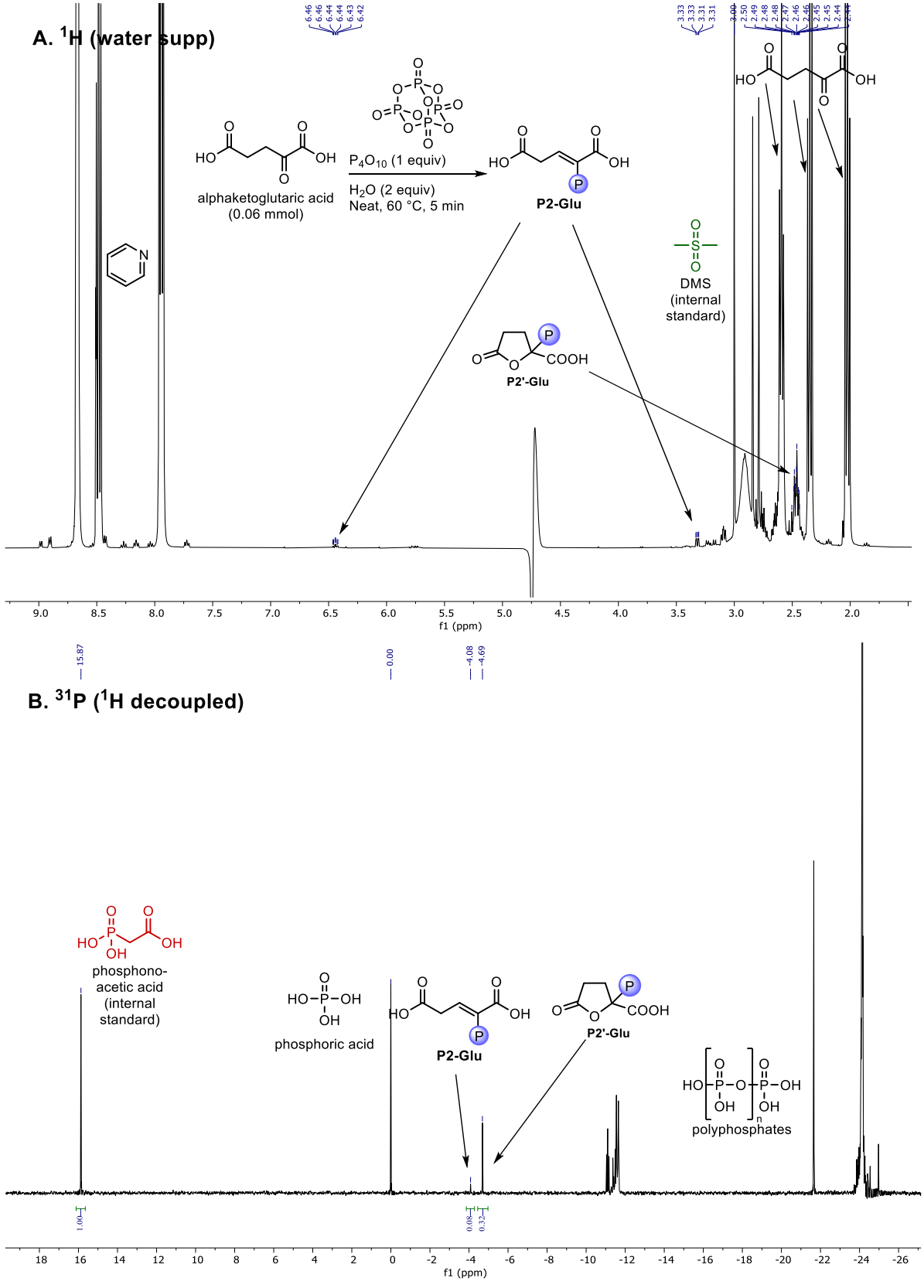

Table S8 Entry 11

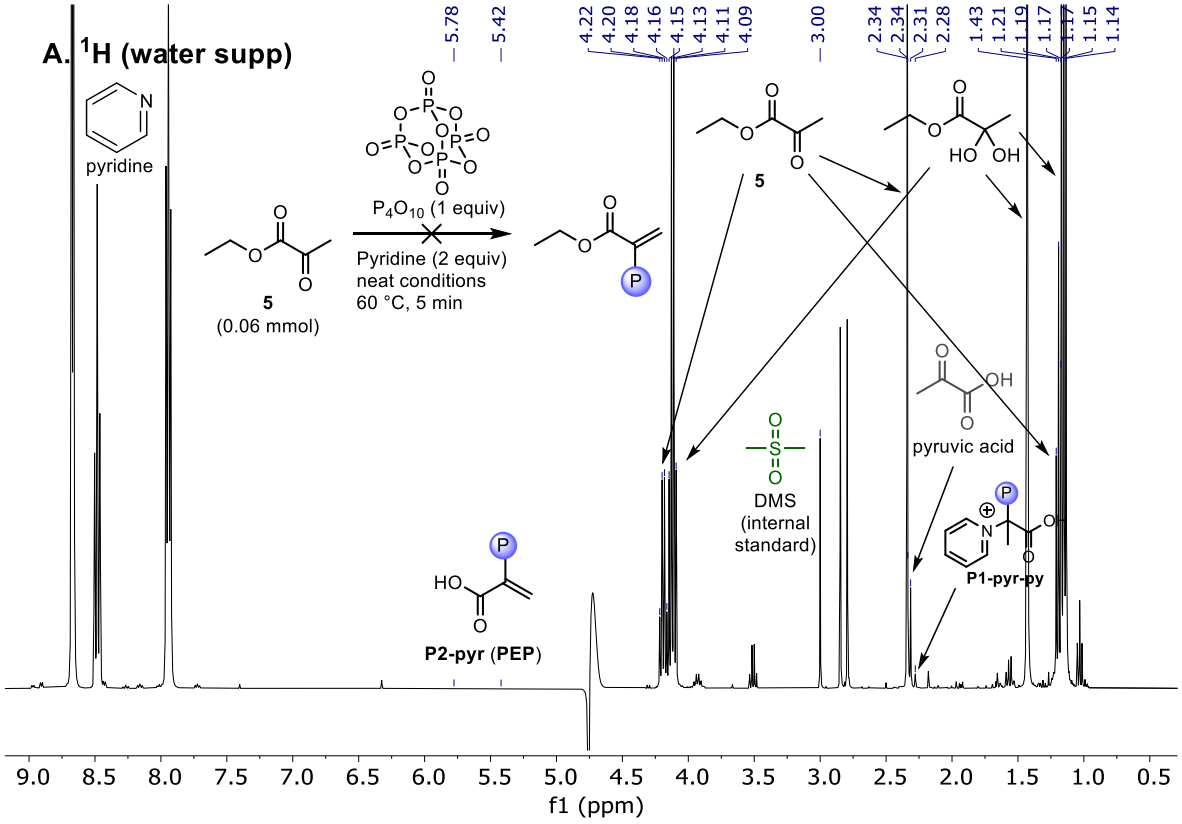

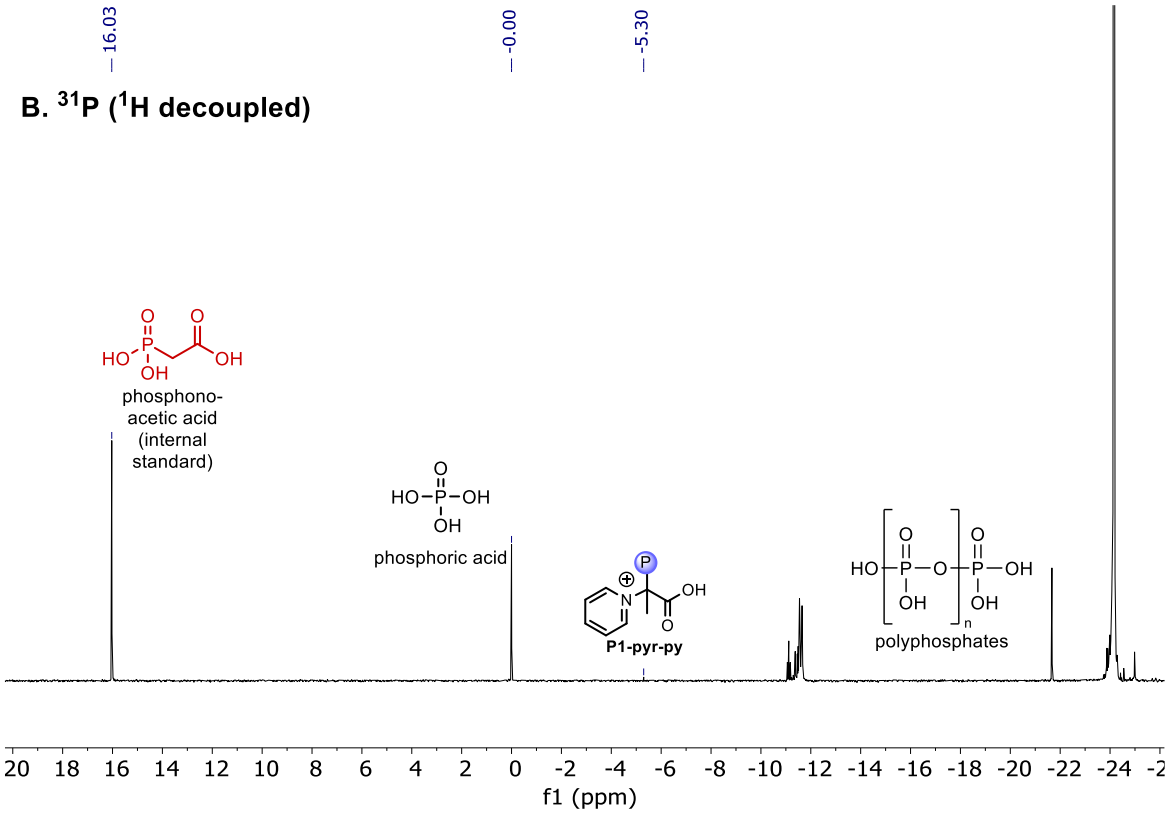

Table S8 Entry 16

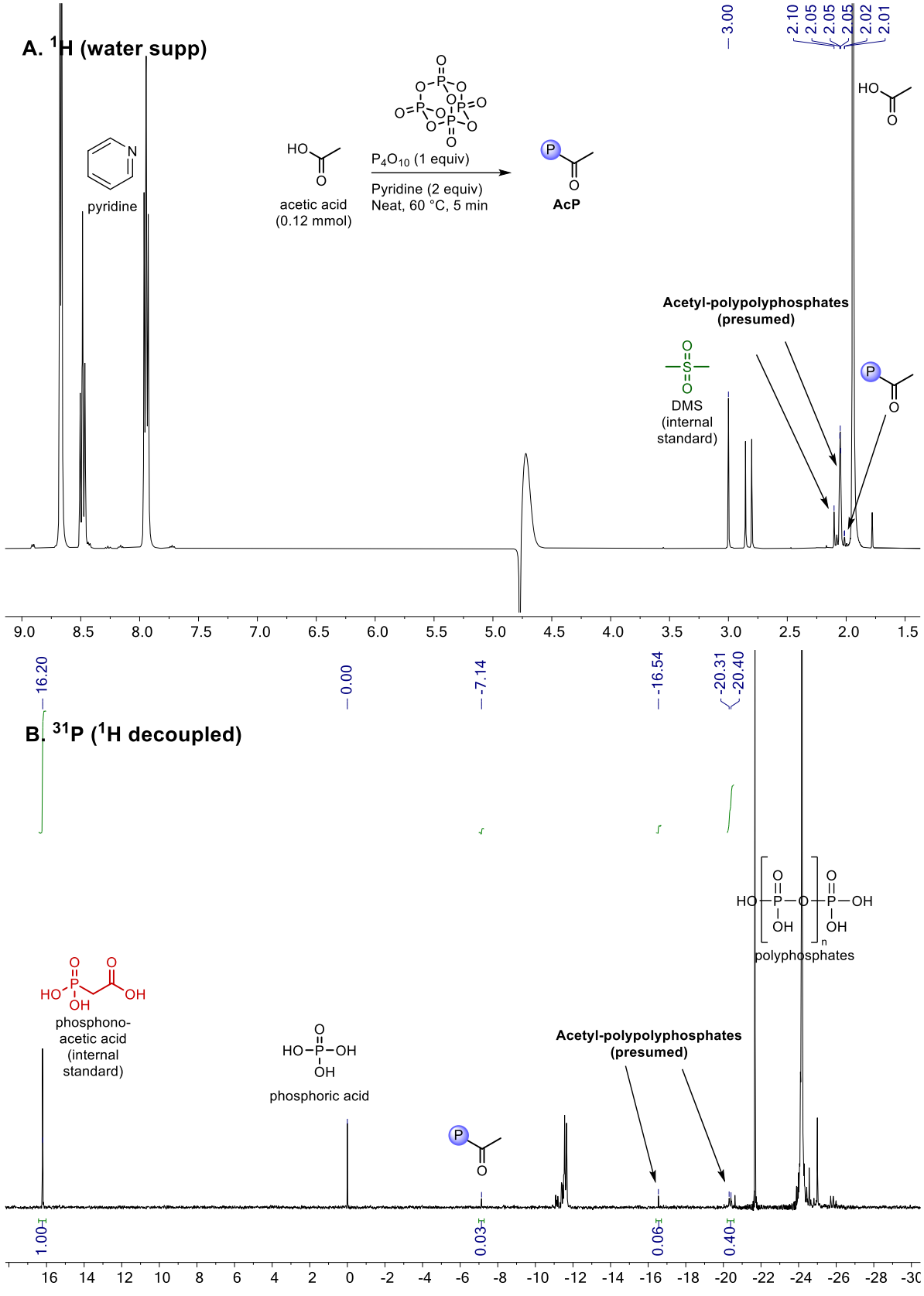

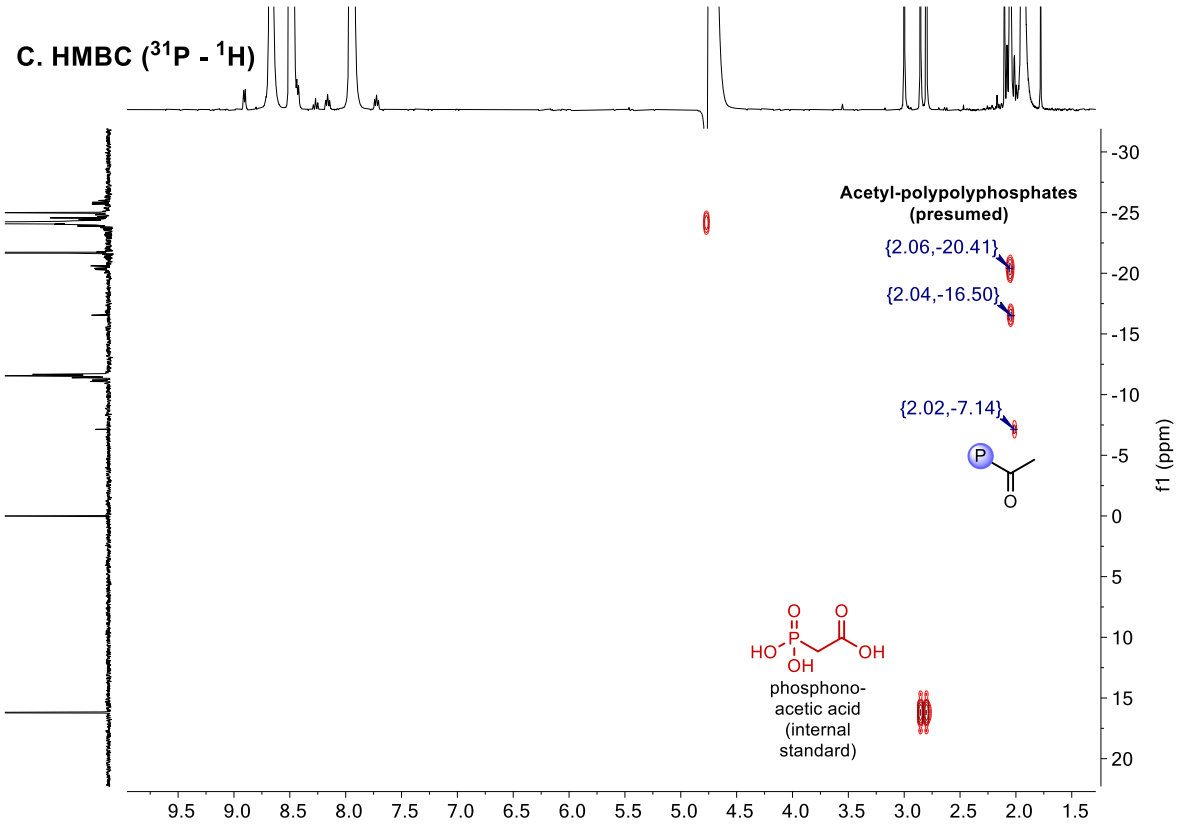
C. HMBC (^{31}P - ^{1}H)
Acetyl-polypolyphosphates
(presumed)
{2.06,-20.41}
{2.04,-16.50}
{2.02,-7.14}
P
O
HO
O
P
O
OH
OH
phosphono-
acetic acid
(internal
standard)
f1 (ppm)
-30
-25
-20
-15
-10
-5
0
5
10
15
20
9.5
9.0
8.5
8.0
7.5
7.0
6.5
6.0
5.5
5.0
4.5
4.0
3.5
3.0
2.5
2.0
1.5

D. Substrate scope in optimized conditions

Reactions were set up as described in general procedure **GP-II**. The reaction was run for 90 min at 60 °C (optimized conditions). Phosphorylated products were quantified by qNMR using ^{1}H NMR.

Table S9. Substrate scope table in optimized conditions with product quantification by ^{1}H NMR.

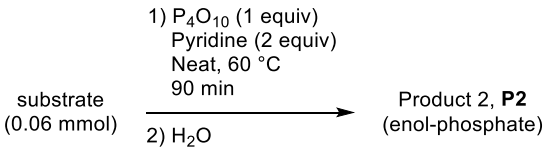

Entry	Mass substrate (mg)	Substrate	P2 product	Integration	Yield P2 (%)
1	6.0 mg	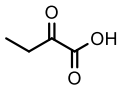	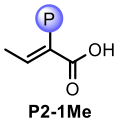 **P2-1Me**	2.9	9.4%
2	7.0 mg	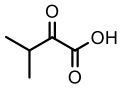	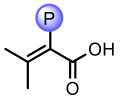 **P2-2Me**	Int.1: 1.0 Int. 2[a]: 6.8	Yield 1: 3.1% Yield 2[a]: 21.4%
3	9.4 mg	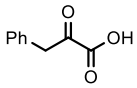	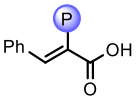 **P2-Ph**	4.8	14.5%
4[a,b]	7.6 mg 8.0 mg[c]	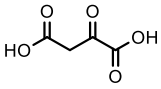	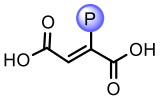 **P2-ox**	Int.1: 1.15 Int. 2[c]: 0.76	Yield 1: 2.7% Yield 2[c]: 1.7%
5[b]	8.7 mg	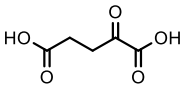	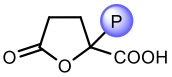 **P2'-Glu**	Int.[d]: 0.34	Yield[d]: 3.4%
	8.7 mg		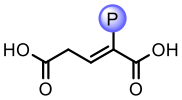 **P2-Glu**	0.22	0.6%
6	4 mg		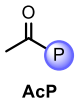 **AcP**	0.36	1.0%

[a] Without pyridine.
[b] The paste was dissolved in 1 M Acetate buffer pH 5 for better stability of the product.
[c] In the presence of pyridine, oxaloacetic acid decarboxylated to pyruvate and was phosphorylated to PEP. Quantification by ^{1}H NMR using the calibration curve of PEP.
[d] Quantification by qNMR using ^{31}P NMR because characteristic peaks of the product were overlapping with those of the substrate on ^{1}H NMR.

E. Study of the reaction progress with phenylpyruvic acid

To determine the influence of the stability of the enol-tautomer toward the transfer of the phosphate from the carboxylate moiety to the enol-phosphate product, the phosphorylation of phenylpyruvic acid was followed over time. As quantitative product analysis requires the quenching of whole reaction mixtures, several identical reactions were prepared and run in parallel. They were then quenched and analyzed at the times stated in Table S10 following the general procedure **GP-II.** The qualitative evolution of each species of the reaction was calculated according to their relative integration compared to the internal standards (phosphonoacetic acid for ^{31}P NMR) using ^{31}P NMR. The reaction was also followed by ^{1}H NMR.

Table S10. Time-dependent table with the two phosphorylated products, integration by ^{31}P NMR.

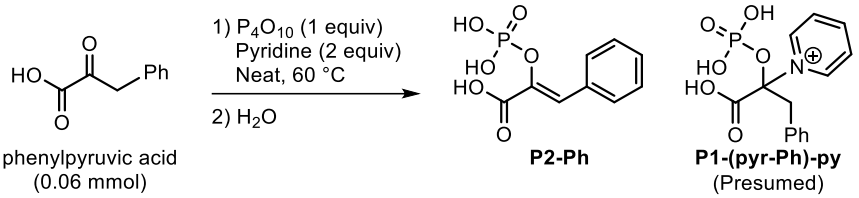

Entry	Time	^{31}P Integration (P2, -4.6 ppm)	^{31}P Integration (P1, -6.7 ppm)
1	1 min	0.02	0
2	2 min	0.08	0
3	5 min	0.94	0
4	10 min	0.95	0.02
5	15 min	1.17	0.02
6	24 h	1.44	0.04
7[a]	30 min	0.05	0

[a] Without the addition of a base.

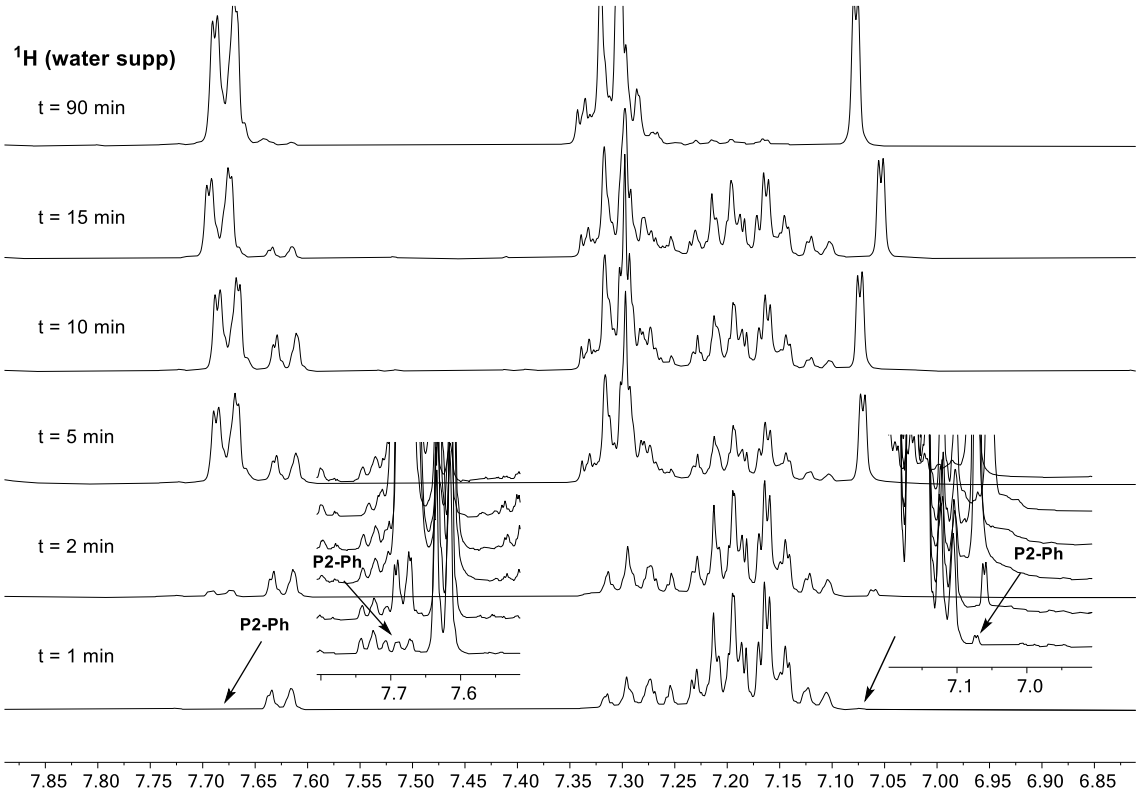

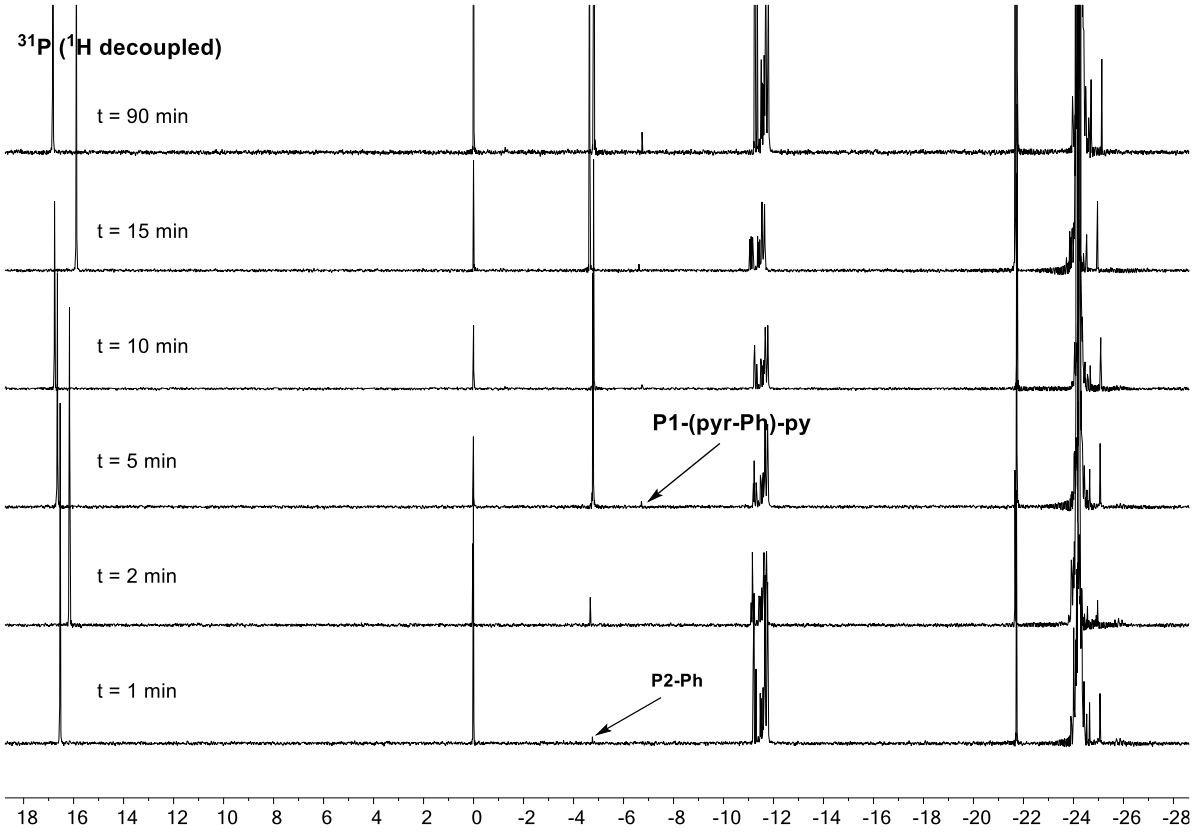

F. From pyruvoyl chloride Pyr-Cl to pyruvoyl phosphate AcP-pyr to enol phosphate of pyruvate PEP

1) Pyruvoyl chloride (Pyr-Cl) synthesis

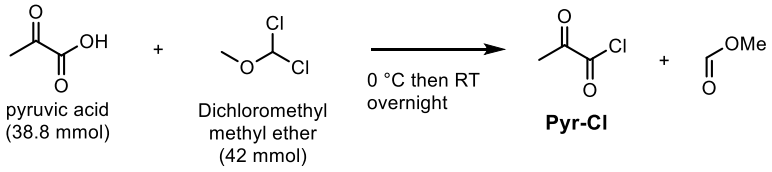

Prepared according to a literature procedure.[2] Dichloromethyl methyl ether (4.82 g, 42.0 mmol) was added dropwise to pyruvic acid (3.42 g, 38.8 mmol) at 0 °C. Evolution of HCl gas was observed immediately. The solution was stirred overnight under argon, at rt. The reaction mixture was directly distilled under vacuum by Kugelrohr distillation to give pyruvoyl chloride **Pyr-Cl** as a colorless oil.

^{1}H NMR (400 MHz, $CDCl_3$) δ 2.52 (s, 3H).

^{13}C NMR (101 MHz, $CDCl_3$) δ 186.0, 167.5, 25.1.

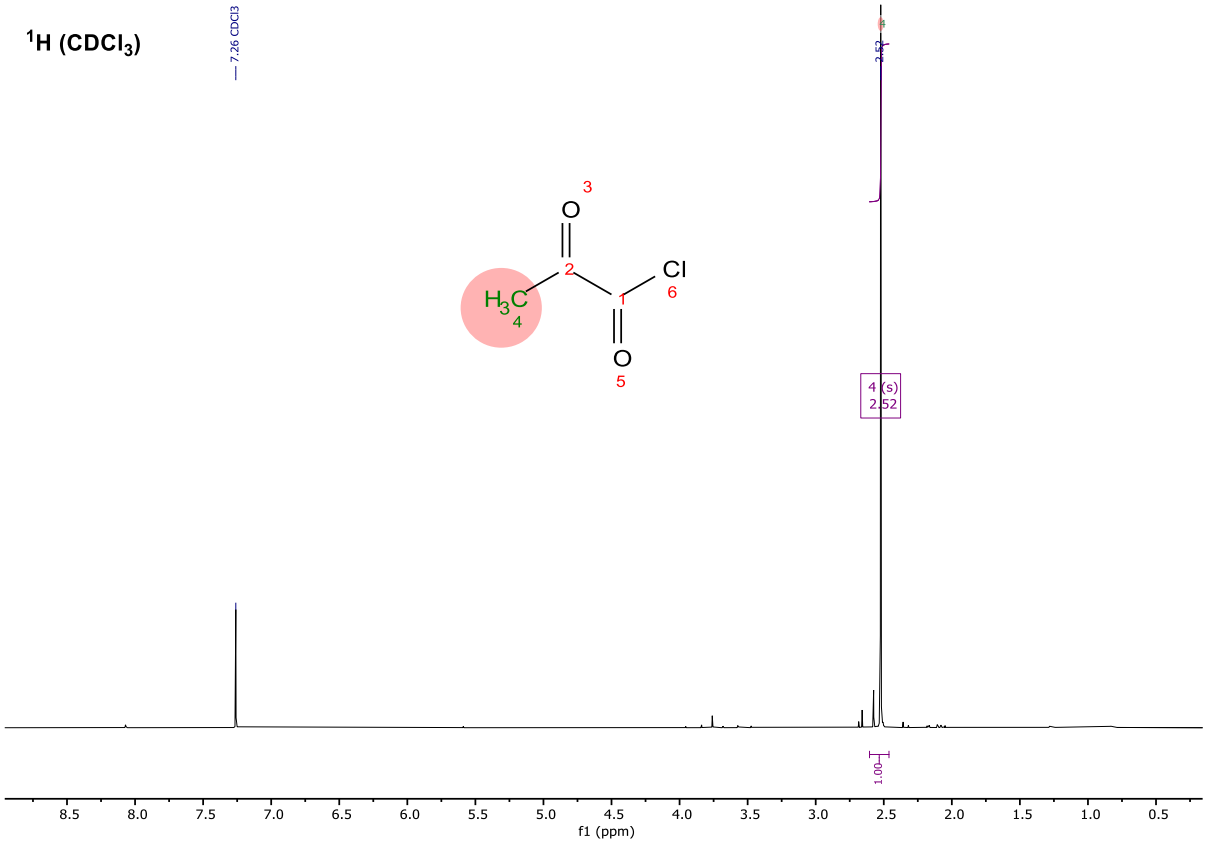
^{1}H (CDCl$_3$)
7.26 CDCl3
2.52
O
3
2
Cl
6
H$_3$C
4
1
O
5
4 (s)
2.52
1.00
8.5
8.0
7.5
7.0
6.5
6.0
5.5
5.0
4.5
4.0
3.5
3.0
2.5
2.0
1.5
1.0
0.5
f1 (ppm)

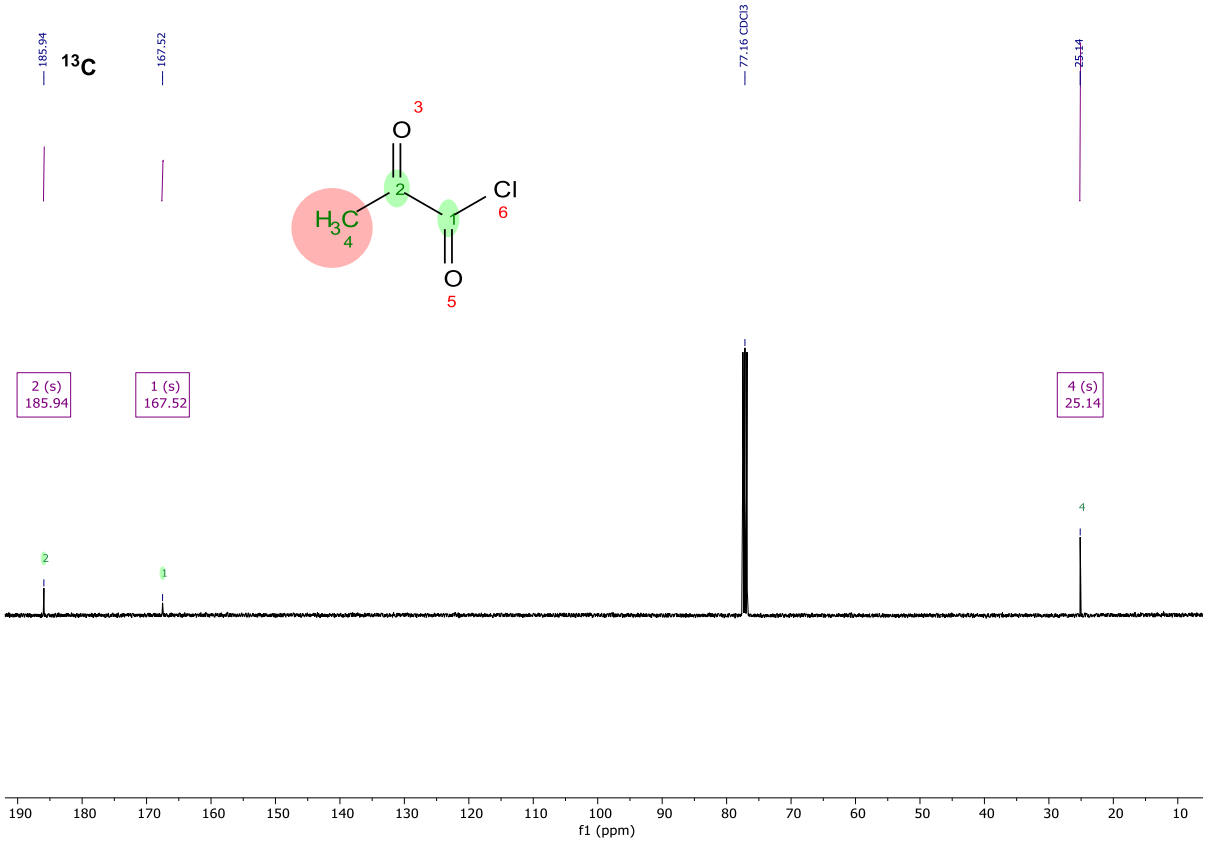
185.94
^{13}C
167.52
77.16 CDCl3
25.14
O
3
2
Cl
6
H$_3$C
4
1
O
5
2 (s)
185.94
1 (s)
167.52
4 (s)
25.14
2
1
4
190
180
170
160
150
140
130
120
110
100
90
80
70
60
50
40
30
20
10
f1 (ppm)

2) From pyruvoyl chloride (Pyr-Cl) to PEP in neat conditions

Pyruvoyl chloride **Pyr-Cl** (0.06 mmol) and the phosphate source (1 equiv) were weighted together in a 2 mL microcentrifuge tube with lid and mixed for 20 s using a vortex. Then, the base was added, and the mixture was centrifuged for 2 min. The retrieved paste was heated at 60 °C for 5 min in a thermoshaker. After the indicated time, 0.8 mL of H_2O was added to the mixture, then NMR tubes were prepared.

Table S11. Alternative synthesis of **PEP** from **Pyr-Cl** in neat conditions with product quantification by ^{1}H NMR.

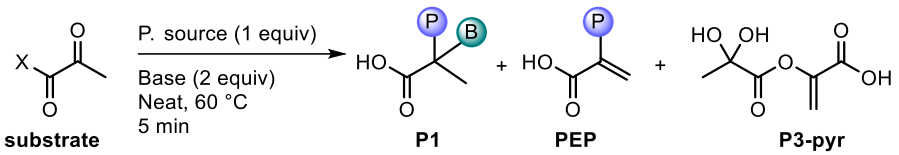

substrate (0.06 mmol) | **P1** | **PEP** | **P3-pyr**

Entry	Substrate	P. source	Base	Products	PEP (yield)
1 **(X = Cl)**		H_3PO_4	Pyridine	**P1-pyr-py** + **PEP** + **P3-pyr**	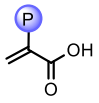 (1.0%)
2 **(X = Cl)**		H_3PO_4	Et_3N	**PEP** + **P3-pyr**	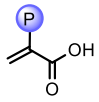 (0.4%)
3 **(X = OH)**		H_3PO_4	Pyridine or Et_3N	/	/
4 **(X = Cl)**		Polyphosphoric acid	Pyridine	**P1-pyr-py** + **PEP** + **P3-pyr**	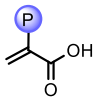 (1.4%)
5 **(X = Cl)**		H_3PO_4	/	Pyrophosphate	/

Table S11 Entry 1

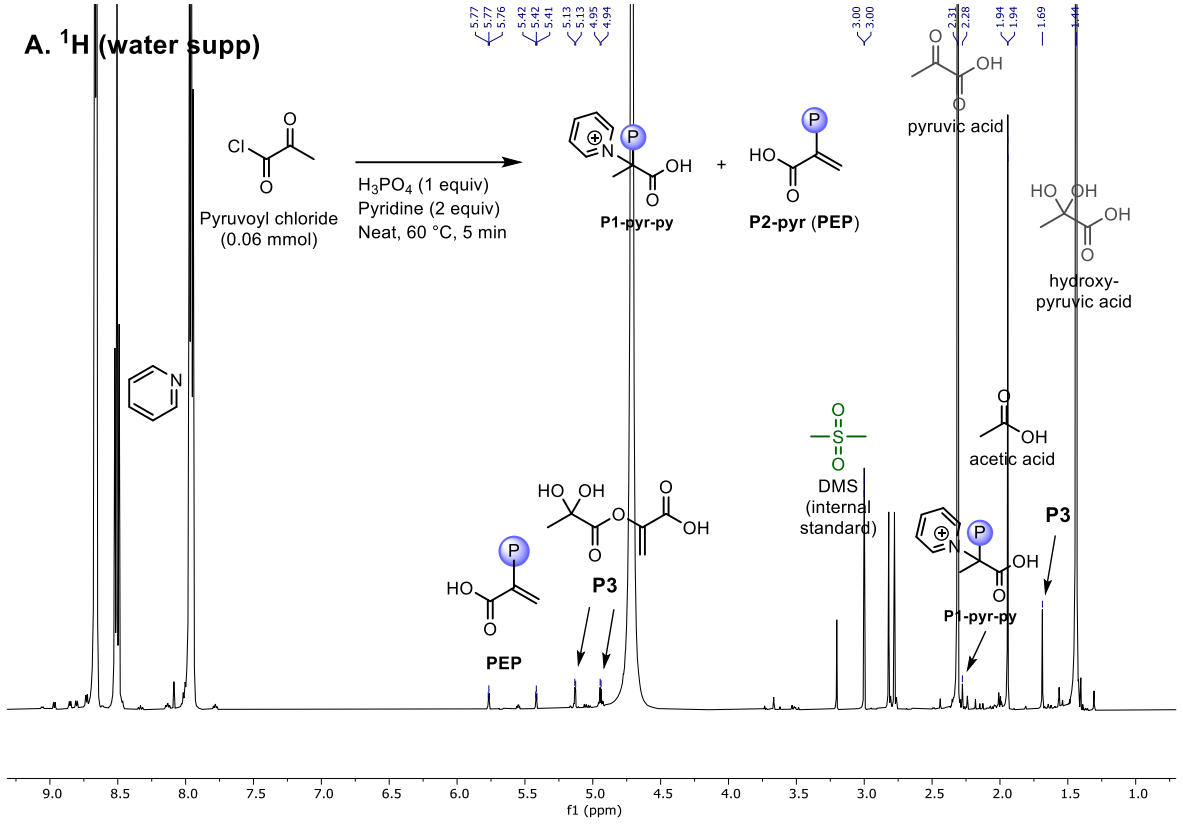

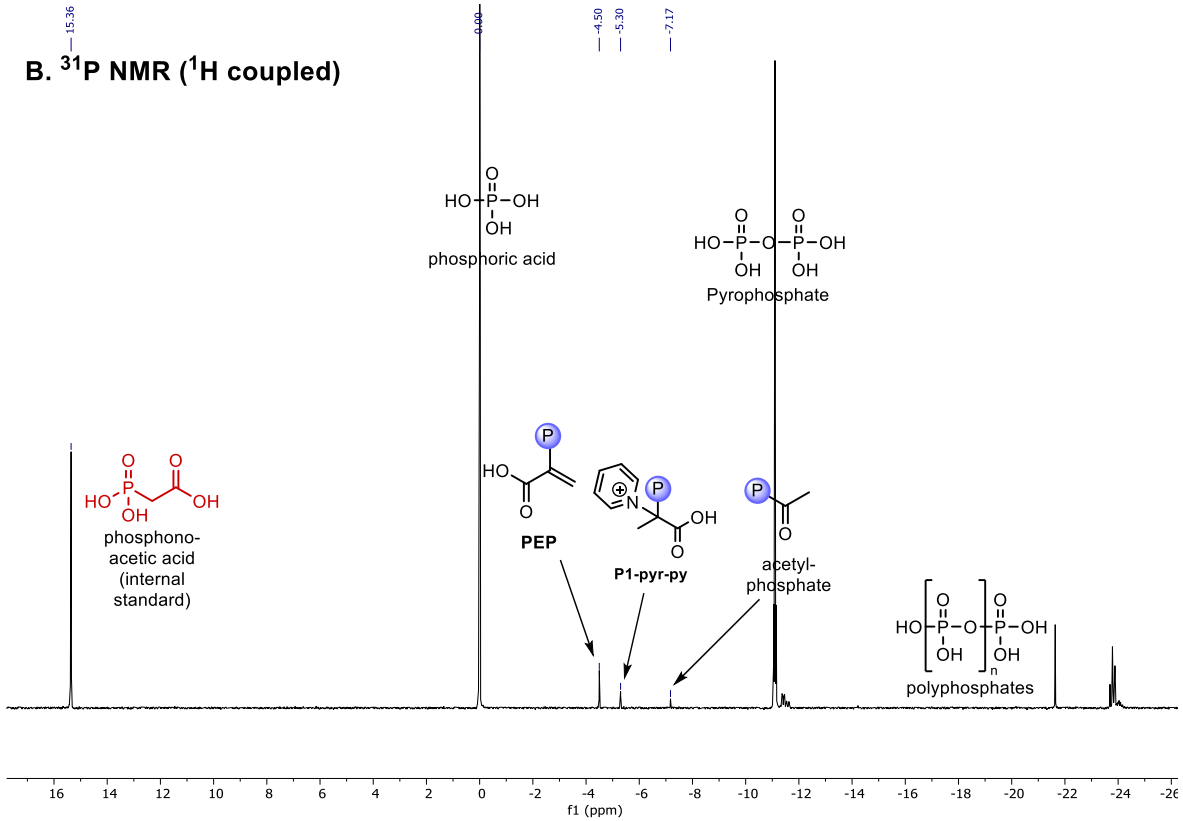

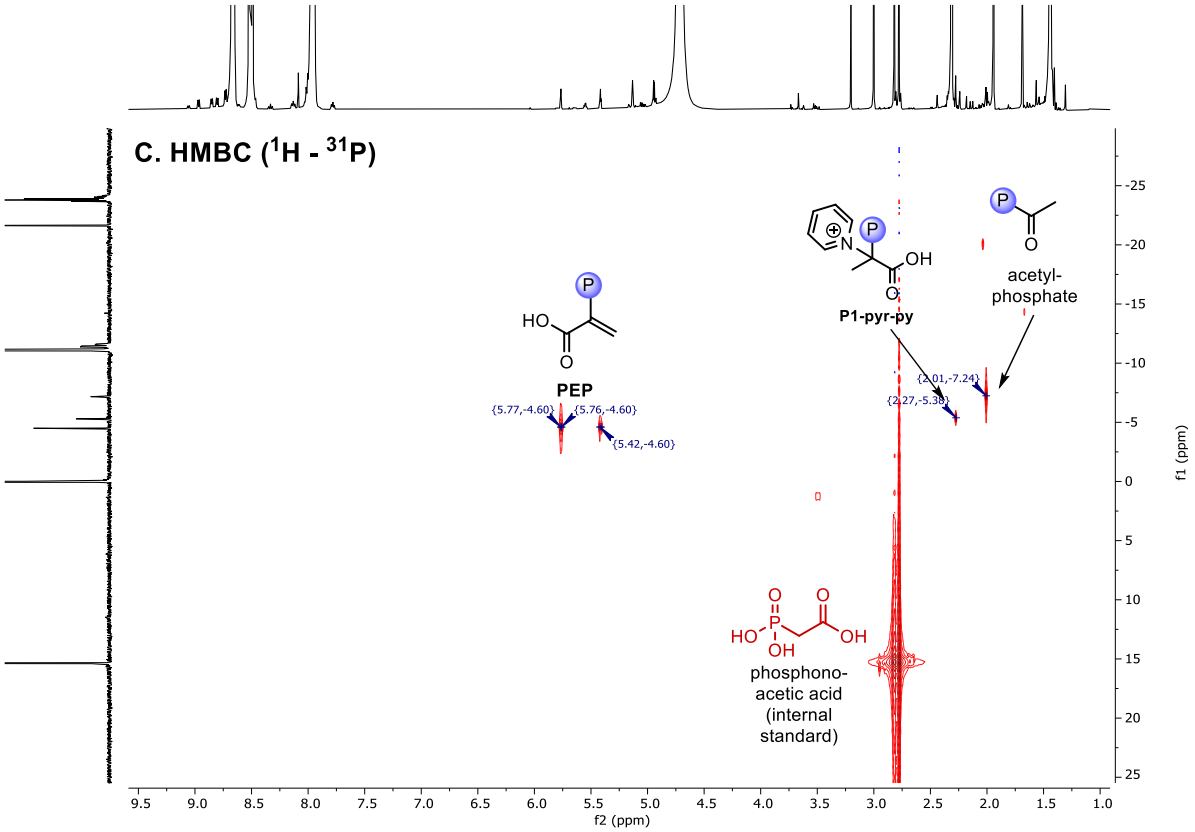

Table S11 Entry 2

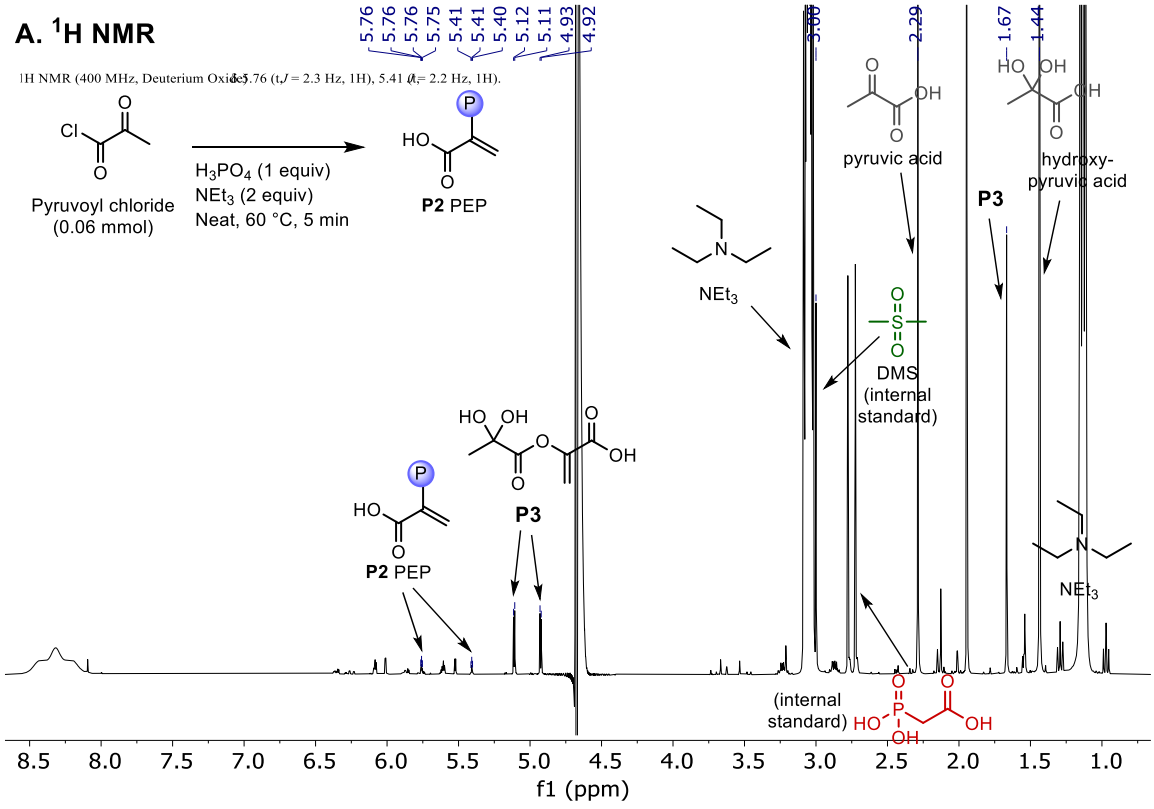

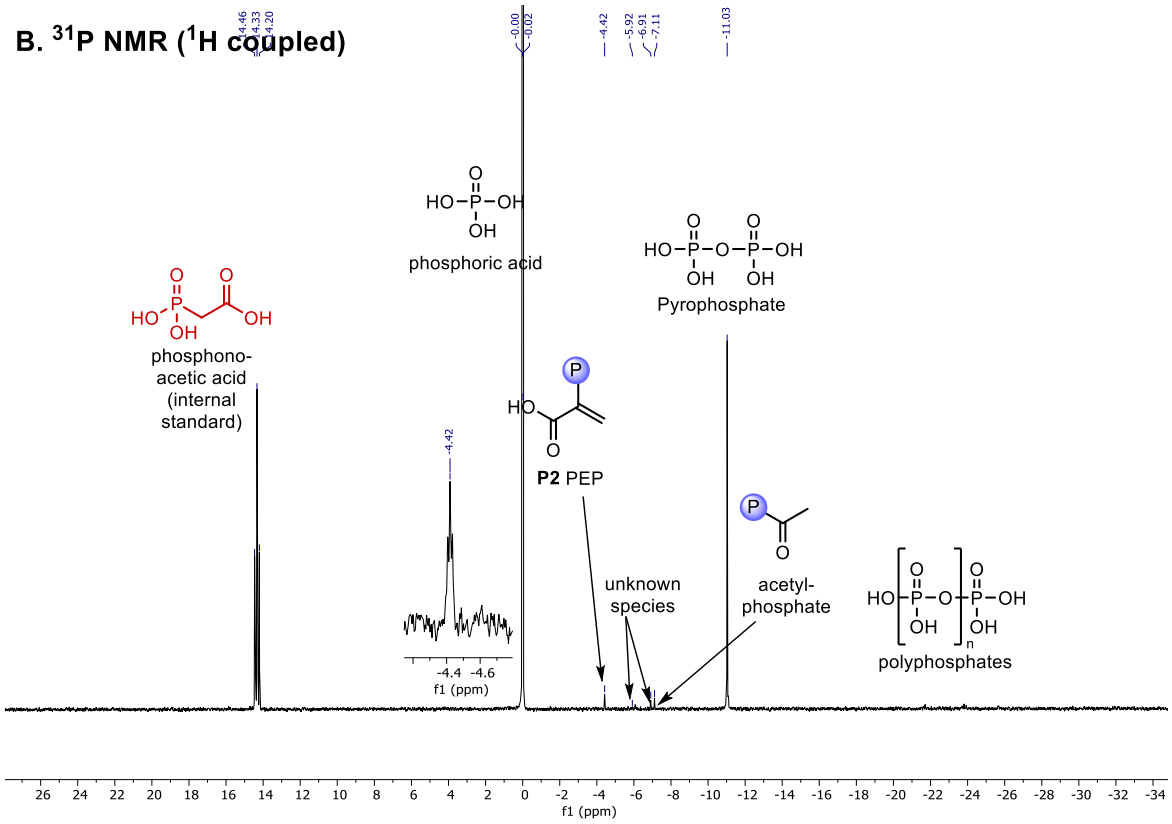

Table S11 Entry 3

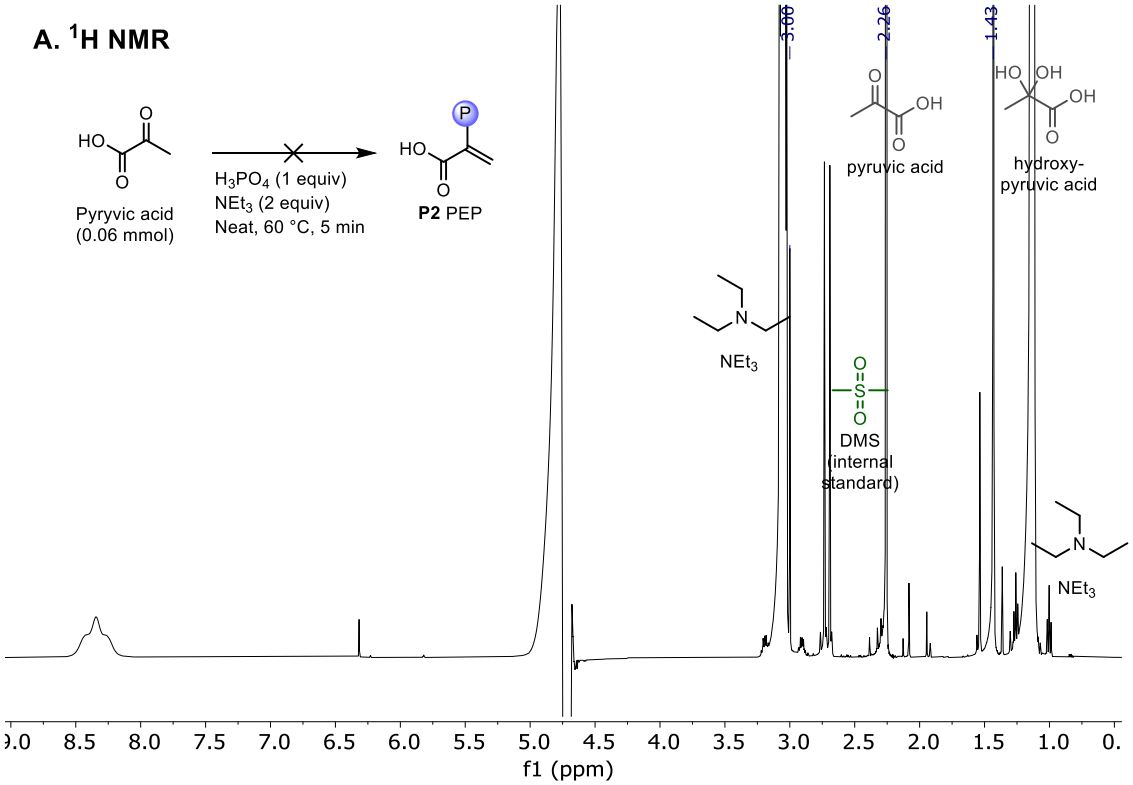

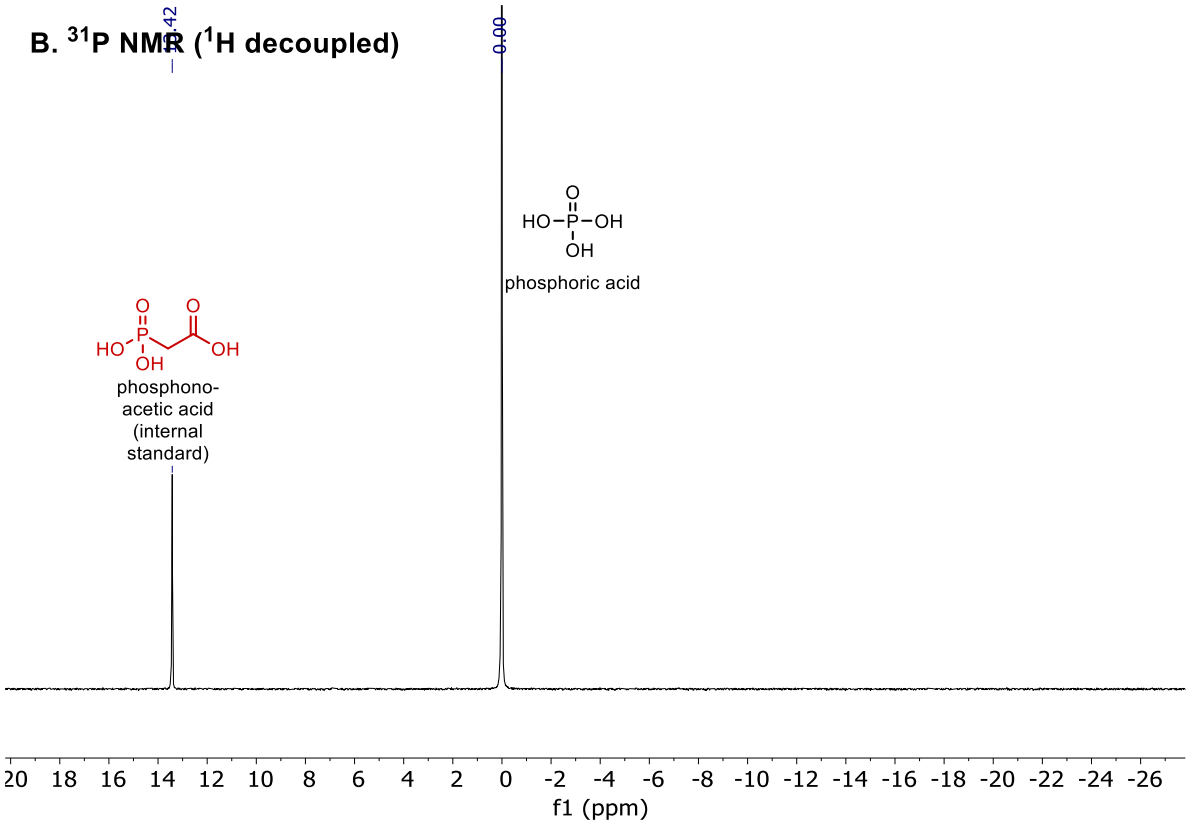

3) Base and phosphate source screening

Table S12. Alternative synthesis of **PEP** from **Pyr-Cl**.

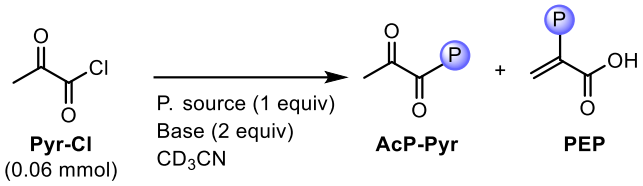

Entry	Phosphate source	Base	Solvent	Time	AcP-Pyr	PEP	Observation
1	H_3PO_4	Et_3N	CD_3CN	3-4 h	No	Yes	Side **P3** + Polyphosphates
2	H_3PO_4	Pyridine	CD_3CN	3-4 h	No	No	Precipitation, pyruvate + acetate
3	Phosphate buffer pH 2	/	/	/	No	No	Phosphate + Pyrophosphate
4	Phosphate buffer pH 6	/	/	/	No	No	Phosphate + pyrophosphate
5[a]	$NBu_4^+H_2PO_4^-$	/	CD_3CN	monitored	Yes	No	Converted to polyphosphates over 30 minutes
6[b]	$NBu_4^+H_2PO_4^-$	Et_3N (after 5 min)	CD_3CN	/	Yes	Yes	**PEP** is only observed after addition of the base

[a] Because of precipitation using the different phosphate source + base, $NBu_4^+H_2PO_4^-$ was used to characterize the acyl-phosphate of pyruvate.

[b] For **PEP** formation, see section V.F.5, p. S59-S60.

Table S12 Entry 1

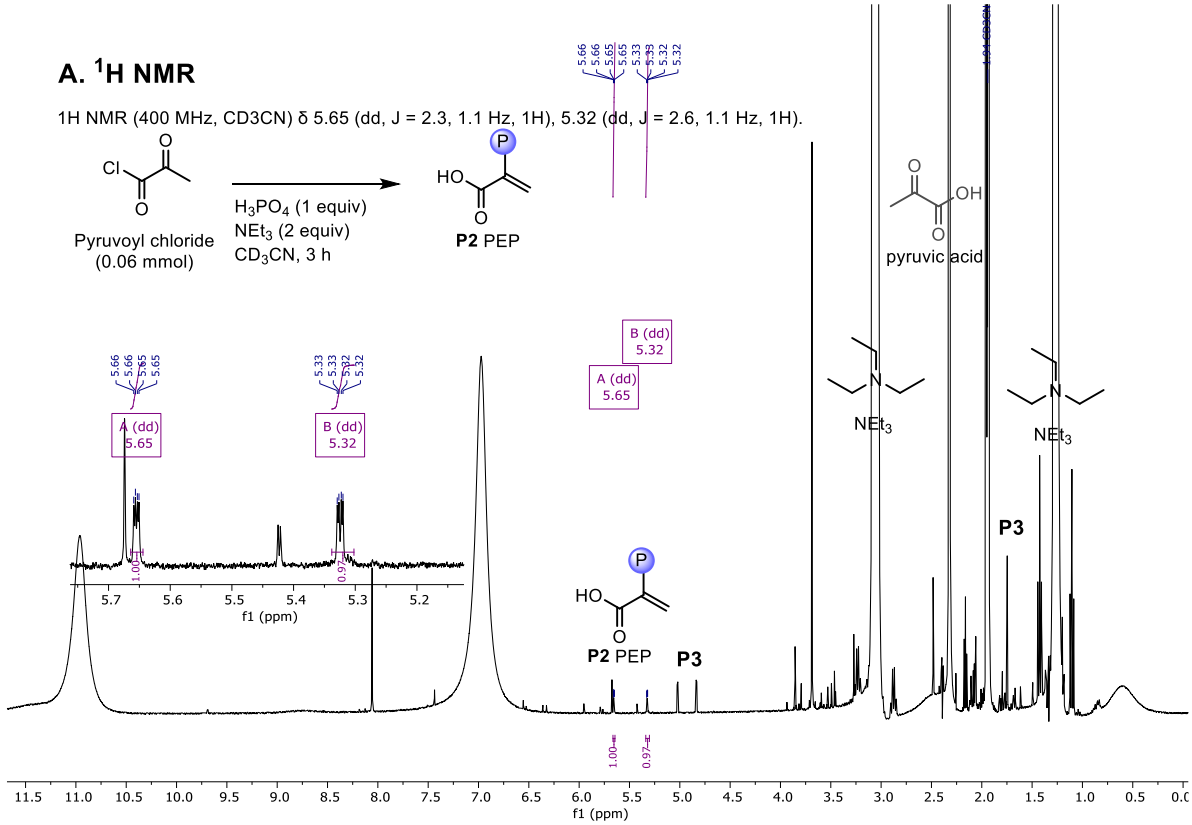

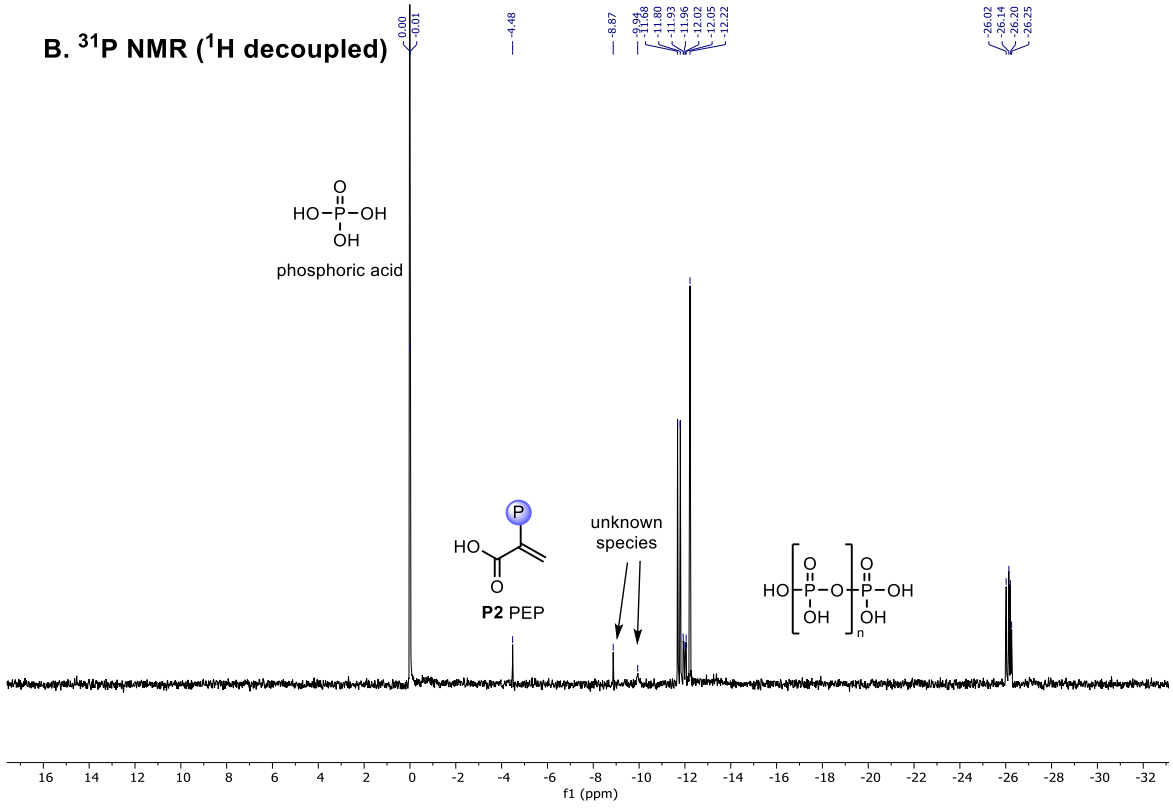

Table S12 Entry 5

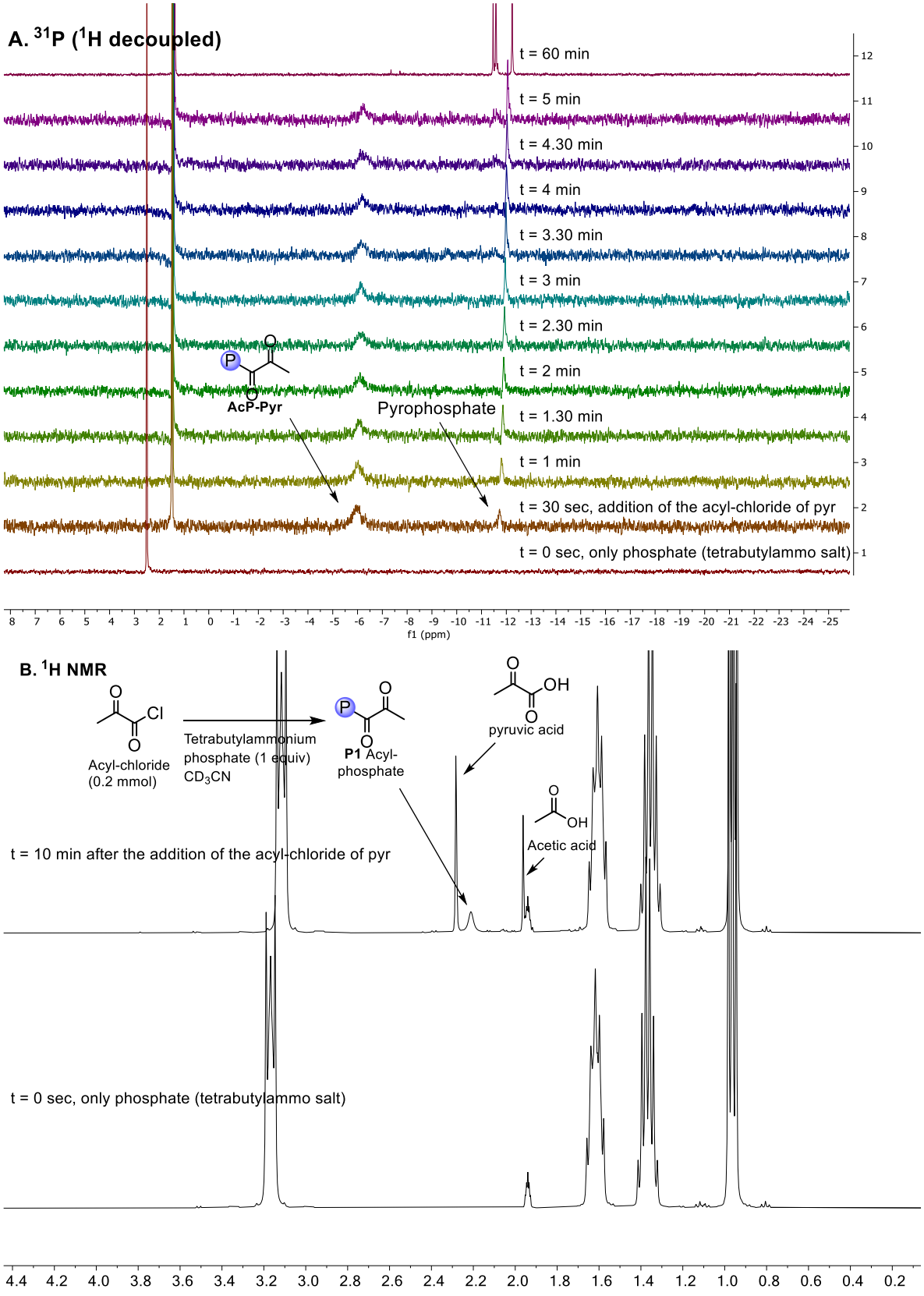

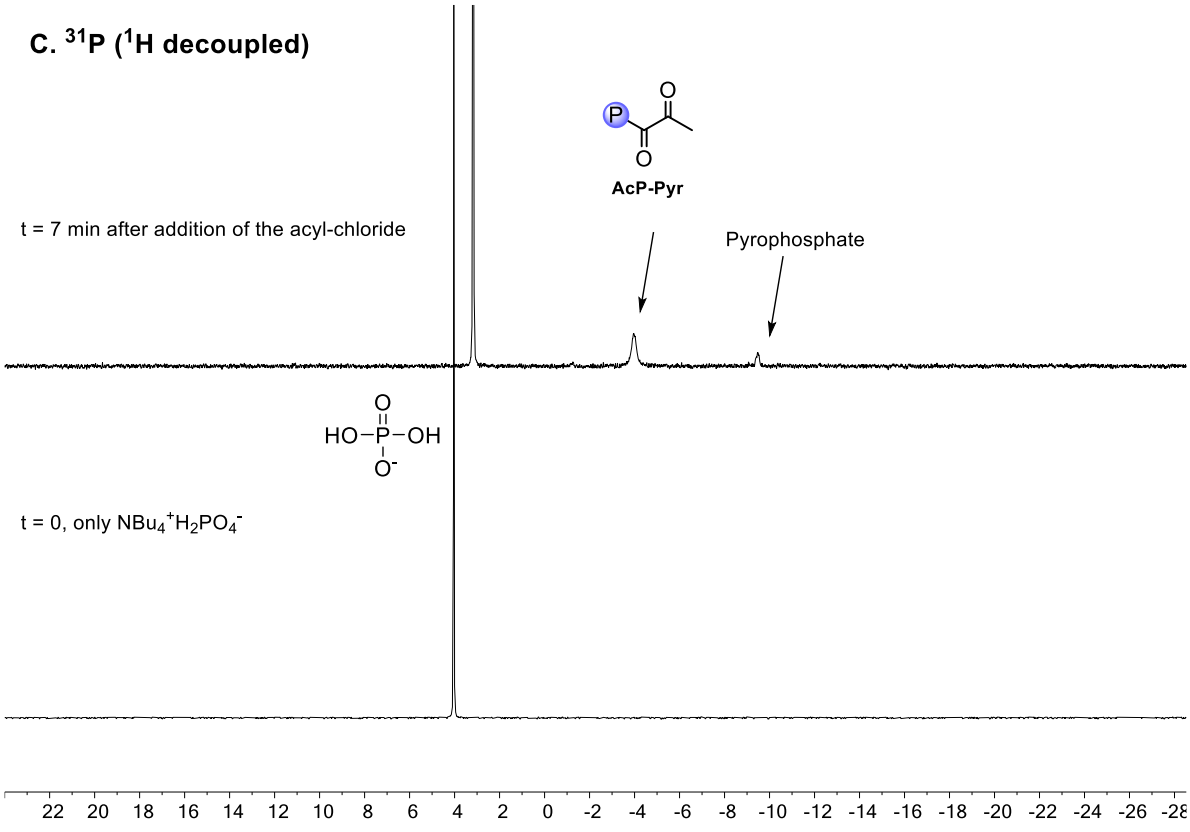
C. 31P (1H decoupled)
AcP-Pyr
t = 7 min after addition of the acyl-chloride
Pyrophosphate
t = 0, only NBu4+H2PO4-
22 20 18 16 14 12 10 8 6 4 2 0 -2 -4 -6 -8 -10 -12 -14 -16 -18 -20 -22 -24 -26 -28

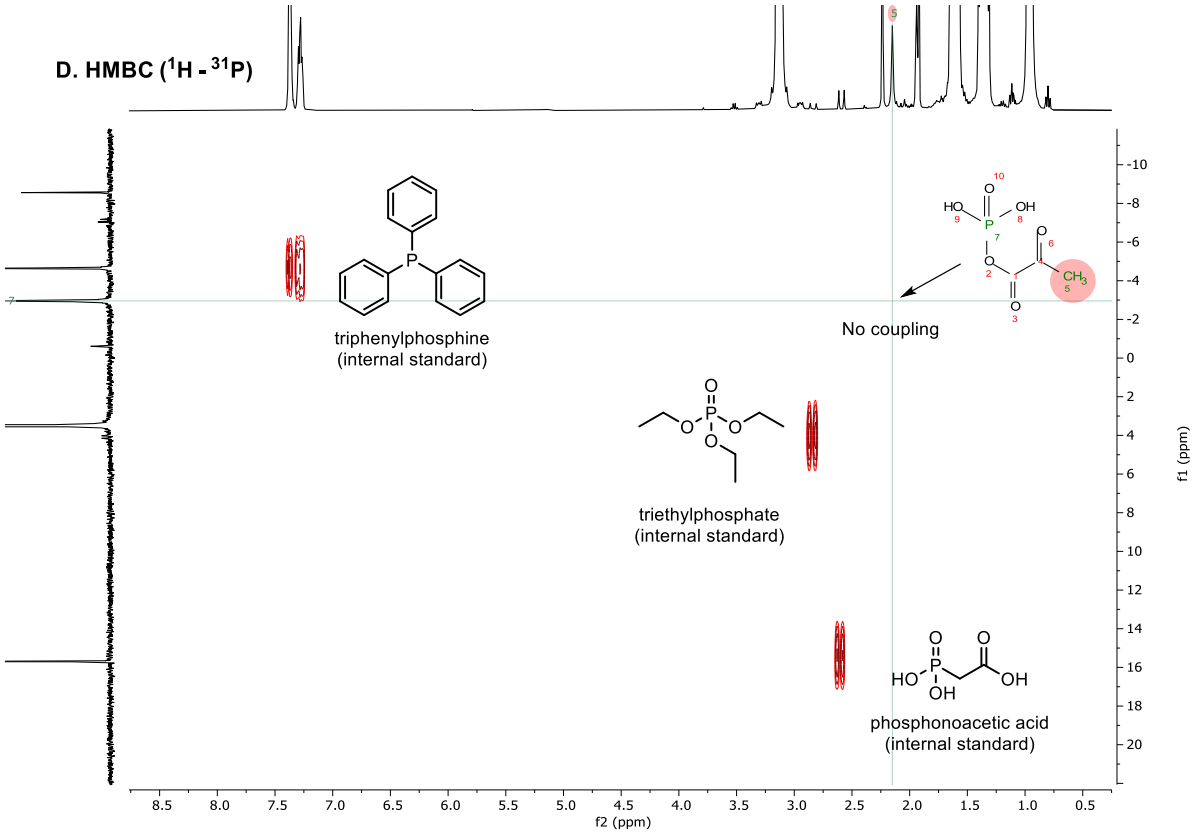
D. HMBC (1H - 31P)
triphenylphosphine
(internal standard)
No coupling
triethylphosphate
(internal standard)
phosphonoacetic acid
(internal standard)
f2 (ppm)
f1 (ppm)

Table S12 Entry 6

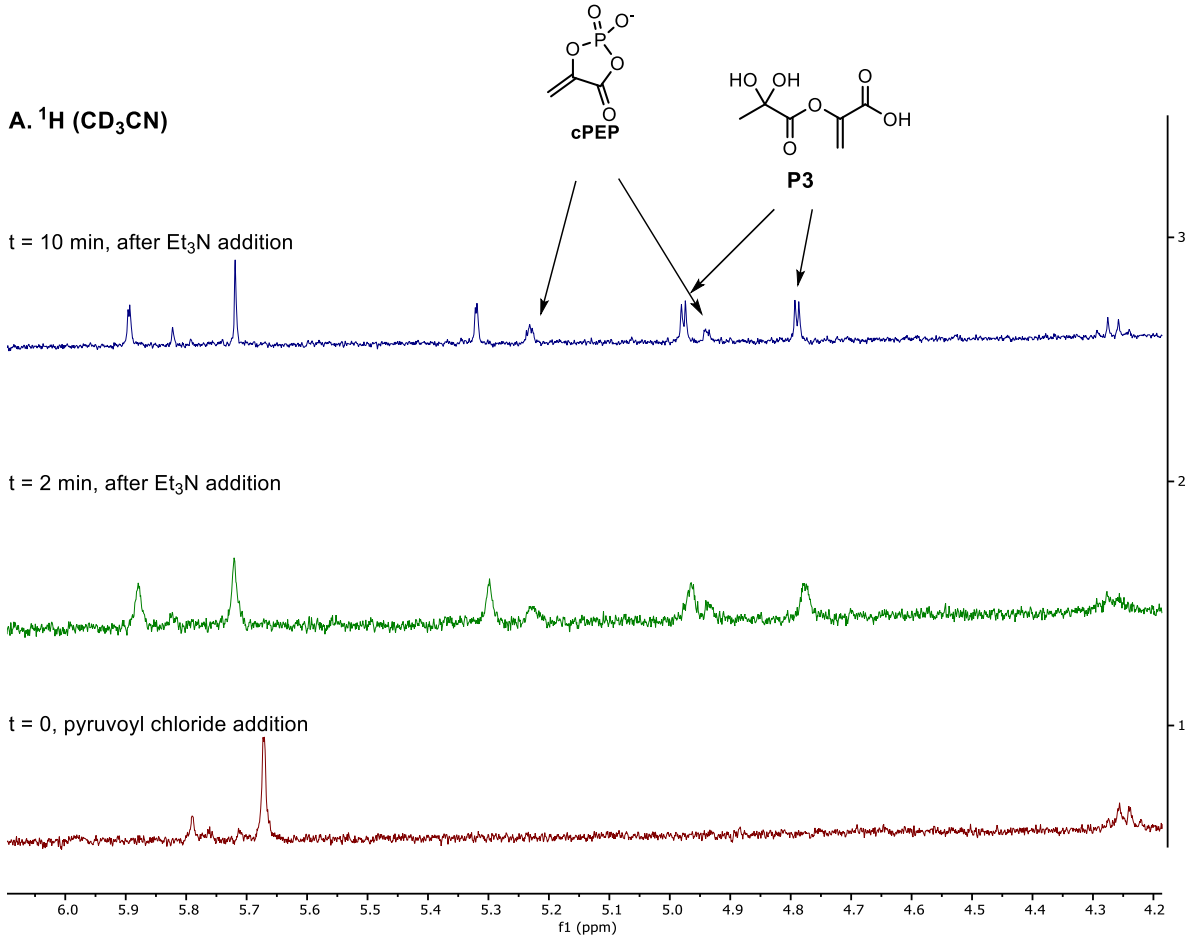

4) Conversion of AcP-Pyr to the Hydroxy-Phosphate of pyruvate P1-OH and P2-PEP in the presence of water

Pyruvoyl chloride **Pyr-Cl** (0.06 mmol) and $NBu_4^+H_2PO_4^-$ (1 equiv) were dissolved in 1 mL of CD_3CN and an NMR tube was prepared (0.6 mL). The reaction was followed by ^1H and ^{31}P NMR. When traces of water were present in the mixture, the **AcP-Pyr** was converted to **P1-OH** (see VI. A14, p. S113 for characterization) and traces of **PEP**.

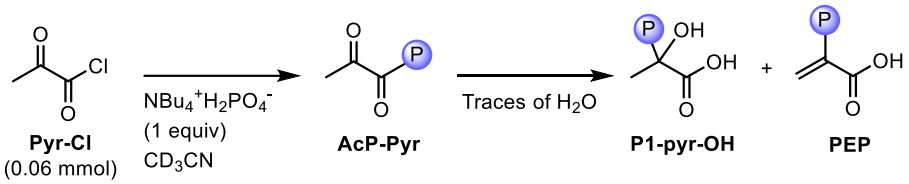

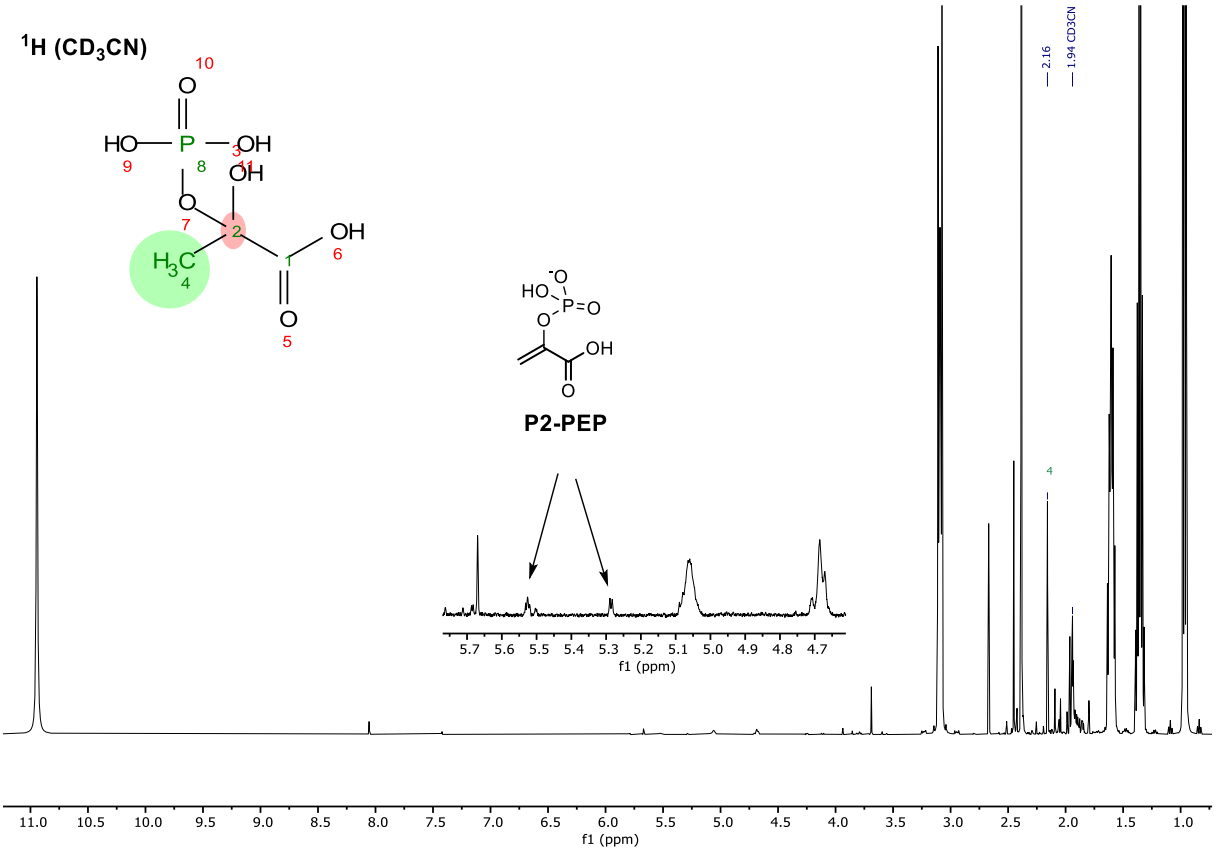

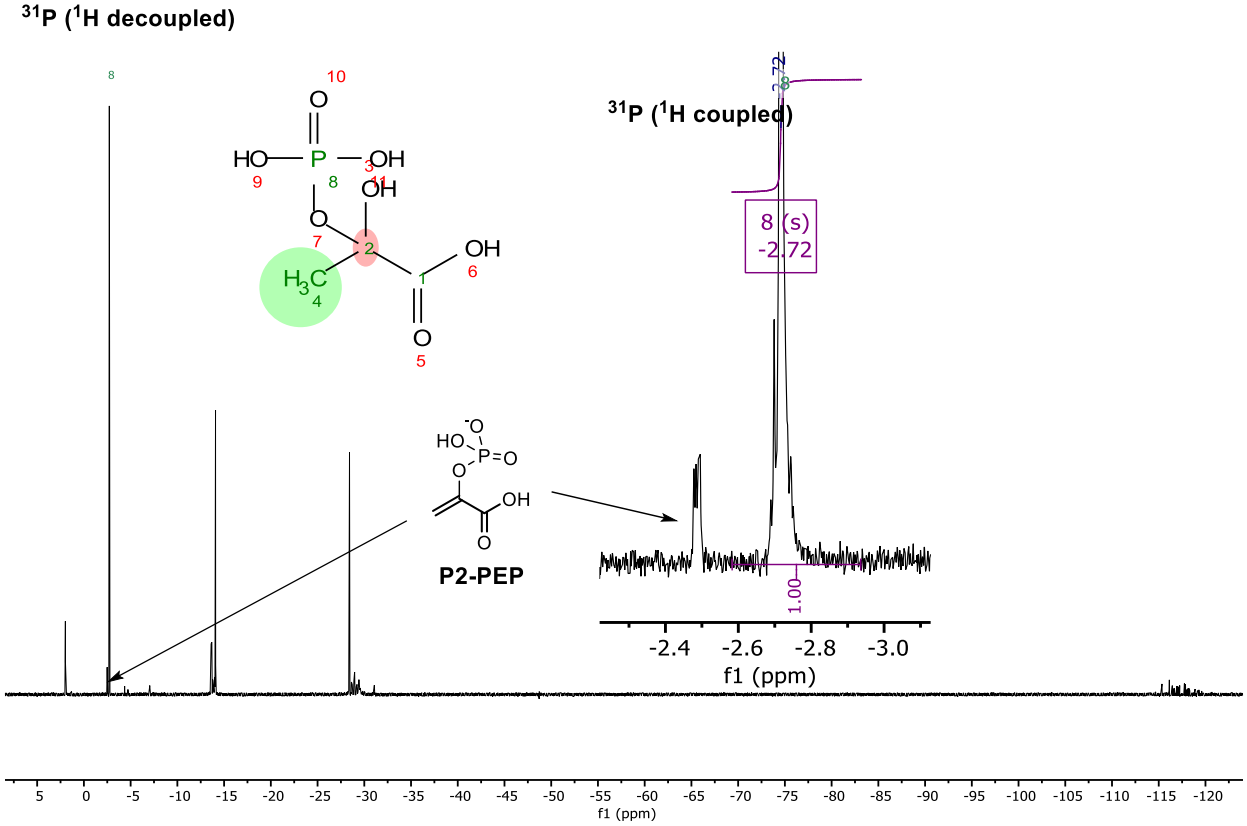

5) Conversion of cPEP to PEP in the presence of Et_3N

$NBu_4^+H_2PO_4^-$ (1 equiv) and Et_3N (2 equiv) were premixed in 1 mL of CD_3CN and an NMR tube was prepared (0.6 mL). Then, pyruvoyl chloride **Pyr-Cl** (0.1 mmol) was added to the mixture and, the reaction was followed by ^1H and ^{31}P NMR spectroscopy. The formation of **cPEP** was observed (see VI. A15, p. S118 for characterization), which converted to **PEP** over time.

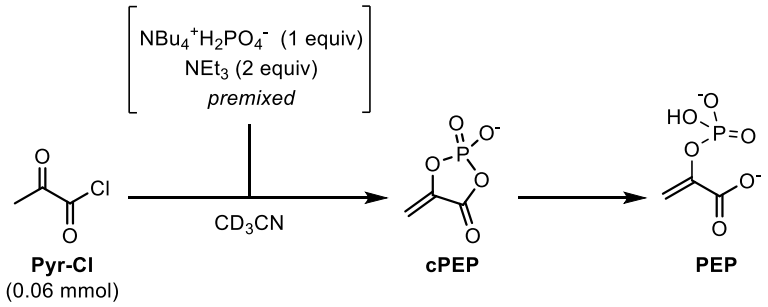

Yields of **PEP** after 36 h: 3% determined by ^1H qNMR (d1 = 45 s,16 scans).

Yields of **P3-pyr** after 36 h: 1% determined by ^1H qNMR (d1 = 45 s,16 scans).

Conversion of cPEP to PEP over time (followed by ^{1}H and ^{31}P NMR).

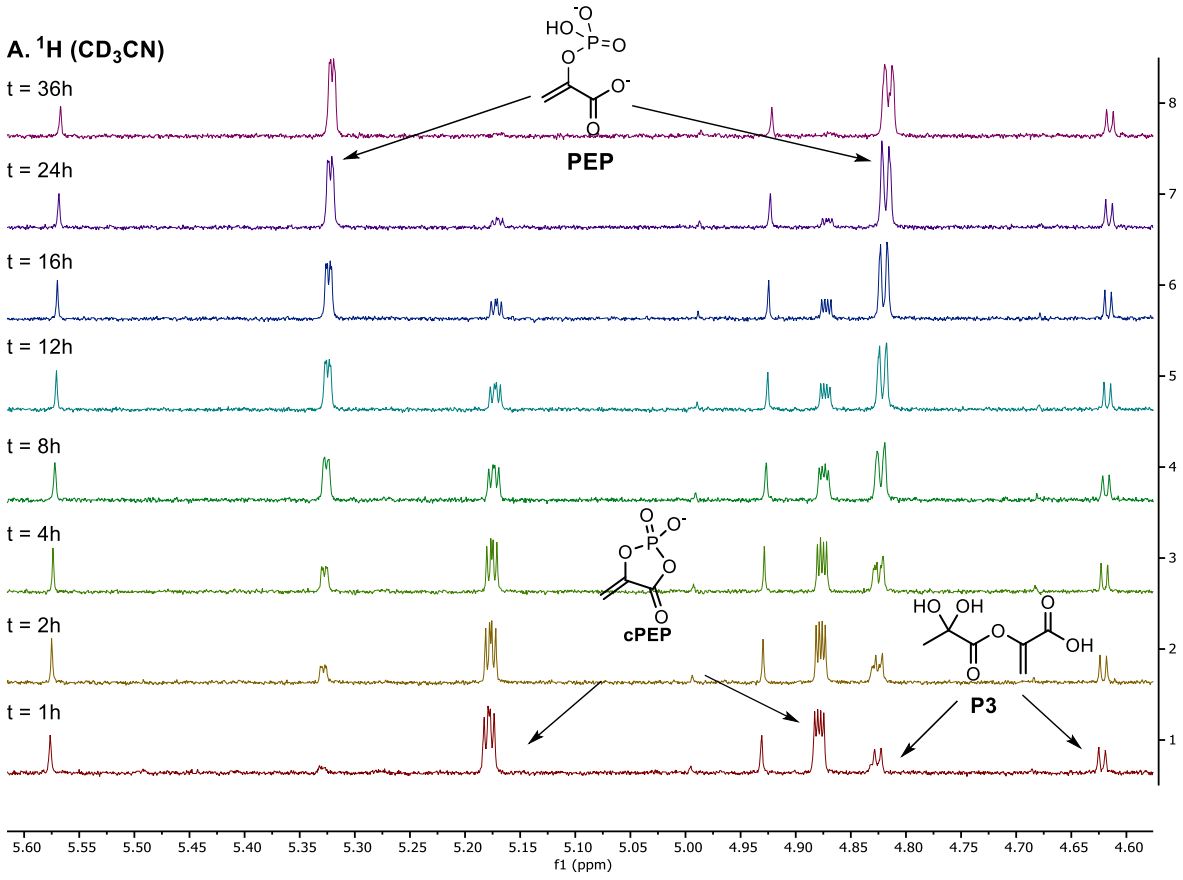

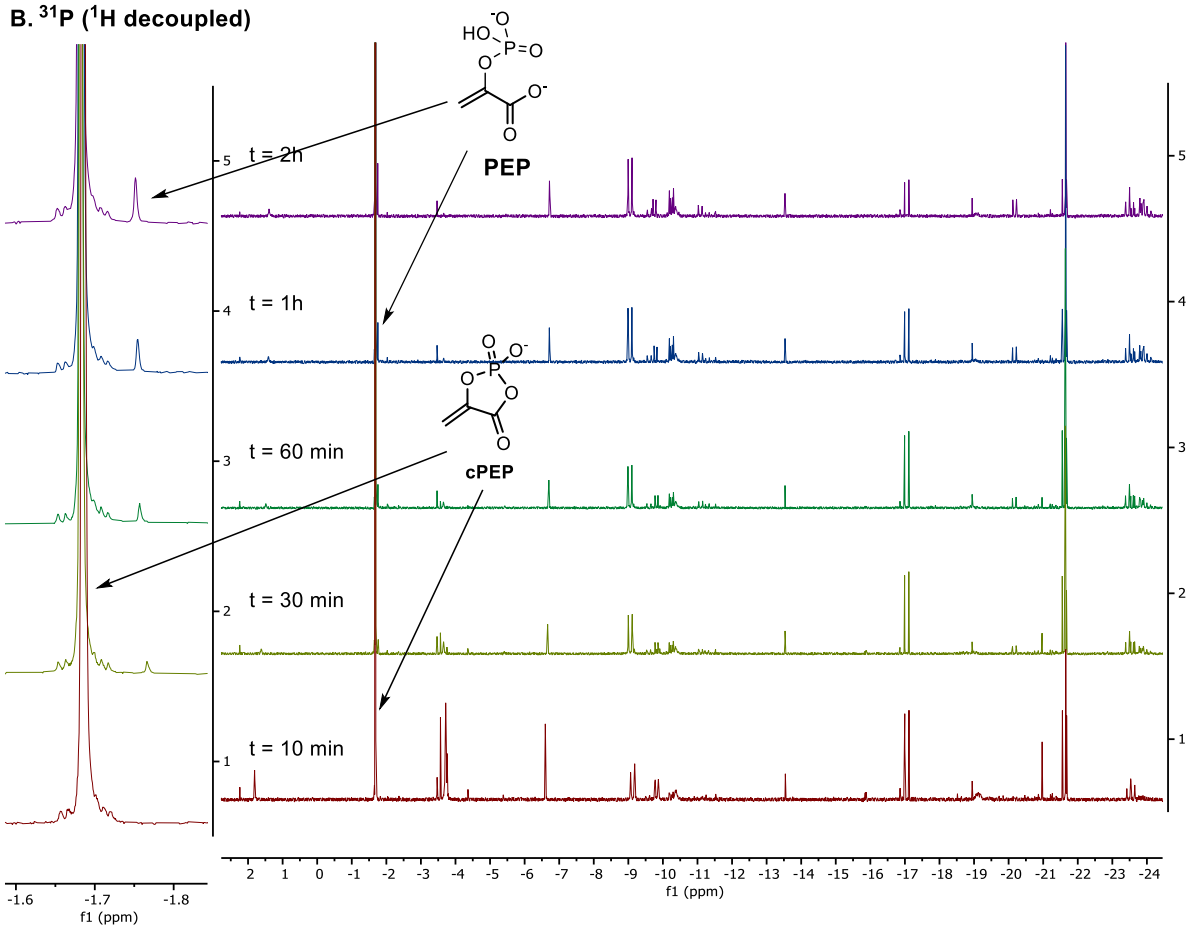
B. 31P (1H decoupled)
PEP
cPEP
t = 2h
t = 1h
t = 60 min
t = 30 min
t = 10 min
f1 (ppm)
f1 (ppm)

VI. Characterization of the products and the paste

A. Characterization of the products of the phosphorylation reaction (scaled-up reactions)

Representative procedure for the scaled-up reactions: The substrate (0.3 mmol) and P_4O_{10} (1 equiv) were weighed together in a 2 mL microcentrifuge tube with lid and mixed for 20 s using a vortex. Then, either pyridine or 1-methylimidazole (2 equiv) was added, and the mixture was centrifuged for 2 min. Unless otherwise specified, the retrieved paste was heated for 5 min at 60 °C in a thermoshaker. After the indicated time, 1 mL of D_2O was added to the mixture and the general procedure **GP-I** was applied for NMR sample preparation.

1) P1-pyr-im characterization (with 1-methylimdazole)

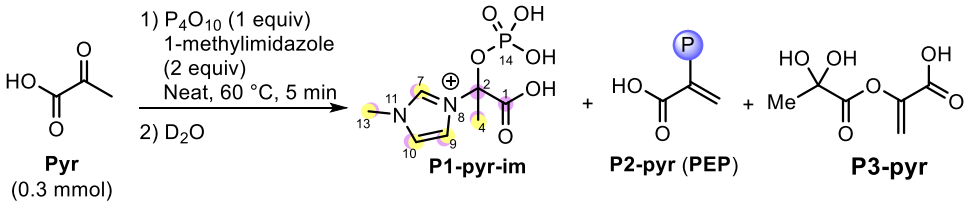

^{1}H NMR (500 MHz, D_2O) δ 8.83 – 8.82 (br, 1 H, H-7), 7.43 (br, 1 H, H-9), 7.27 (br, 1 H, H-10), 3.70 (s, 3 H, H-13), 2.02 (s, 3 H, H-4) ppm.

^{13}C NMR (126 MHz, D_2O) δ 170.0 (d, J_{CP} = 8.5 Hz, C-1), 135.6 (C-7), 123.5 (C-9), 120.2 (C-10), 88.7 (d, J_{CP} = 6.6 Hz, C-2), 36.0 (C-13), 22.6 (d, J_{CP} = 2.8 Hz, C-4) ppm.

^{31}P NMR (202 MHz, D_2O) δ -5.41 (s) ppm.

^{15}N NMR (36 MHz, D_2O) δ 173.03 (N-11), 195.28 (N-8) ppm.

HRMS (ESI$^+$): Calcd m/z for [$C_7H_{12}O_6N_2P^+$] [M^+]: 251.0427; Found: 251.0428 (0.2046 ppm).

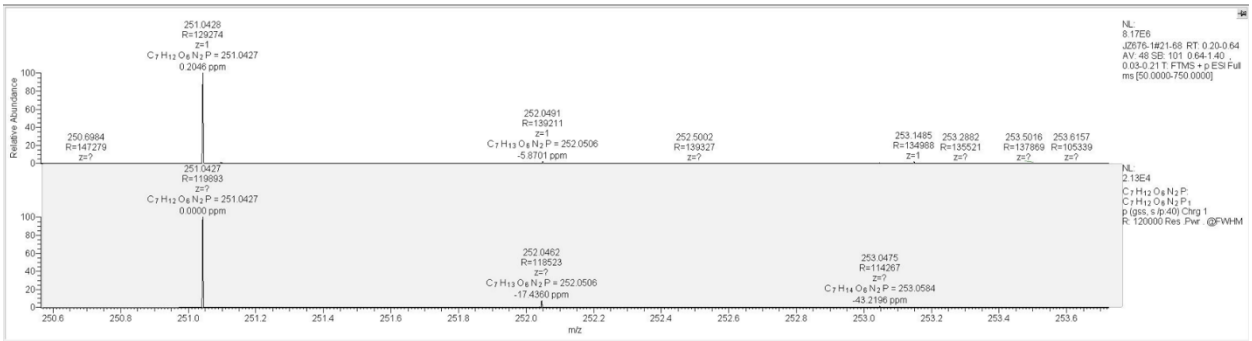

The product **P1** was assigned as a phosphorylated covalent adduct of pyruvate and the base (see below). While **P1** refers to the general structure of the intermediate, **P1-pyr-py** and **P1-pyr-im,** respectively refer to the phosphorylated adduct containing pyridine (**Py**) and 1-methylimidazole (**Im**), respectively.

The structure of **P1-pyr-im** was attributed based on the following observations. The HMQC (^{1}H - ^{31}P) NMR showed a correlation between the -CH_3 (δ = 2.02 ppm) of the pyruvate moiety (C-4) and the phosphate peak (-5.23 ppm) with no associated coupling constant, suggesting a long distance (at least 4 bonds distance) between the two chemical groups. ^{13}C NMR and ^{1}H, ^{13}C-2D spectra showed two parts of the molecule. The first part proved to be the pyruvate moiety with the protons of the -CH_3 (H-4) having a direct correlation with the C-3 at 22.3 ppm ($J_{C\text{-}P}$ = 2.8 Hz) and two second correlations with the C-1 at 169.9 ppm ($J_{C\text{-}P}$ = 8.5 Hz) and with the C-2 at 88.6 ppm ($J_{C\text{-}P}$ = 6.6 Hz) detected by HMBC. The second part was the **Im** moiety, with three distinct peaks at 8.83 ppm (H-7), 7.43 ppm (H-9) and 7.27 ppm (H-10) integrating for 1 proton and the -CH_3 at 3.7 ppm (H-13) integrating for 3 protons (as well as the -CH_3 moiety of pyruvate

at 2.02 ppm). These protons of the **Im** showed direct correlations with their respective carbons (i.e., C-7, C-9, C-10, and C-13. A NOESY spectrum showed correlation between protons H-7 and H-9 of the **Im** moiety with the -CH_3 of the pyruvate moiety. In addition, a HOESY spectrum (which might show correlations between the phosphate and the protons of the **Im** moiety) showed correlation between protons H-7 and H-9 and the phosphate of the molecule. Finally, a ^{1}H, ^{15}N-HMBC experiment allowed us to indirectly measure the ^{15}N signals. This experiment revealed the two nitrogen atoms N-11 (at 173 ppm) and N-8 (at 195 ppm) of **Im**; N-11 showing the main correlation with H-13, and further ones with H-7 and H-9 but no correlation with H-10; N-8 showing the main correlation with H-3 of the pyruvate moiety, with H-7, and H-10, but no correlation with H-9.

The product was not purified because of the low yields obtained, the poor stability of this kind of product on silica, and the poor solubility of the paste.

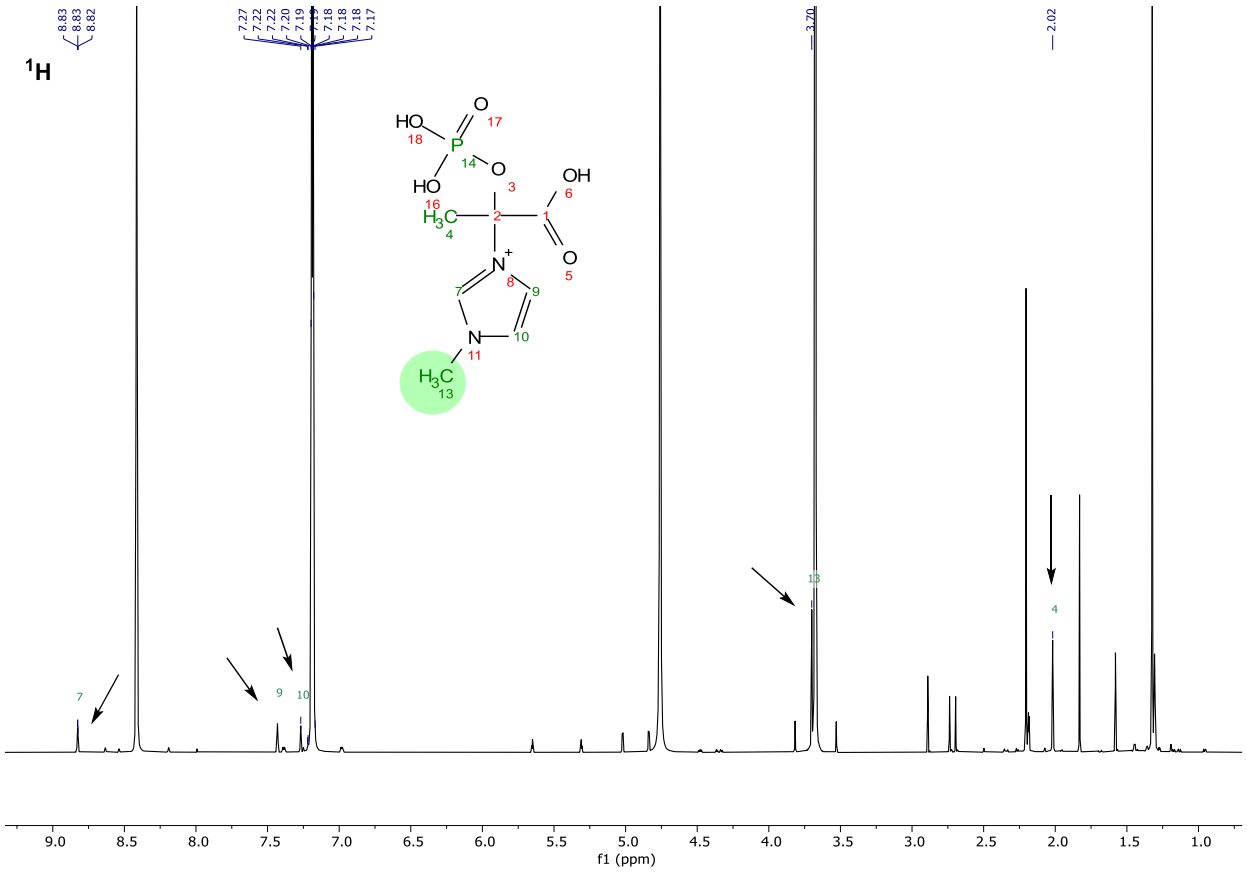

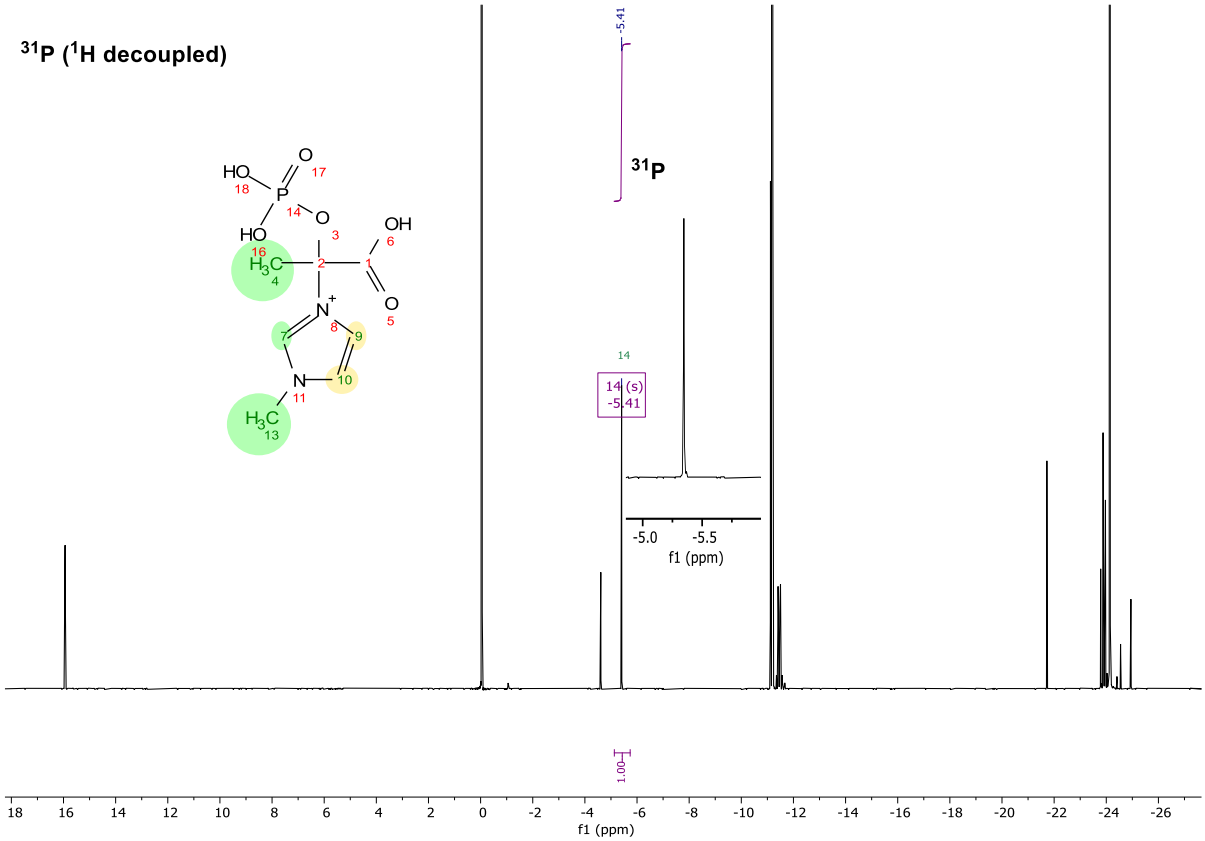
31P (1H decoupled)
31P
-5.41
14 (s)
-5.41
-5.0
-5.5
f1 (ppm)
1.00
f1 (ppm)

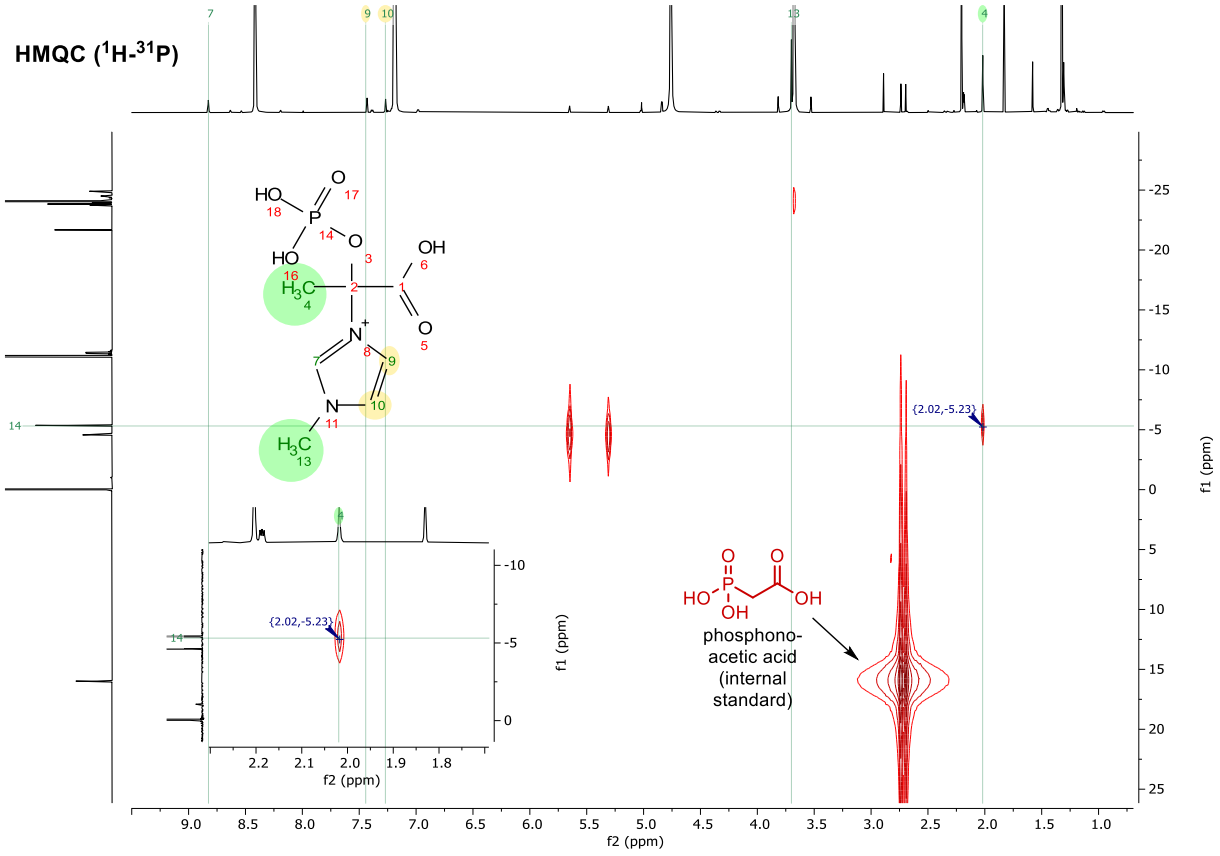
HMQC (1H-31P)
{2.02,-5.23}
phosphono-
acetic acid
(internal
standard)
f2 (ppm)
f1 (ppm)

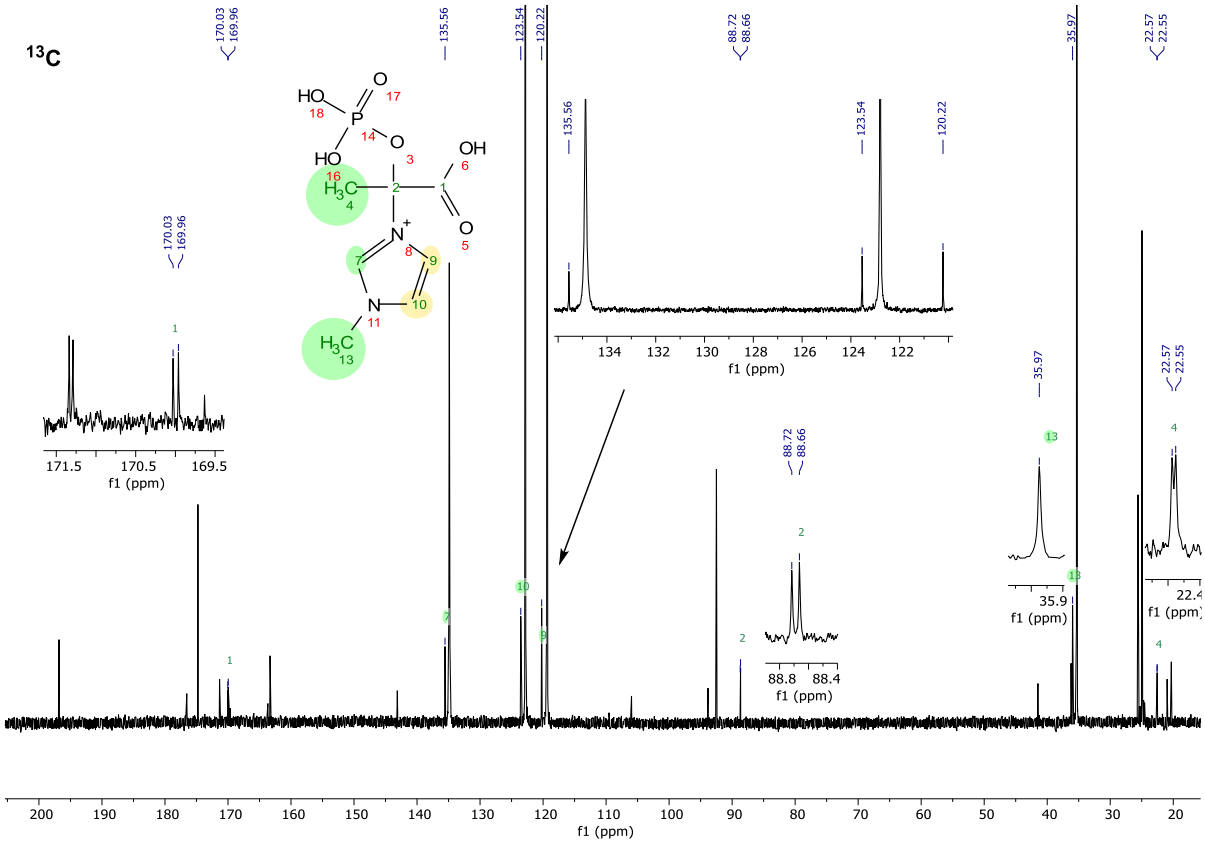
13C
170.03
169.96
135.56
123.54
120.22
88.72
88.66
35.97
22.57
22.55
f1 (ppm)

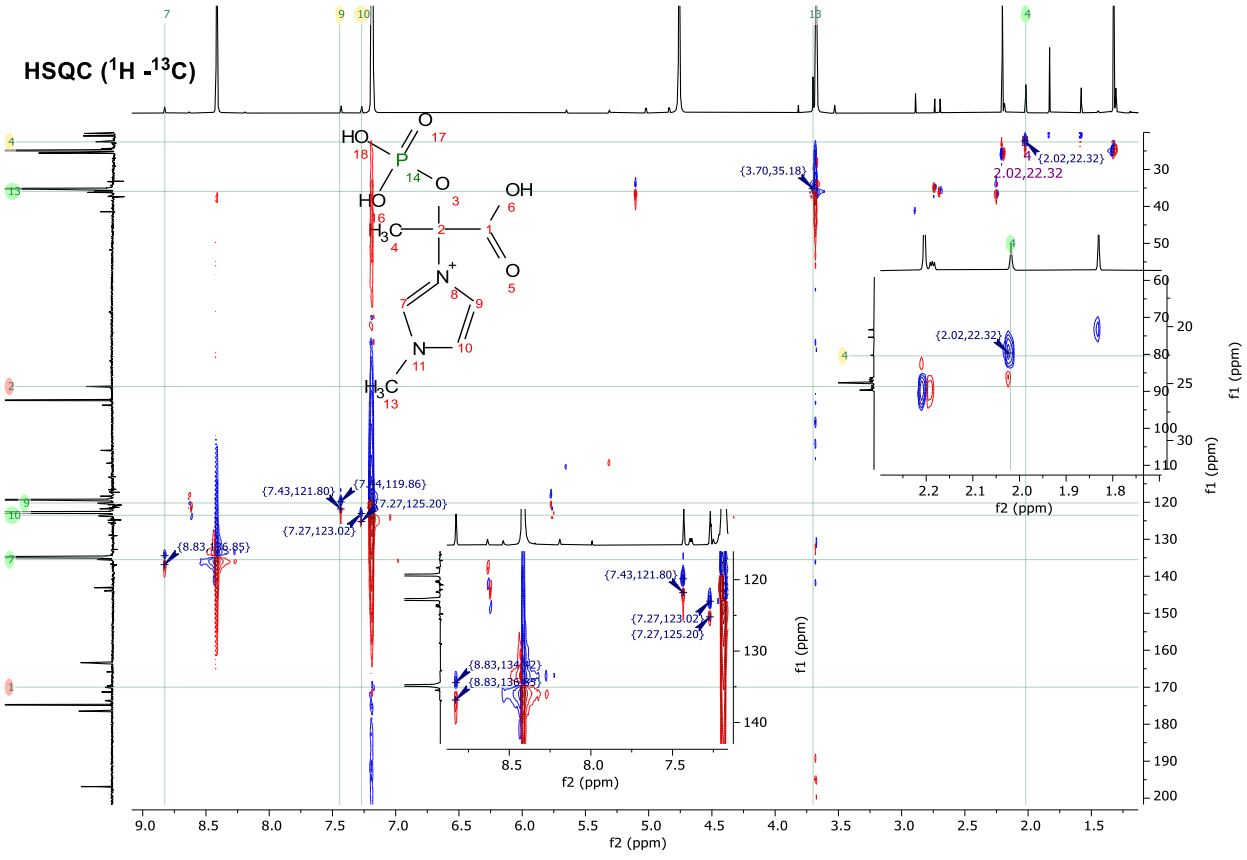
HSQC (1H -13C)
f2 (ppm)
f1 (ppm)

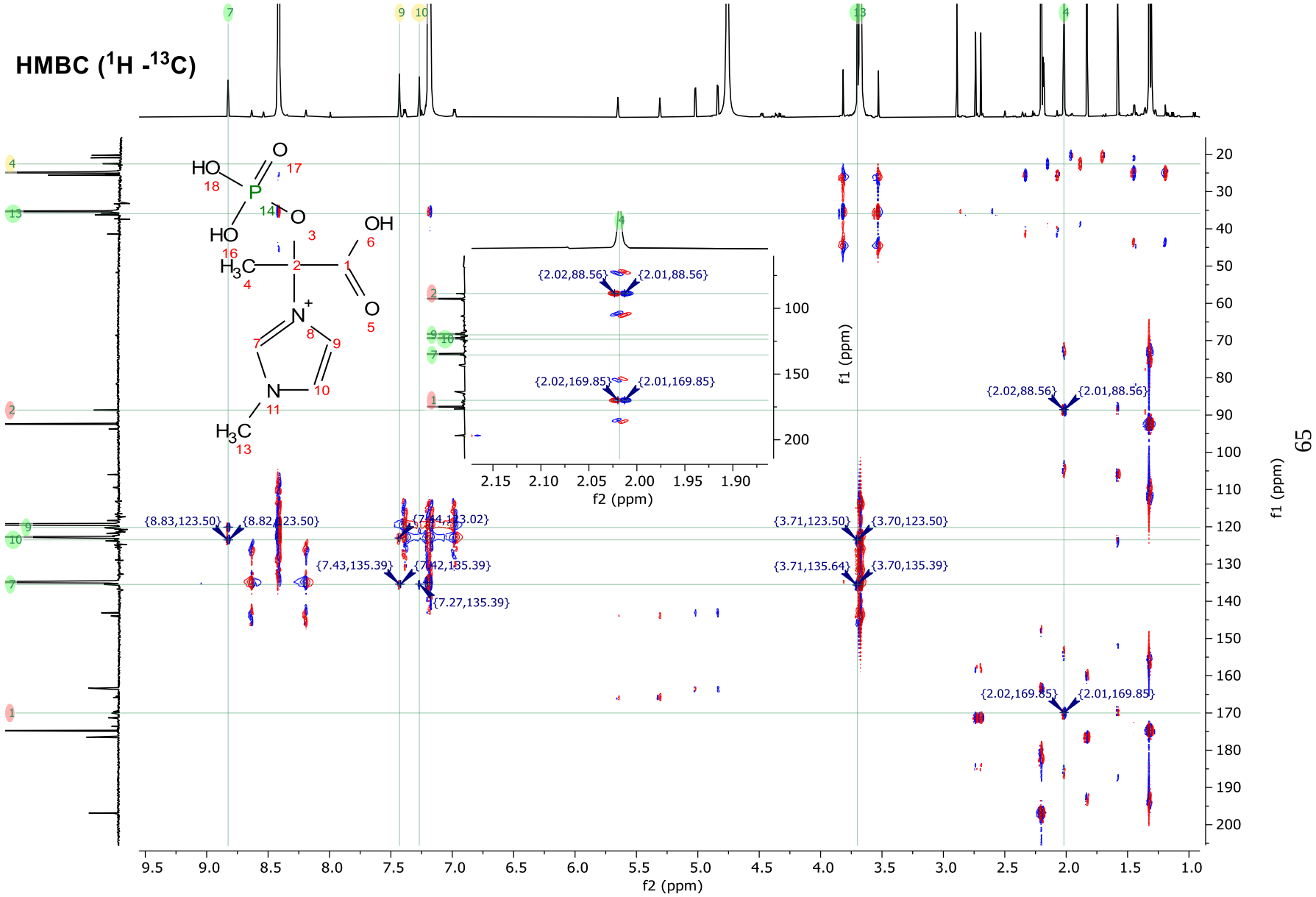
HMBC (^{1}H -^{13}C)
f2 (ppm)
f1 (ppm)
{8.83,123.50}
{8.82,123.50}
{7.43,135.39}
{7.42,135.39}
{7.27,135.39}
{3.71,123.50}
{3.70,123.50}
{3.71,135.64}
{3.70,135.39}
{2.02,88.56}
{2.01,88.56}
{2.02,169.85}
{2.01,169.85}

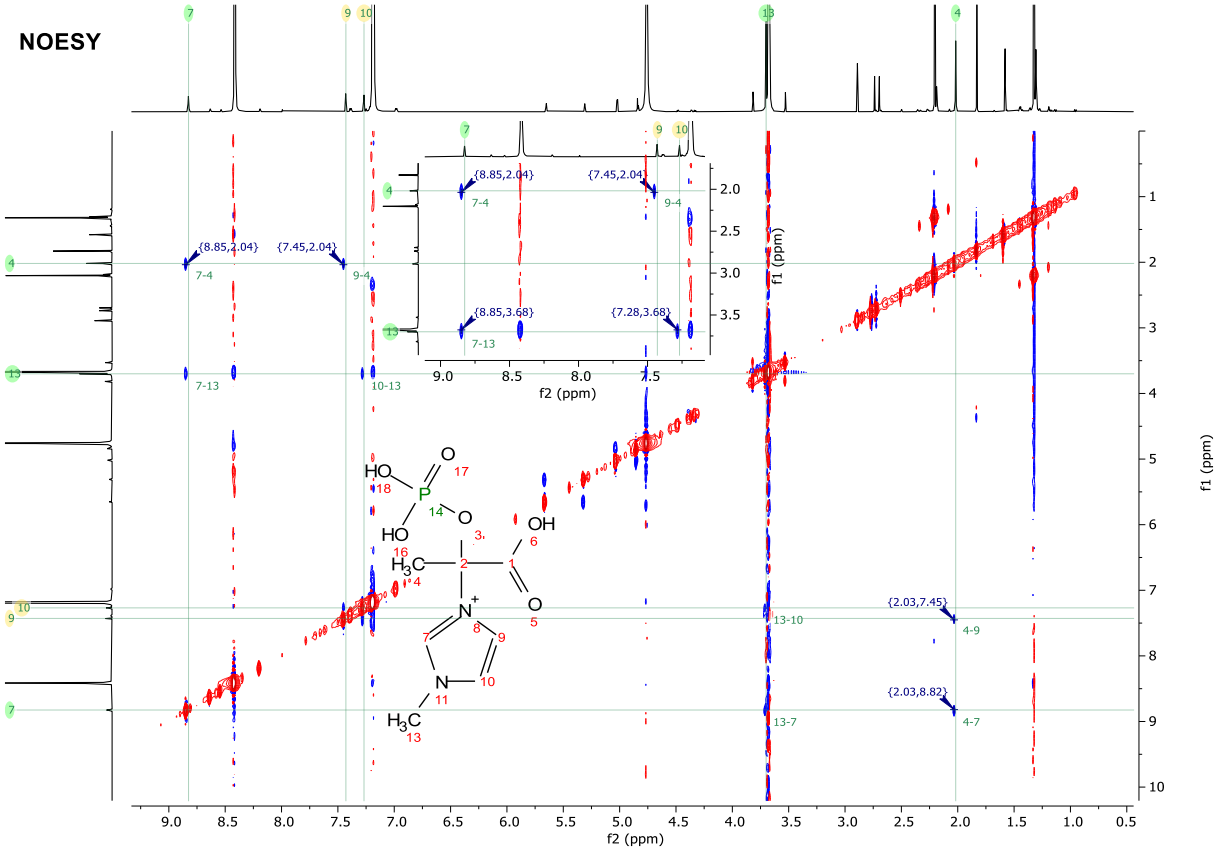
NOESY
{8.85,2.04}
{7.45,2.04}
7-4
9-4
{8.85,3.68}
{7.28,3.68}
7-13
10-13
13-10
13-7
{2.03,7.45}
4-9
{2.03,8.82}
4-7
f2 (ppm)
f1 (ppm)

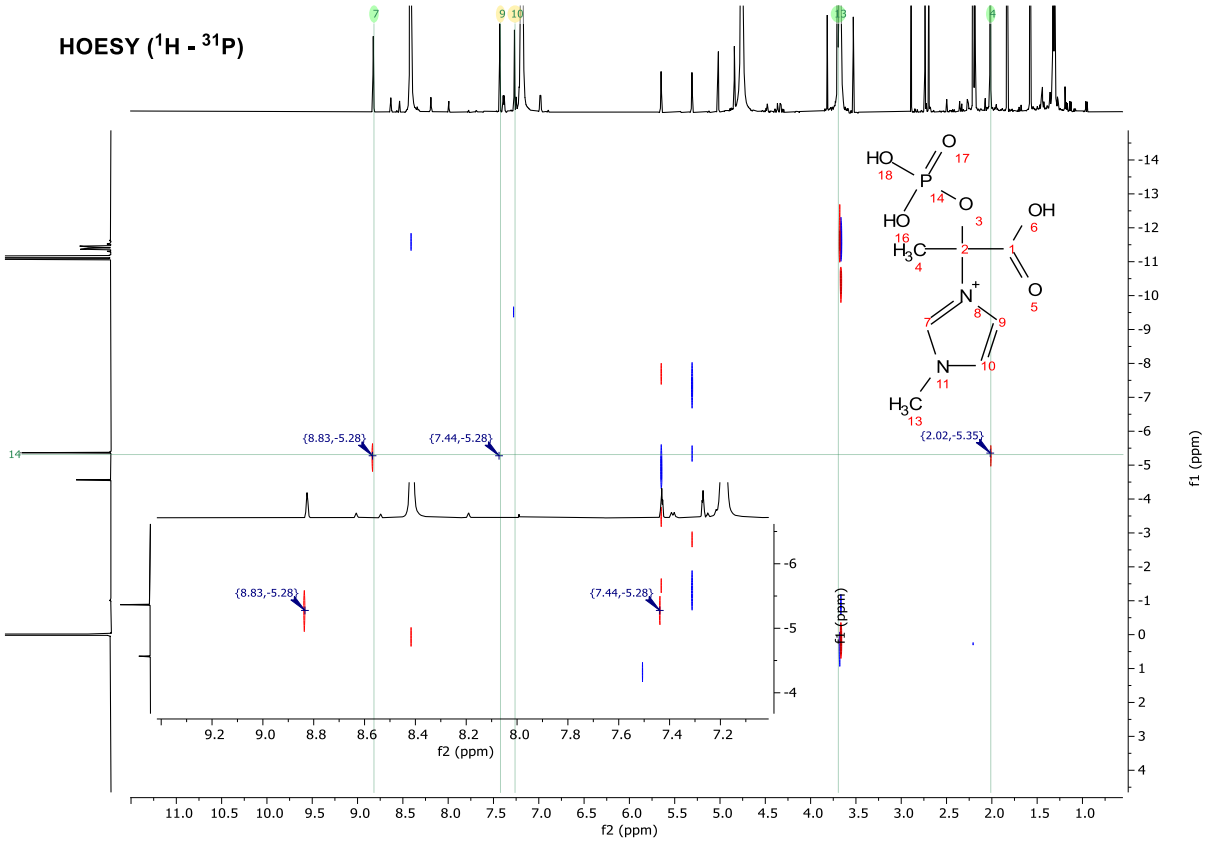
HOESY (1H - 31P)
{8.83,-5.28}
{7.44,-5.28}
{2.02,-5.35}
f2 (ppm)
f1 (ppm)

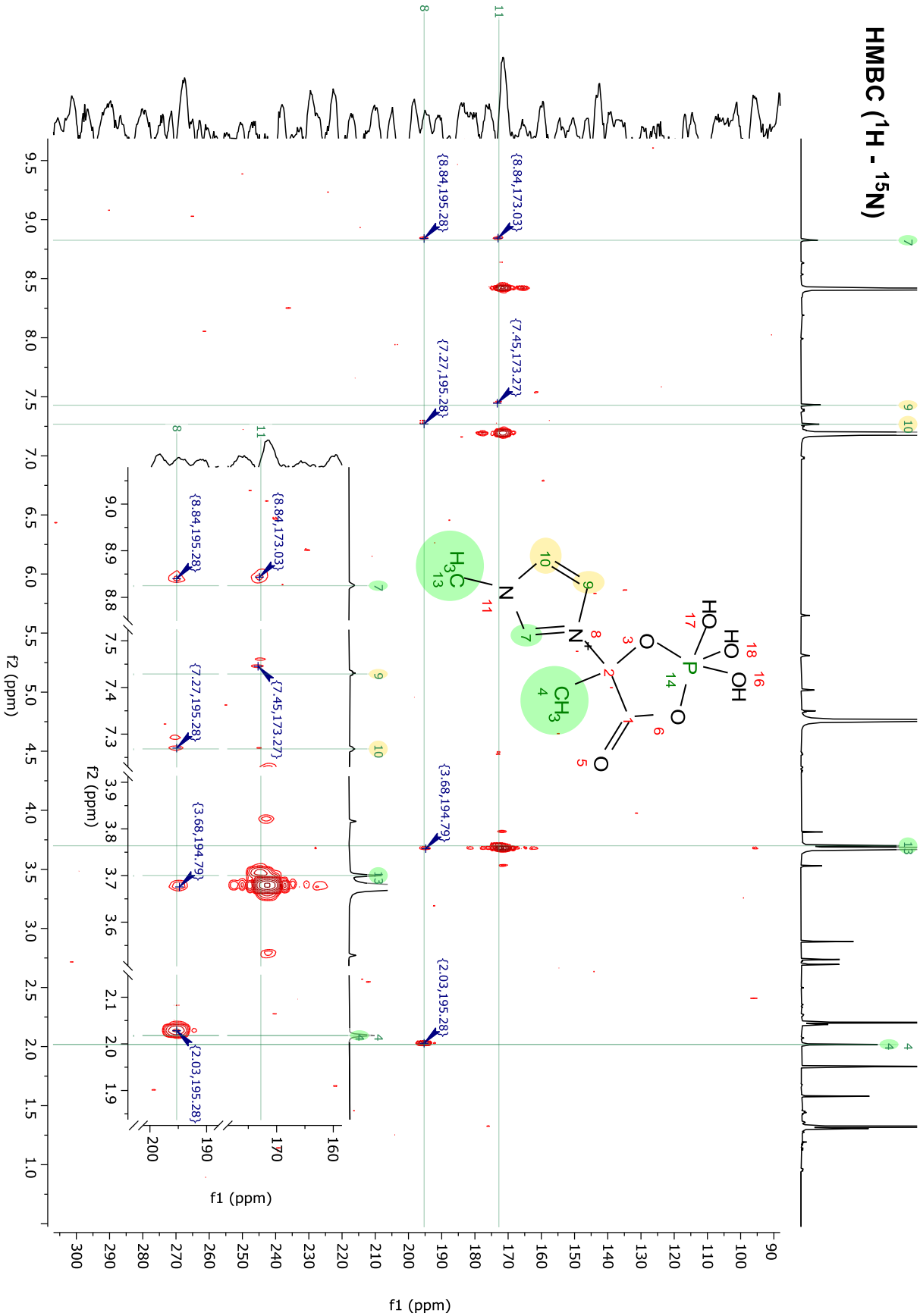
HMBC (^{1}H - ^{15}N)
{8.84,173.03}
{8.84,195.28}
{7.45,173.27}
{7.27,195.28}
{3.68,194.79}
{2.03,195.28}
f1 (ppm)
f2 (ppm)

The NMR data for product **P1** could potentially be assigned either to a linear (Fig. S4A, left) or a cyclized form (Fig. S4A, right). The phosphorous-carbon coupling constants $J_{C\text{-}P}$ were used to differentiate these species.

The C-1 and C-2 atoms of **P1-pyr-im** show similar/close coupling constants ($J_{C\text{-}P}$ = 8.5 Hz and $J_{C\text{-}P}$ = 6.6 Hz respectively) with the phosphate group while C-4 has a smaller value ($J_{C\text{-}P}$ = 2.8 Hz). Similarly, the phosphorylated adduct obtained with **Py** as base (**P1-pyr-py**) shows the same characteristics: C-1: $J_{C\text{-}P}$ = 9.6 Hz; C-2: $J_{C\text{-}P}$ = 7.9 Hz; C-4: $J_{C\text{-}P}$ = 1.8 Hz (see below, section VI.A2, p. S69). **PEP** has similar characteristics in aqueous solution: C-1: $J_{C\text{-}P}$ = 6.8 Hz; C-2: $J_{C\text{-}P}$ = 7.1 Hz; C-3: $J_{C\text{-}P}$ =4.0 Hz (Fig. S4B, left).

The similar magnitude of the $J_{C\text{-}P}$ of C1 and C2 had been interpreted by Baccolini and co-workers to originate from the formation of a 5-membered cyclic phosphate (Fig. S4B, left).[3]

According to our computations, such a five-membered structure does not correspond to a minima but rather to a transition state of phosphoryl transfer (see SI VII.C, Fig. S7, p. S145). Furthermore, we computed the $J_{C\text{-}P}$ as a function of the dihedral angle for **PEP** (see SI VII.D, Fig. S8, p. S146). These computations indicated that $J_{C\text{-}P}$ between C-1 and phosphorous varies greatly and is largest for a C-C-O-P dihedral angle of 180 °. Thus, $J_{C\text{-}P}$ is not a suitable measure for distance between C-1 and P and even is largest when these two groups are farthest away. Accordingly, we discard the cyclic form of **P1** and suggest the open structure (Fig. S4A, left).

Further evidence for this interpretation comes from measurement of $J_{C\text{-}P}$ of **PEP** and its dimethyl ester (Fig. S4B),[4] the latter of which cannot cyclize: similar coupling constant are observed in both cases, contrasting the proposed cyclic structure of **PEP**.

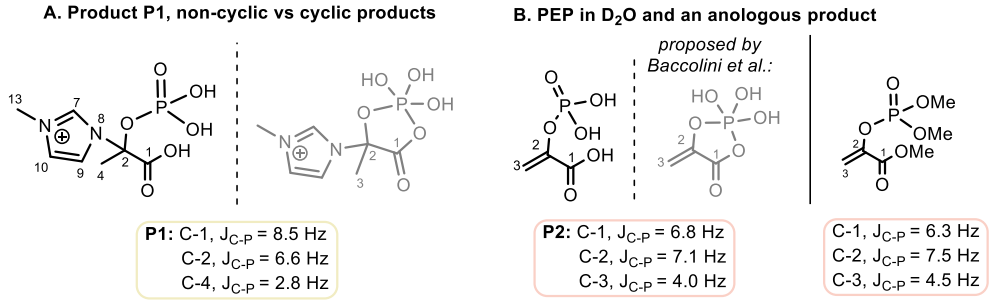

Figure S4. (A) Product **P1** and its two plausible forms according to the observed coupling constants $J_{C\text{-}P}$. (B) Two plausible representations of **PEP** (left) in solution according to its associated coupling constants $J_{C\text{-}P}$. An analogous product (right) and its associated coupling constants $J_{C\text{-}P}$.

2) P1-pyr-py characterization (with pyridine)

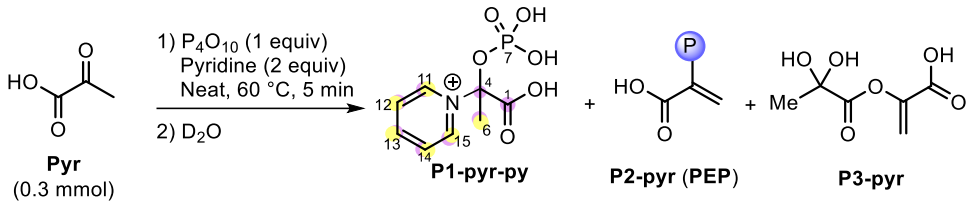

^{1}H NMR (500 MHz, D_2O) δ 8.97 – 8.95 (br, 2 H, H-11; H-15), 8.74 – 8.63 (br, 2 H, H-12, H-14), 8.02 – 7.88 (br, H-13), both overlapping with pyridine peaks, 2.28 (s, 3 H, H-6) ppm.

^{13}C NMR (126 MHz, D_2O) δ 170.6 (d, J_{CP} = 9.6 Hz, C-1), 146.9 (2 C, C-11, C-15), 141.1 (2 C, C-12, C-14, 127.3 (C-13), both overlapping with pyridine peaks, 96.5 (d, J_{CP} = 7.9 Hz, C-4), 22.0 (d, J_{CP} = 1.8 Hz, C-6) ppm.

^{31}P NMR (202 MHz, D_2O) δ -5.41 (s) ppm.

HRMS (ESI $^{+}$): Calcd m/z for [$C_8H_{11}O_6NP^{+}$] [M^{+}]: 248.0319; Found: 248.0322 (1.4024 ppm).

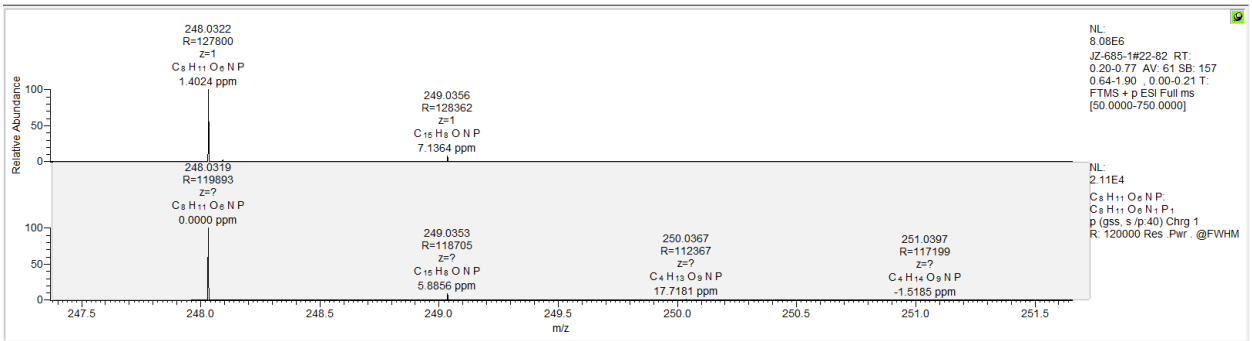

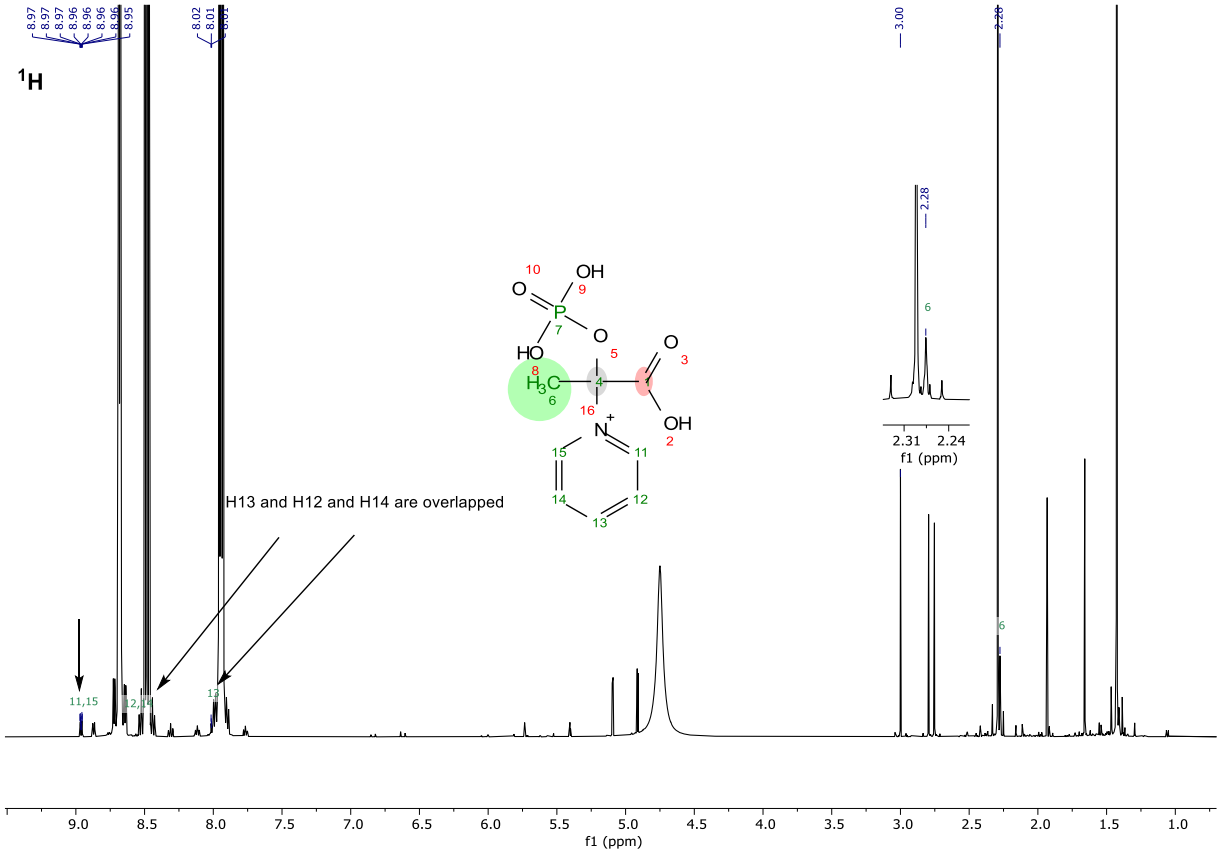
1H
H13 and H12 and H14 are overlapped
f1 (ppm)

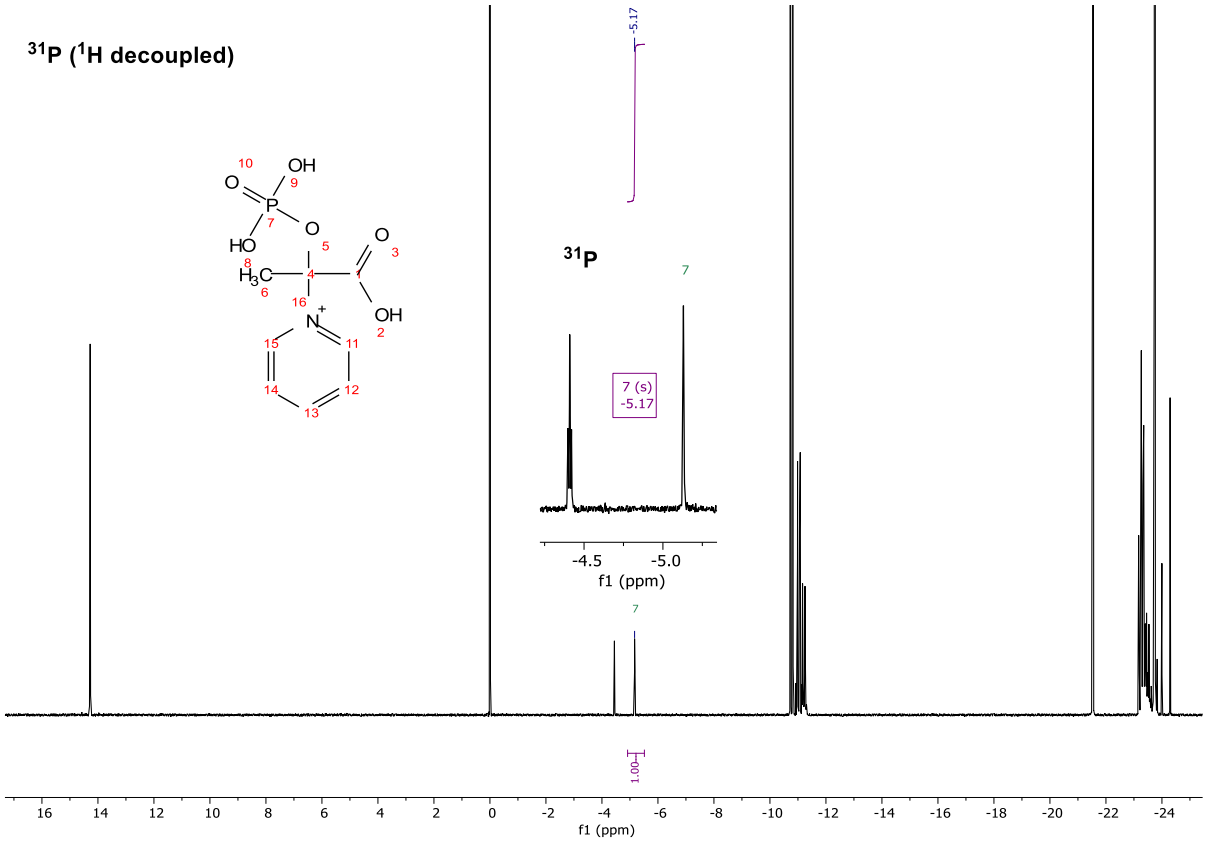
31P (1H decoupled)
31P
7 (s)
-5.17
f1 (ppm)

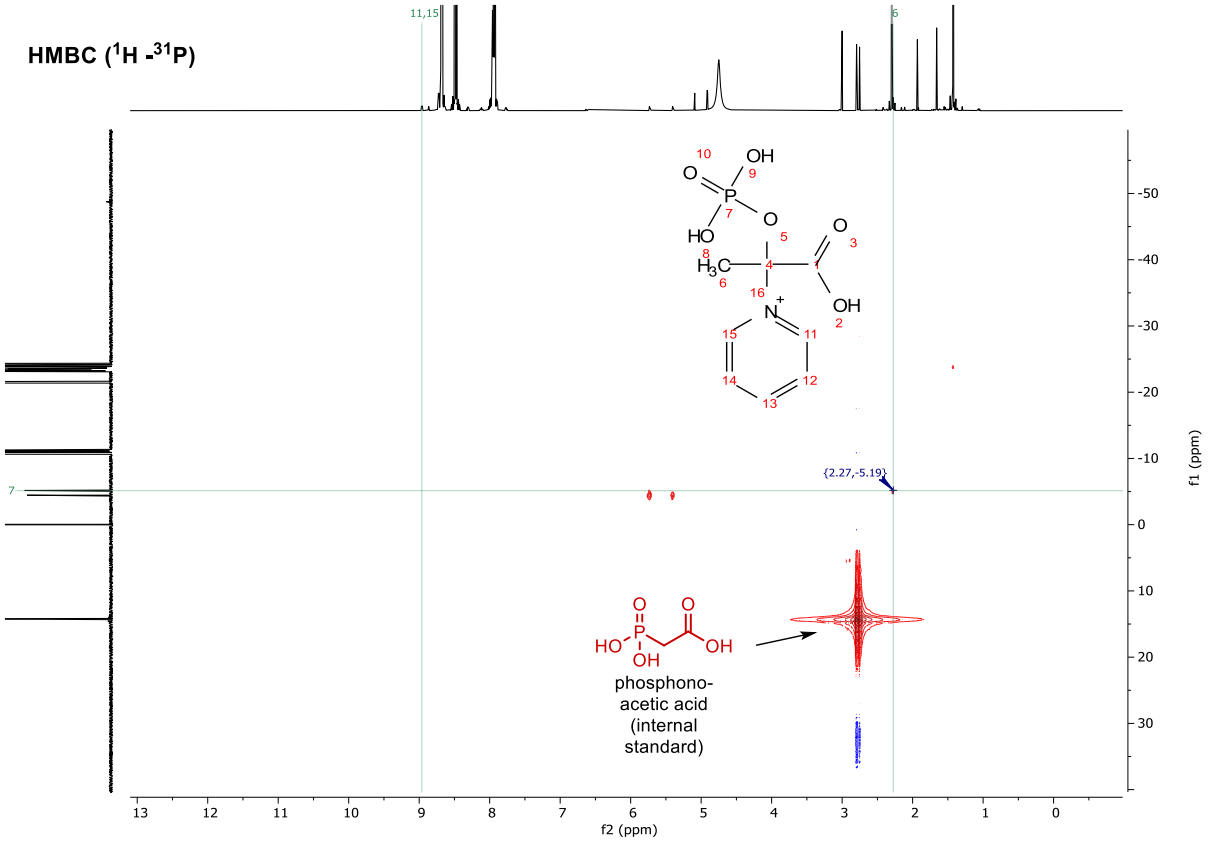
HMBC (^{1}H -^{31}P)
{2.27,-5.19}
phosphono-
acetic acid
(internal
standard)
f2 (ppm)
f1 (ppm)

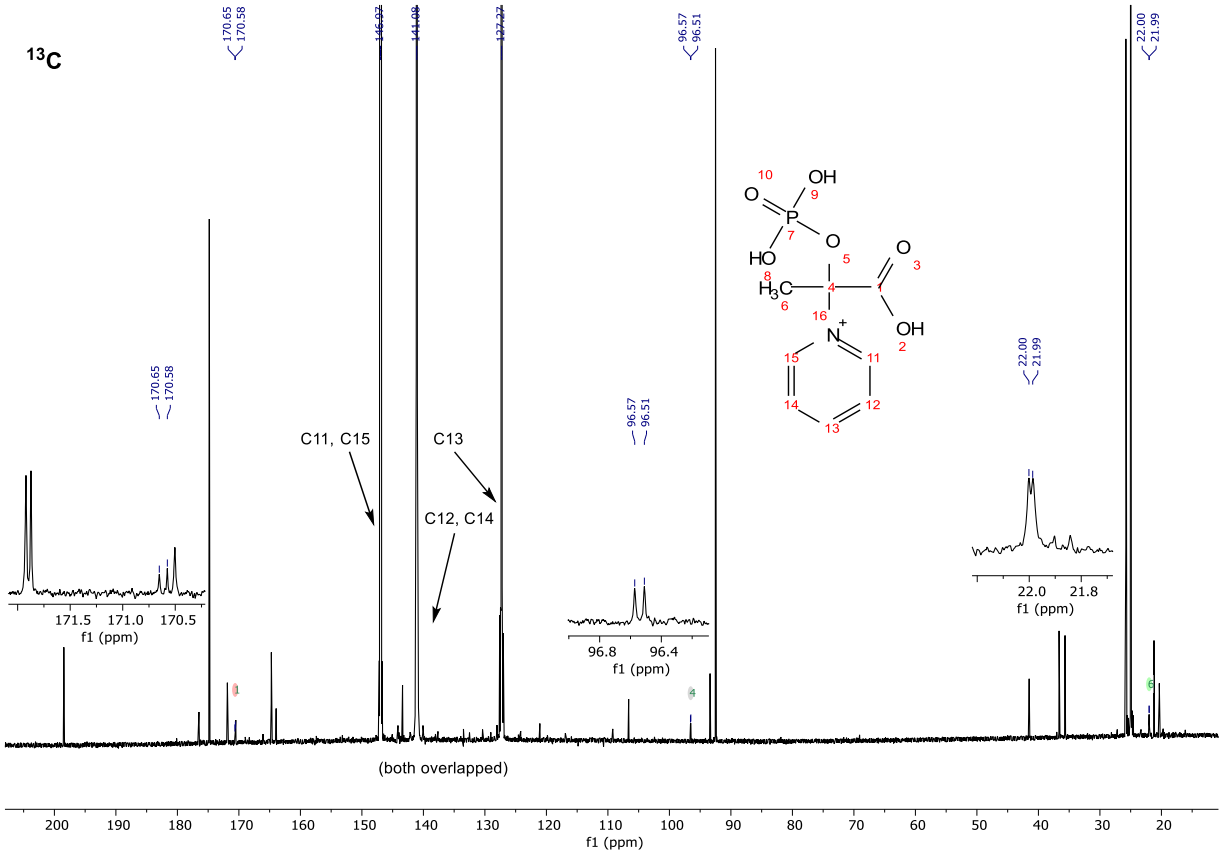
^{13}C
C11, C15
C13
C12, C14
(both overlapped)
f1 (ppm)

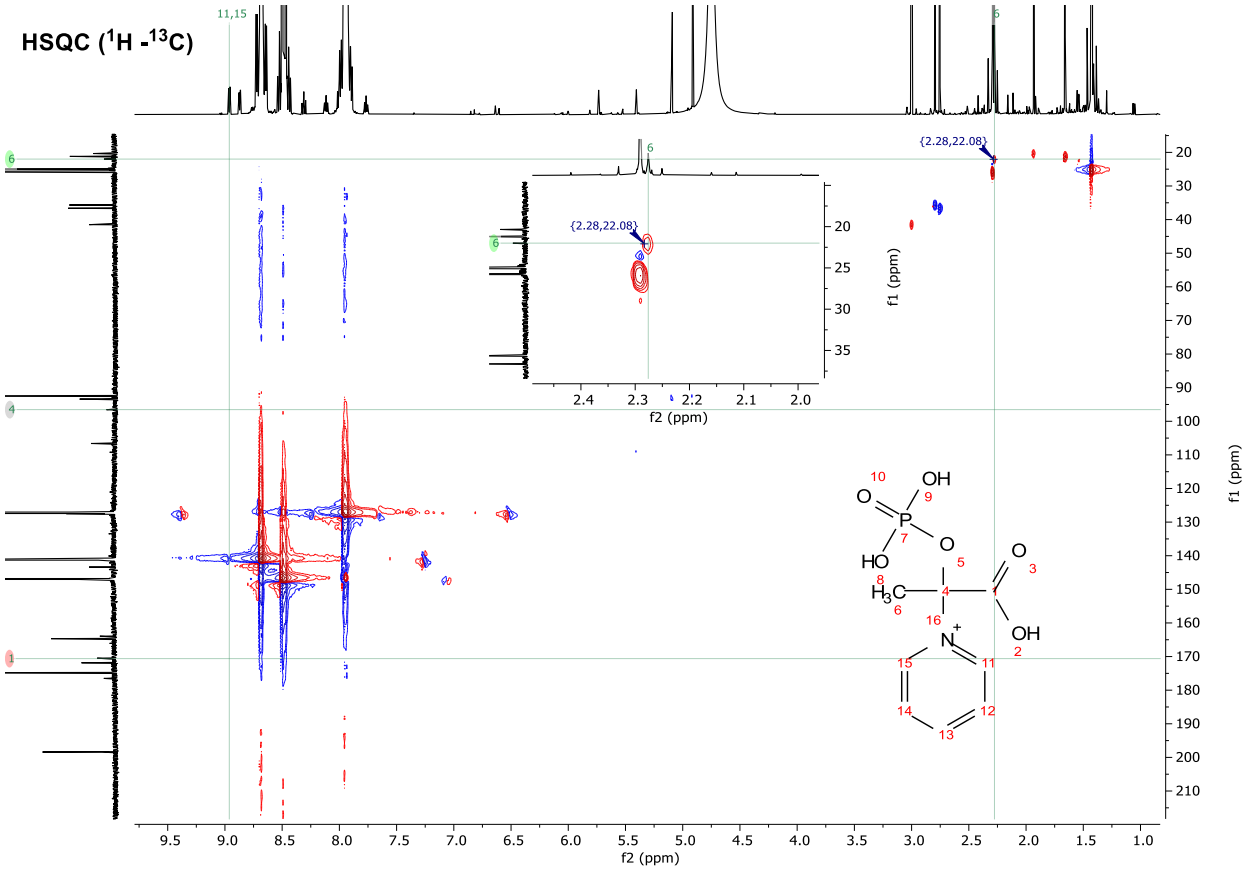
HSQC (^{1}H -^{13}C)
11,15
6
4
1
{2.28,22.08}
f2 (ppm)
f1 (ppm)
OH
O
P
HO
H_3C
N
+

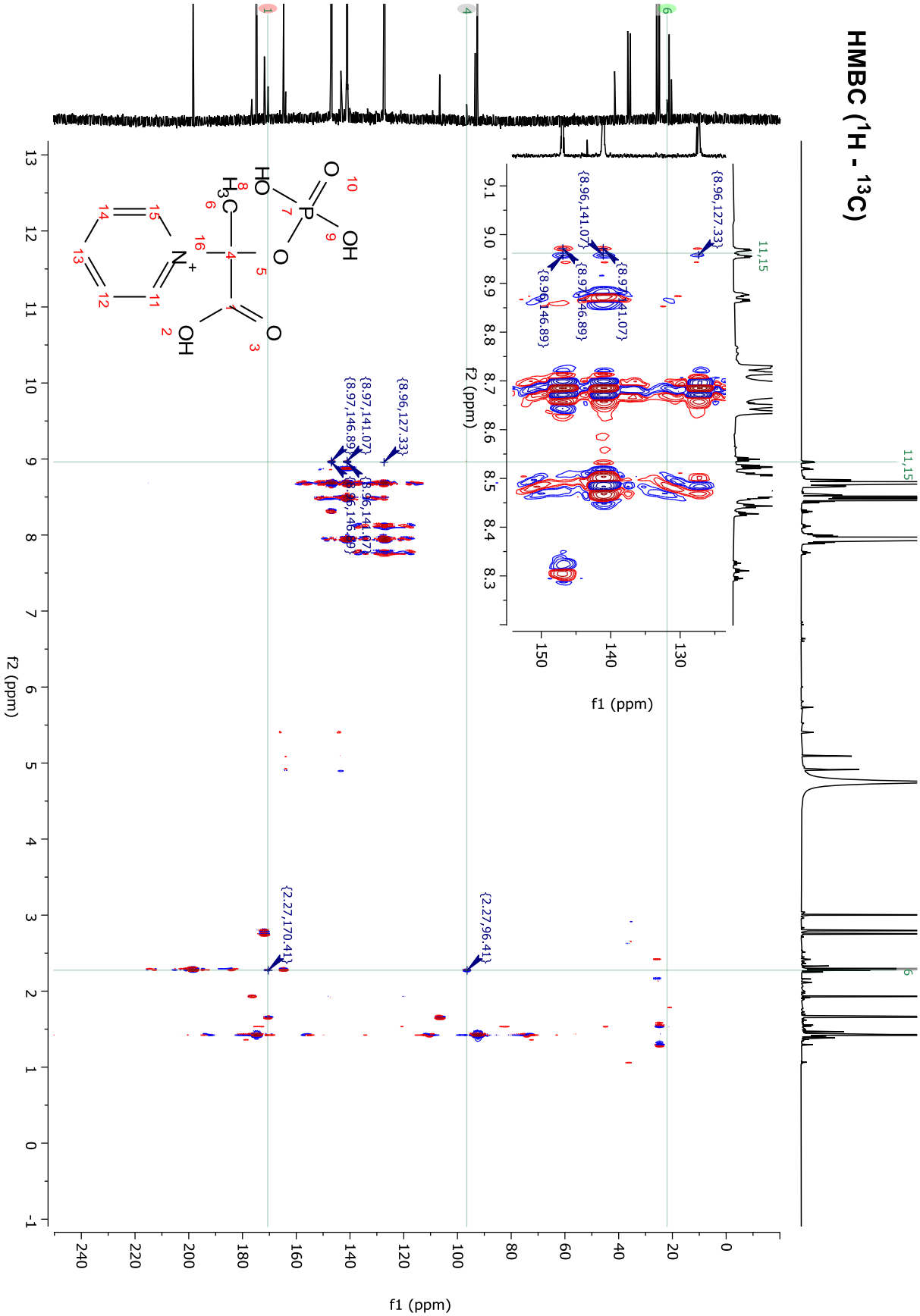
HMBC (^{1}H - ^{13}C)
f1 (ppm)
f2 (ppm)
{8.96,127.33}
{8.97,141.07}
{8.97,146.89}
{2.27,170.41}
{2.27,96.41}
11,15
6
1
4
OH
HO
O
P
N+

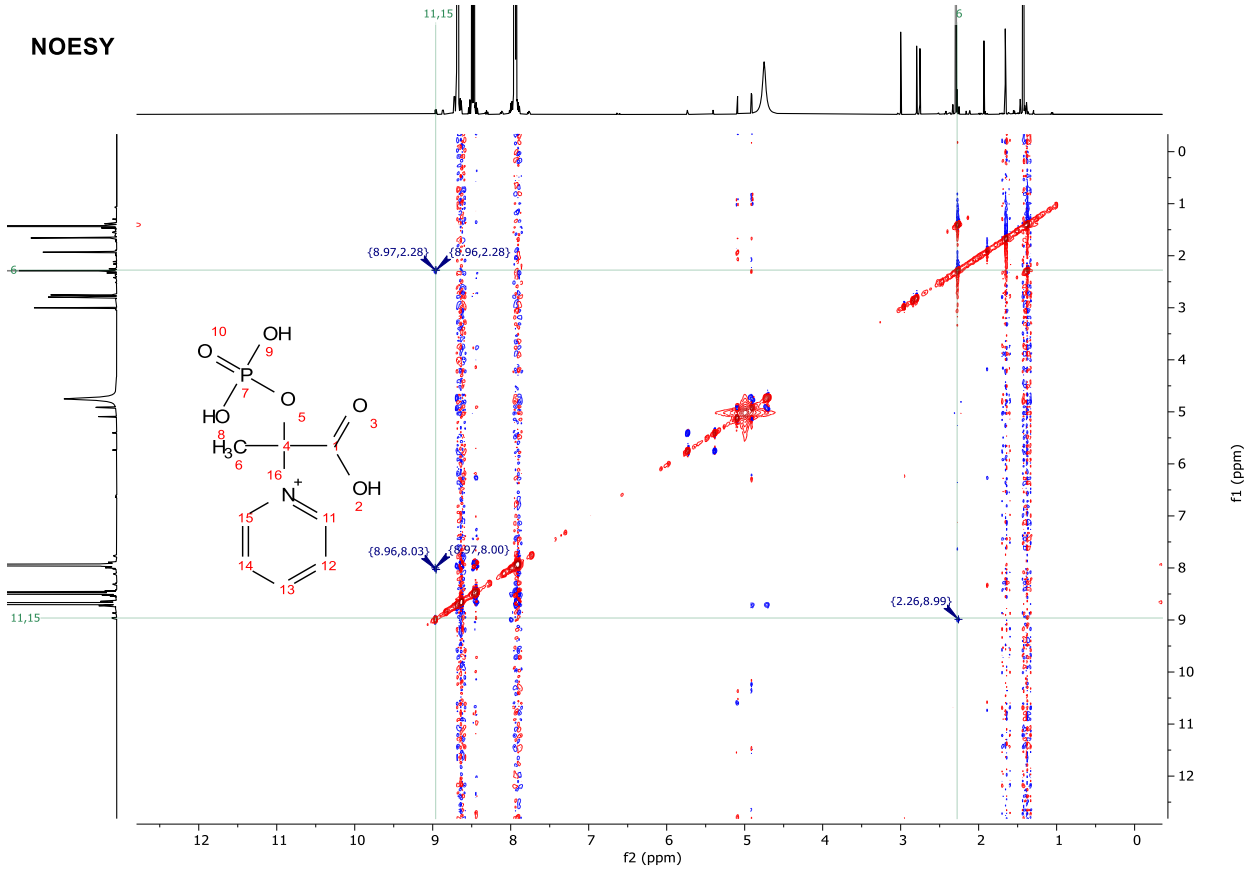

3) PEP (P2-pyr) characterization

^{1}H NMR (500 MHz, D_2O) δ 5.73 (t, J_{HH} = 2.3 Hz, J_{HP} = 2.3 Hz 1 H), 5.40 (t, J_{HH} = 2.2 Hz, J_{HP} = 2.2 Hz, 1 H) ppm.

^{13}C NMR (126 MHz, D_2O) δ 165.8 (d, J_{CP} = 6.8 Hz, C-1), 143.9 (d, J_{CP} = 7.1 Hz, C-2)), 109.7 (d, J_{CP} = 4.0 Hz, C-3) ppm.

^{31}P NMR (202 MHz, D_2O) δ -4.41 (t, J_{HP} = 2.2 Hz) ppm.

HRMS (ESI $^{-}$): Calcd m/z for $[C_3H_4O_6P]$ $[M-H]^{-}$: 166.9751; Found: 166.9742 (-5.4274 ppm).

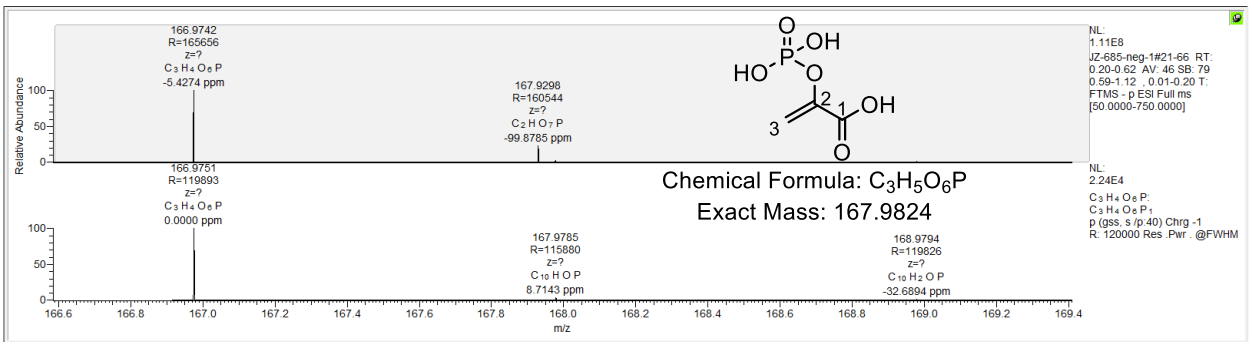

4) P3-pyr characterization (in CD_3CN)

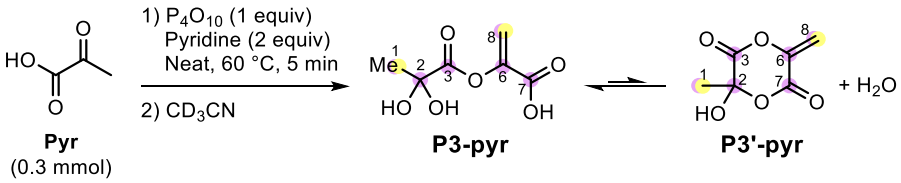

P3-pyr, which was observed after dissolving the paste in water, could be characterized in CD_3CN, where **P3-pyr** proved to be the main species after suspending the paste. In water, **P3-pyr** proved to be stable at room temperature in acidic conditions, but hydrolyzed when the solution was heated at 90 °C (Table S6). The NMR shifts observed correspond could also be those of the cyclic form **P3'-pyr**. Both **P3-pyr** and **P3'-pyr** were observed by HRMS (see below).

^{1}H NMR (500 MHz, CD_3CN) δ 5.08 (d, J_{HH} = 2.8 Hz, 1 H, H-8), 4.88 (d, J_{HH} 2.8 Hz, 1 H, H-8), 1.80 (s, 3 H, H-1) ppm.

^{13}C NMR (126 MHz, CD_3CN) δ 169.2 (C-3), 163.4(C-7), 145.4(C-6), 106.3(C-8), 90.9(C-2), 21.1(C-1) ppm.

HRMS (ESI$^-$): Calcd m/z for $[C_6H_6O_6]$ $[M-H]^{\cdot-}$: 175.0248; Found: 175.0240 (-4.7237 ppm).

HRMS (ESI$^-$): Calcd m/z for $[C_6H_5O_5]$ $[M-H]^{\cdot-}$: 157.0142; Found: 157.0133 (-5.7813 ppm).

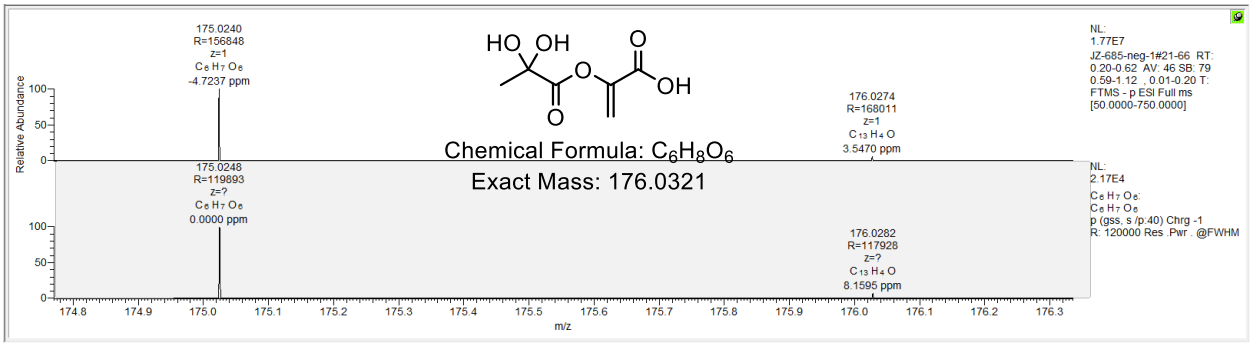

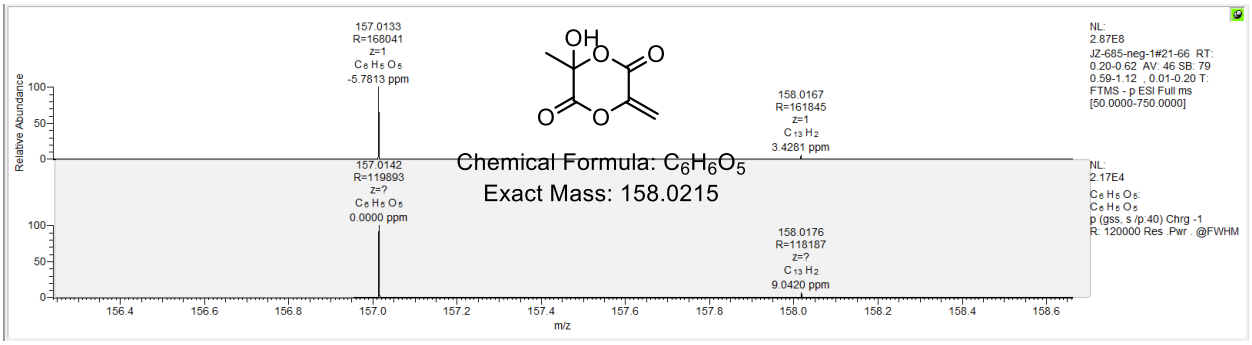

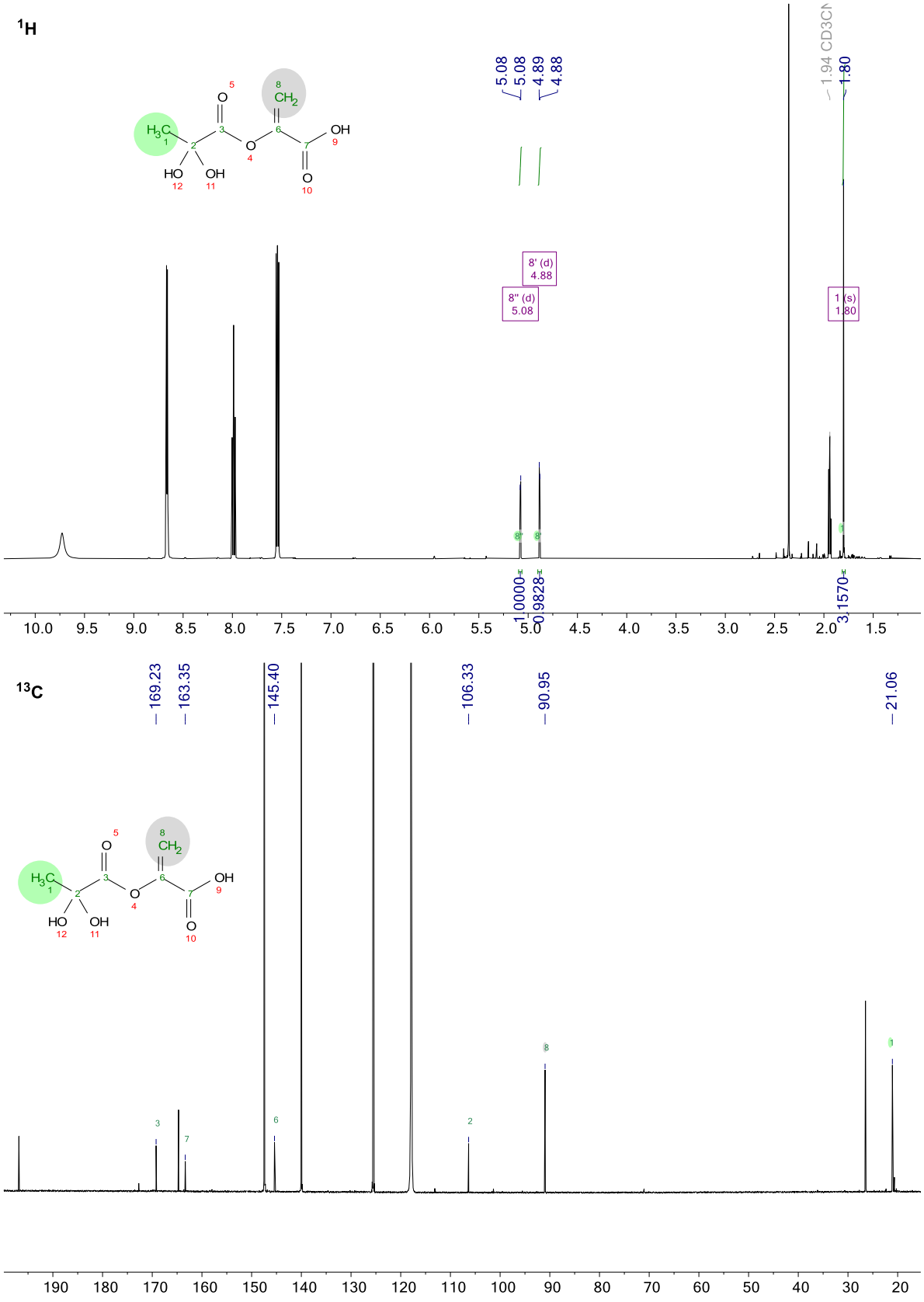
1H
5.08
5.08
4.89
4.88
1.94 CD3CN
1.80
8' (d)
4.88
8'' (d)
5.08
1 (s)
1.80
1.0000
0.9828
3.1570
13C
169.23
163.35
145.40
106.33
90.95
21.06

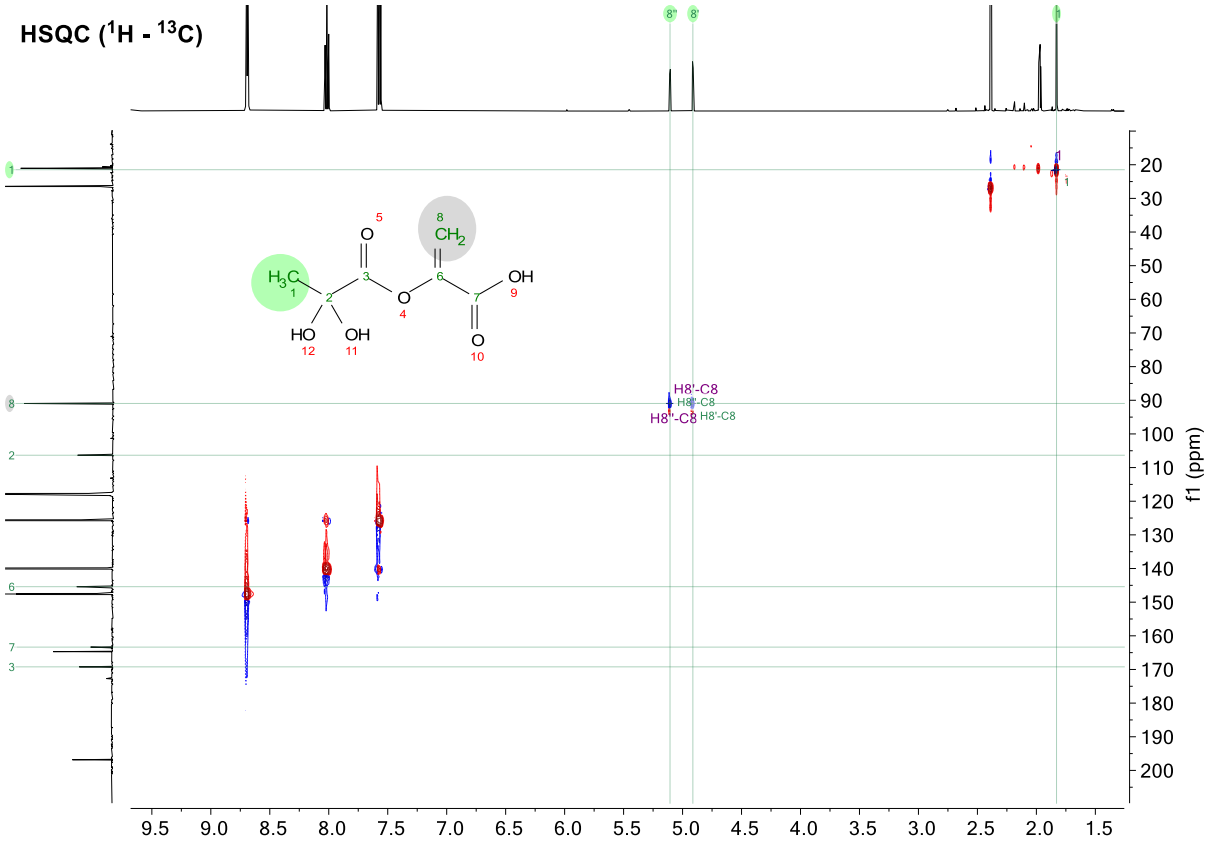
HSQC (^{1}H - ^{13}C)
H8''-C8
H8'-C8
f1 (ppm)

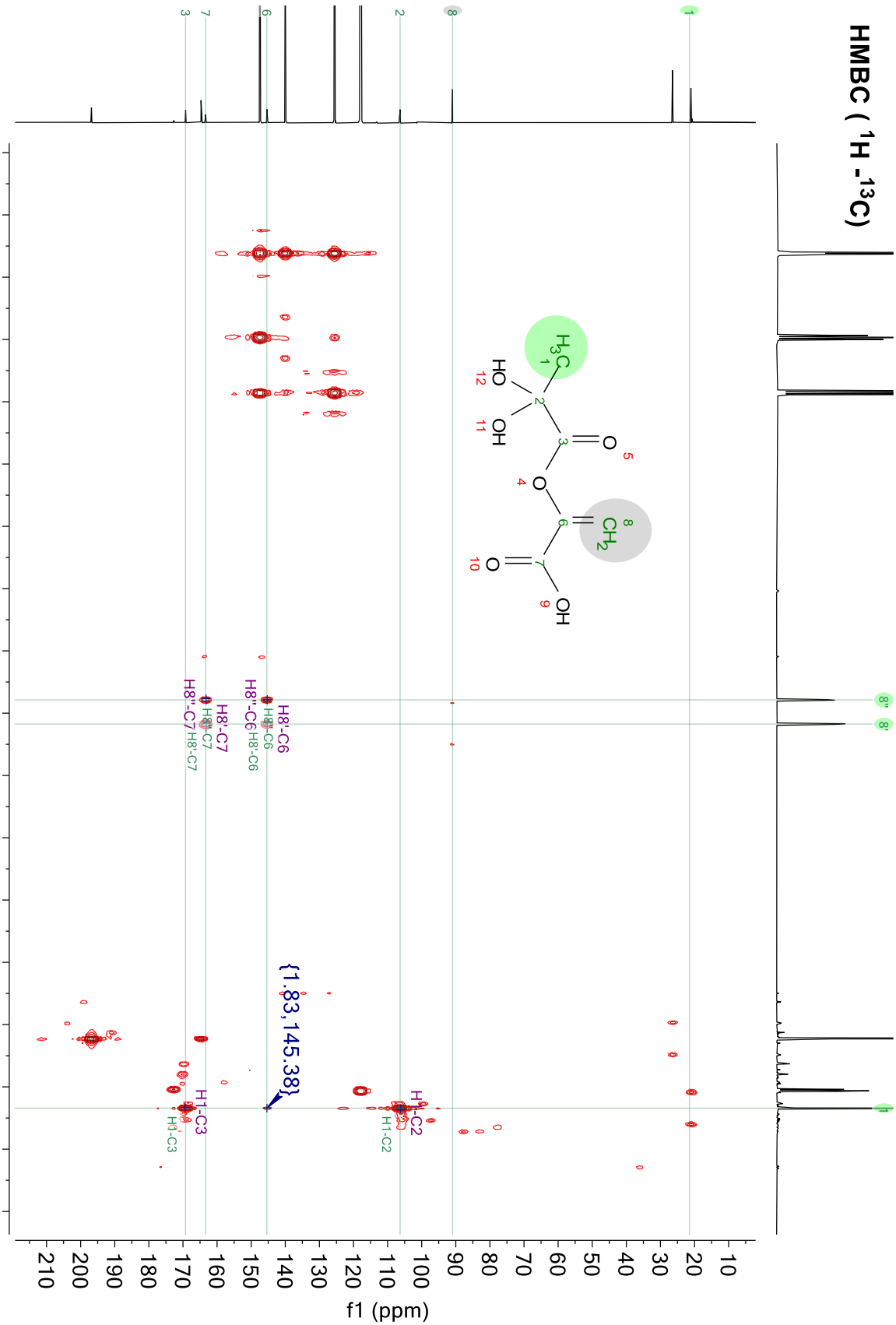
HMBC (1H -13C)
f1 (ppm)
{1.83,145.38}
H8'-C6
H8''-C6
H8'-C7
H8''-C7
H1-C2
H1-C3

5) Characterization of the different species in solution (in D_2O)

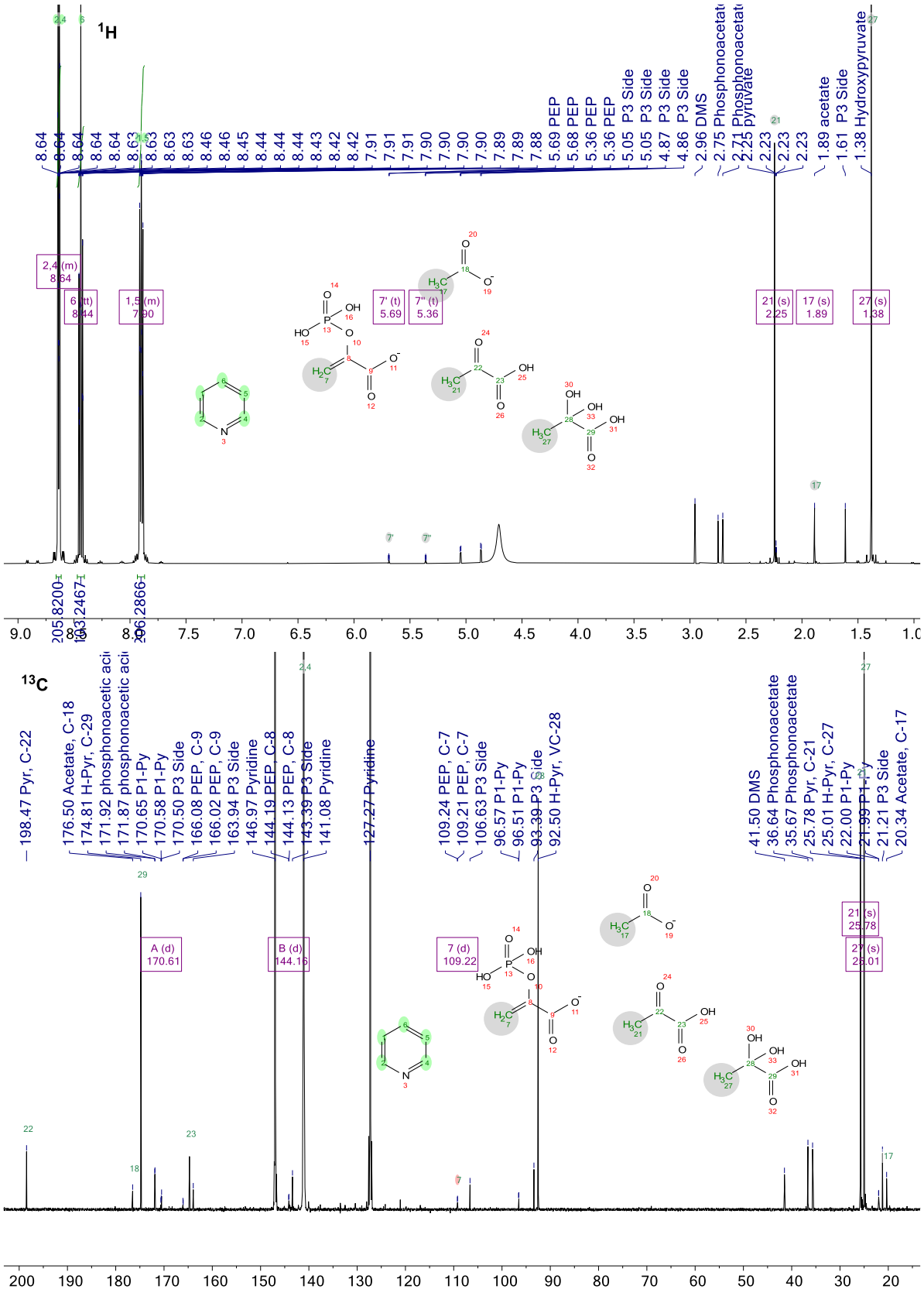

6) Enolphosphate of phenylpyruvic acid, P2-Ph

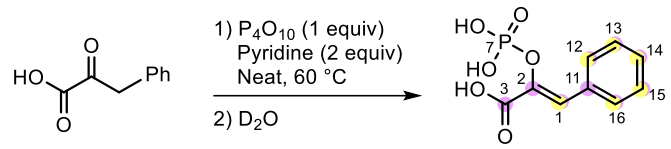

phenylpyruvic acid
(0.3 mmol)

P2-Ph

^{1}H NMR (500 MHz, D_2O) δ 7.64 – 7.62 (m, 2 H, H-12, H-16), 7.30 – 7.23 (m, 3 H, H-13, H-14, H-15), 7.00 (d, J_{HP} = 1.8 Hz, 1 H, H-1) ppm.

^{13}C NMR (126 MHz, D_2O) δ 167.1 (d, J_{CP} = 1.2 Hz, C-3), 137.0 (d, J_{CP} = 8.3 Hz, C-2), 131.9 (d, J_{CP} = 2.2 Hz, C-11), 130.3 (C-12, C-16), 129.8 (C-13, C-14, C-15), 125.6 (d, J_{CP} = 6.4 Hz, C-1) ppm.

^{31}P NMR (202 MHz, D_2O) δ -4.72 (d, J_{HP} = 1.7 Hz) ppm.

HRMS (ESI$^+$): Calcd m/z for $[C_9H_{10}O_6P]$ $[M+H]^+$: 245.0210; Found: 245.0210 (0.2968 ppm).

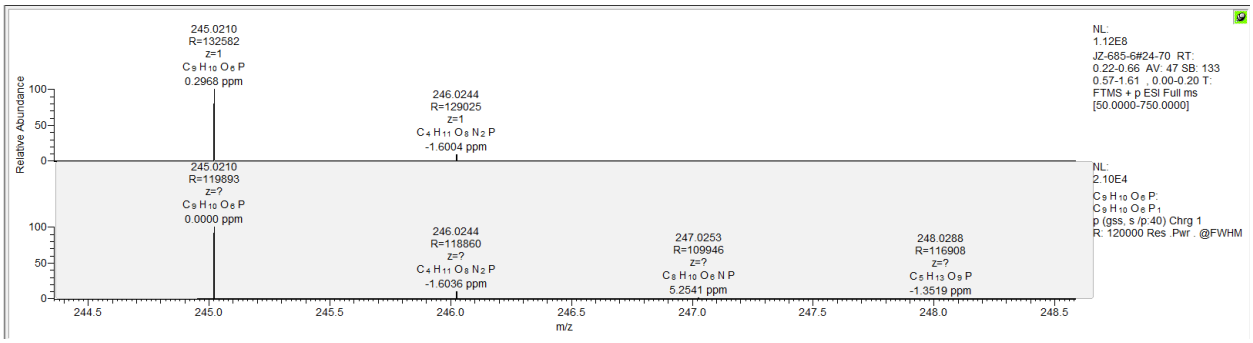

^{1}H NMR chemical shifts are in accordance with a previously reported synthesis of **P2-Ph**.[4]

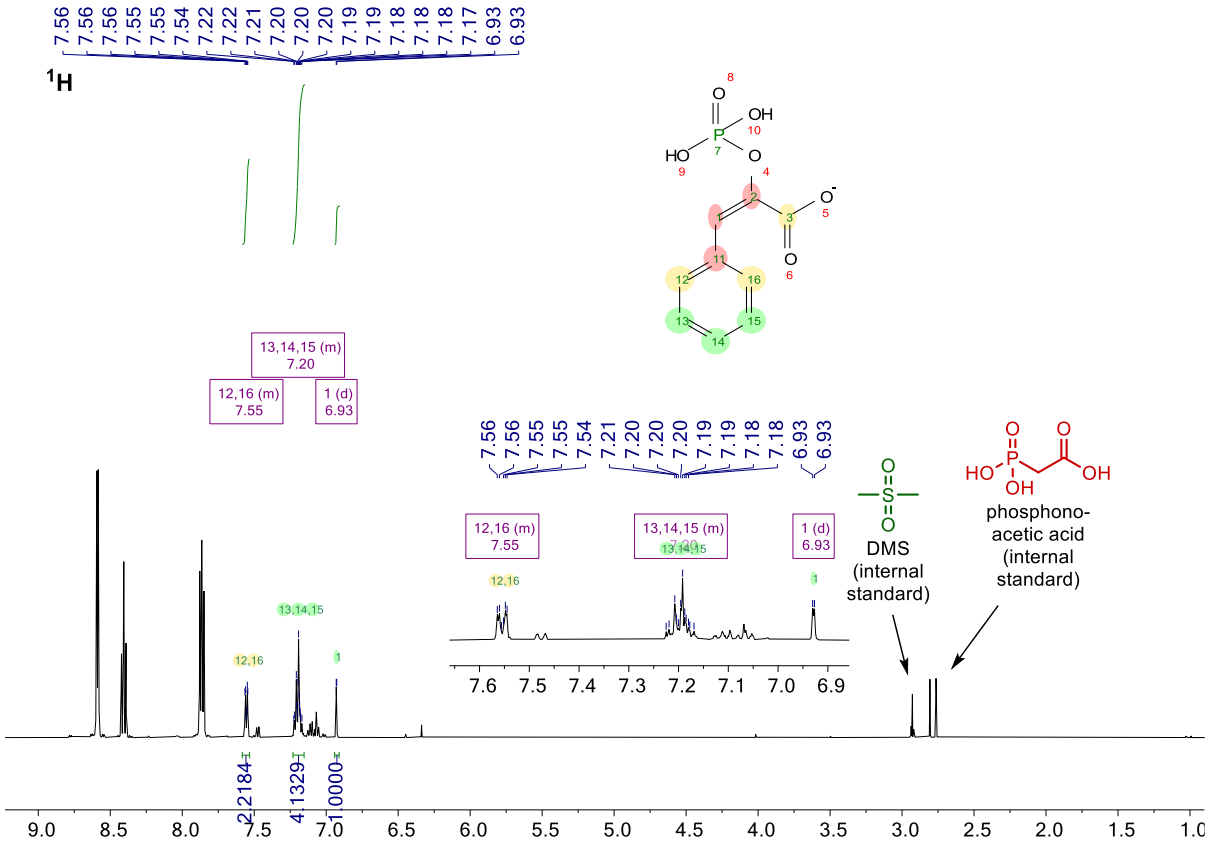
7.56 7.56 7.56 7.55 7.55 7.54 7.22 7.22 7.21 7.20 7.20 7.20 7.19 7.19 7.18 7.18 7.18 7.17 6.93 6.93
1H
13,14,15 (m) 7.20
12,16 (m) 7.55
1 (d) 6.93
DMS (internal standard)
phospho-acetic acid (internal standard)
2.2184
4.1329
1.0000

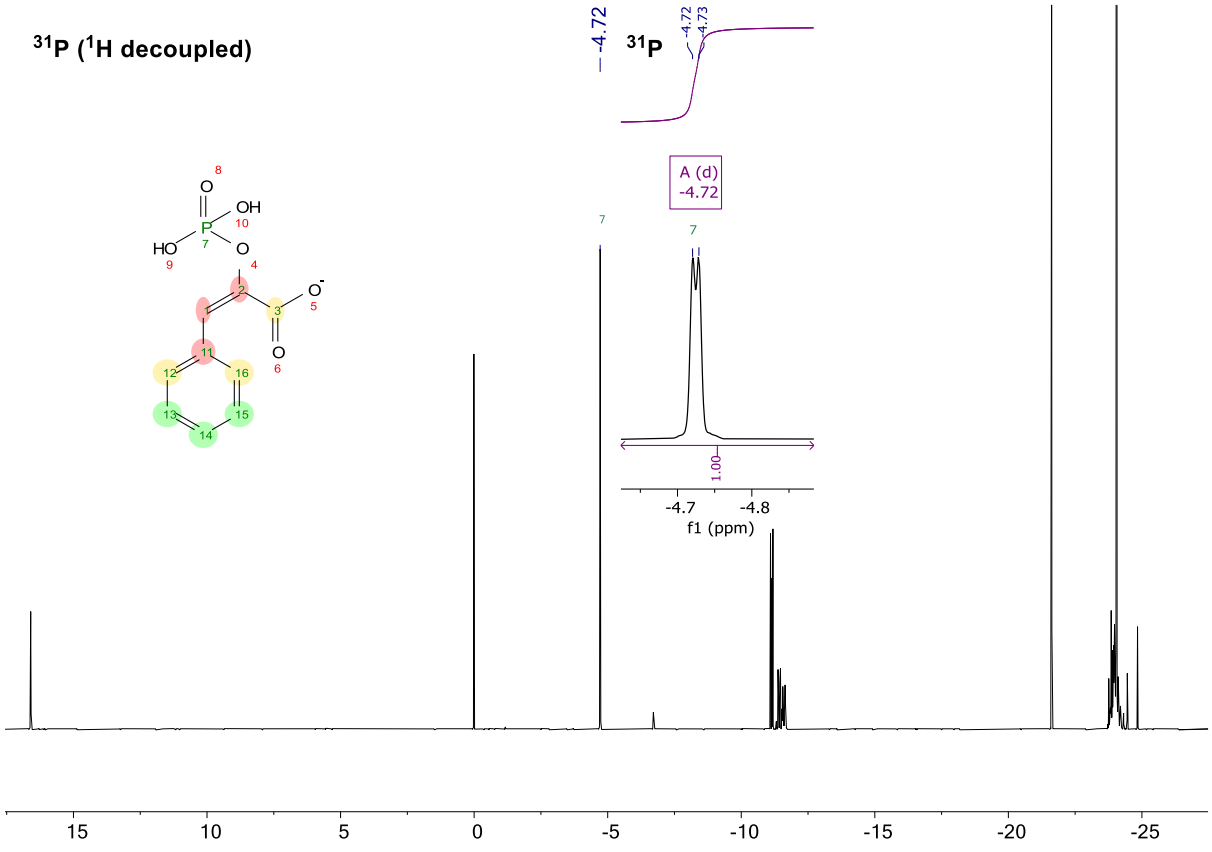
31P (1H decoupled)
-4.72
31P
A (d) -4.72
1.00
f1 (ppm)

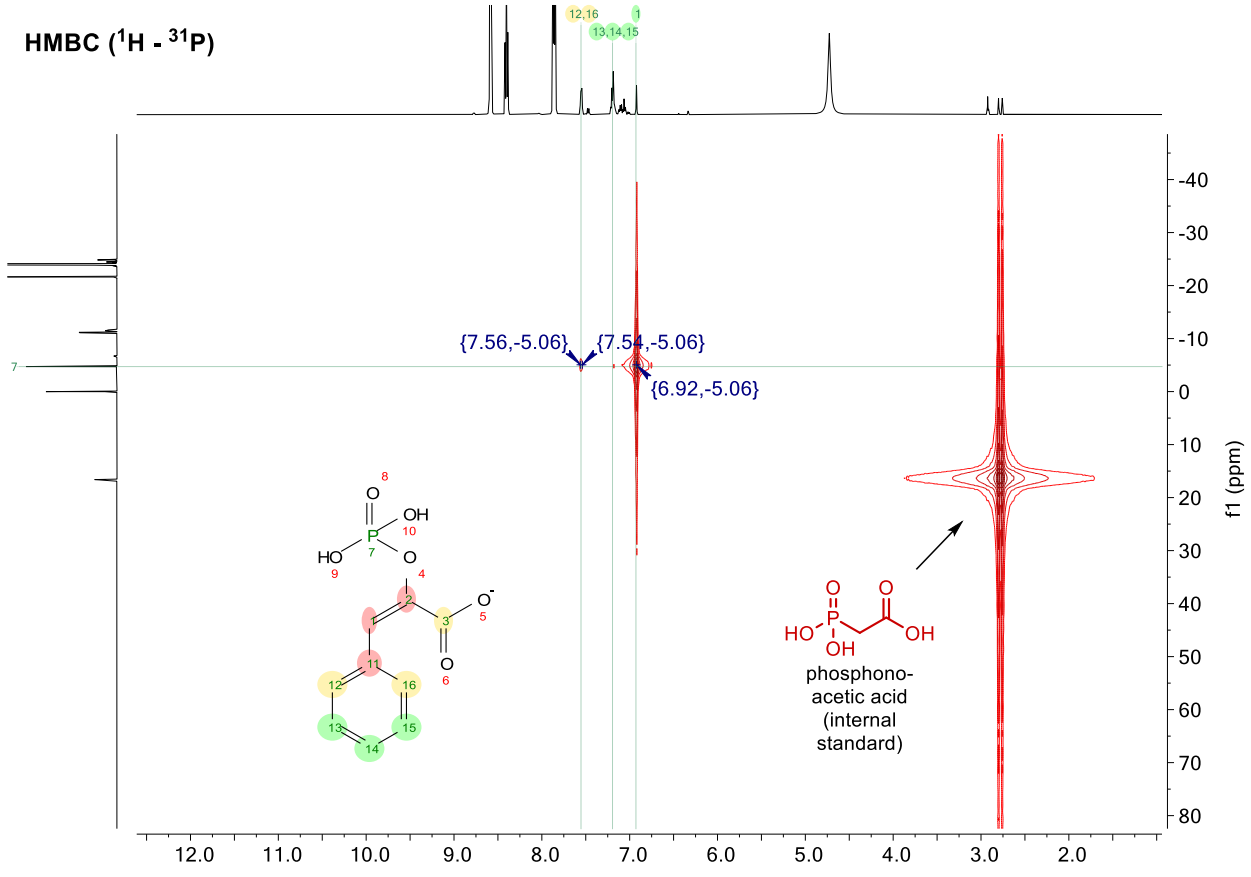
HMBC (^{1}H - ^{31}P)
12,16
13,14,15
1
{7.56,-5.06}
{7.54,-5.06}
{6.92,-5.06}
phosphono-
acetic acid
(internal
standard)
f1 (ppm)
12.0
11.0
10.0
9.0
8.0
7.0
6.0
5.0
4.0
3.0
2.0

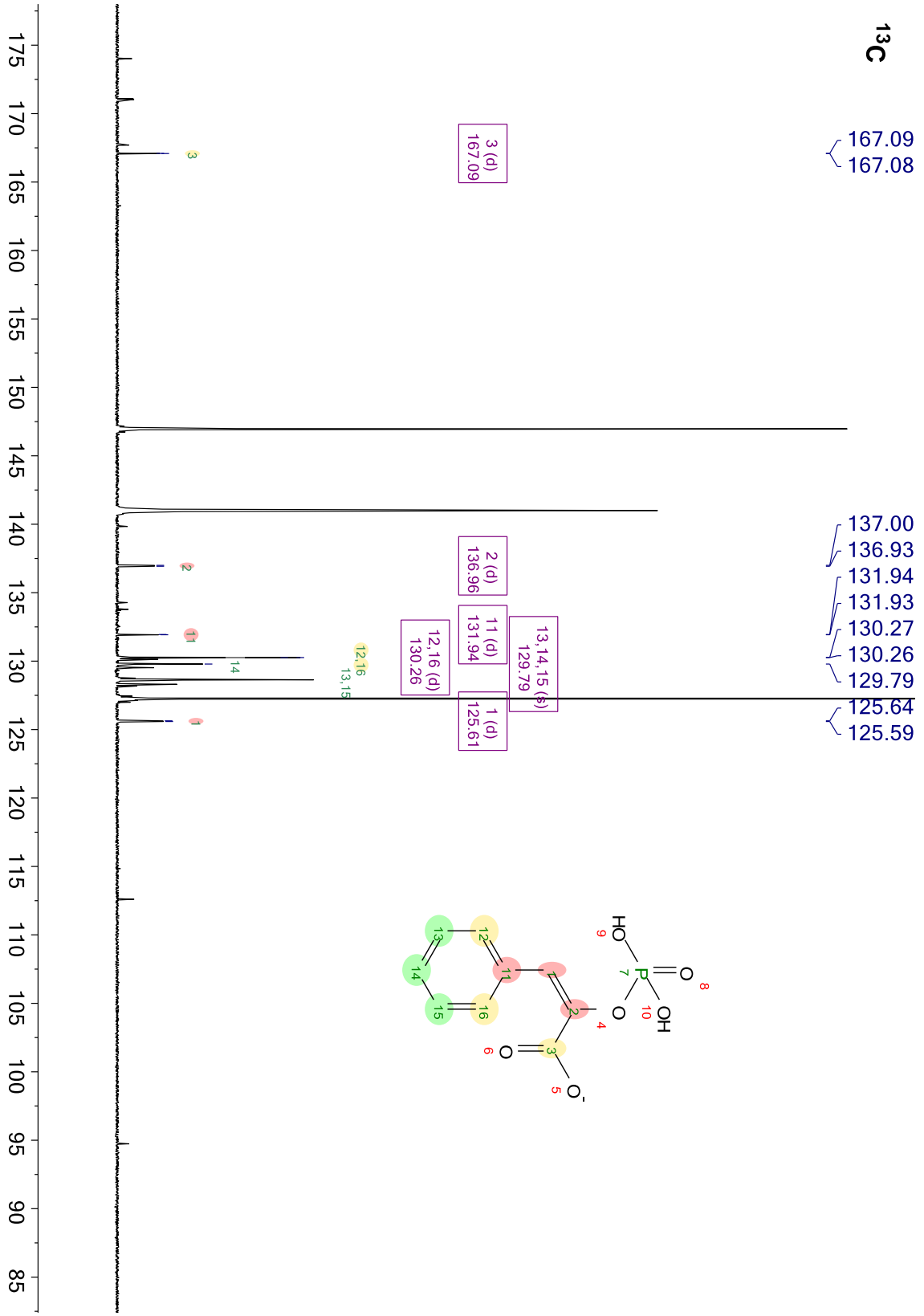
13C
167.09
167.08
137.00
136.93
131.94
131.93
130.27
130.26
129.79
125.64
125.59
3 (d)
167.09
2 (d)
136.96
11 (d)
131.94
12,16 (d)
130.26
13,14,15 (s)
129.79
1 (d)
125.61
HO
O
P
O
OH
O
O
O
O
175
170
165
160
155
150
145
140
135
130
125
120
115
110
105
100
95
90
85

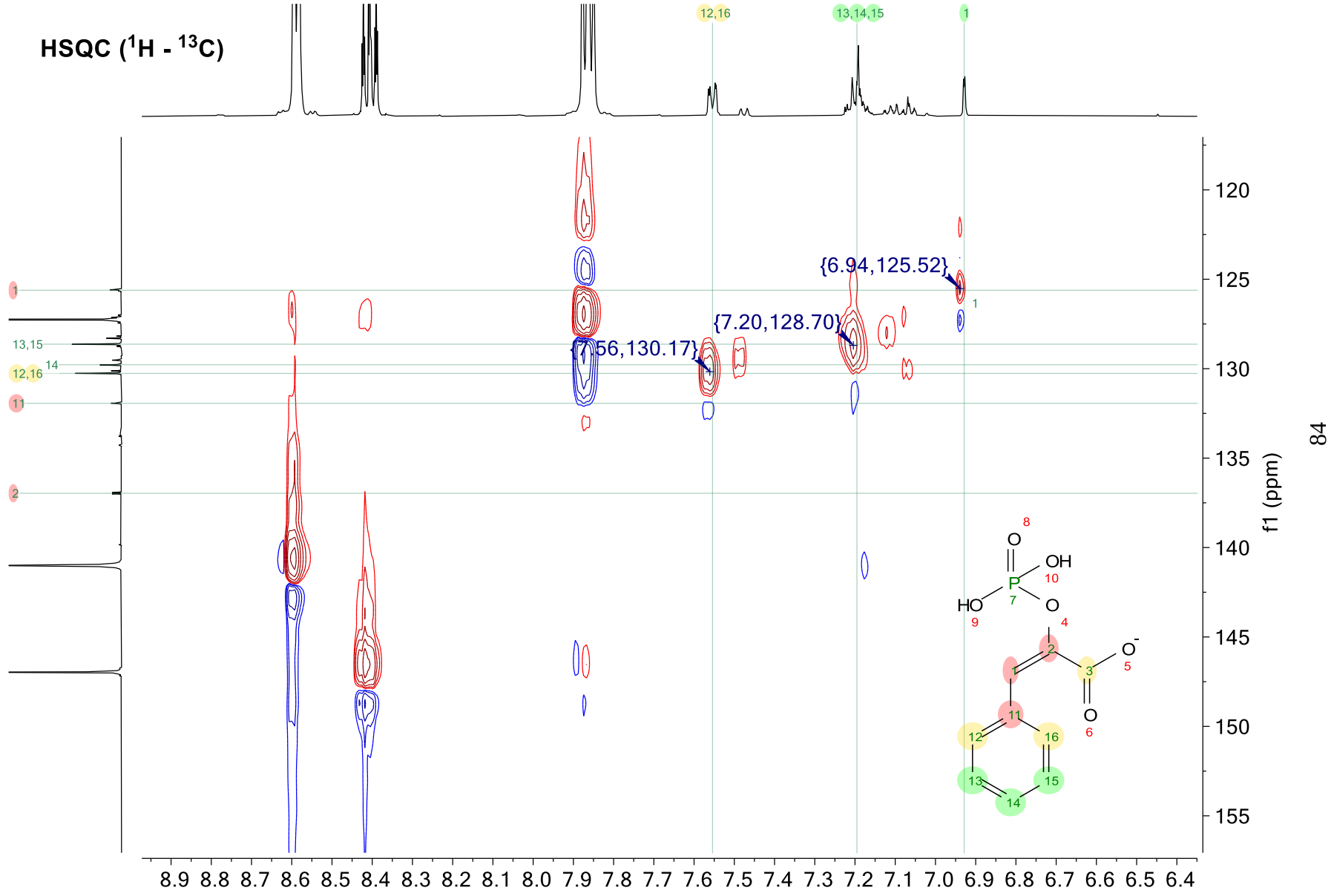
HSQC (^{1}H - ^{13}C)
12,16
13,14,15
1
{6.94,125.52}
{7.20,128.70}
{7.56,130.17}
13,15
12,16
14
11
2
f1 (ppm)
84
8.9 8.8 8.7 8.6 8.5 8.4 8.3 8.2 8.1 8.0 7.9 7.8 7.7 7.6 7.5 7.4 7.3 7.2 7.1 7.0 6.9 6.8 6.7 6.6 6.5 6.4
120 125 130 135 140 145 150 155
OH
HO
P
O

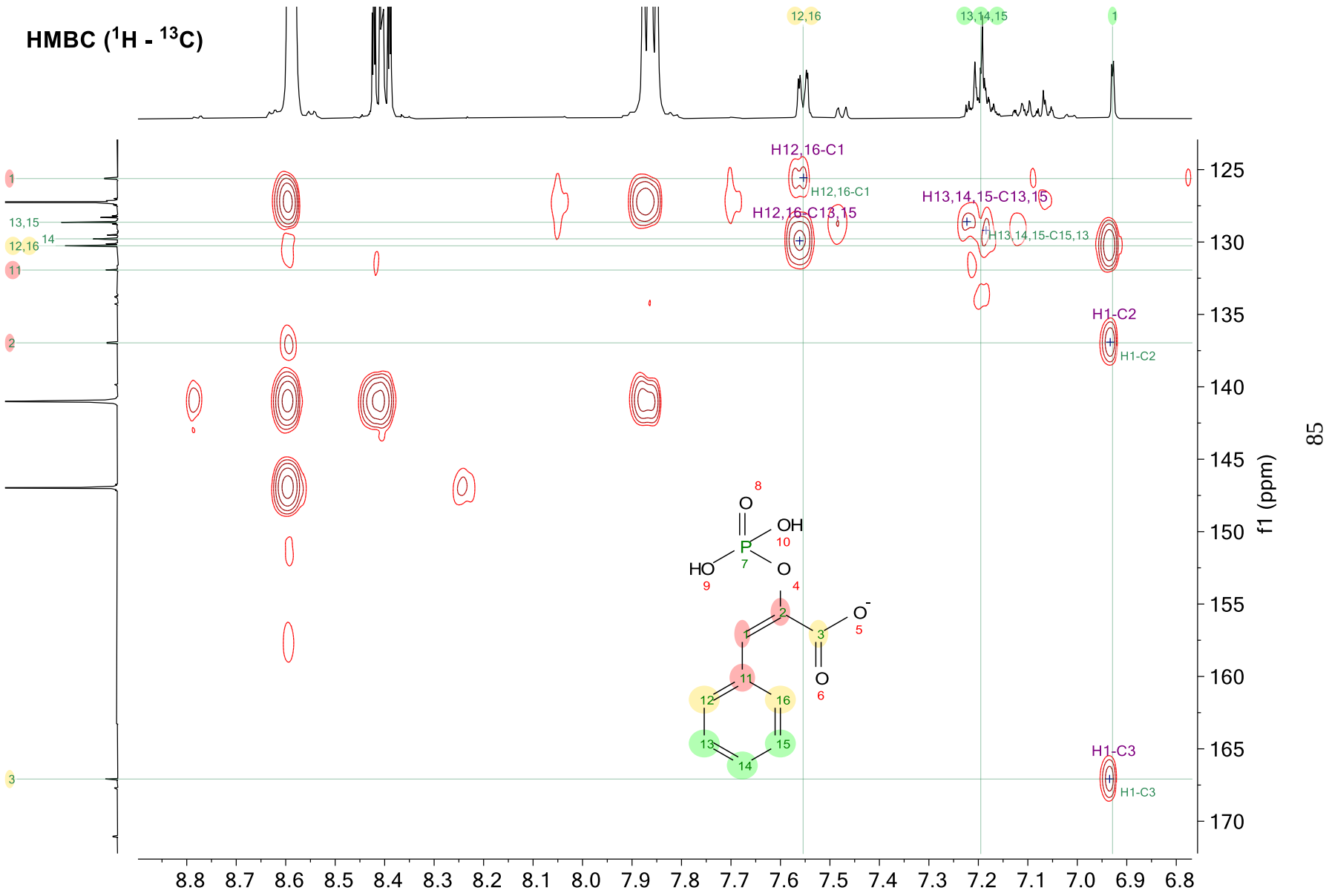
HMBC (^{1}H - ^{13}C)
12,16
13,14,15
1
H12,16-C1
H12,16-C1
H12,16-C13,15
H13,14,15-C13,15
H13,14,15-C15,13
H1-C2
H1-C2
H1-C3
H1-C3
13,15
12,16
14
11
2
3
8
O
OH
10
P
7
HO
9
O
4
2
1
3
O
5
O
6
11
12
16
13
15
14
125
130
135
140
145
150
155
160
165
170
f1 (ppm)
8.8
8.7
8.6
8.5
8.4
8.3
8.2
8.1
8.0
7.9
7.8
7.7
7.6
7.5
7.4
7.3
7.2
7.1
7.0
6.9
6.8

7) Enolphosphate of dimethylpyruvic acid P2-2Me

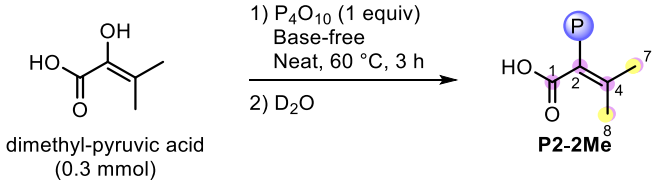

dimethyl-pyruvic acid
(0.3 mmol)

P2-2Me

^{1}H NMR (500 MHz, D_2O) δ 1.94 (d, J_{HP} = 3.2 Hz, 3 H, H-1), 1.79 (d, J_{HP} = 2.4 Hz, 3 H, H-4) ppm.

^{13}C NMR (126 MHz, D_2O) δ 166.4 (d, J_{CP} = 1.0 Hz, C-5), 140.7 (d, J_{CP} = 6.1 Hz C-3), 132.7 (d, J_{CP} = 8.4 Hz C-2), 19.9 (br, C-4), 19.1 (br, C-1) ppm.

^{31}P NMR (202 MHz, D_2O) δ -3.48 (dq, J_{HP} = 3.3 Hz, J_{HP} = 2.3 Hz) ppm.

HRMS (ESI$^-$): Calcd m/z for $[C_5H_8O_6P]$ $[M-H]^-$: 195.0064; Found: 195.0058 (-3.2168 ppm).

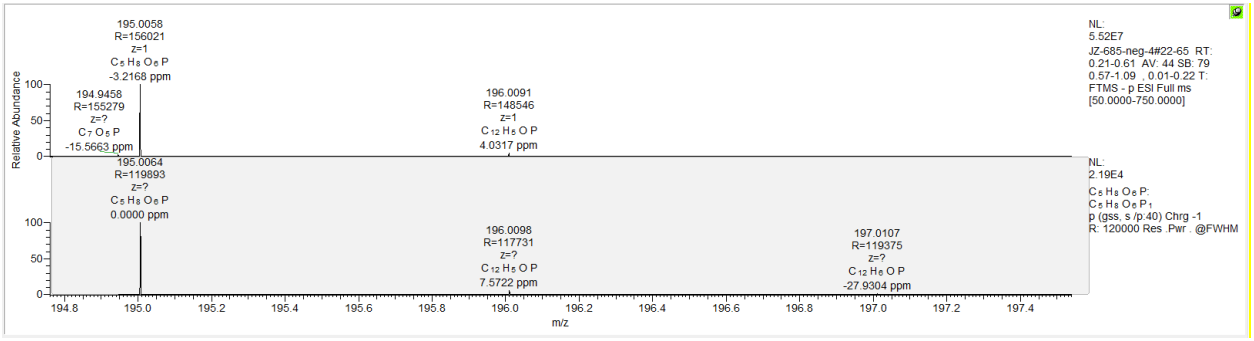

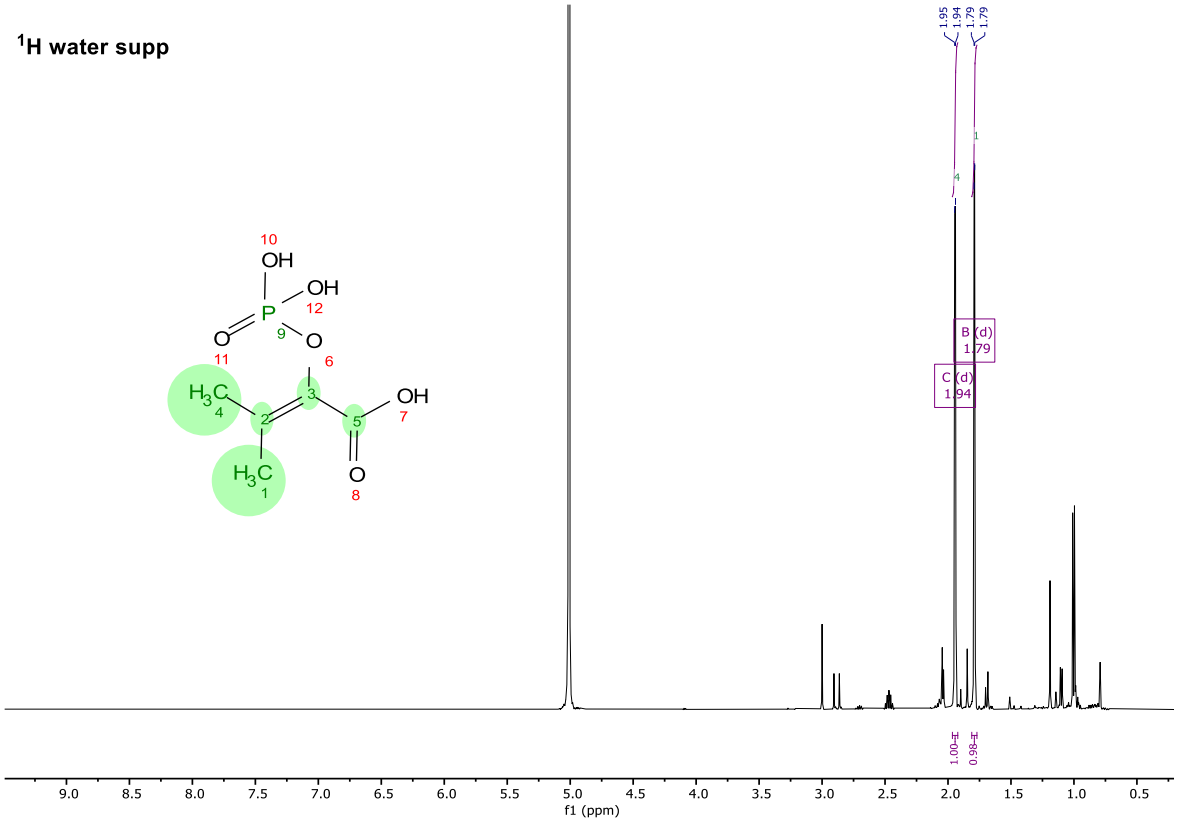

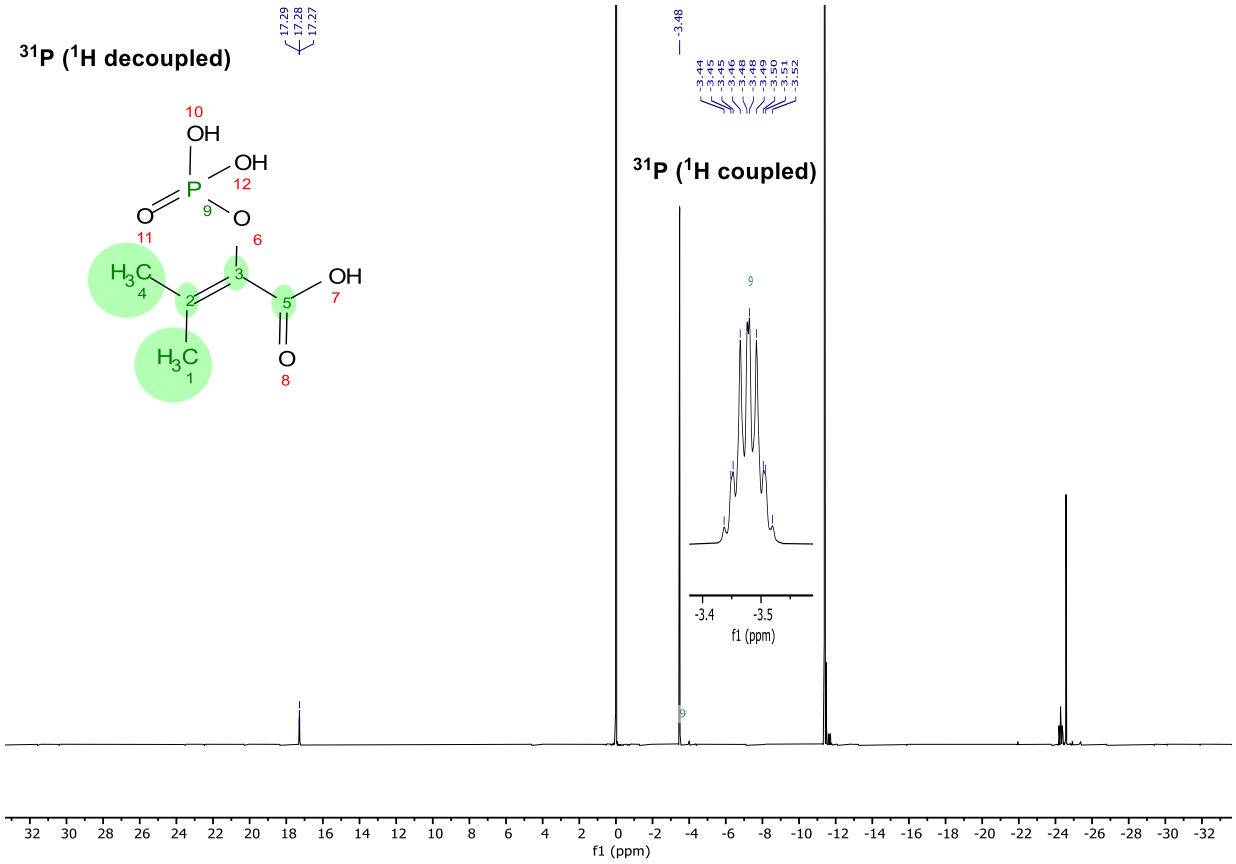
31P (1H decoupled)
31P (1H coupled)
f1 (ppm)

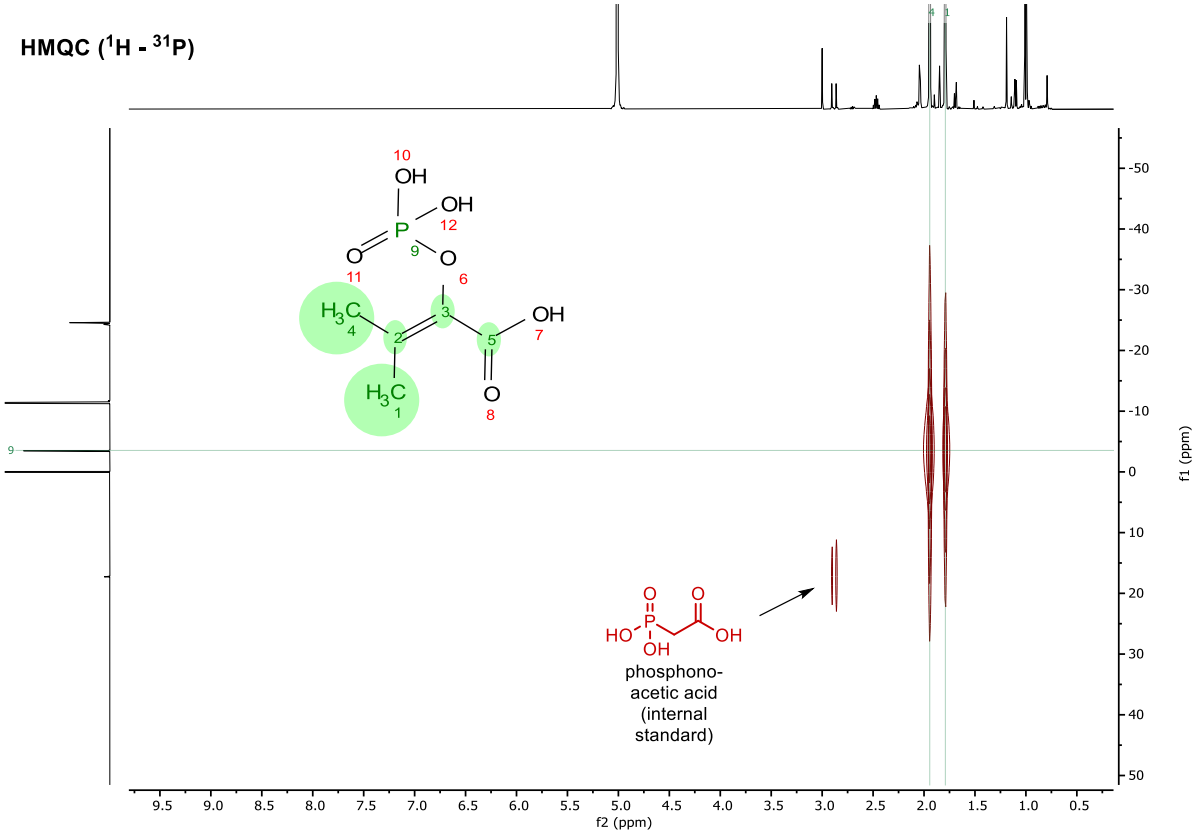
HMQC (1H - 31P)
phosphono-
acetic acid
(internal
standard)
f2 (ppm)
f1 (ppm)

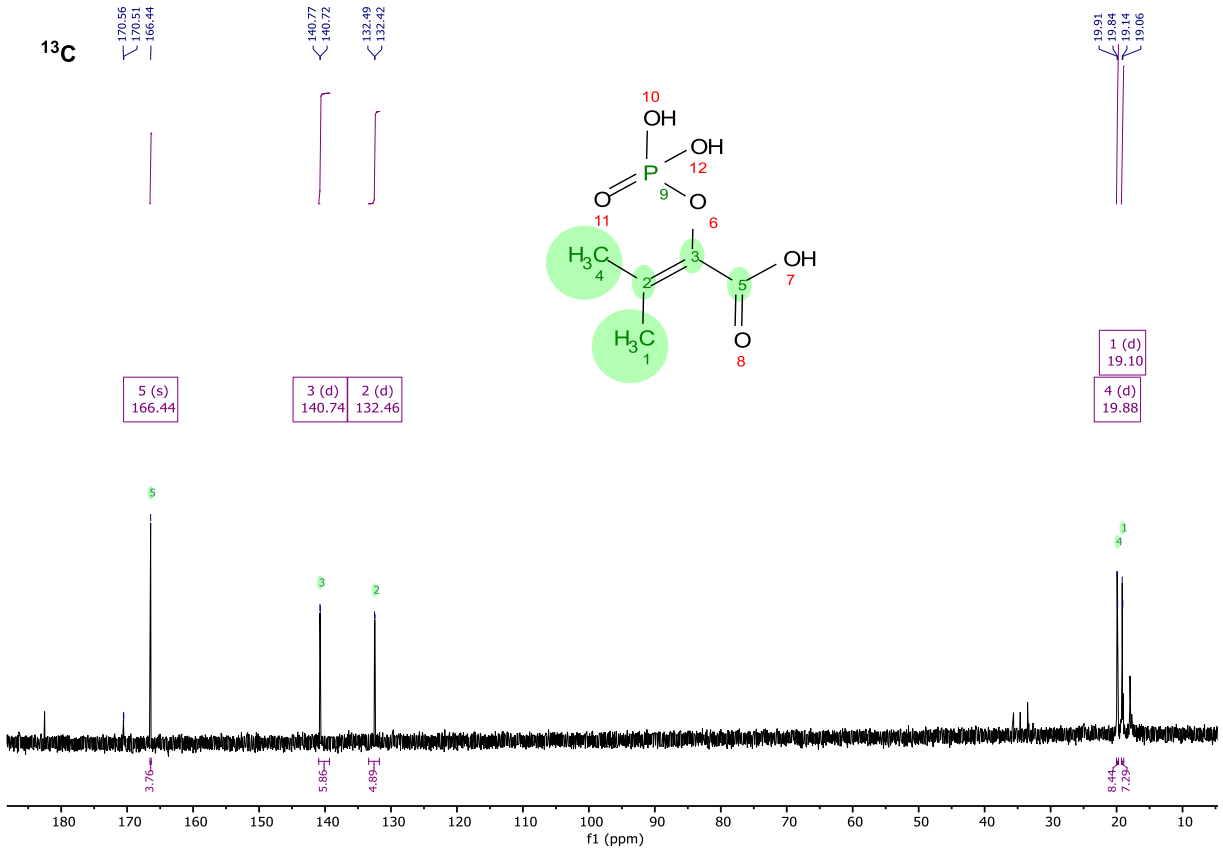
13C
170.56
170.51
166.44
140.77
140.72
132.49
132.42
19.91
19.84
19.14
19.06
5 (s)
166.44
3 (d)
140.74
2 (d)
132.46
1 (d)
19.10
4 (d)
19.88
f1 (ppm)

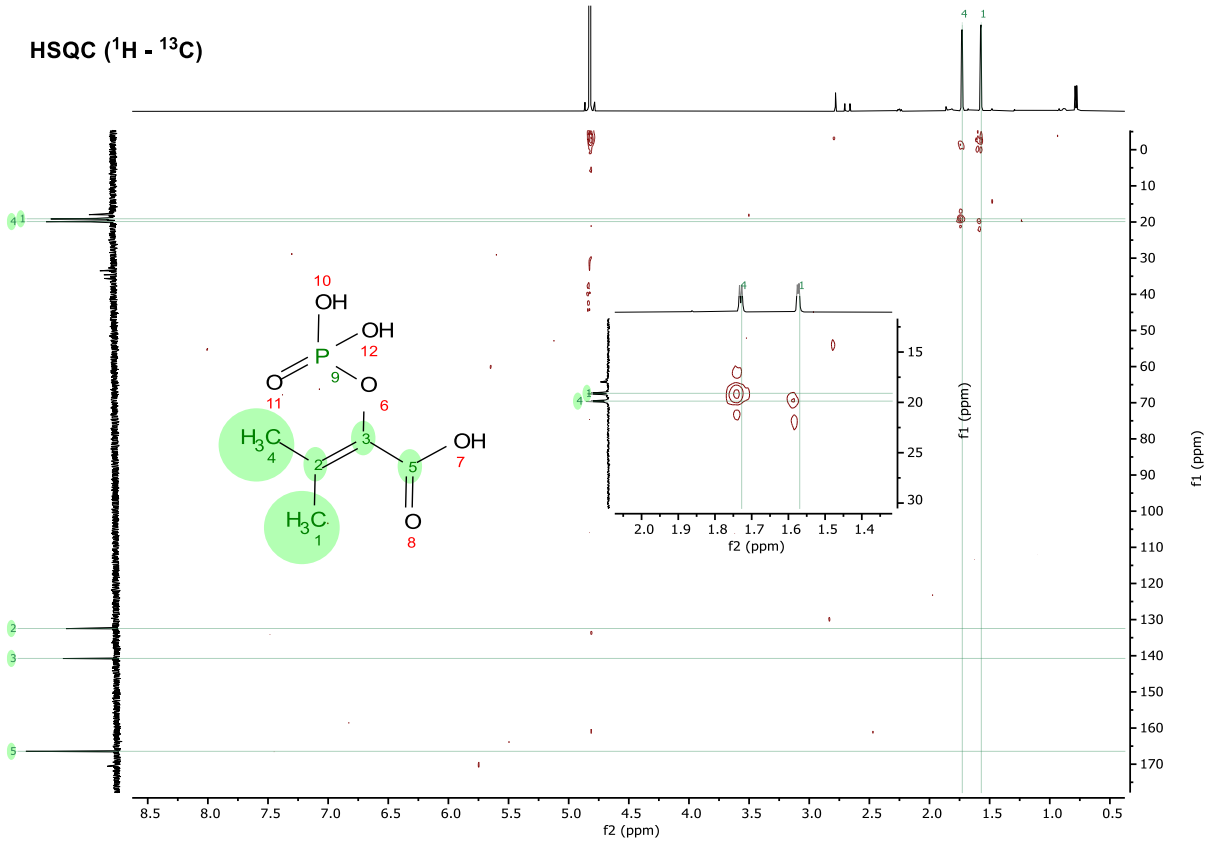
HSQC (1H - 13C)
f2 (ppm)
f1 (ppm)

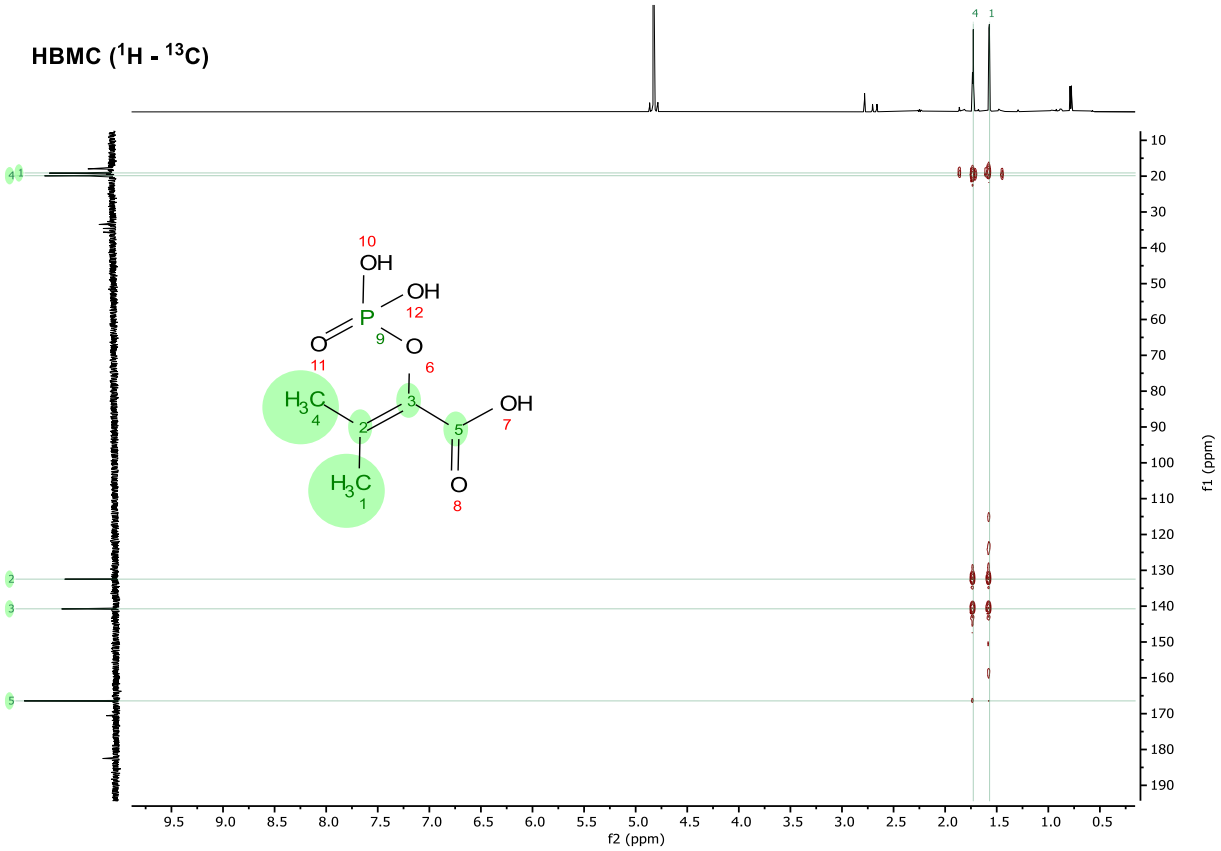

8) Hydroxy-phosphate of trimethylpyruvic acid (pyr-3Me) with Im P1-(pyr-3Me)-im

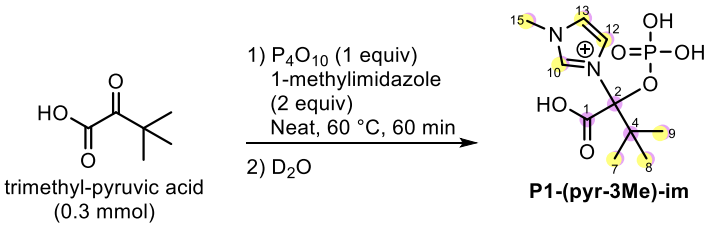

^{1}H NMR (500 MHz, D_2O) δ 9.12 – 9.11 (br, 1 H, H-10), 7.74 – 7.73 (br, 1 H, H-12), 7.36 – 7.35 (br, 1 H, H-13), 3.82 (s, 3 H, H-15), 0.86 (s, 9 H, H-7, H-8, H-9) ppm.

^{13}C NMR (126 MHz, D_2O) δ 168.1 (d, J_{CP} = 2.6 Hz, C-1), 136.1 (br, C-10), 123.6 (br, C-12), 122.5 (br, C-13), 96.9 (d, J_{CP} = 9.6 Hz, C-2) 40.0 (d, J_{CP} = 7.7 Hz, C-4), 36.0 (br, C-15), 23.9 (3 C,C-7, C-8, C-9) ppm.

^{31}P NMR (202 MHz, D_2O) δ -3.66 (s) ppm.

HRMS (ESI$^+$): Calcd m/z for [$C_{10}H_{18}O_6N_2P^+$] [M]$^+$: 293.0897; Found: 293.0895 (-0.7891 ppm).

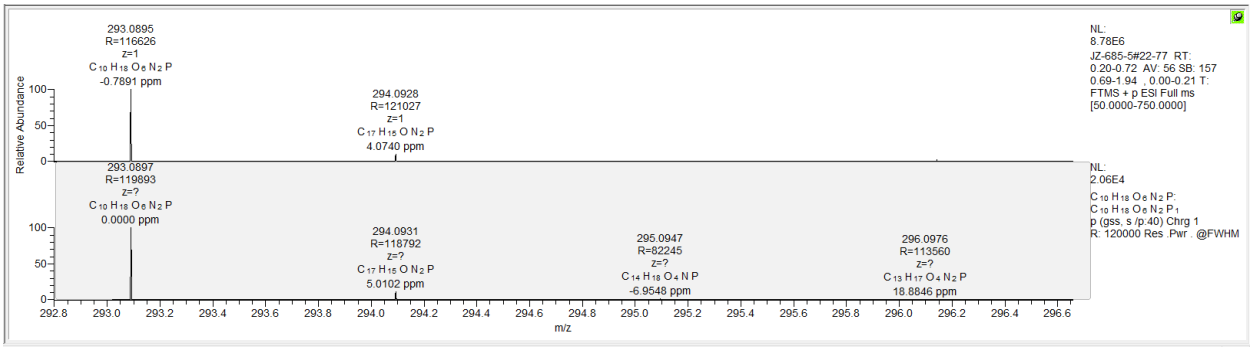
293.0895
R=116626
z=1
C 10 H 18 O 6 N 2 P
-0.7891 ppm
294.0928
R=121027
z=1
C 17 H 15 O N 2 P
4.0740 ppm
293.0897
R=119893
z=?
C 10 H 18 O 6 N 2 P
0.0000 ppm
294.0931
R=118792
z=?
C 17 H 15 O N 2 P
5.0102 ppm
295.0947
R=82245
z=?
C 14 H 18 O 4 N P
-6.9548 ppm
296.0976
R=113560
z=?
C 13 H 17 O 4 N 2 P
18.8846 ppm
Relative Abundance
m/z
NL:
8.78E6
JZ-685-5#22-77 RT:
0.20-0.72 AV: 56 SB: 157
0.69-1.94 , 0.00-0.21 T:
FTMS + p ESI Full ms
[50.0000-750.0000]
NL:
2.06E4
C 10 H 18 O 6 N 2 P:
C 10 H 18 O 6 N 2 P 1
p (gss, s /p:40) Chrg 1
R: 120000 Res .Pwr . @FWHM

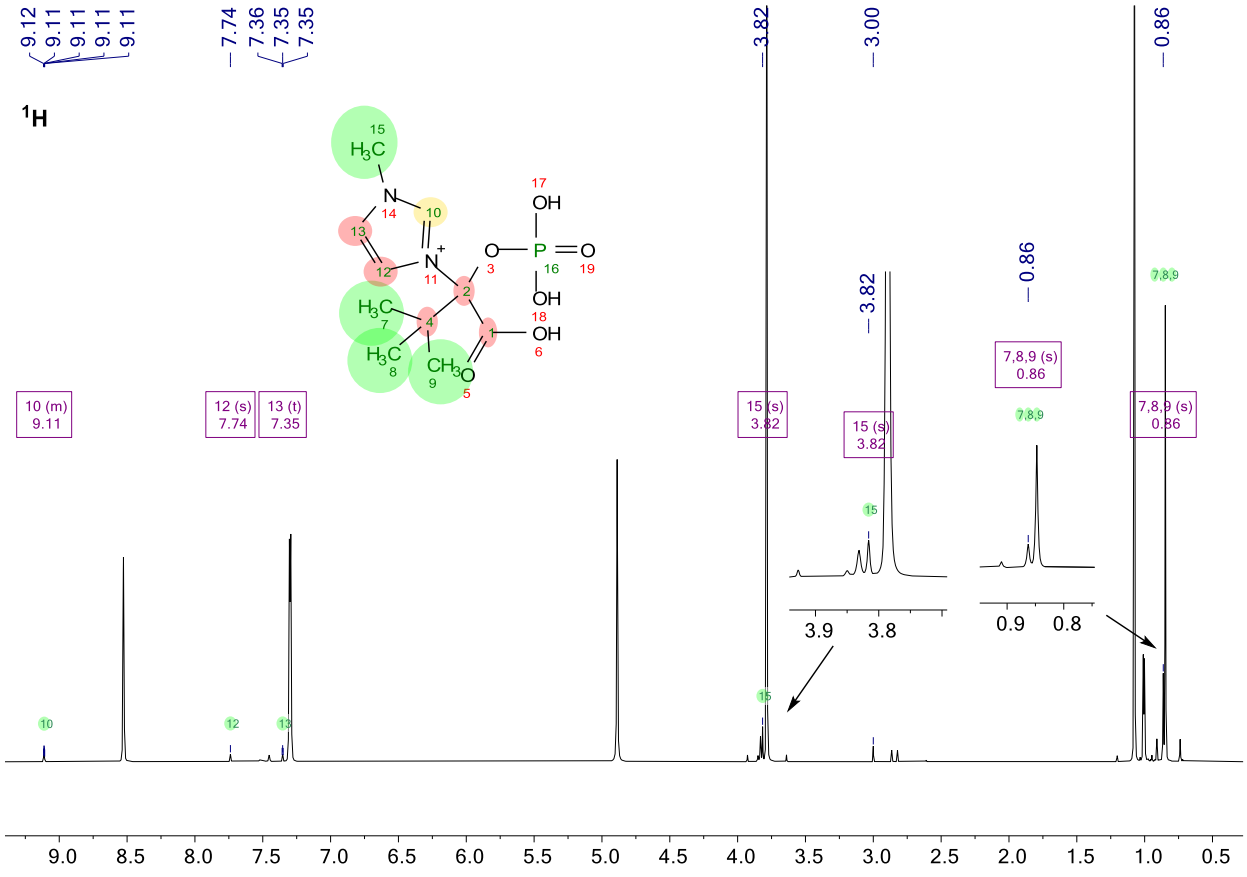
9.12
9.11
9.11
9.11
9.11
7.74
7.36
7.35
7.35
3.82
3.00
0.86
1H
10 (m)
9.11
12 (s)
7.74
13 (t)
7.35
15 (s)
3.82
15 (s)
3.82
7,8,9 (s)
0.86
7,8,9 (s)
0.86
7,8,9
3.9
3.8
0.9
0.8
9.0
8.5
8.0
7.5
7.0
6.5
6.0
5.5
5.0
4.5
4.0
3.5
3.0
2.5
2.0
1.5
1.0
0.5

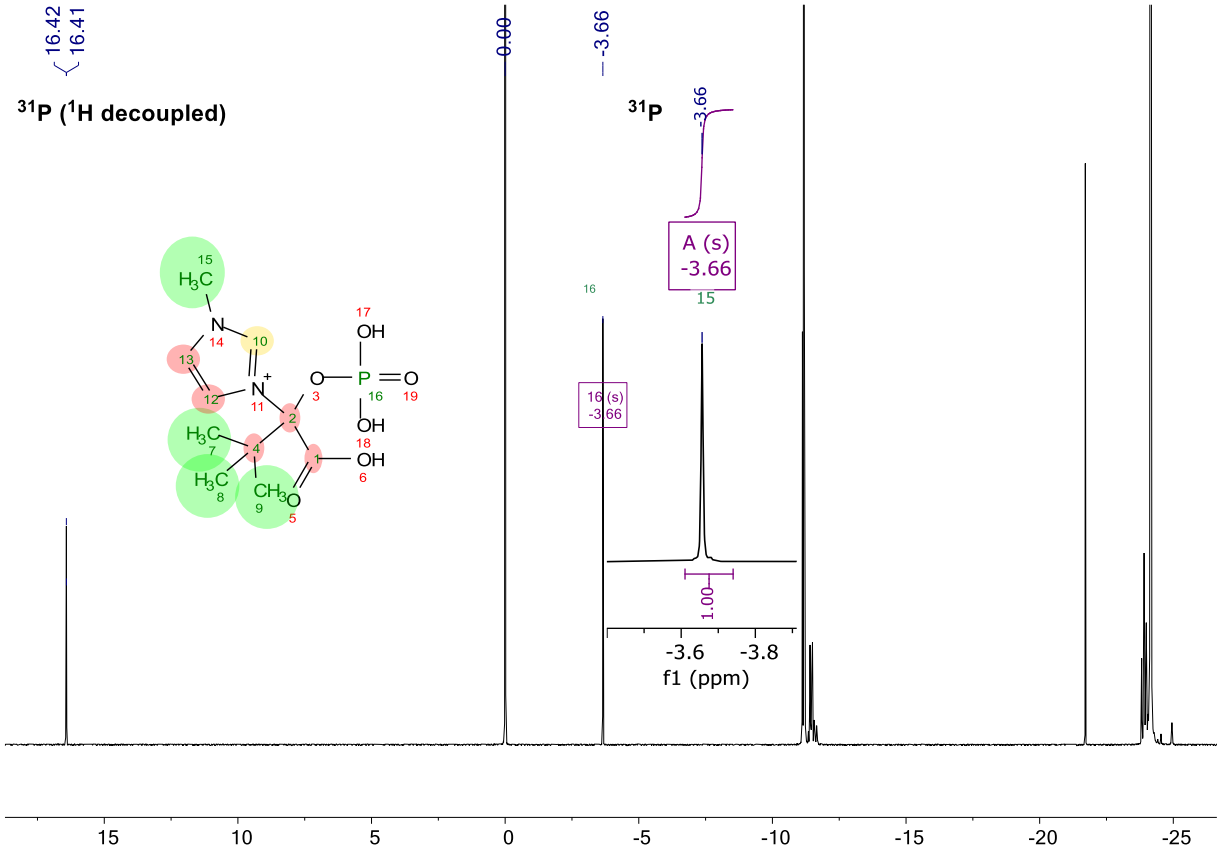
16.42
16.41
0.00
-3.66
31P (1H decoupled)
31P
-3.66
A (s)
-3.66
15
16
16 (s)
-3.66
1.00
-3.6
-3.8
f1 (ppm)
15
10
5
0
-5
-10
-15
-20
-25

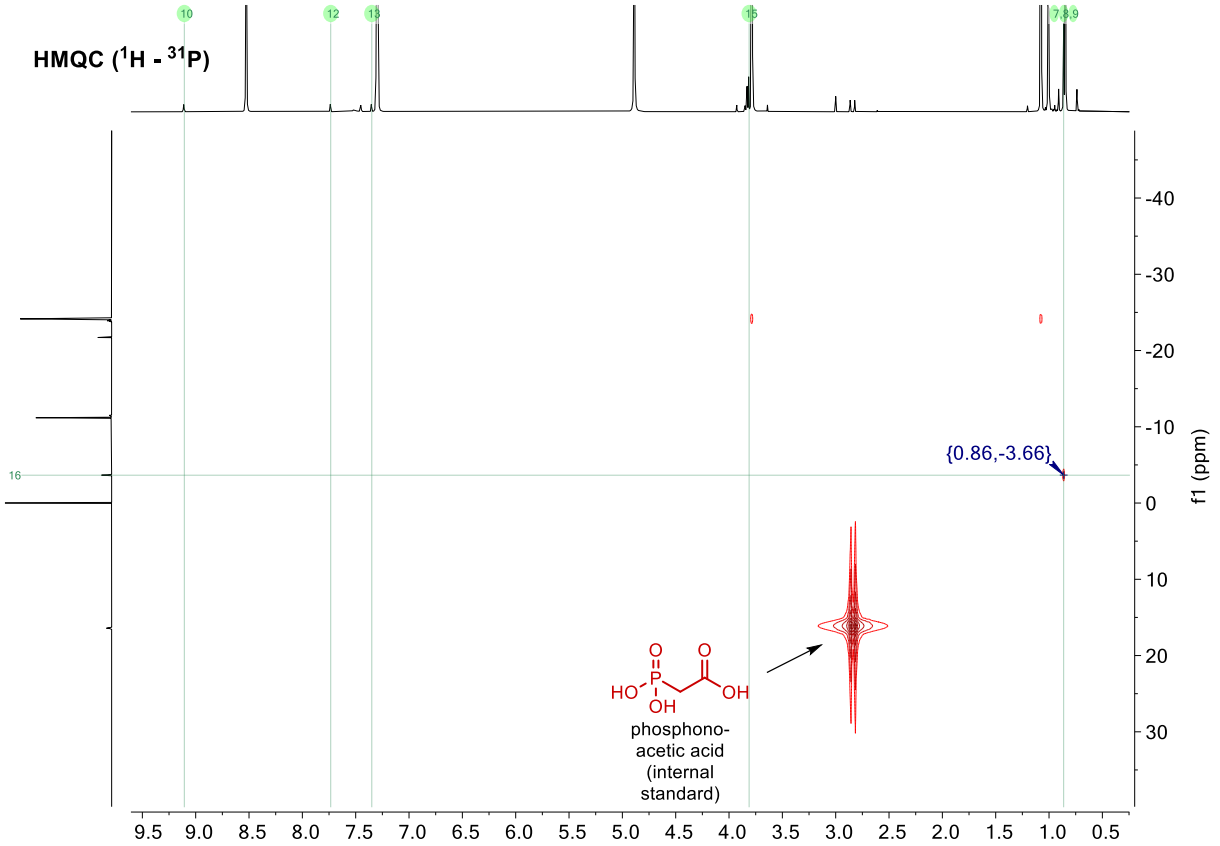
HMQC (1H - 31P)
10
12
13
15
7,8,9
16
{0.86,-3.66}
-40
-30
-20
-10
0
10
20
30
f1 (ppm)
9.5
9.0
8.5
8.0
7.5
7.0
6.5
6.0
5.5
5.0
4.5
4.0
3.5
3.0
2.5
2.0
1.5
1.0
0.5
phosphono-
acetic acid
(internal
standard)

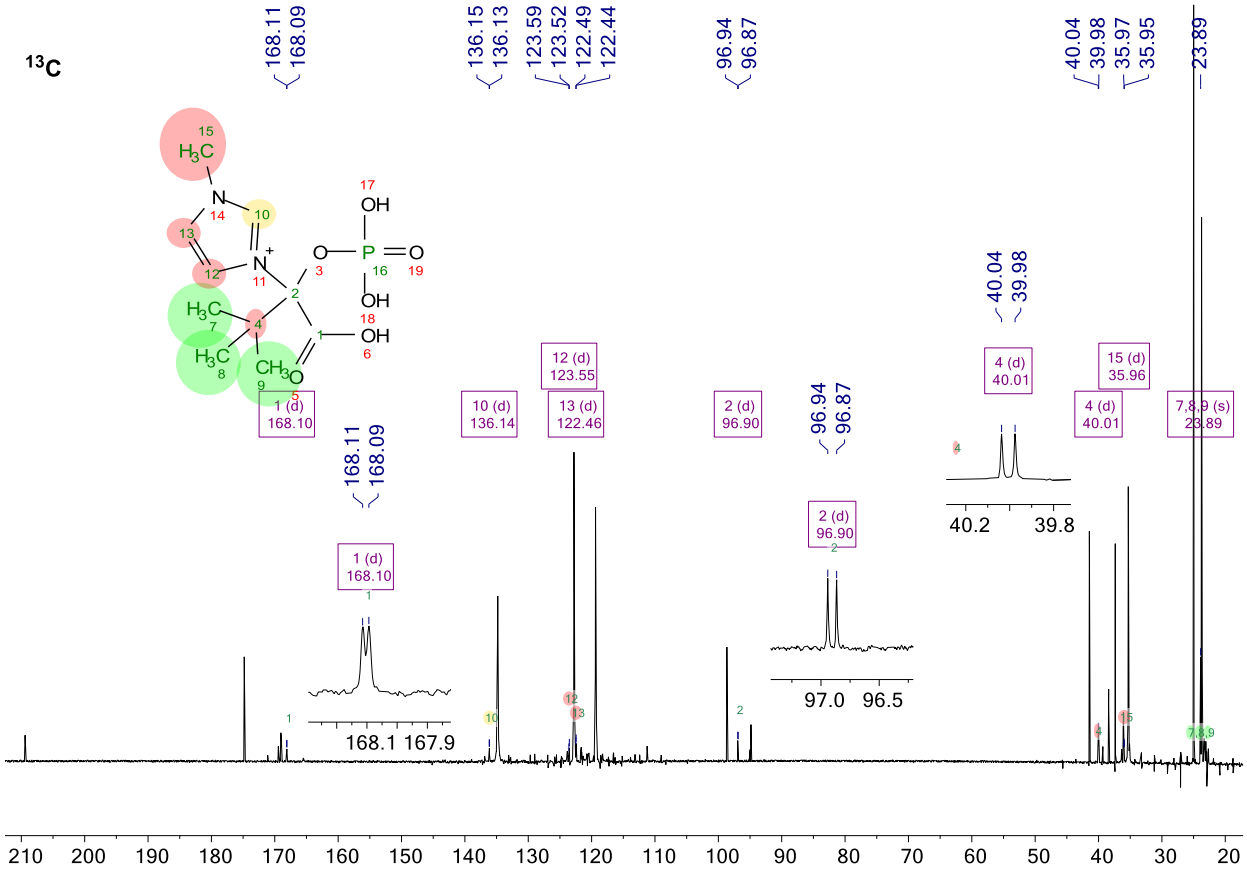
13C
168.11
168.09
136.15
136.13
123.59
123.52
122.49
122.44
96.94
96.87
40.04
39.98
35.97
35.95
23.89
1 (d)
168.10
10 (d)
136.14
12 (d)
123.55
13 (d)
122.46
2 (d)
96.90
4 (d)
40.01
15 (d)
35.96
7,8,9 (s)
23.89
168.1 167.9
97.0 96.5
40.2 39.8
210 200 190 180 170 160 150 140 130 120 110 100 90 80 70 60 50 40 30 20

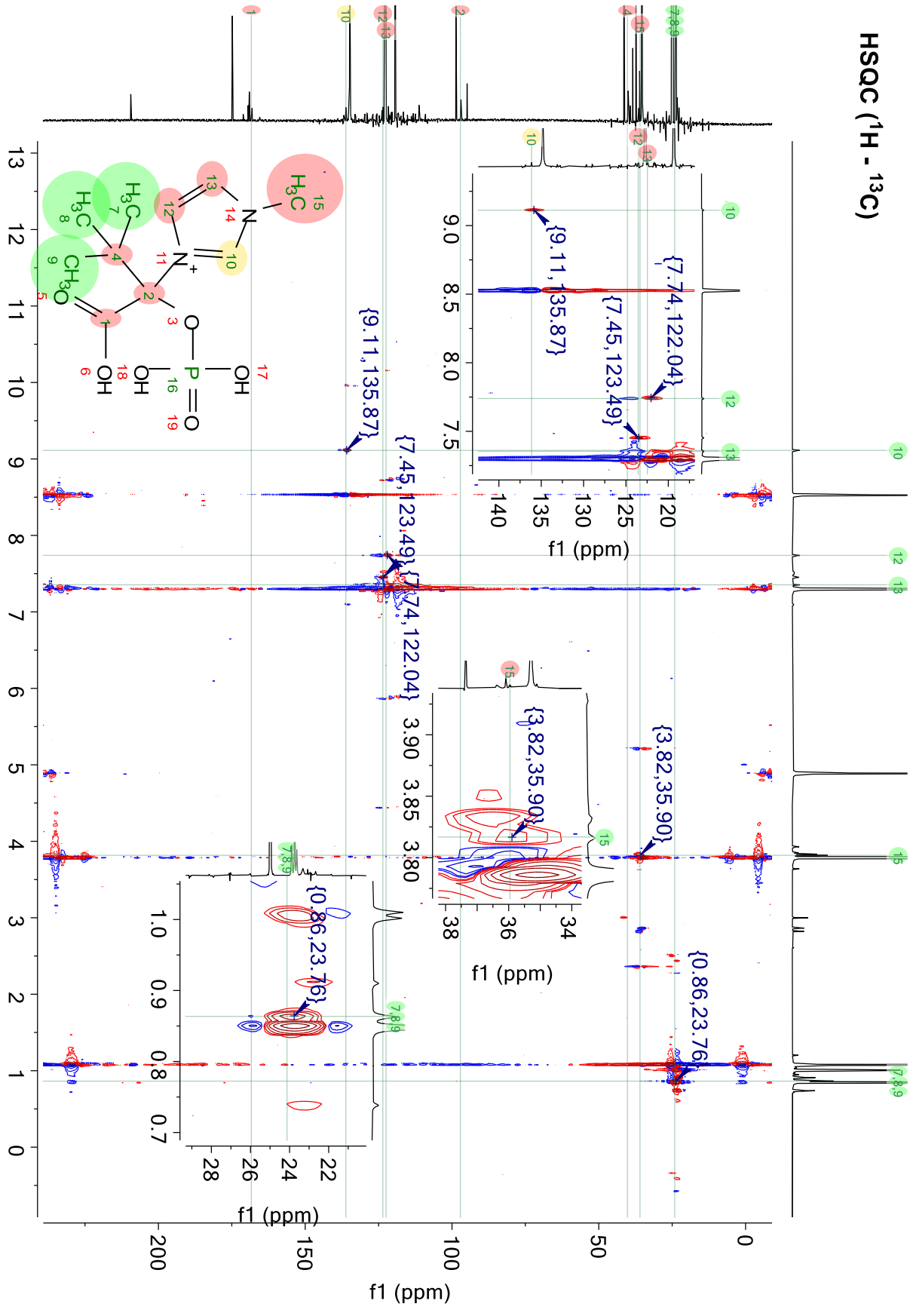
HSQC (^{1}H - ^{13}C)
f1 (ppm)
{9.11,135.87}
{7.74,122.04}
{7.45,123.49}
{3.82,35.90}
{0.86,23.76}

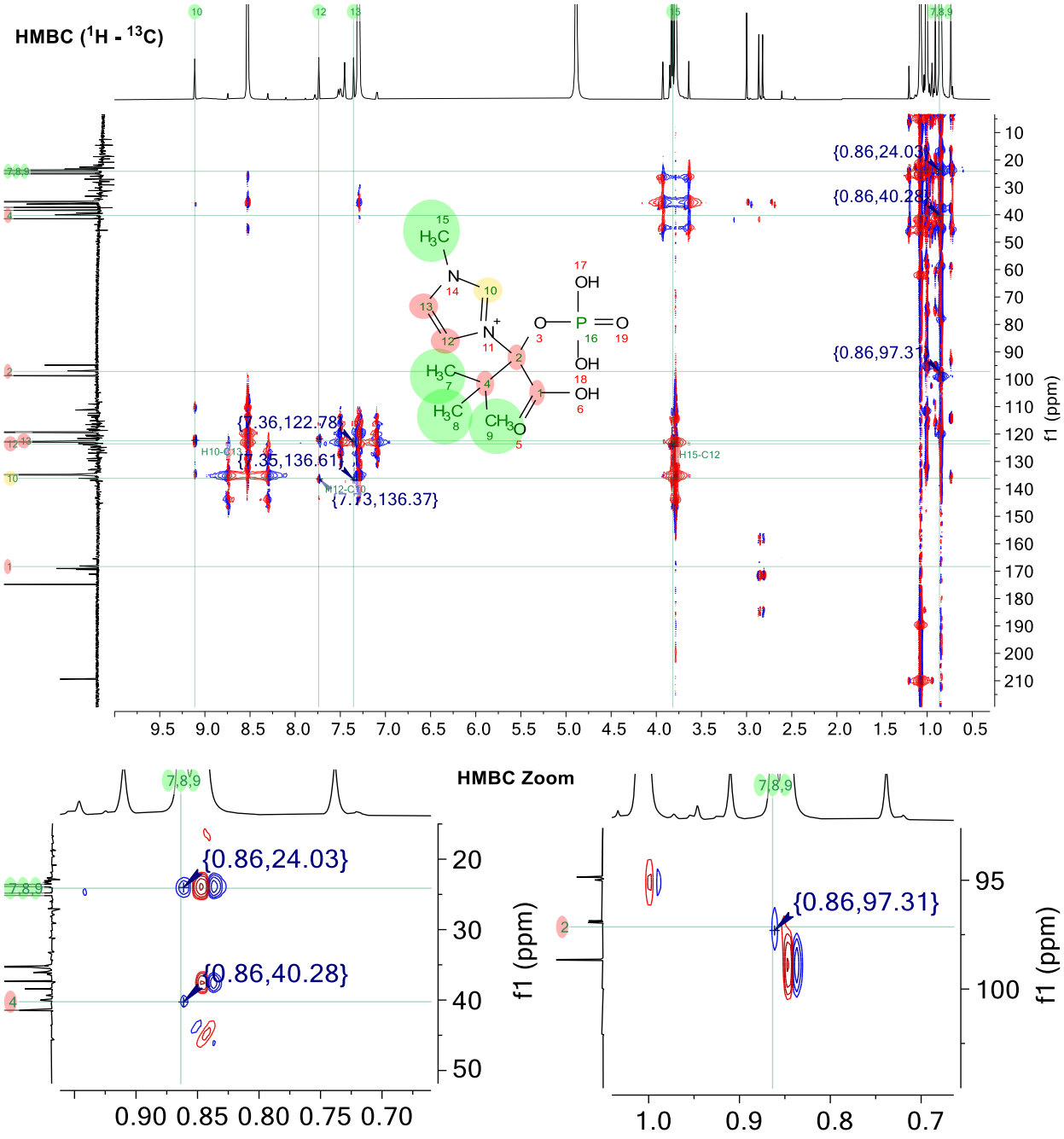
HMBC (^{1}H - ^{13}C)
{0.86,24.03}
{0.86,40.28}
{0.86,97.31}
{7.36,122.78}
{7.35,136.61}
{7.73,136.37}
H10-C13
H12-C10
H15-C12
f1 (ppm)
HMBC Zoom
{0.86,24.03}
{0.86,40.28}
{0.86,97.31}
f1 (ppm)
f1 (ppm)

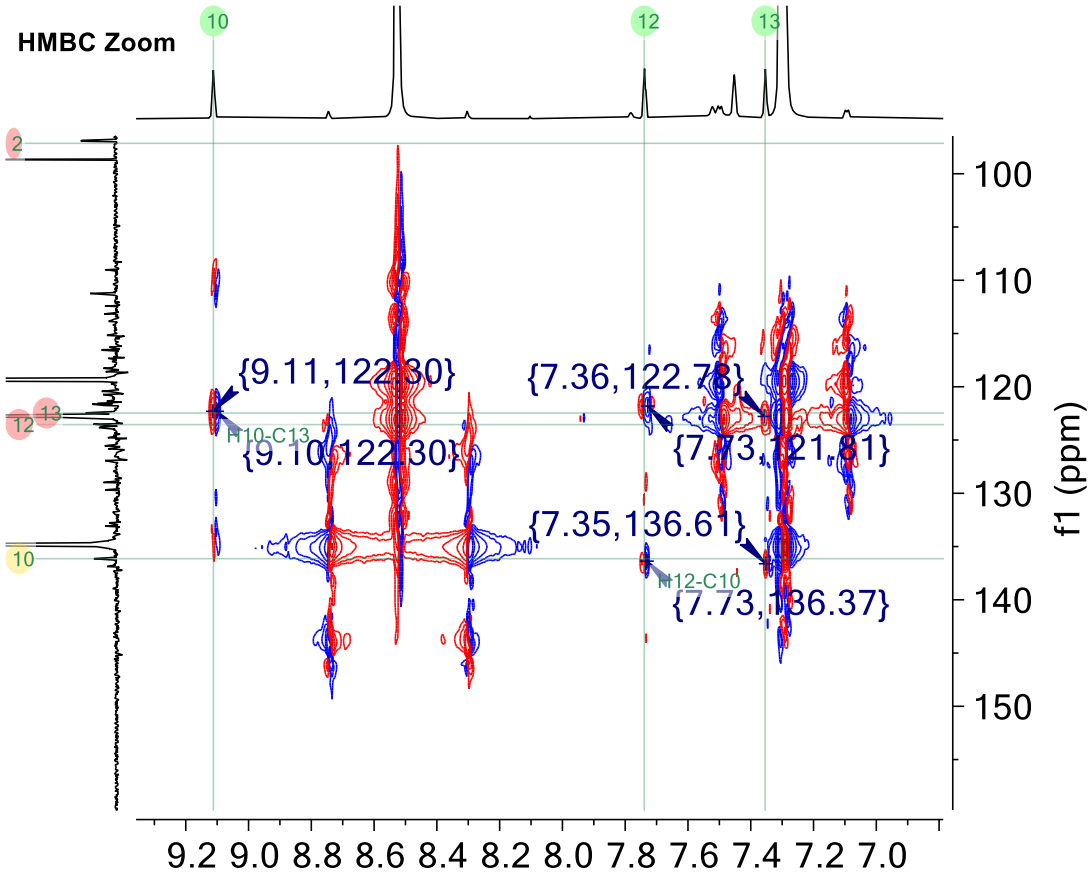
HMBC Zoom
10
12
13
2
12
13
10
{9.11,122.30}
H10-C13
{9.10,122.30}
{7.36,122.78}
{7.73,121.81}
{7.35,136.61}
H12-C10
{7.73,136.37}
100
110
120
130
140
150
f1 (ppm)
9.2 9.0 8.8 8.6 8.4 8.2 8.0 7.8 7.6 7.4 7.2 7.0

9) Enol-phosphate of methylpyruvic acid P2-1Me – Z-isomer according to $J_{C\text{-}P}$[5,6]

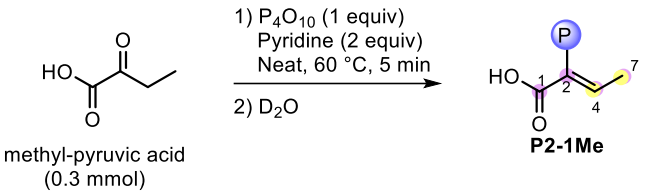

methyl-pyruvic acid
(0.3 mmol)

P2-1Me

^{1}H NMR (500 MHz, D_2O) δ 6.46 - 6.41 (qd, J_{CH} = 7.2 Hz, J_{HP} = 2.4 Hz, 1 H, H-4), 1.71 – 1.67 (dd, J_{CH} = 7.2 Hz J_{HP} = 2.9 Hz, 3 H, H-7) ppm.

^{13}C NMR (126 MHz, D_2O) δ 166.1 (d, J_{CP} = 1.3 Hz, C-1), 138.4 (d, J_{CP} = 8.3 Hz, C-2), 127.8 (d, J_{CP} = 5.6 Hz, C-4), 10.9 (C-7) ppm.

^{31}P NMR (202 MHz, D_2O) δ –3.86 (t, J_{HP} = 1.3 Hz) ppm.

HRMS (ESI$^+$): Calcd m/z for $[C_4H_8O_6P]$ $[M+H]^+$: 183.0053; Found: 183.0054 (0.6006 ppm).

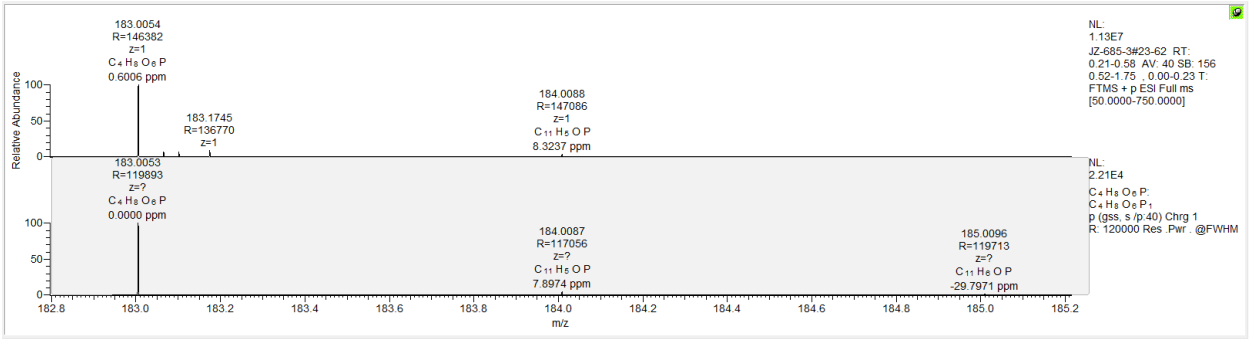

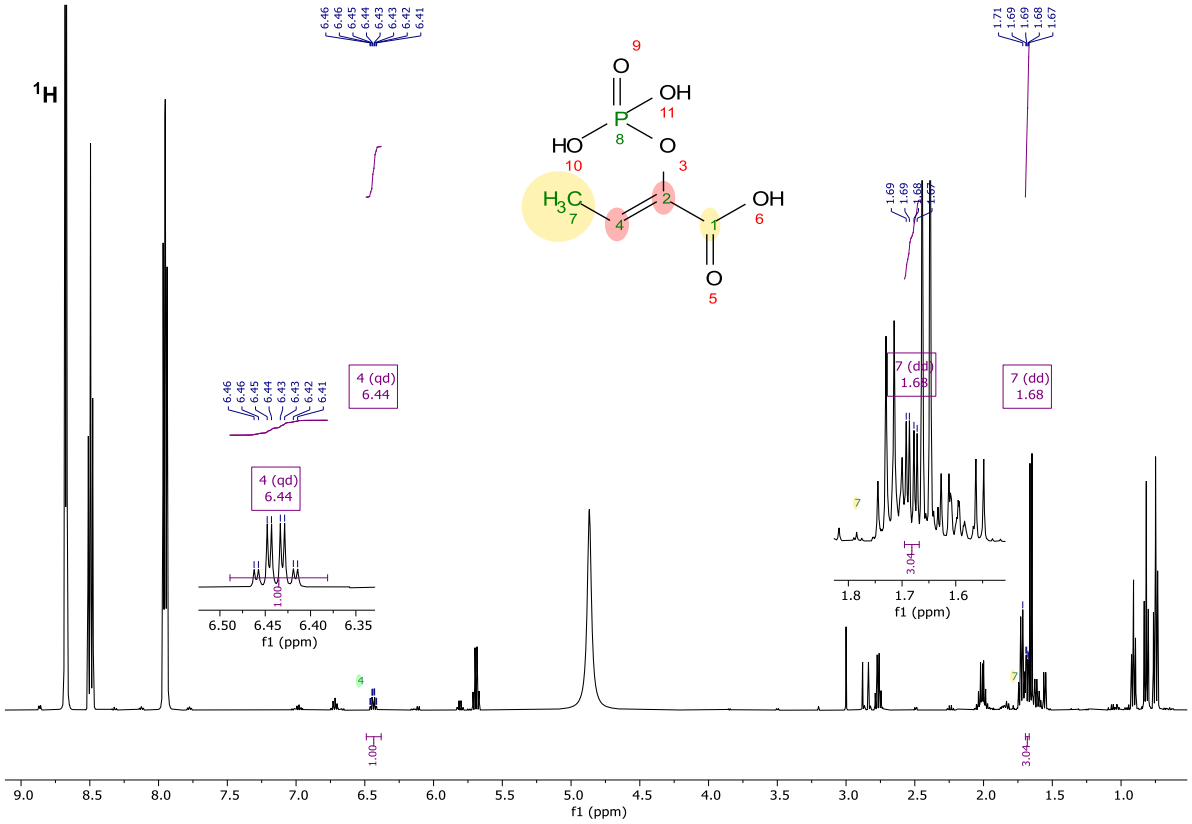
^{1}H
4 (qd)
6.44
7 (dd)
1.68
f1 (ppm)

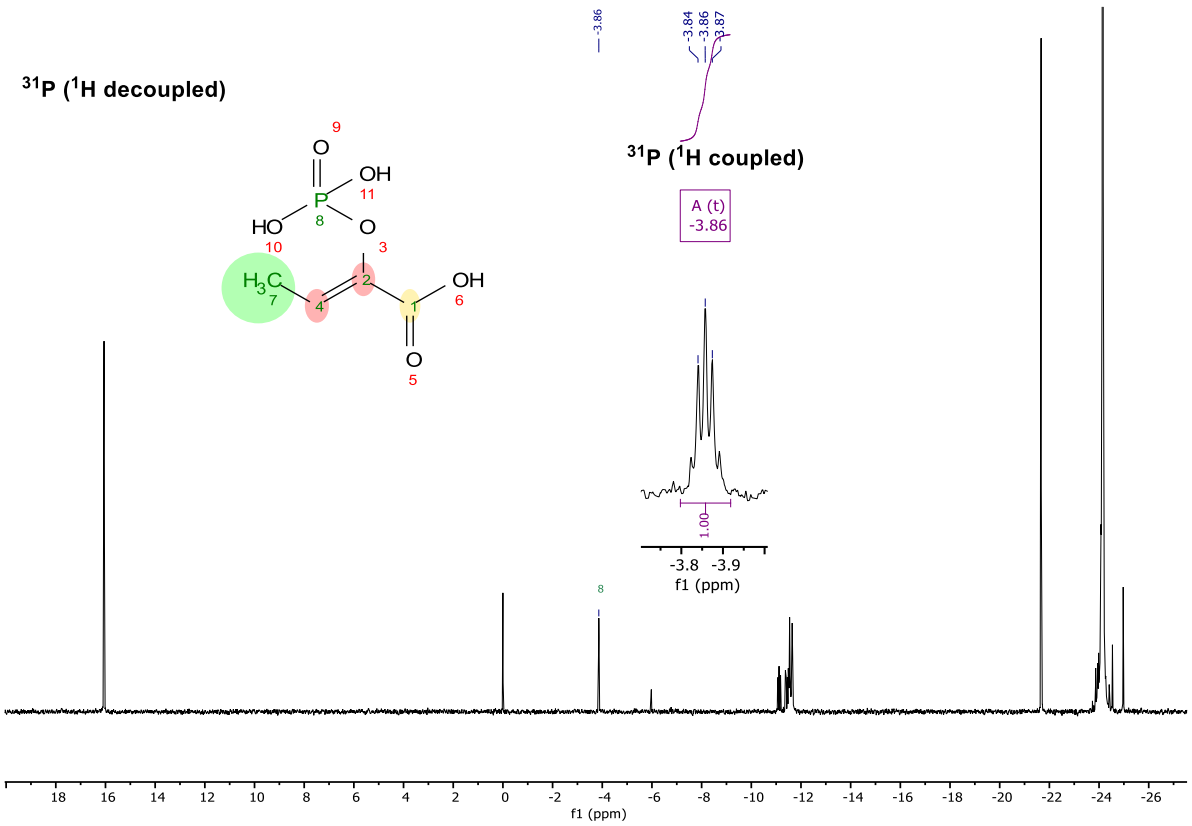
^{31}P (^{1}H decoupled)
^{31}P (^{1}H coupled)
A (t)
-3.86
f1 (ppm)

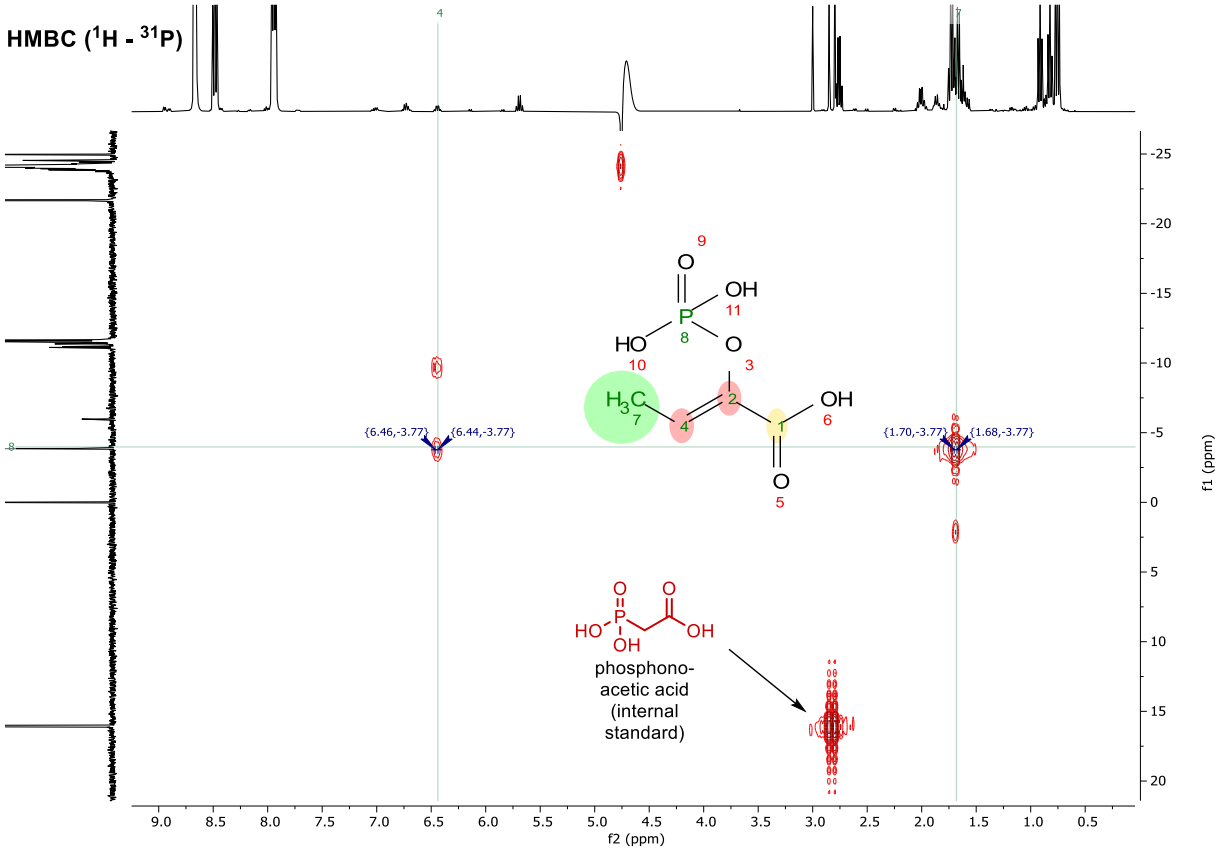
HMBC (^{1}H - ^{31}P)
{6.46,-3.77}
{6.44,-3.77}
{1.70,-3.77}
{1.68,-3.77}
phosphono-
acetic acid
(internal
standard)
f2 (ppm)
f1 (ppm)

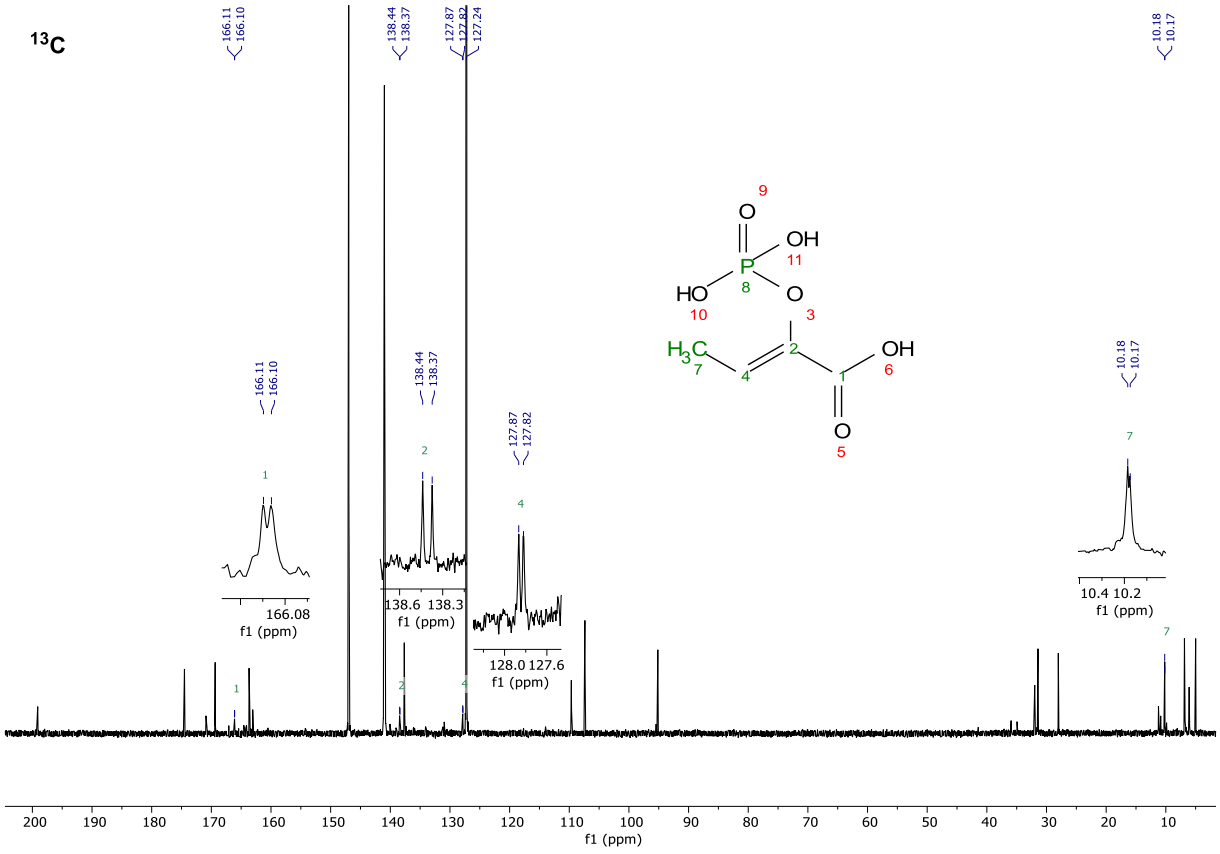
^{13}C
166.11
166.10
138.44
138.37
127.87
127.82
127.24
10.18
10.17
166.08
f1 (ppm)
138.6 138.3
f1 (ppm)
128.0 127.6
f1 (ppm)
10.4 10.2
f1 (ppm)
f1 (ppm)

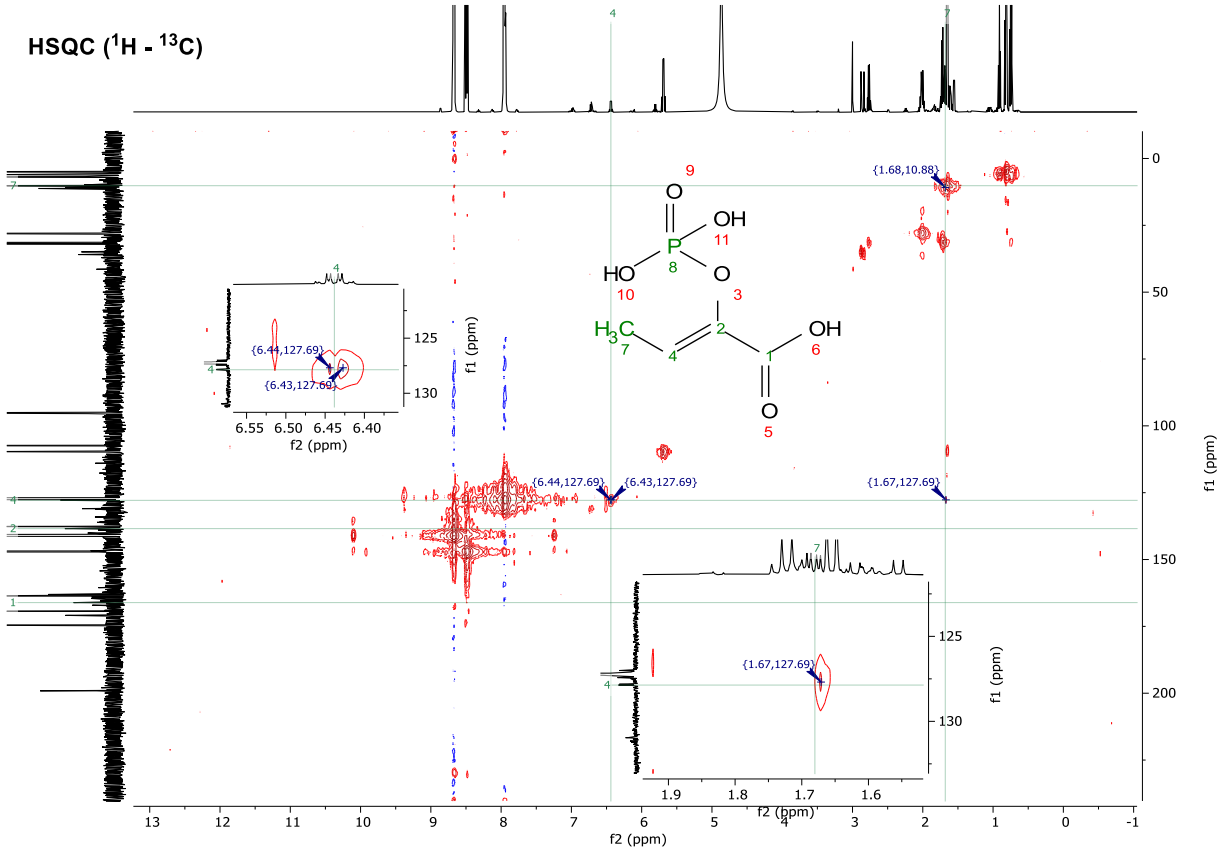
HSQC (^{1}H - ^{13}C)
{1.68,10.88}
{6.44,127.69}
{6.43,127.69}
{1.67,127.69}
f2 (ppm)
f1 (ppm)

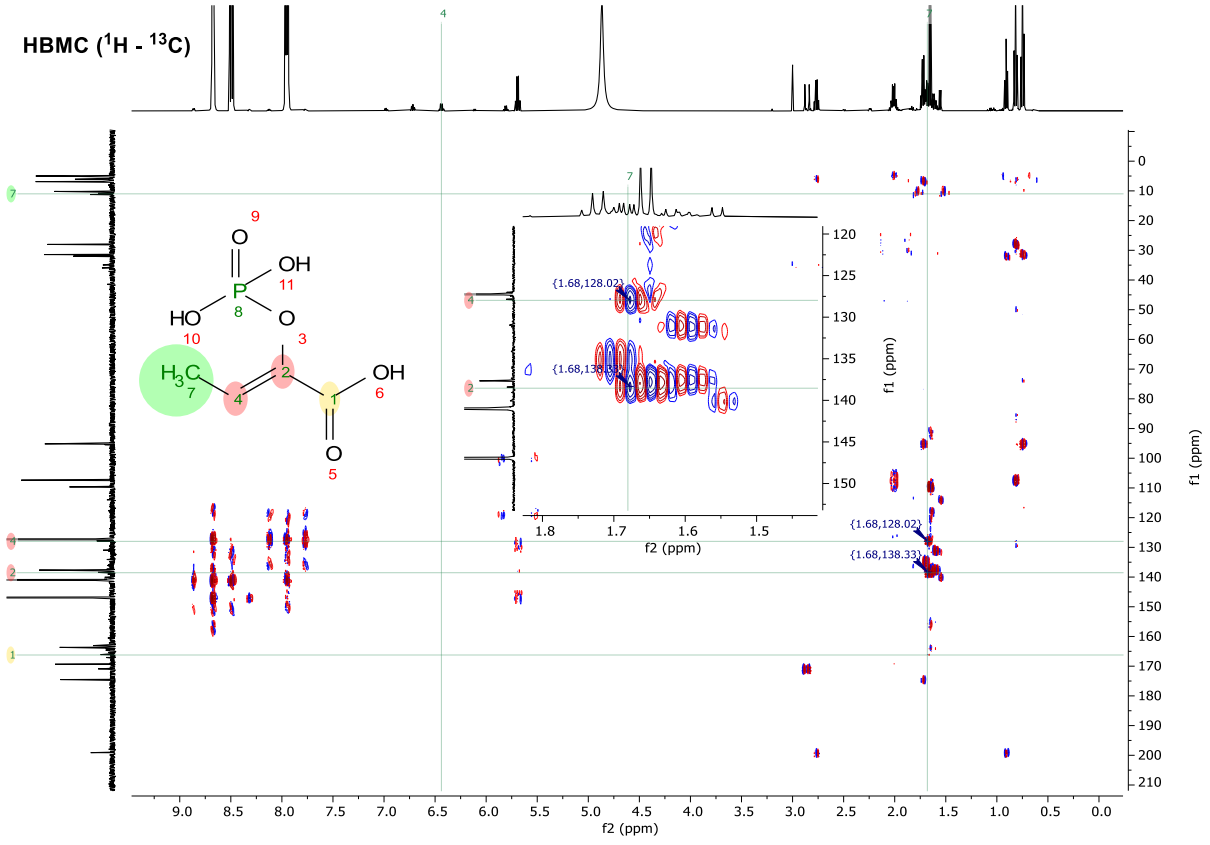
HBMC (^{1}H - ^{13}C)
{1.68,128.02}
{1.68,138.33}
f2 (ppm)
f1 (ppm)

10) Enol-phosphate of α-ketoglutaric acid P2-glu

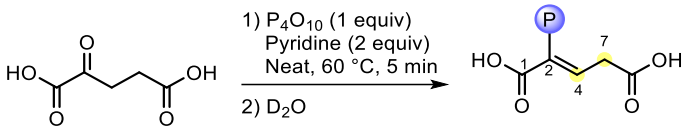

alphaketoglutaric acid
(0.3 mmol)

P2-Glu

^{1}H NMR (500 MHz, D_2O) δ 6.49 - 6.46 (td, J_{CH} = 7.3 Hz, J_{HP} = 2.4 Hz, 1 H, H-4), 3.34 – 3.32 (dd, J_{CH} = 7.3 Hz, J_{HP} = 2.4 Hz, 2 H, H-7) ppm.

Because of low yields, the carbon NMR of **P2-glu** was not assigned.

^{31}P NMR (202 MHz, D_2O) δ –4.16 (q, J_{HP} = 2.5 Hz) ppm.

HRMS (ESI$^+$): Calcd m/z for [$C_5H_8O_8P$] [M+H]$^+$: 226.9951; Found: 226.9952 (0.3309 ppm).

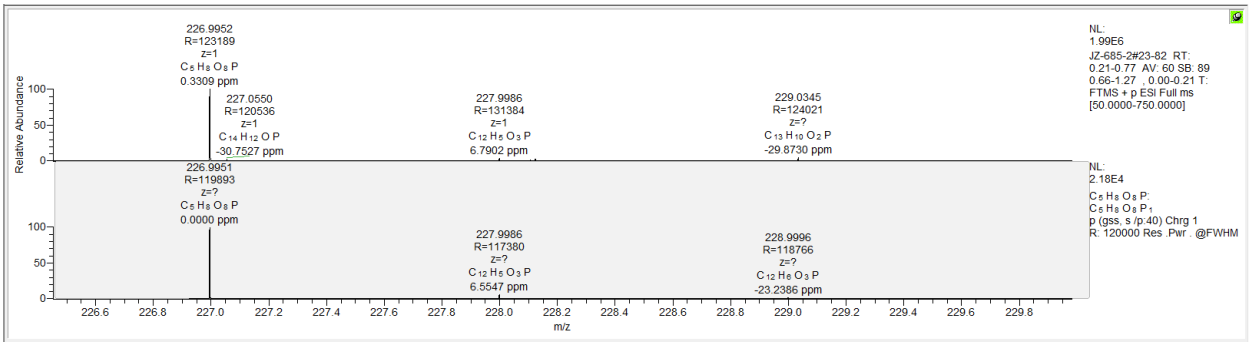

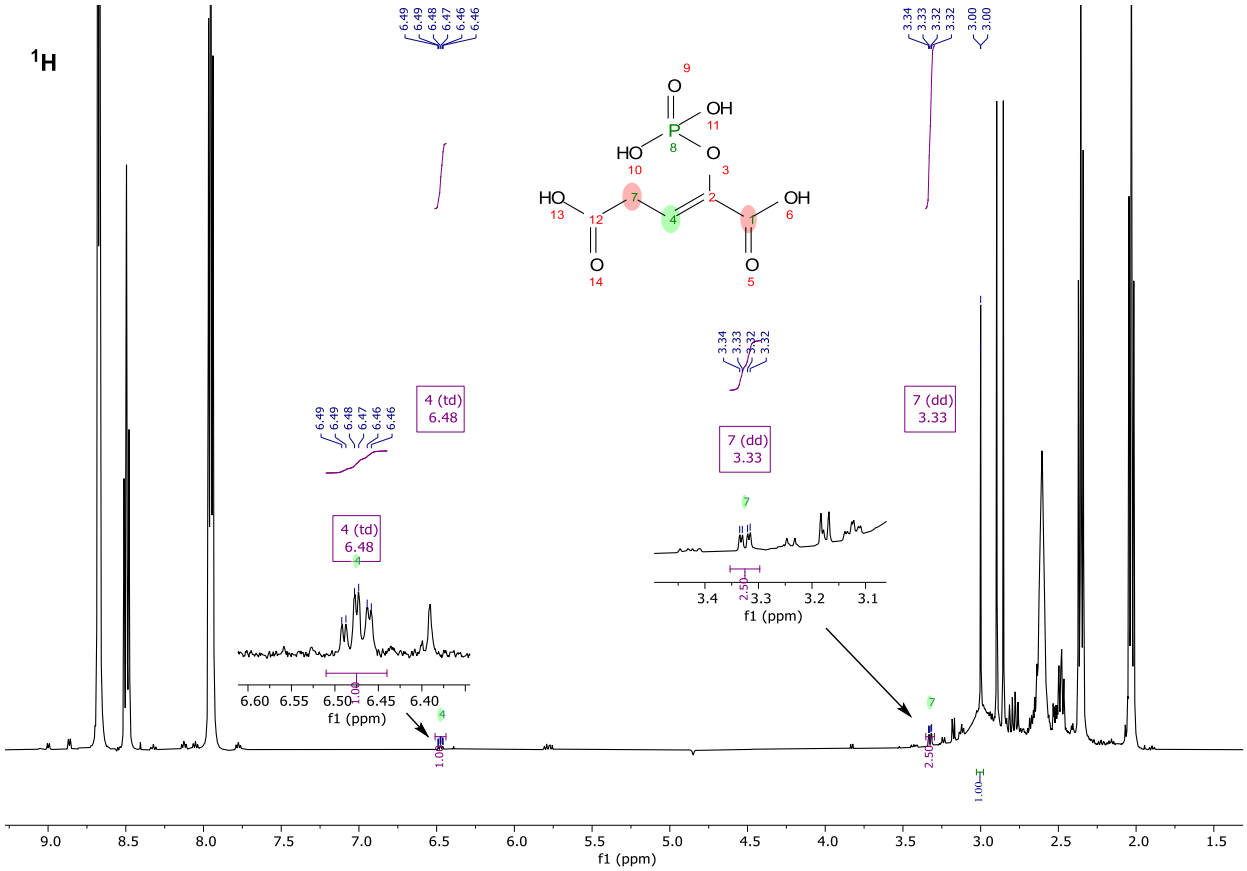
1H
4 (td)
6.48
7 (dd)
3.33
f1 (ppm)

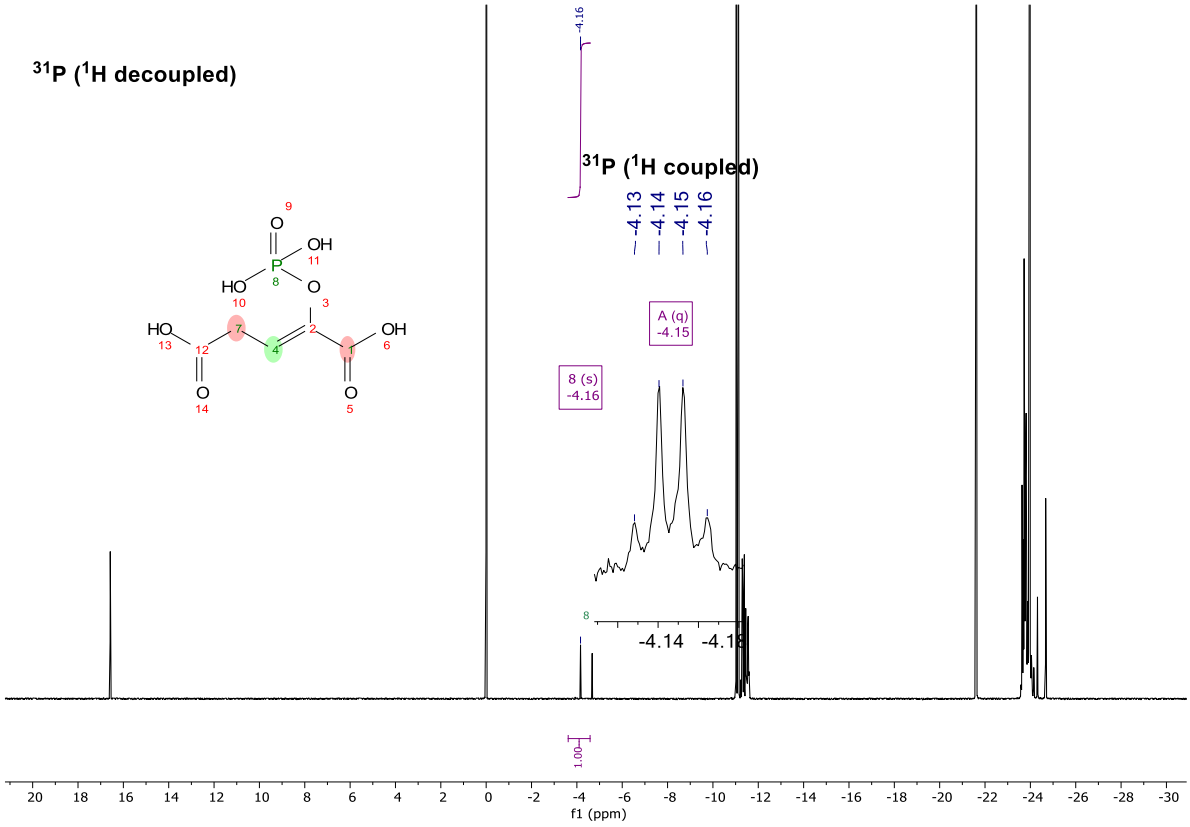
31P (1H decoupled)
31P (1H coupled)
-4.13
-4.14
-4.15
-4.16
A (q)
-4.15
8 (s)
-4.16
f1 (ppm)

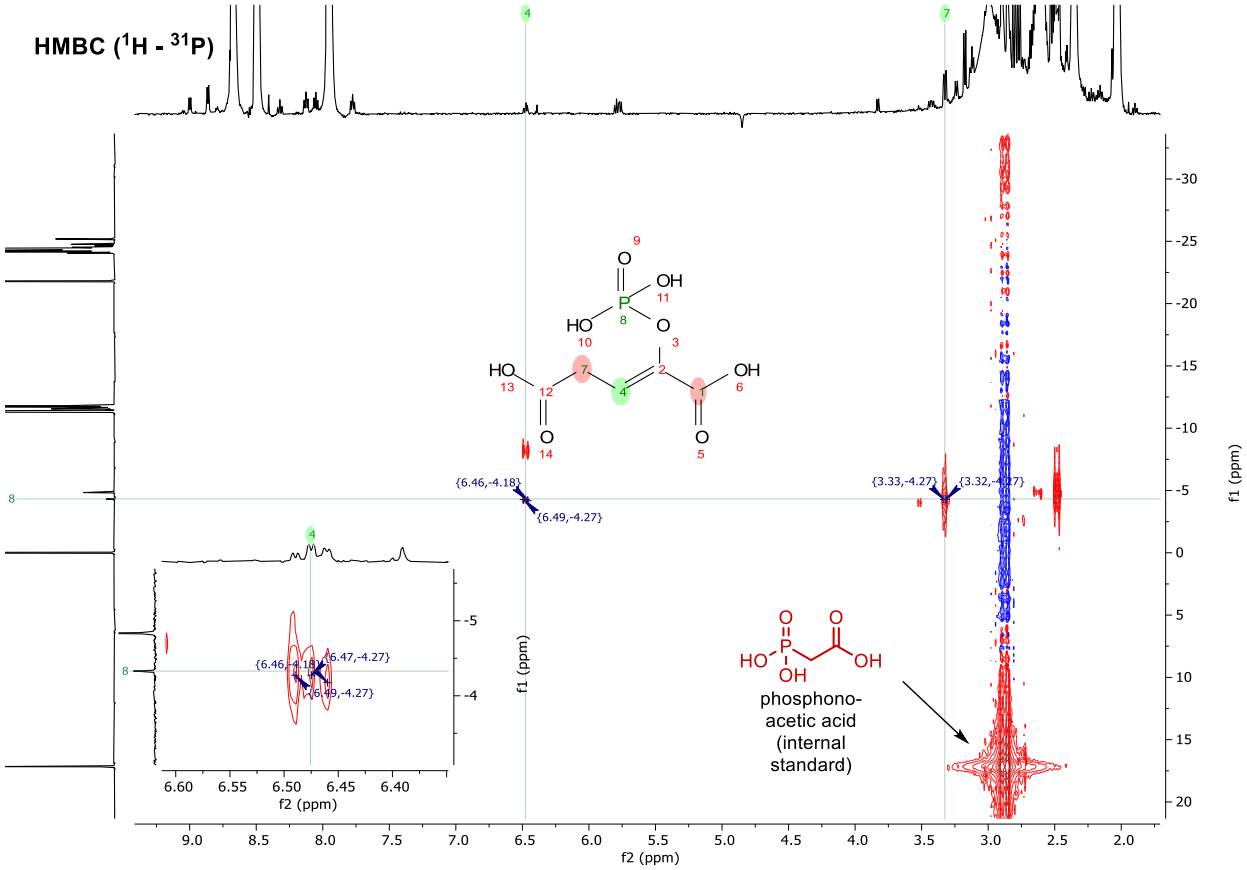
HMBC (^{1}H - ^{31}P)
{6.46,-4.18}
{6.49,-4.27}
{3.33,-4.27}
{3.32,-4.27}
{6.47,-4.27}
phosphono-
acetic acid
(internal
standard)
f2 (ppm)
f1 (ppm)

11) Phosphorylated cyclic form of α-ketoglutaric acid P2'-glu

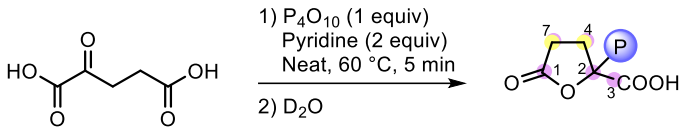

alphaketoglutaric acid (0.3 mmol)

P2'-Glu

^{1}H NMR (500 MHz, D_2O) δ 3.5 – 3.44 (br, 4 H, H-4, H-7, both are overlapping) ppm.

^{13}C NMR (126 MHz, D_2O) δ 177.1 (br, C-1), 170.3 (d, J_{CP} = 2.6 Hz, C-3), 103.2 (d, J_{CP} = 7.7 Hz C-2), 32.4 (br, C-4), 26.5 (d, J_{CP} = 7.7 Hz C-7, deducted from ^{13}C NMR) ppm.

^{31}P NMR (202 MHz, D_2O) δ –4.68 (t, J_{HP} = 1.5 Hz) ppm.

HRMS (ESI$^-$): Calcd m/z for $[C_5H_6O_8P]$ $[M-H]^-$: 224.9806; Found: 226.9802 (-1.5296 ppm).

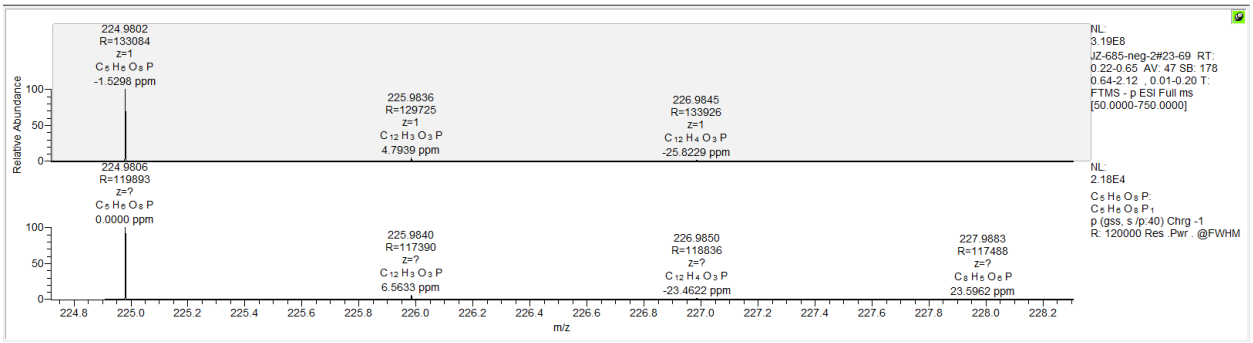

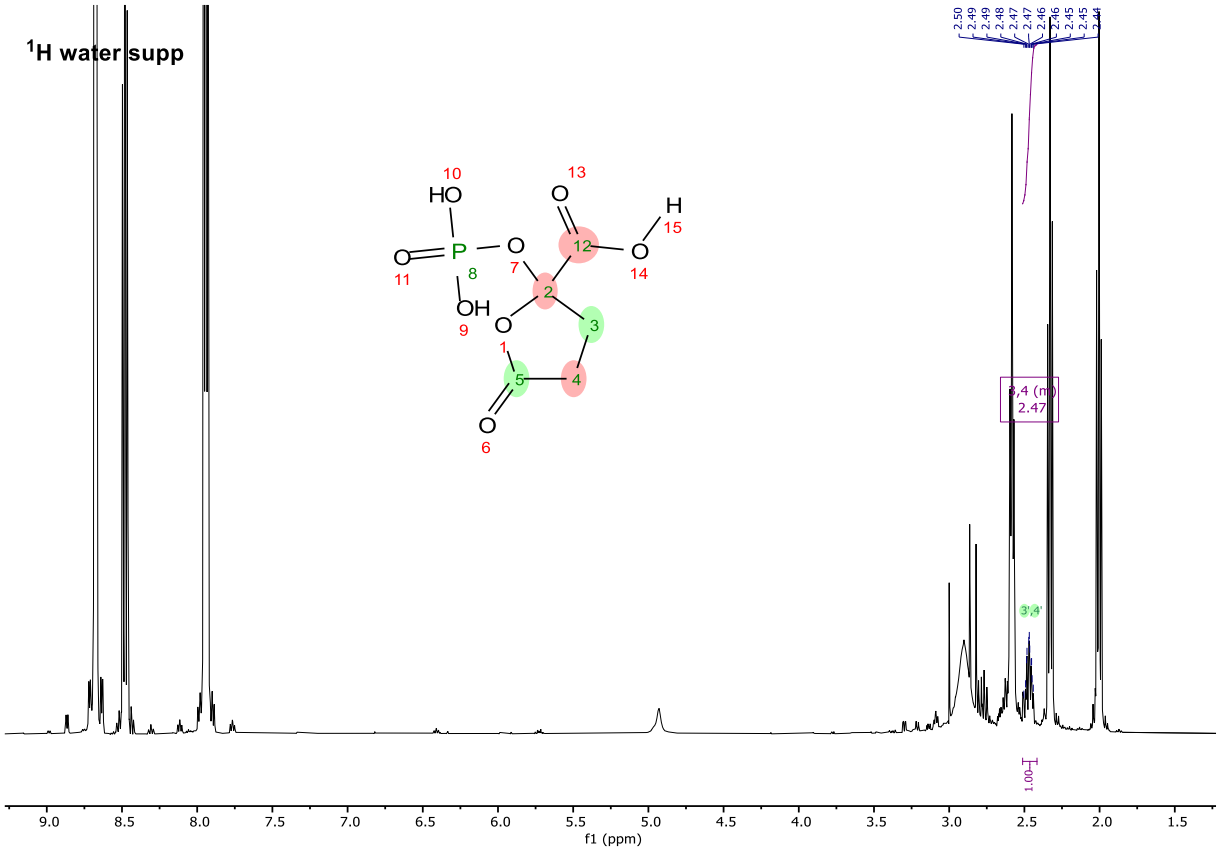
^{1}H water supp
2.50
2.49
2.49
2.48
2.47
2.47
2.46
2.46
2.45
2.45
2.44
2,4 (m)
2.47
3',4'
1.00
9.0
8.5
8.0
7.5
7.0
6.5
6.0
5.5
5.0
4.5
4.0
3.5
3.0
2.5
2.0
1.5
f1 (ppm)

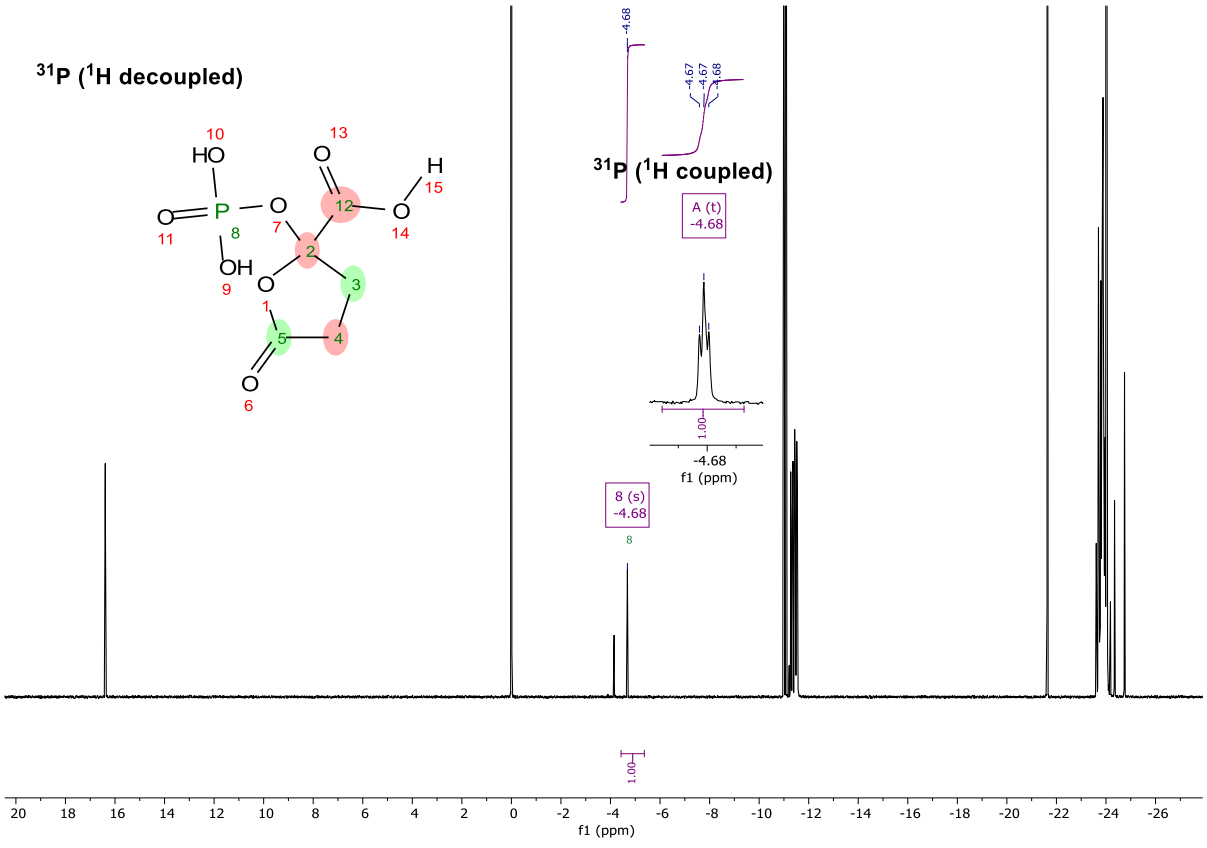
^{31}P (^{1}H decoupled)
^{31}P (^{1}H coupled)
-4.68
-4.67
-4.67
-4.68
A (t)
-4.68
1.00
-4.68
f1 (ppm)
8 (s)
-4.68
8
1.00
20
18
16
14
12
10
8
6
4
2
0
-2
-4
-6
-8
-10
-12
-14
-16
-18
-20
-22
-24
-26
f1 (ppm)

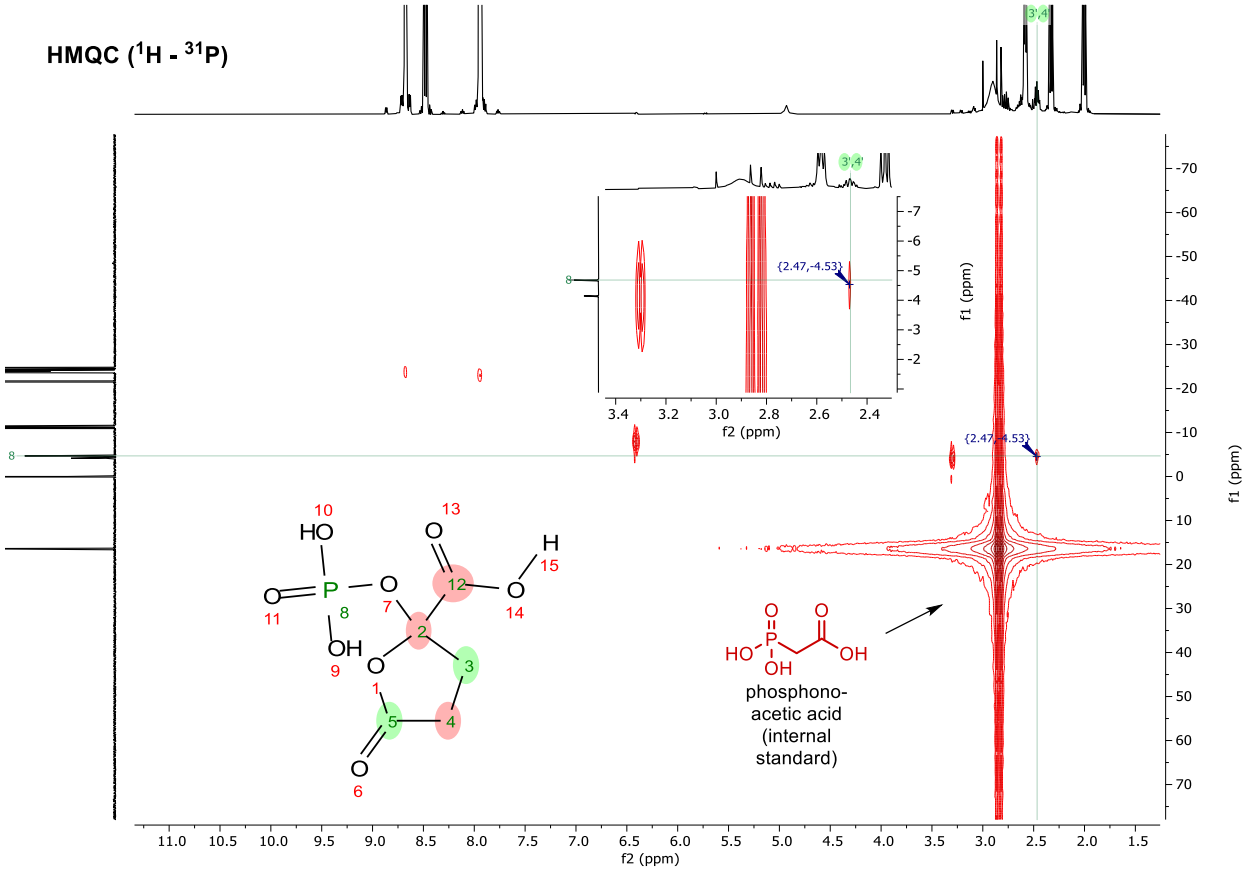
HMQC (^{1}H - ^{31}P)
3',4'
{2.47,-4.53}
f1 (ppm)
f2 (ppm)
phosphono-
acetic acid
(internal
standard)

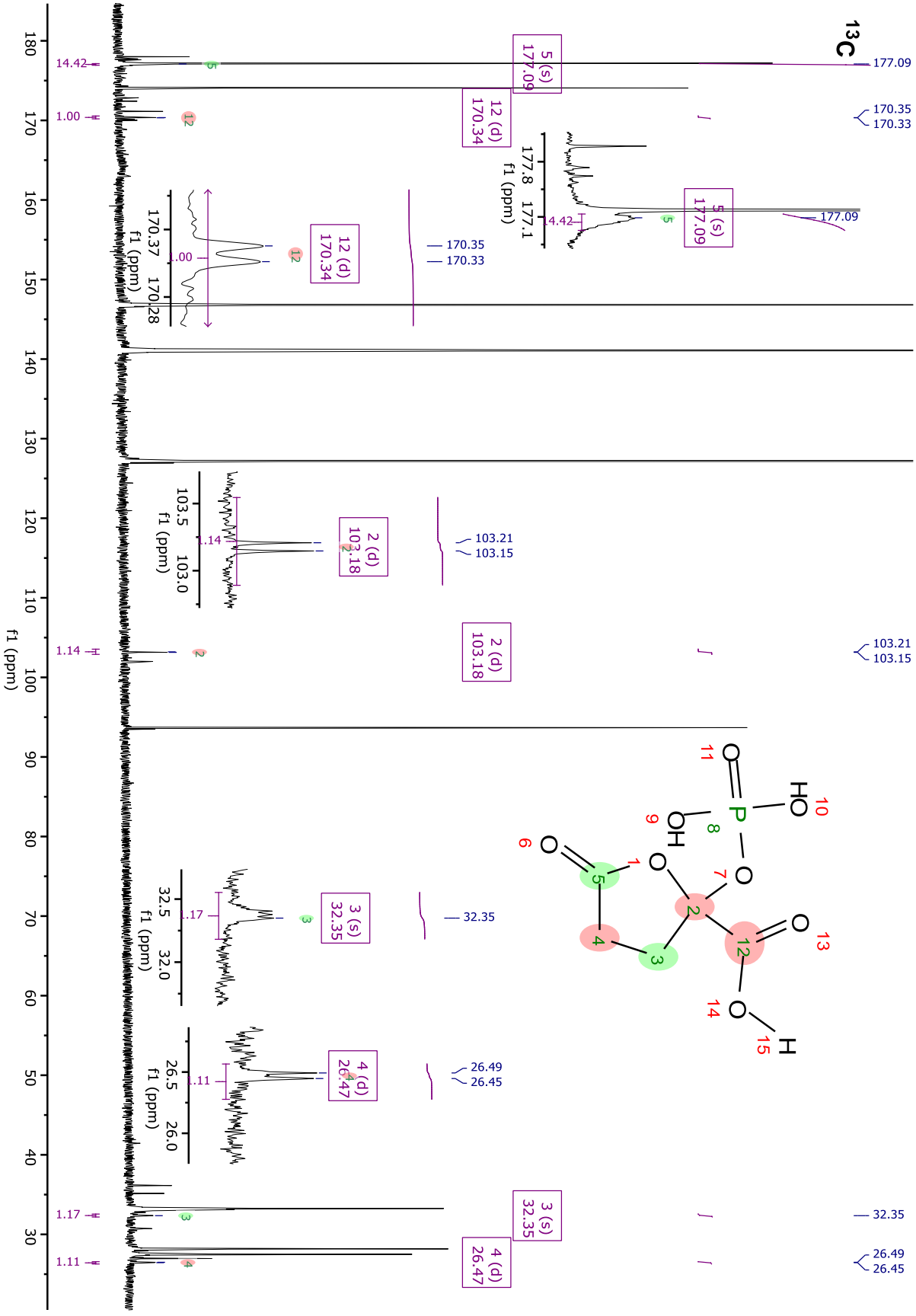
13C
f1 (ppm)
5 (s) 177.09
12 (d) 170.34
2 (d) 103.18
3 (s) 32.35
4 (d) 26.47
177.09
170.35
170.33
103.21
103.15
32.35
26.49
26.45
14.42
1.00
1.14
1.17
1.11
HO
OH
O
P
O
O
O
O
O
H
1
2
3
4
5
6
7
8
9
10
11
12
13
14
15

12) Enol-phosphate of oxaloacetic acid P2-ox

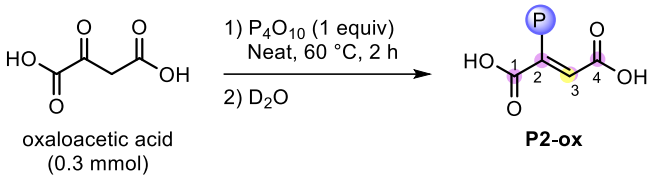

^{1}H NMR (500 MHz, D_2O) δ 5.94 (d, J_{HP} = 1.7 Hz, H-3) ppm.

^{13}C NMR (126 MHz, D_2O) δ 171.2 (d, J_{CP} = 6.1 Hz, C-4), 166.1 (d, J_{CP} = 7.1 Hz, C-1), 151.4 (d, J_{CP} = 8.4 Hz C-2), 109.4 (d, J_{CP} = 3.9 Hz C-3) ppm.

^{31}P NMR (202 MHz, D_2O) δ –5.38 (q, J_{HP} = 1.4 Hz) ppm.

HRMS (ESI^{-}): Calcd m/z for [$C_4H_4O_8P$] [M-H]$^{-}$: 210.9649; Found: 210.9641 (-3.8068 ppm).

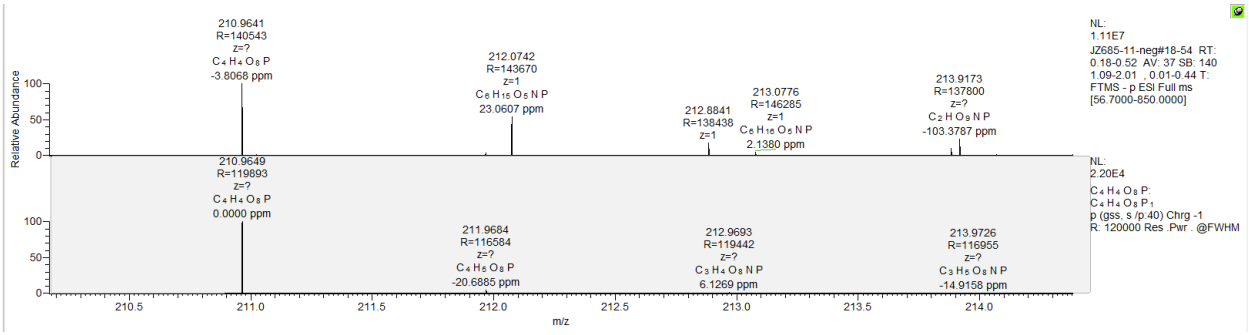

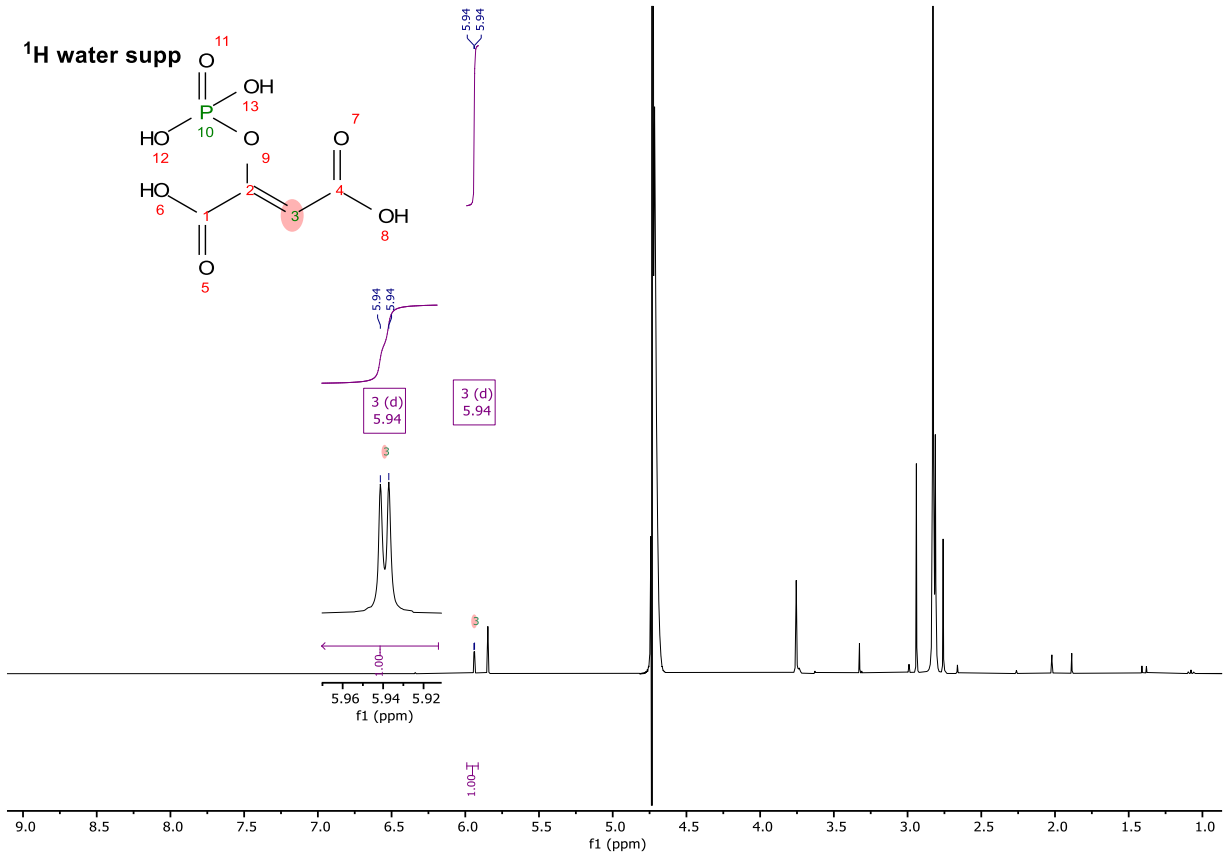

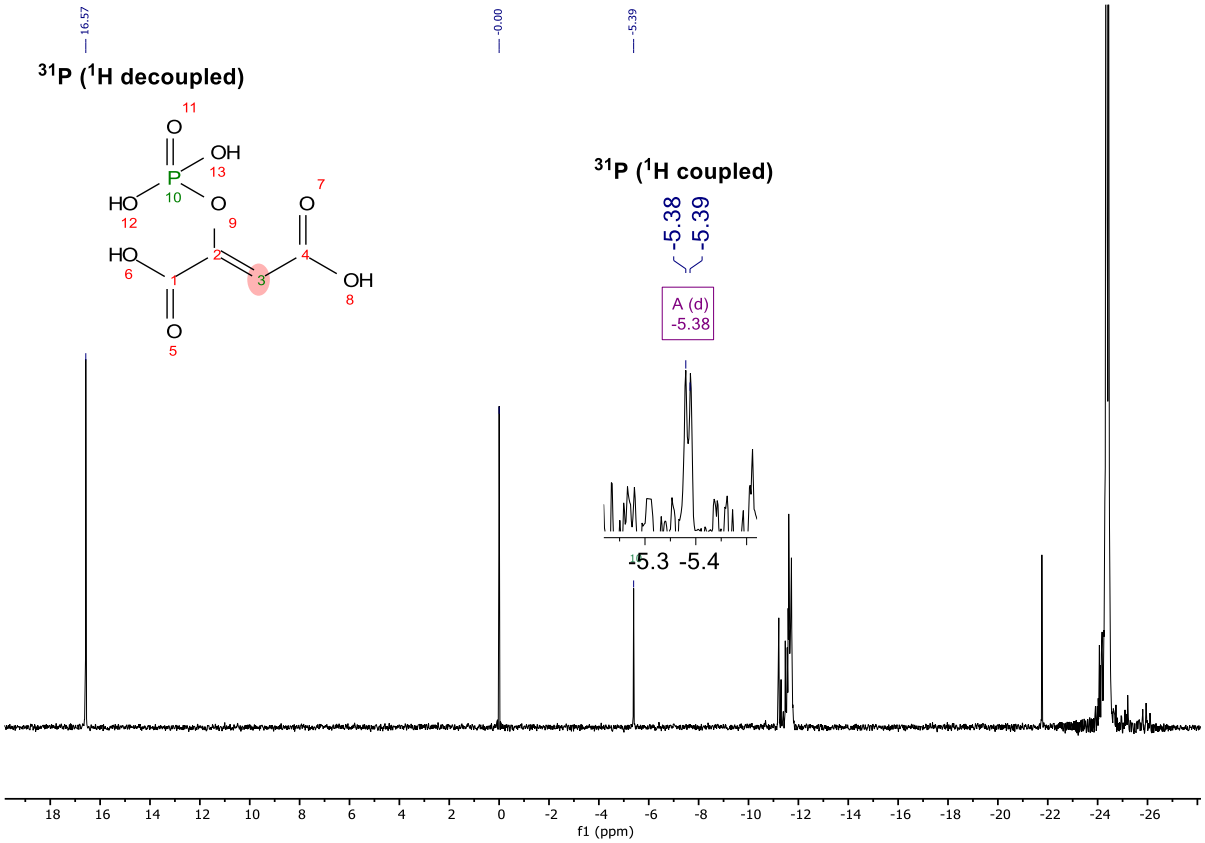
31P (1H decoupled)
31P (1H coupled)
-5.38
-5.39
A (d)
-5.38
-5.3 -5.4
f1 (ppm)

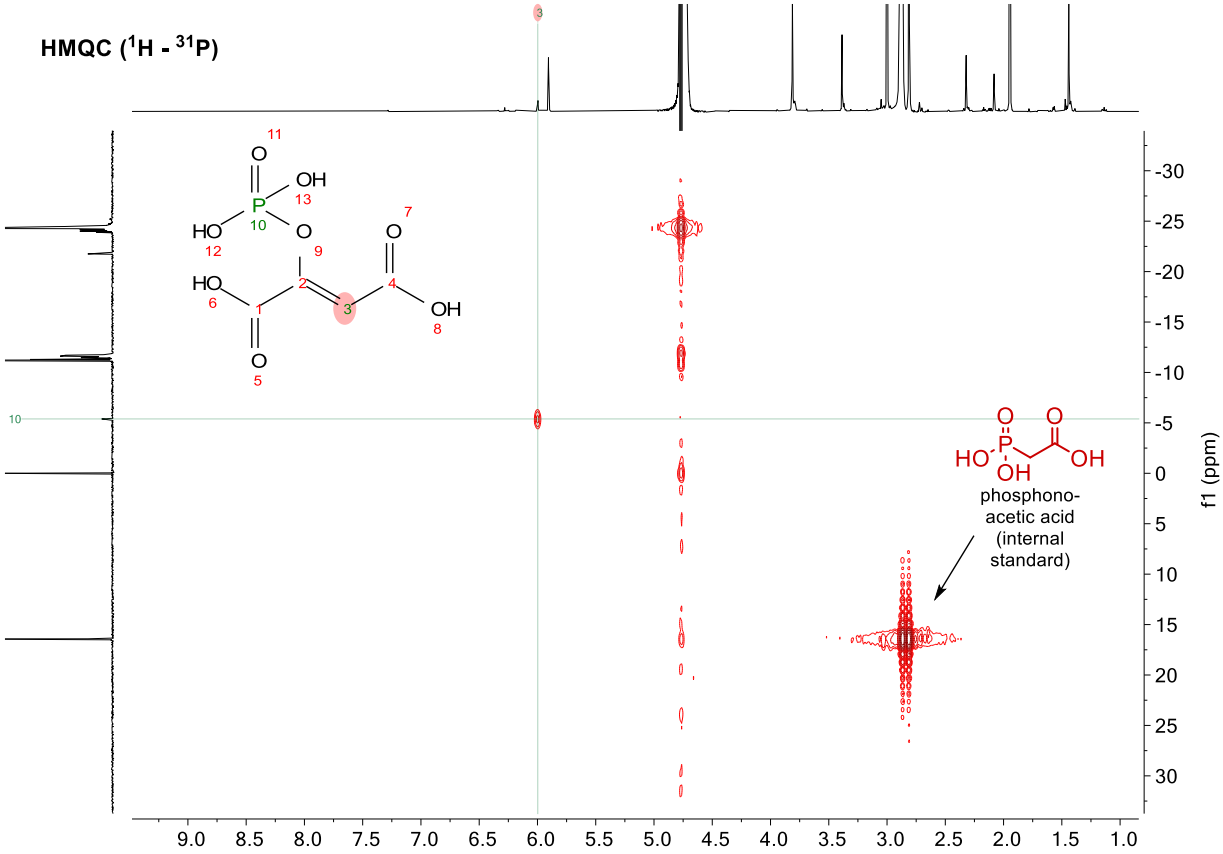
HMQC (1H - 31P)
phosphono-
acetic acid
(internal
standard)
f1 (ppm)

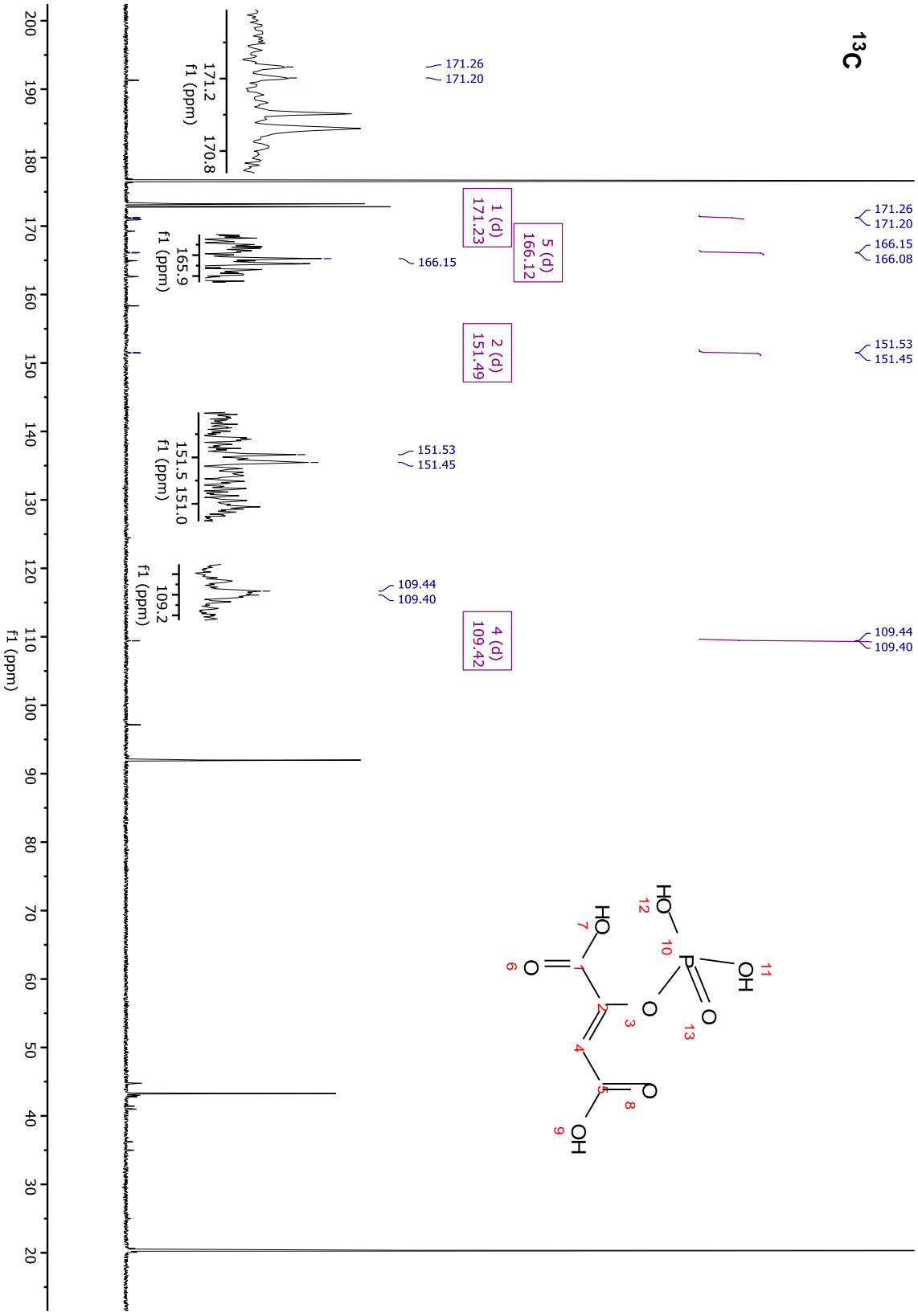

The ^{13}C NMR spectrum was recorded in 1 M acetate buffer at pH 5 to limit the hydrolysis of **P2-ox**.

13) From levulinic acid to its non-phosphorylated base-adduct

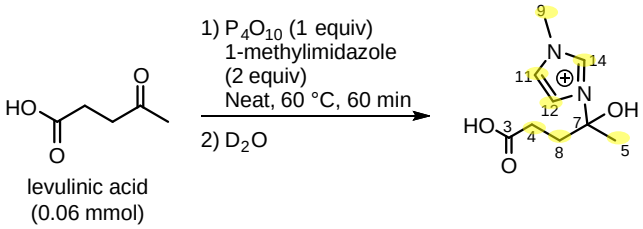

^{1}H NMR (500 MHz, D_2O) δ 8.95 – 8.94 (m,1 H, H-14), 7.61 – 7.60 (t, J_{H-H} = 2 Hz, 1 H, H-12), 7.43 – 7.42 (t, J_{H-H} = 1.9 Hz, 1 H, H-11), 3.79 (s, 3 H, H-9), 2.79-2.67 (m, 4 H, H-4, H-8), 1.9 (s, 3 H, H-5) ppm.

HRMS (ESI$^+$): Calcd m/z for $[C_9H_{15}O_3N_2]$ $[M+H]^+$: 199.1077; Found: 199.1078 (0.2633 ppm)

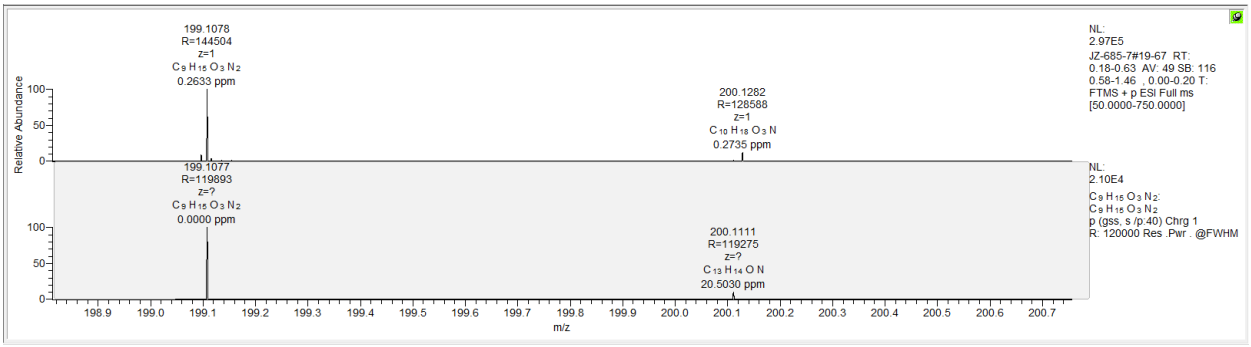

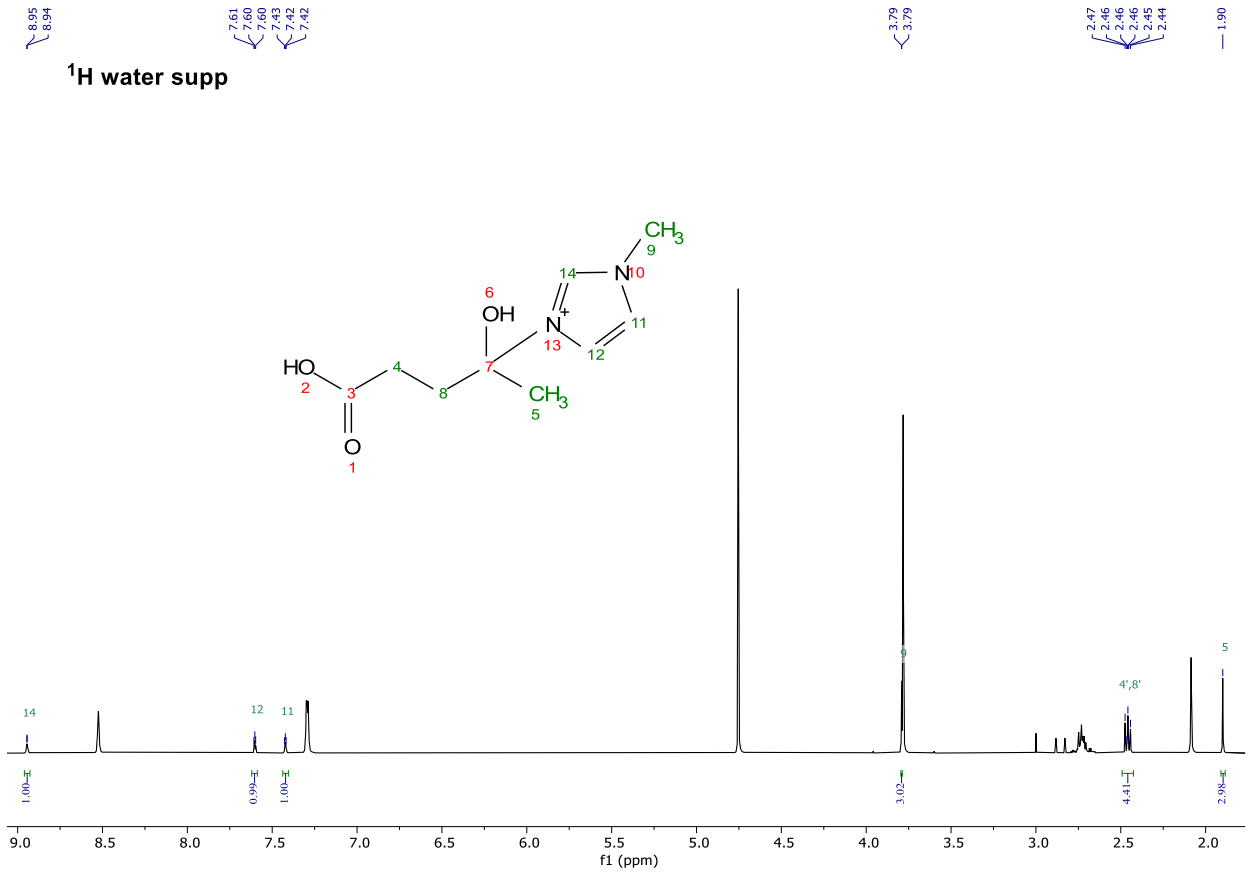
8.95
8.94
7.61
7.60
7.60
7.43
7.42
7.42
3.79
3.79
2.47
2.46
2.46
2.46
2.45
2.44
1.90
1H water supp
CH3
9
N
10
14
6
OH
N+
13
11
12
HO
2
3
4
7
8
CH3
5
O
1
14
12
11
9
4',8'
5
1.00
0.99
1.00
3.02
4.41
2.98
9.0
8.5
8.0
7.5
7.0
6.5
6.0
5.5
5.0
4.5
4.0
3.5
3.0
2.5
2.0
f1 (ppm)

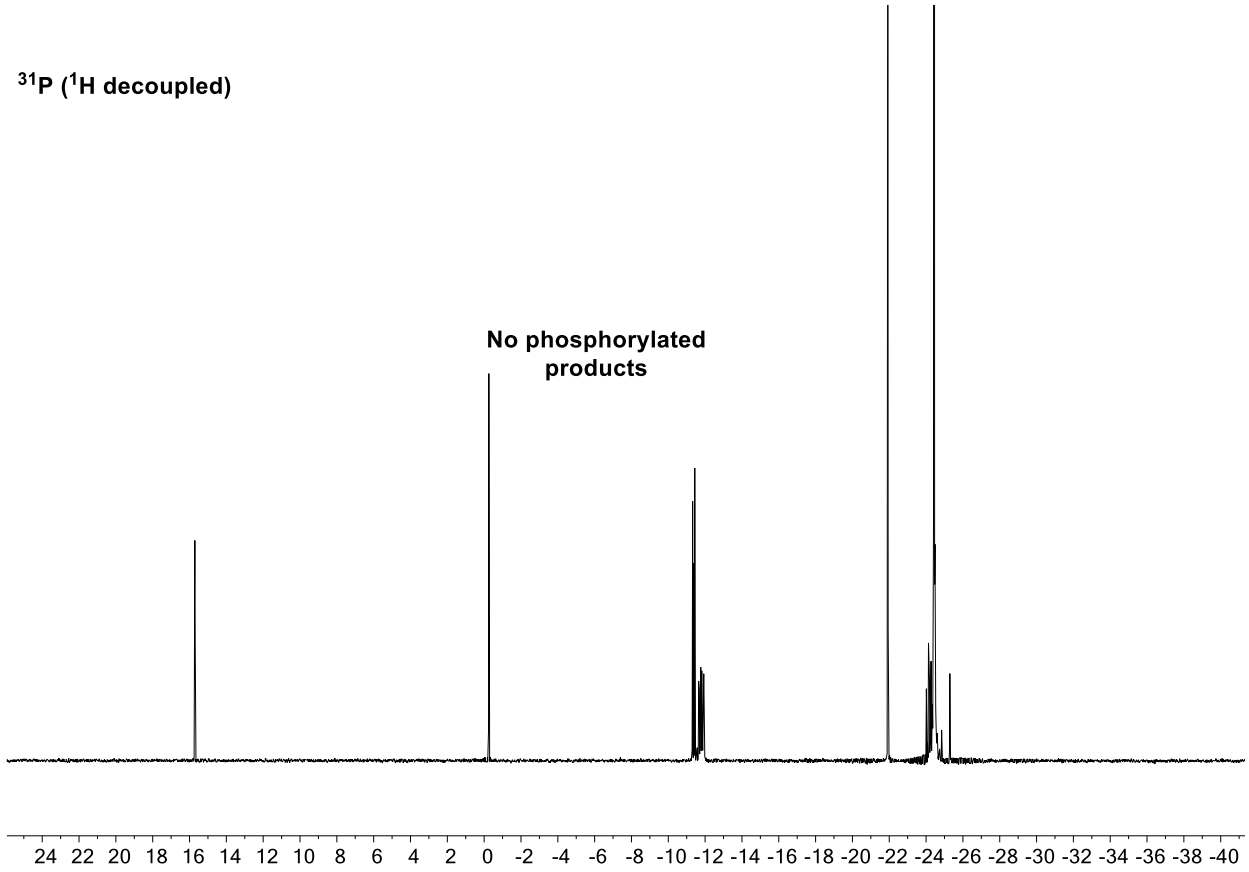

Interestingly, when the reaction was performed from levulinic acid (a γ-ketoacid) using 1-methylimidazole, the nucleophilic attack occurred on the ketone, generating the in-situ hydroxylate, but no phosphorylated product was observed. The observation of a hydroxy-phosphate product (**P1** product) could be the result of the phosphorylation of an *in-situ* generated hydroxylate without going through an acyl-phosphate intermediate. However, no phosphorylated products were observed in that case, favoring the mechanism through an acyl-phosphate intermediate. This intermediate was not observed using pyridine or triethylamine.

14) P1-pyr-OH characterization

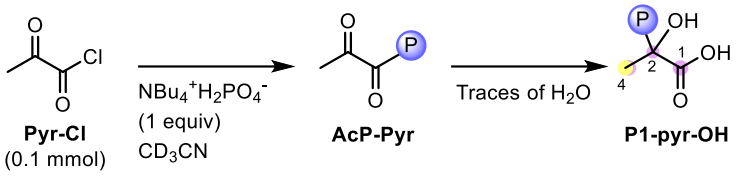

Pyruvoyl chloride **Pyr-Cl** (0.1 mmol) and $NBu_4^+H_2PO_4^-$ (1 equiv) were dissolved in 1 mL of CD_3CN and an NMR tube was prepared (0.6 mL). When traces of water were present in the mixture, the **AcP-Pyr** was converted to **P1-pyr-OH** (characterization below).

^{1}H NMR (500 MHz, D_2O) δ 2.16 (s, 3 H, H-4) ppm.

^{13}C NMR (126 MHz, D_2O) δ 164.2 (d, J_{CP} = 11.2 Hz, C-1), 96.0 (d, J_{CP} = 5.4 Hz C-2), 27.8 (d, J_{CP} = 7.6 Hz, C-4) ppm.

^{31}P NMR (202 MHz, D_2O) δ -2.7 (s) ppm.

HRMS (ESI^-): Calcd m/z for $[C_3H_6O_7P]$ $[M-H]^-$: 184.9857; Found: 184.9849 (-4.2261 ppm).

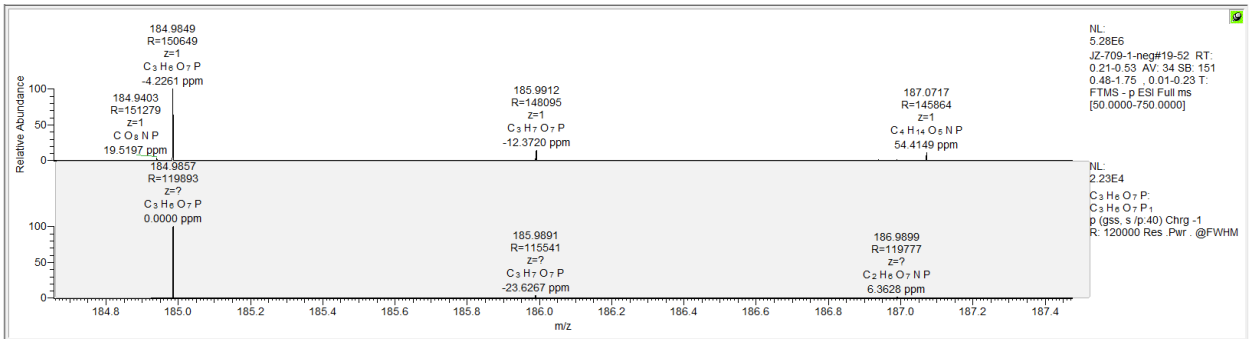

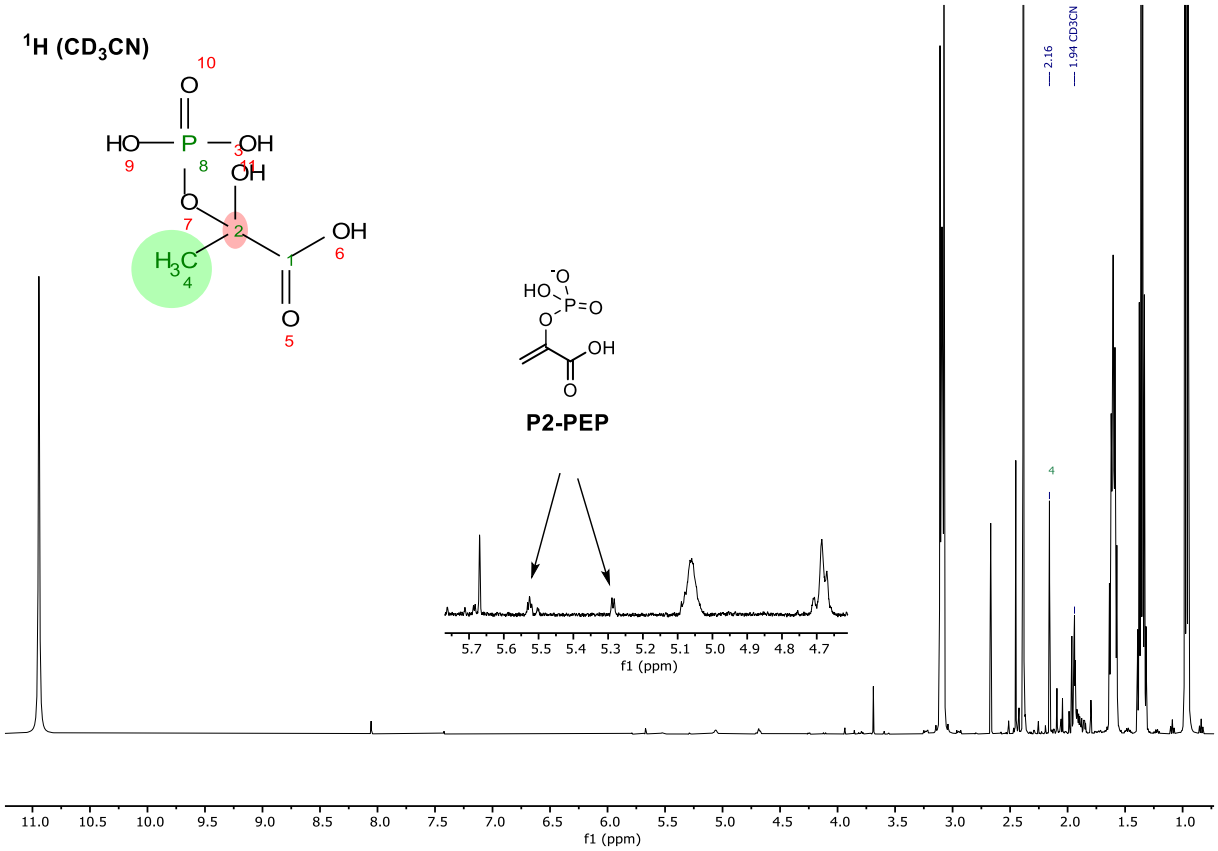
^{1}H (CD_3CN)
P2-PEP
2.16
1.94 CD3CN
f1 (ppm)

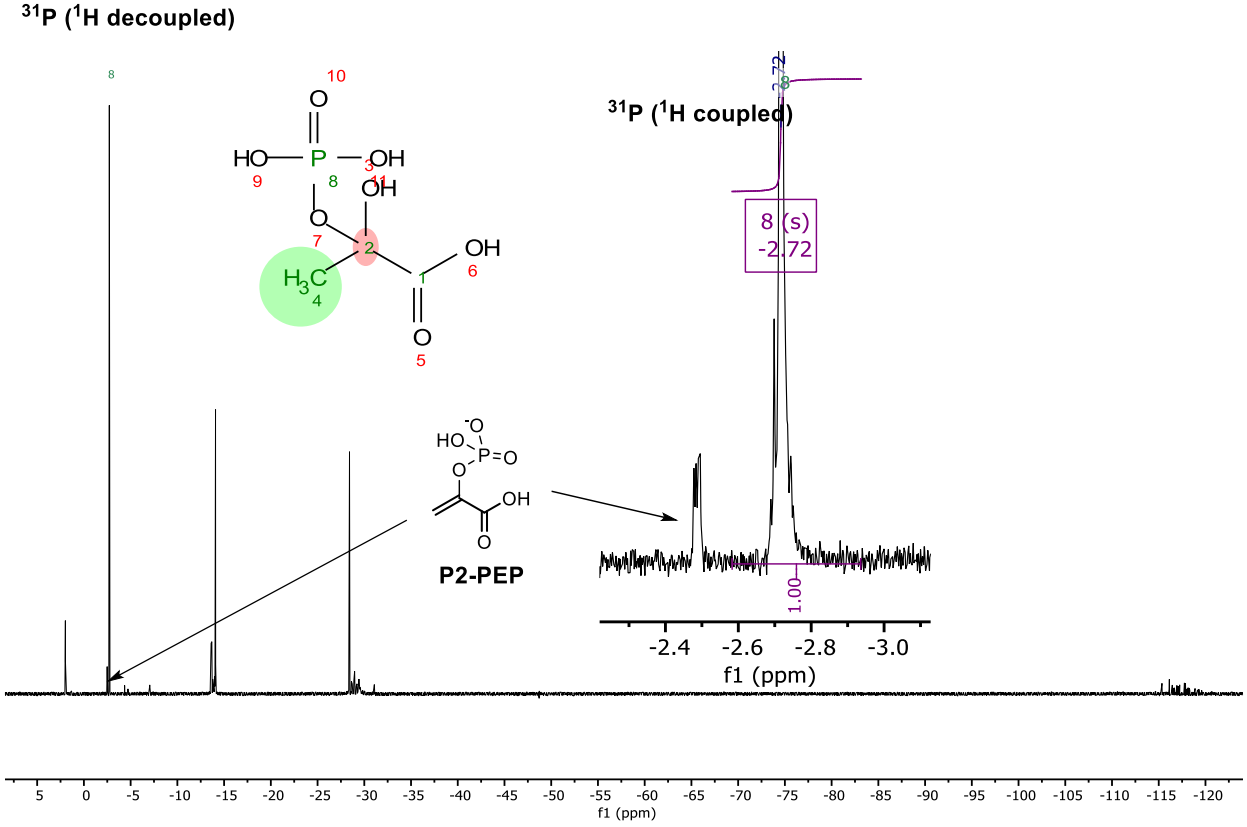
^{31}P (^{1}H decoupled)
^{31}P (^{1}H coupled)
8 (s)
-2.72
P2-PEP
f1 (ppm)

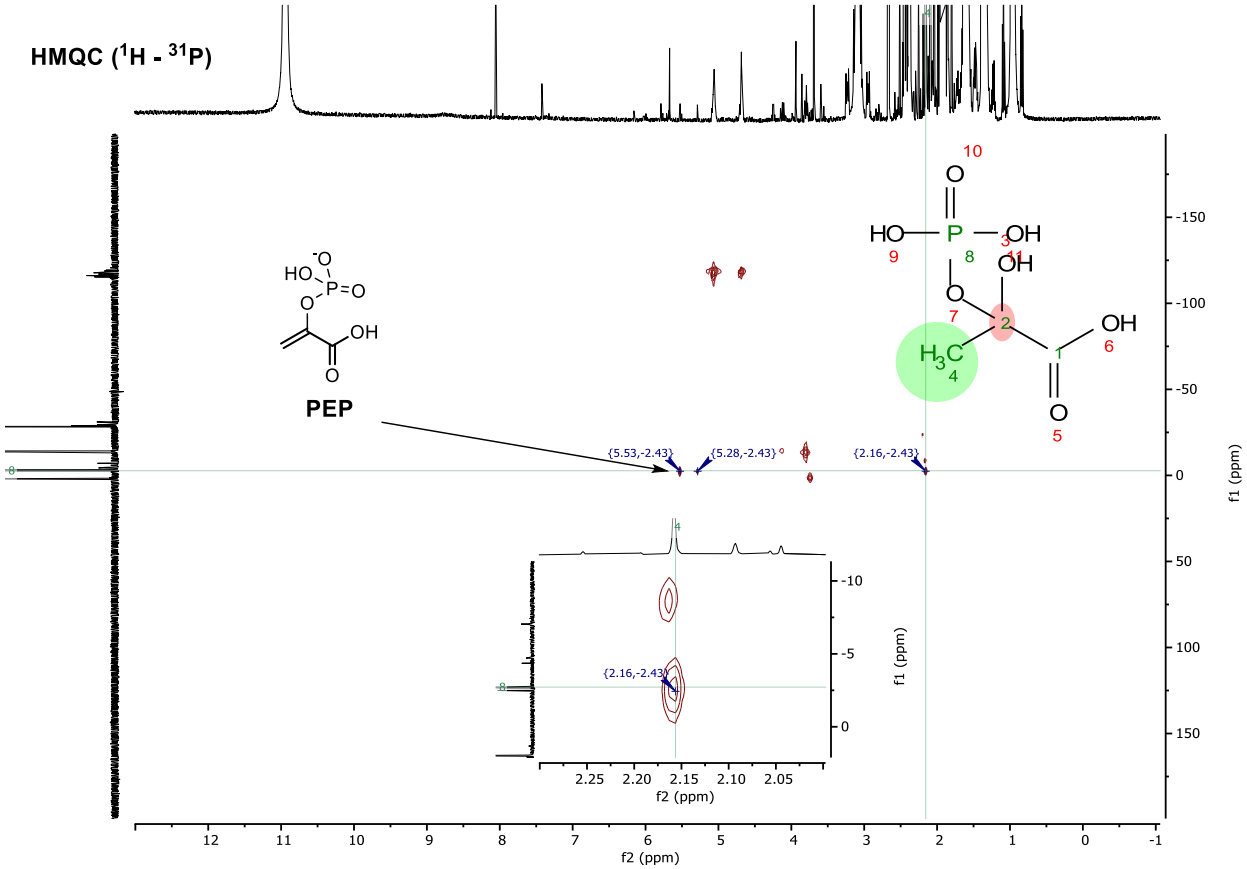
HMQC (^{1}H - ^{31}P)
PEP
{5.53,-2.43}
{5.28,-2.43}
{2.16,-2.43}
f2 (ppm)
f1 (ppm)

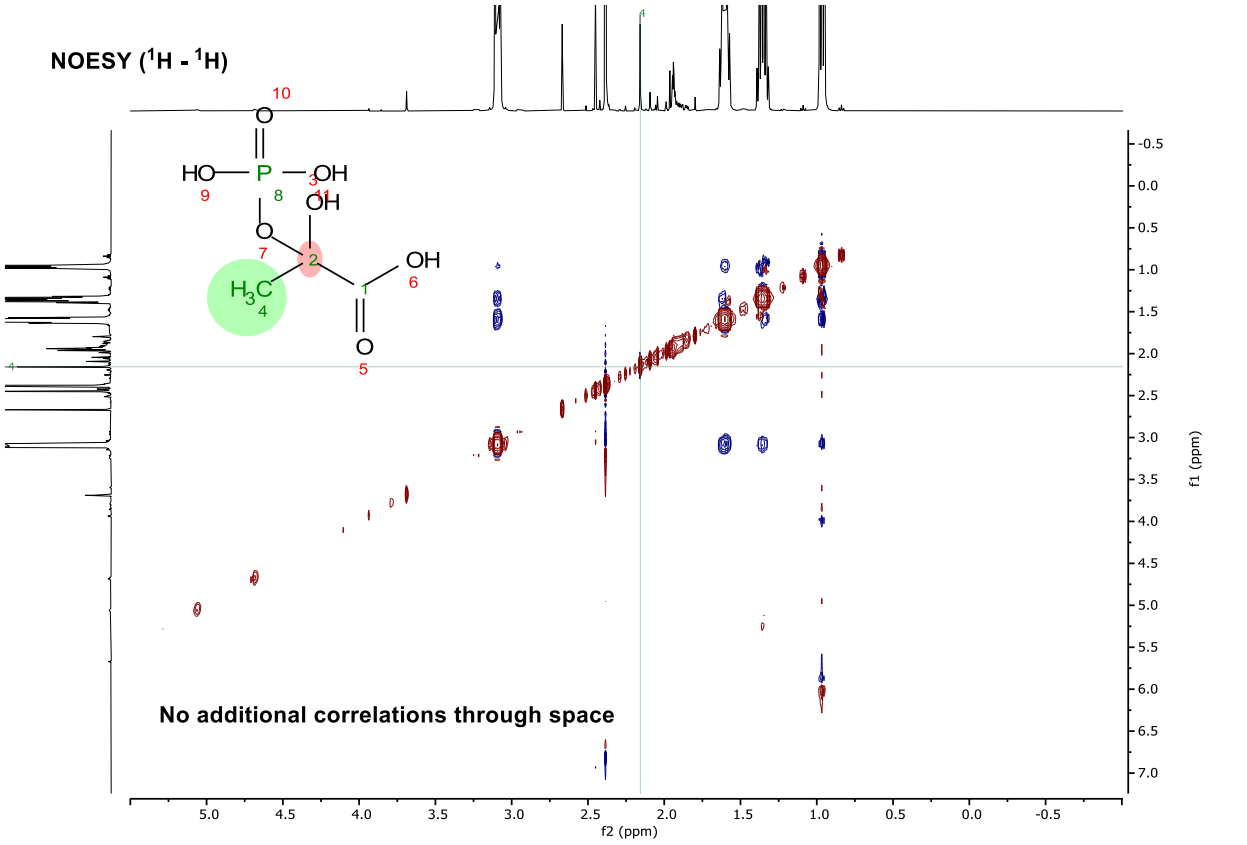
NOESY (^{1}H - ^{1}H)
No additional correlations through space
f2 (ppm)
f1 (ppm)

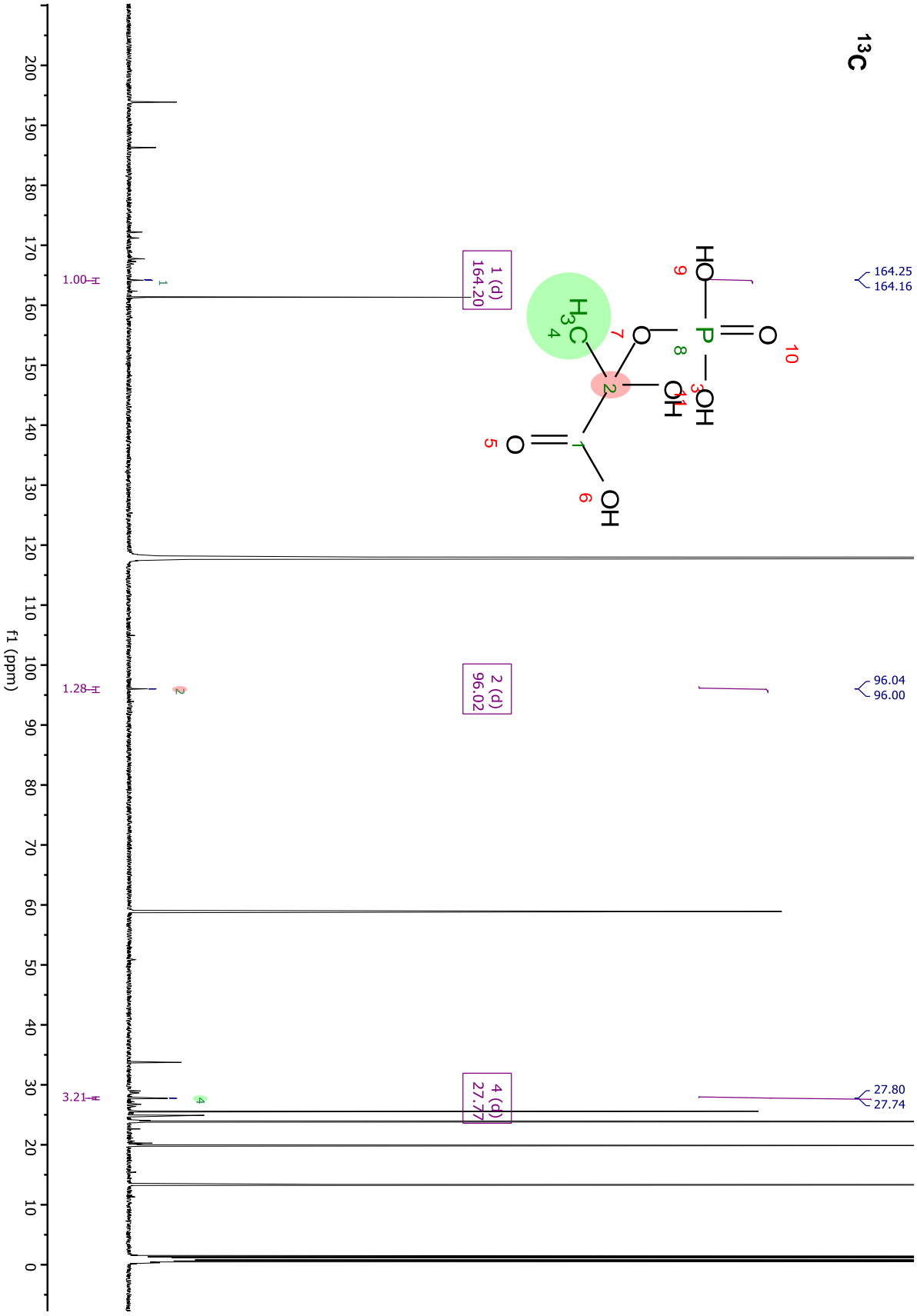
13C
f1 (ppm)
1.00
1.28
3.21
1 (d)
164.20
2 (d)
96.02
4 (d)
27.77
164.25
164.16
96.04
96.00
27.80
27.74

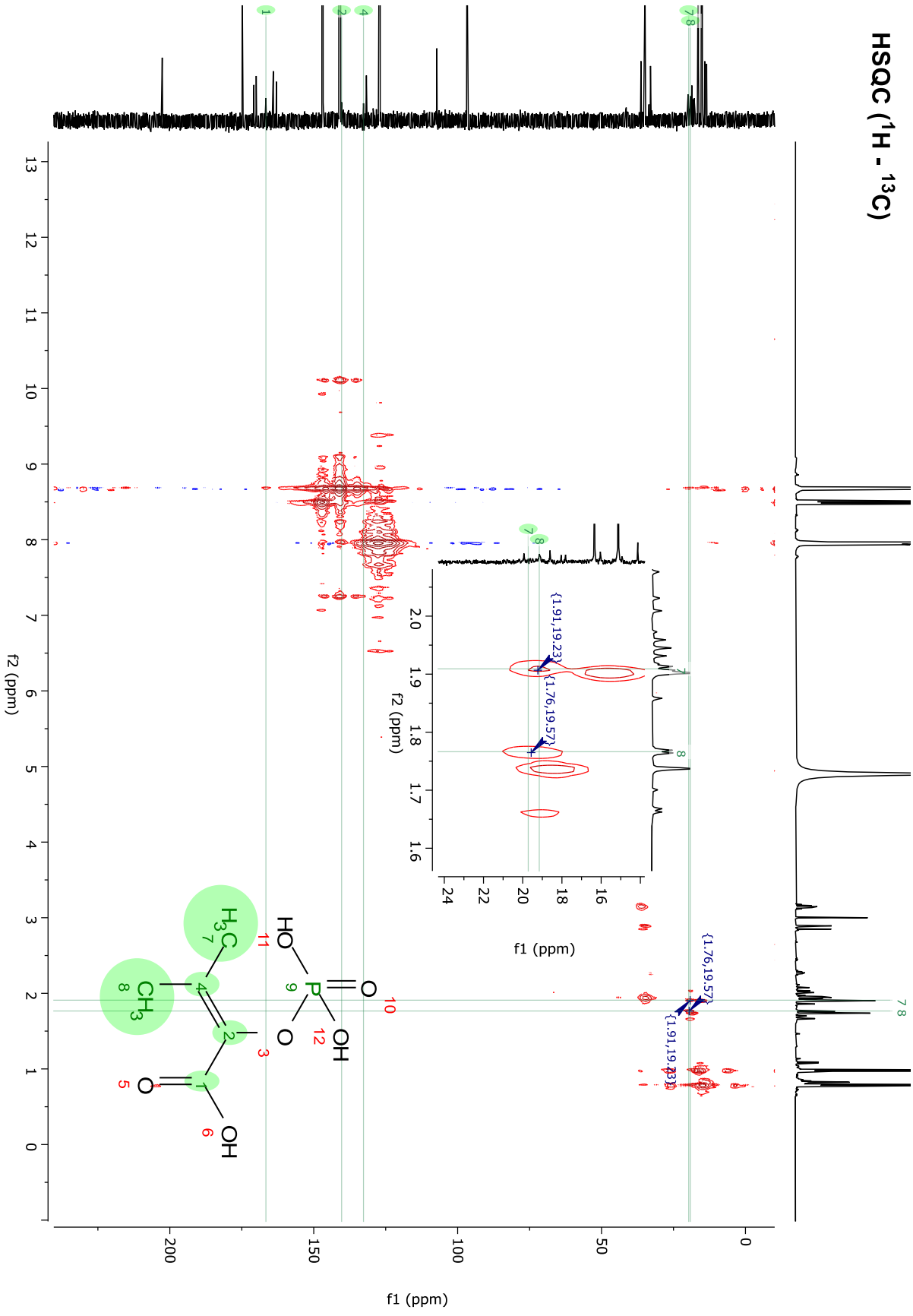
HSQC (^{1}H - ^{13}C)
f1 (ppm)
f2 (ppm)
{1.91,19.23}
{1.76,19.57}
H3C
CH3
HO
OH
O
P

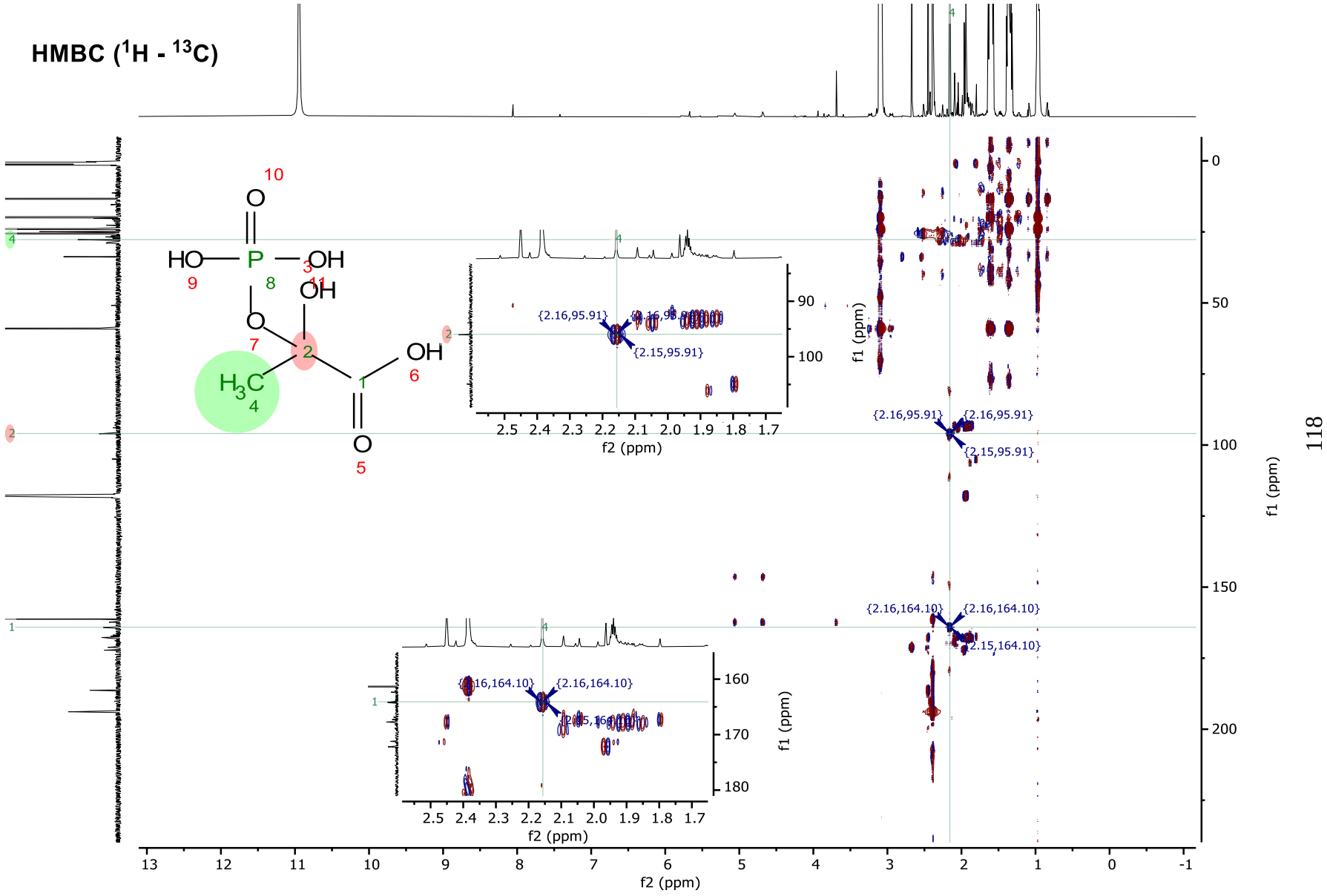
HMBC (^{1}H - ^{13}C)
HO
P
OH
OH
O
O
OH
H_3C
{2.16,95.91}
{2.15,95.91}
{2.16,164.10}
{2.15,164.10}
f2 (ppm)
f1 (ppm)

15) cPEP characterization

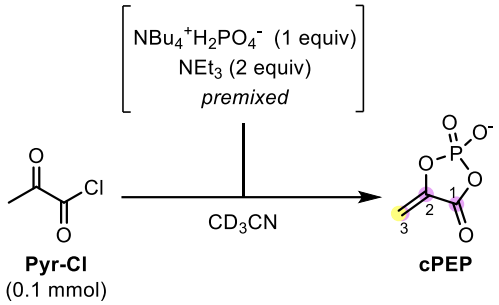

$NBu_4^+H_2PO_4^-$ (1 equiv) and Et_3N (2 equiv) were premixed in 1 mL of CD_3CN and an NMR tube was prepared (0.6 mL). Then, pyruvoyl chloride **Pyr-Cl** (0.1 mmol) was added to the mixture and the formation of **cPEP** was observed (characterization below).

^{1}H NMR (500 MHz, D_2O) δ 5.18 (t/dd, J_{HH} = 2.2 Hz, J_{HP} = 1.4 Hz H-3), 4.88 (dd, J_{HH} = 2.2 Hz, J_{HP} = 1.1 Hz H-3) ppm.

^{13}C NMR (126 MHz, D_2O) δ 161.4 (d, J_{CP} = 7.4 Hz, C-1), 148.0 (d, J_{CP} = 2.7 Hz C-2), 95.2 (d, J_{CP} = 11.1 Hz, C-3) ppm.

^{31}P NMR (202 MHz, D_2O) δ -1.7 (t, J_{HP} = 1.3 Hz) ppm.

HRMS (ESI^-): Calcd m/z for $[C_3H_2O_5P]$ $[M-H]^-$: 148.9645; Found: 148.9634 (-7.5668 ppm).

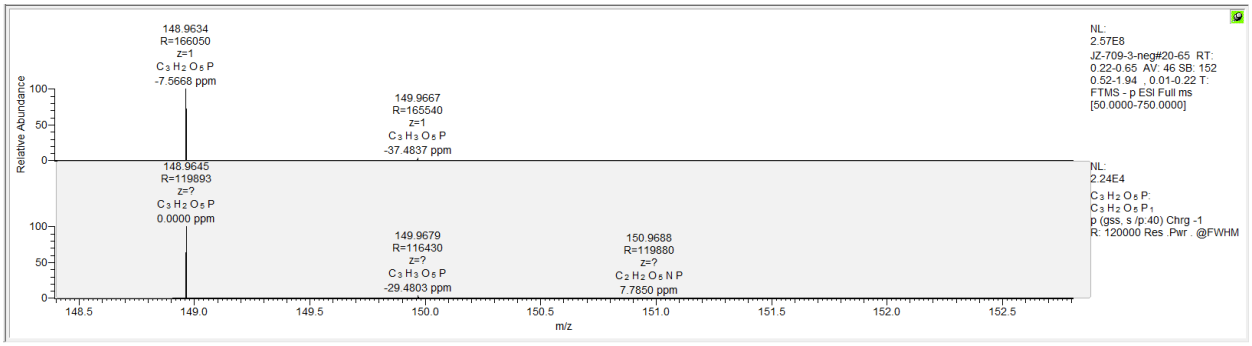

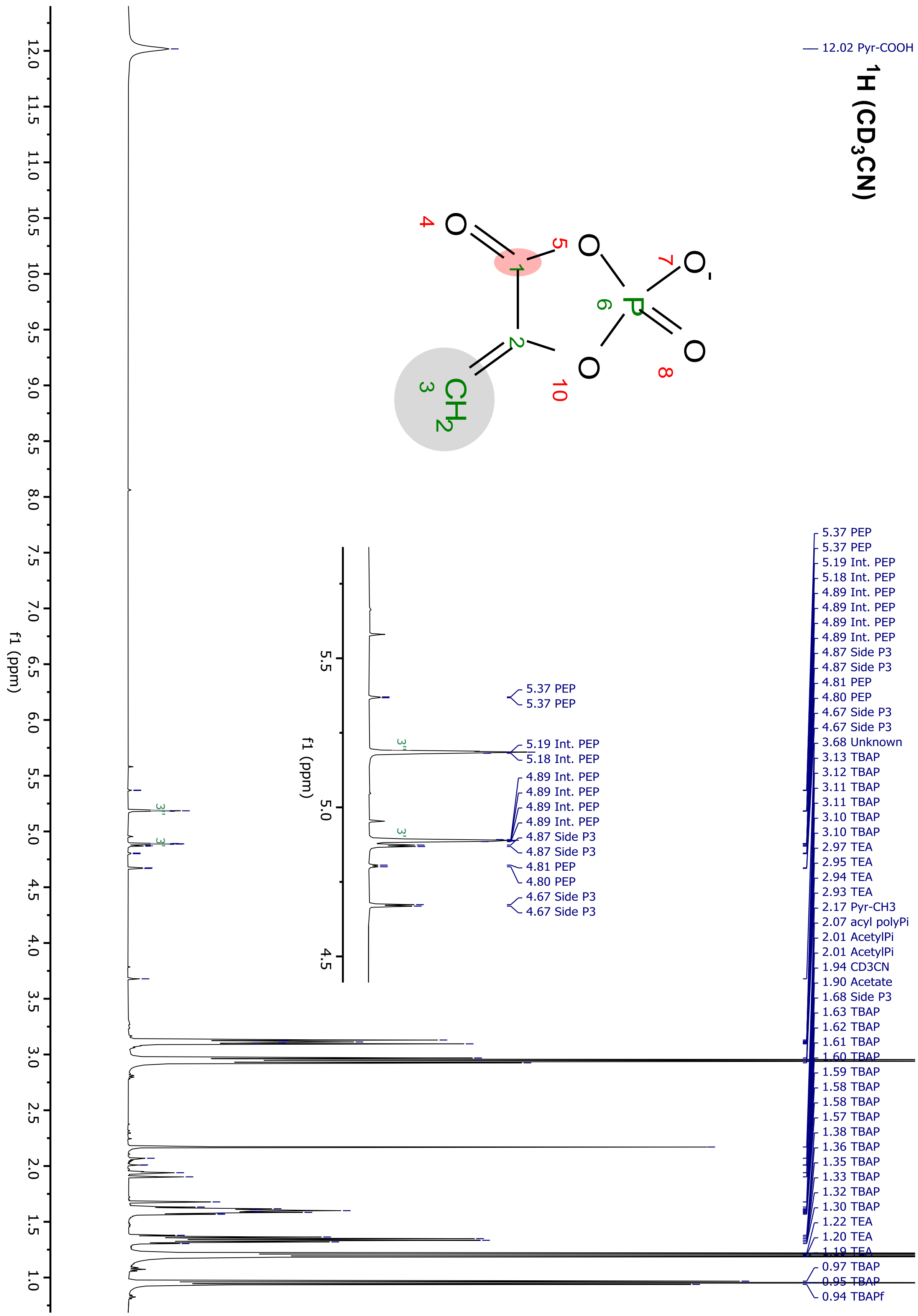
1H (CD3CN)
12.02 Pyr-COOH
5.37 PEP
5.37 PEP
5.19 Int. PEP
5.18 Int. PEP
4.89 Int. PEP
4.89 Int. PEP
4.89 Int. PEP
4.89 Int. PEP
4.87 Side P3
4.87 Side P3
4.81 PEP
4.80 PEP
4.67 Side P3
4.67 Side P3
3.68 Unknown
3.13 TBAP
3.12 TBAP
3.11 TBAP
3.11 TBAP
3.10 TBAP
3.10 TBAP
2.97 TEA
2.95 TEA
2.94 TEA
2.93 TEA
2.17 Pyr-CH3
2.07 acyl polyPi
2.01 AcetylPi
2.01 AcetylPi
1.94 CD3CN
1.90 Acetate
1.68 Side P3
1.63 TBAP
1.62 TBAP
1.61 TBAP
1.60 TBAP
1.59 TBAP
1.58 TBAP
1.58 TBAP
1.57 TBAP
1.38 TBAP
1.36 TBAP
1.35 TBAP
1.33 TBAP
1.32 TBAP
1.30 TBAP
1.22 TEA
1.20 TEA
1.19 TEA
0.97 TBAP
0.95 TBAP
0.94 TBAPf
f1 (ppm)

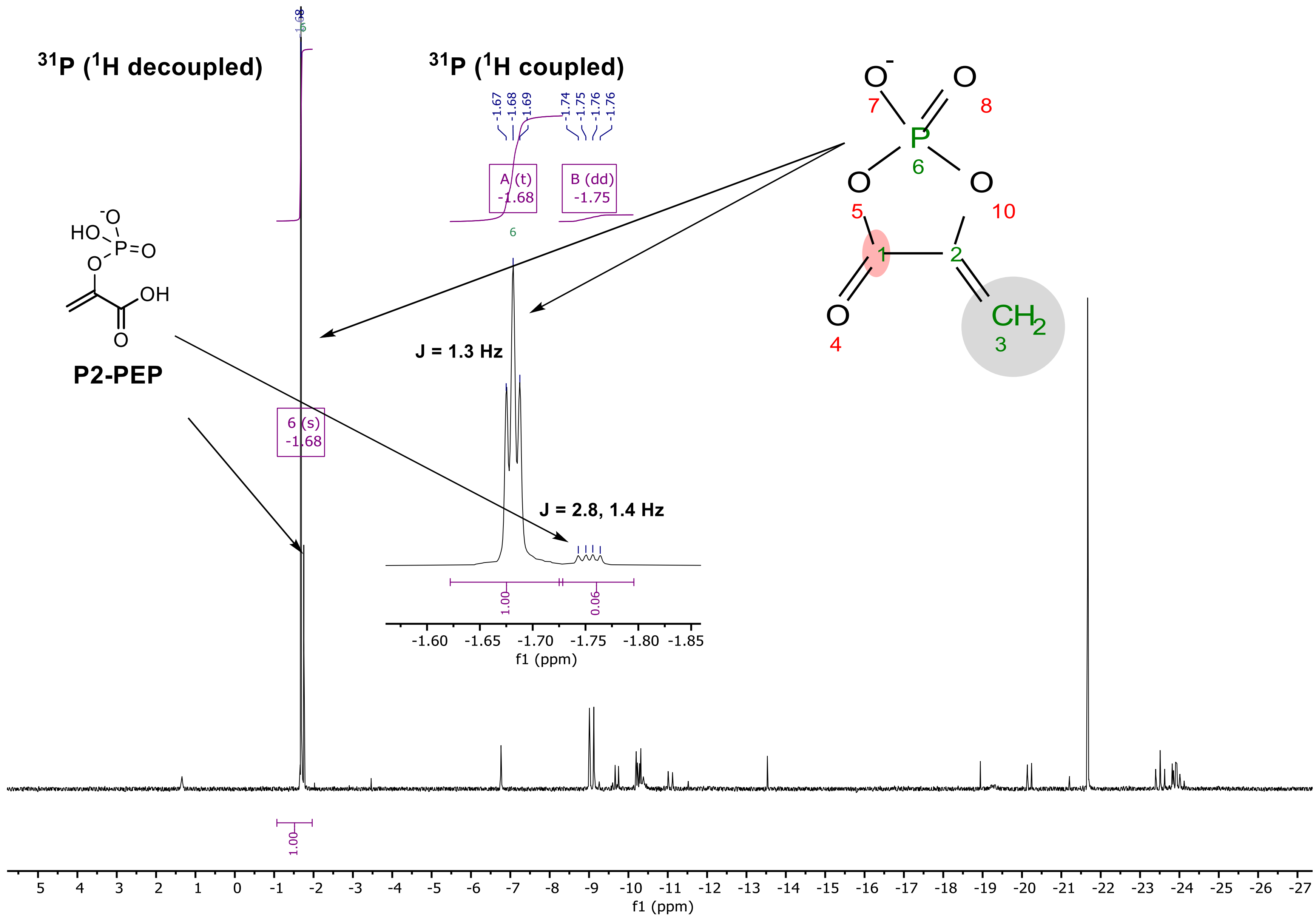

31P (1H decoupled)
31P (1H coupled)
P2-PEP
6 (s)
-1.68
A (t)
-1.68
B (dd)
-1.75
-1.67
-1.68
-1.69
-1.74
-1.75
-1.76
-1.76
J = 1.3 Hz
J = 2.8, 1.4 Hz
1.00
0.06
-1.60 -1.65 -1.70 -1.75 -1.80 -1.85
f1 (ppm)
5 4 3 2 1 0 -1 -2 -3 -4 -5 -6 -7 -8 -9 -10 -11 -12 -13 -14 -15 -16 -17 -18 -19 -20 -21 -22 -23 -24 -25 -26 -27
f1 (ppm)

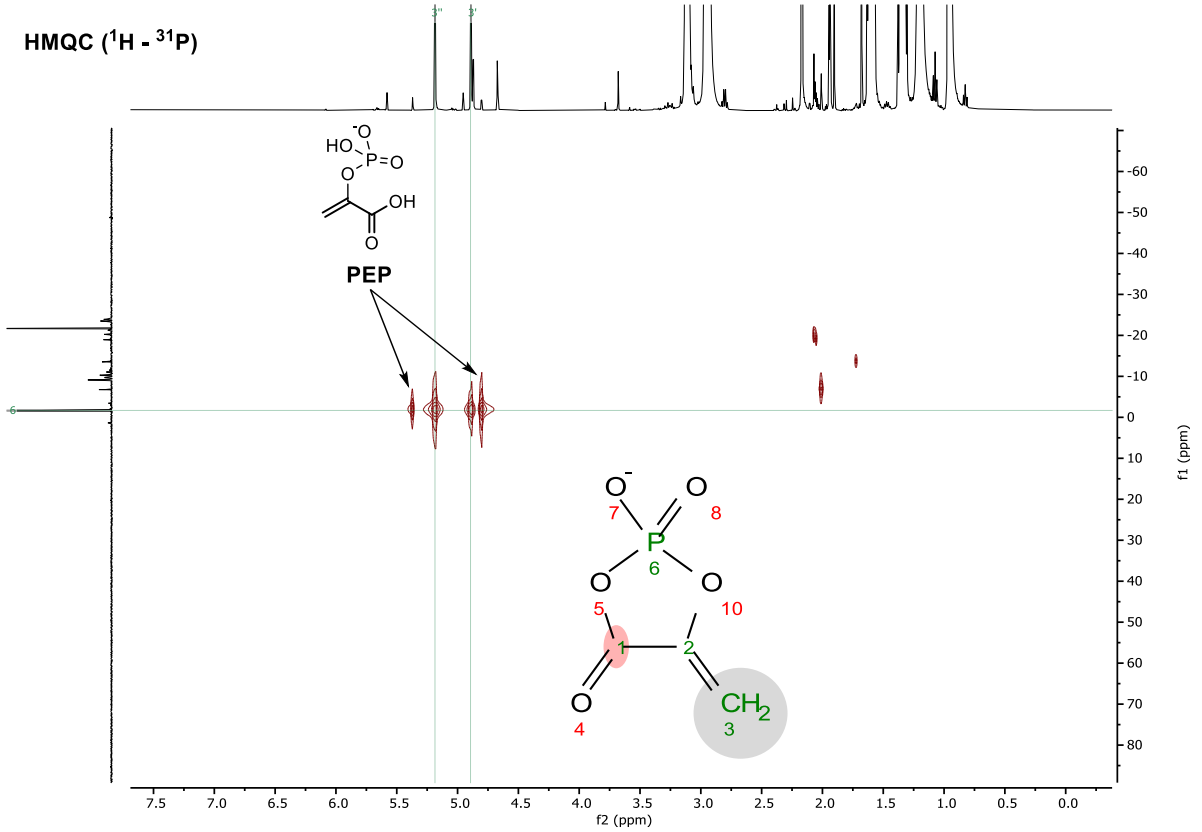
HMQC (^{1}H - ^{31}P)
PEP
f2 (ppm)
f1 (ppm)

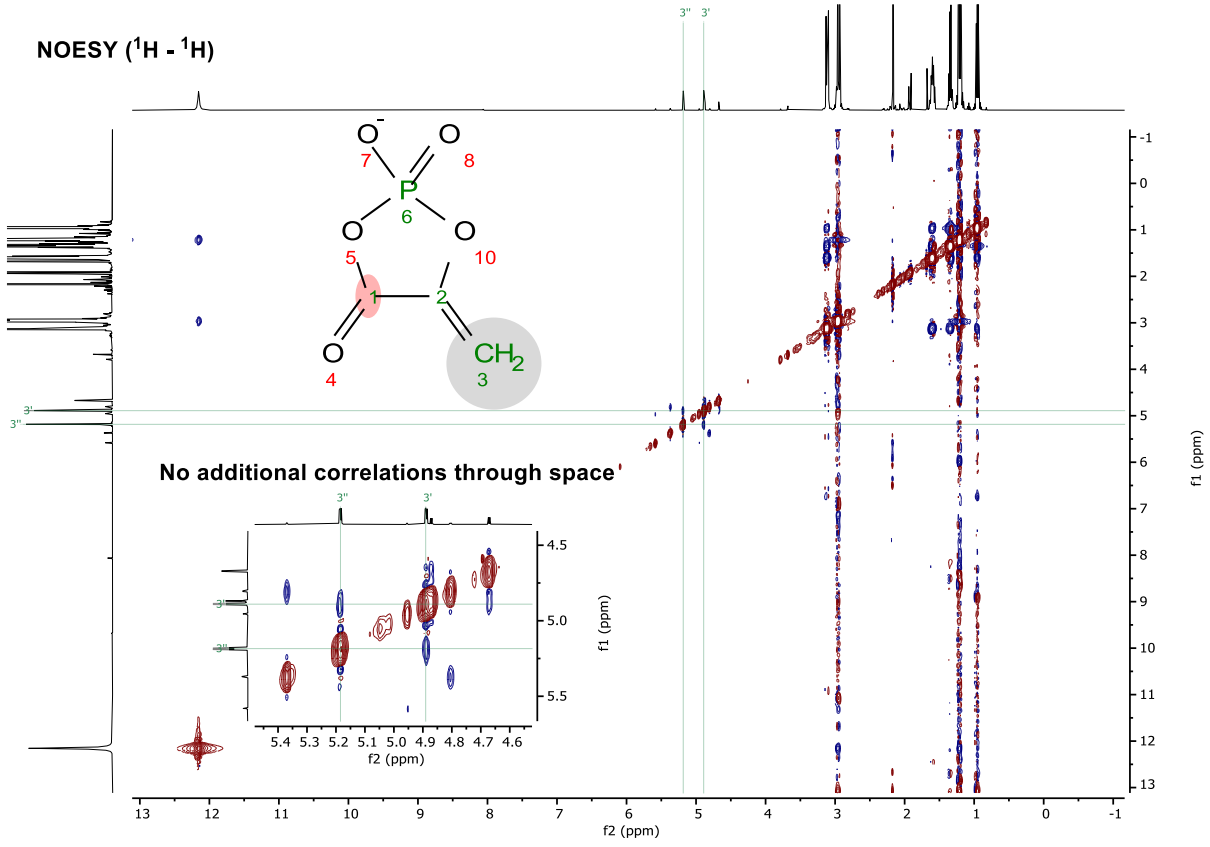
NOESY (^{1}H - ^{1}H)
No additional correlations through space
f2 (ppm)
f1 (ppm)

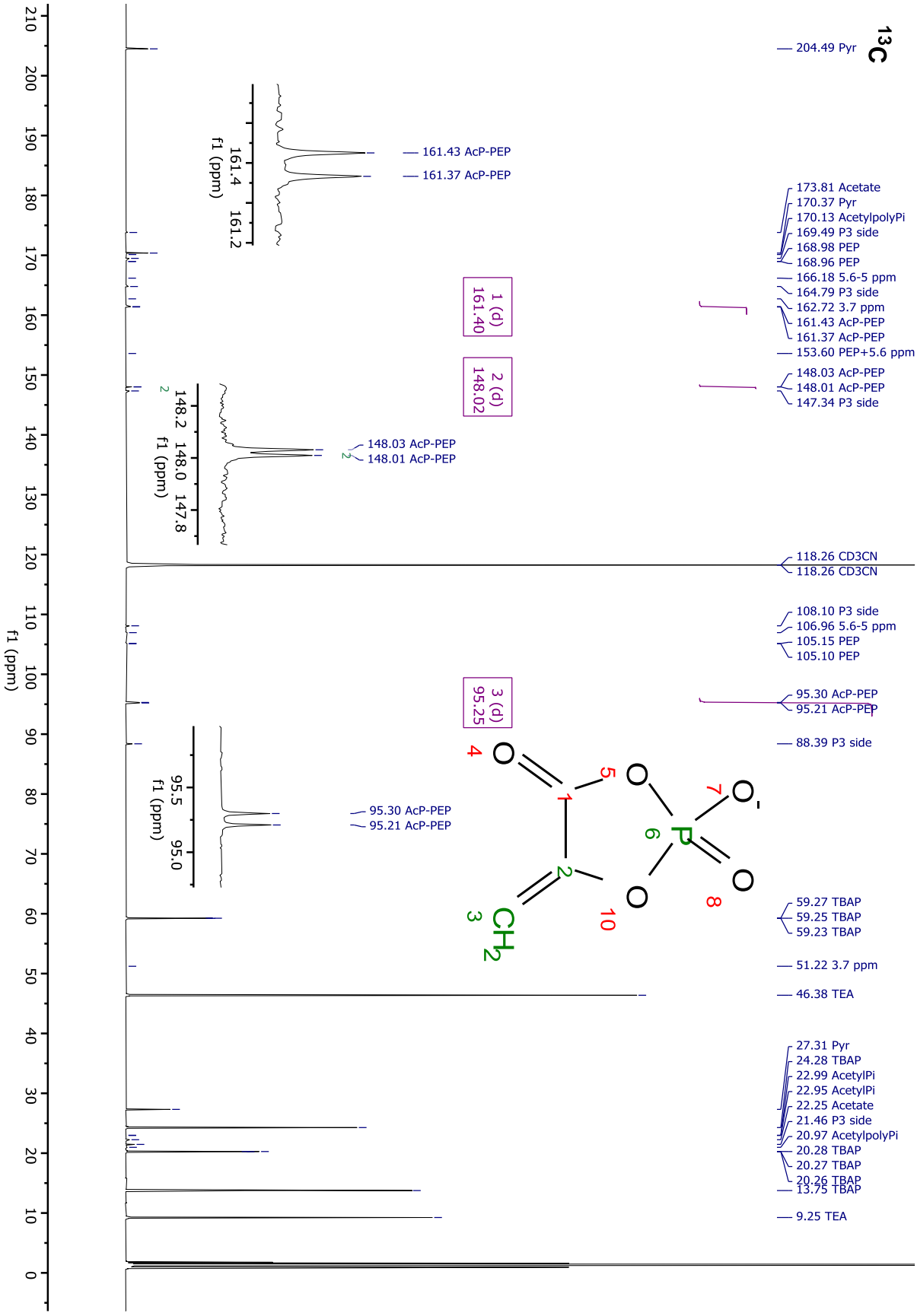
13C
204.49 Pyr
173.81 Acetate
170.37 Pyr
170.13 AcetylpolyPi
169.49 P3 side
168.98 PEP
168.96 PEP
166.18 5.6-5 ppm
164.79 P3 side
162.72 3.7 ppm
161.43 AcP-PEP
161.37 AcP-PEP
153.60 PEP+5.6 ppm
148.03 AcP-PEP
148.01 AcP-PEP
147.34 P3 side
118.26 CD3CN
118.26 CD3CN
108.10 P3 side
106.96 5.6-5 ppm
105.15 PEP
105.10 PEP
95.30 AcP-PEP
95.21 AcP-PEP
88.39 P3 side
59.27 TBAP
59.25 TBAP
59.23 TBAP
51.22 3.7 ppm
46.38 TEA
27.31 Pyr
24.28 TBAP
22.99 AcetylPi
22.95 AcetylPi
22.25 Acetate
21.46 P3 side
20.97 AcetylpolyPi
20.28 TBAP
20.27 TBAP
20.26 TBAP
13.75 TBAP
9.25 TEA
1 (d) 161.40
2 (d) 148.02
3 (d) 95.25
161.43 AcP-PEP
161.37 AcP-PEP
148.03 AcP-PEP
148.01 AcP-PEP
95.30 AcP-PEP
95.21 AcP-PEP
f1 (ppm)

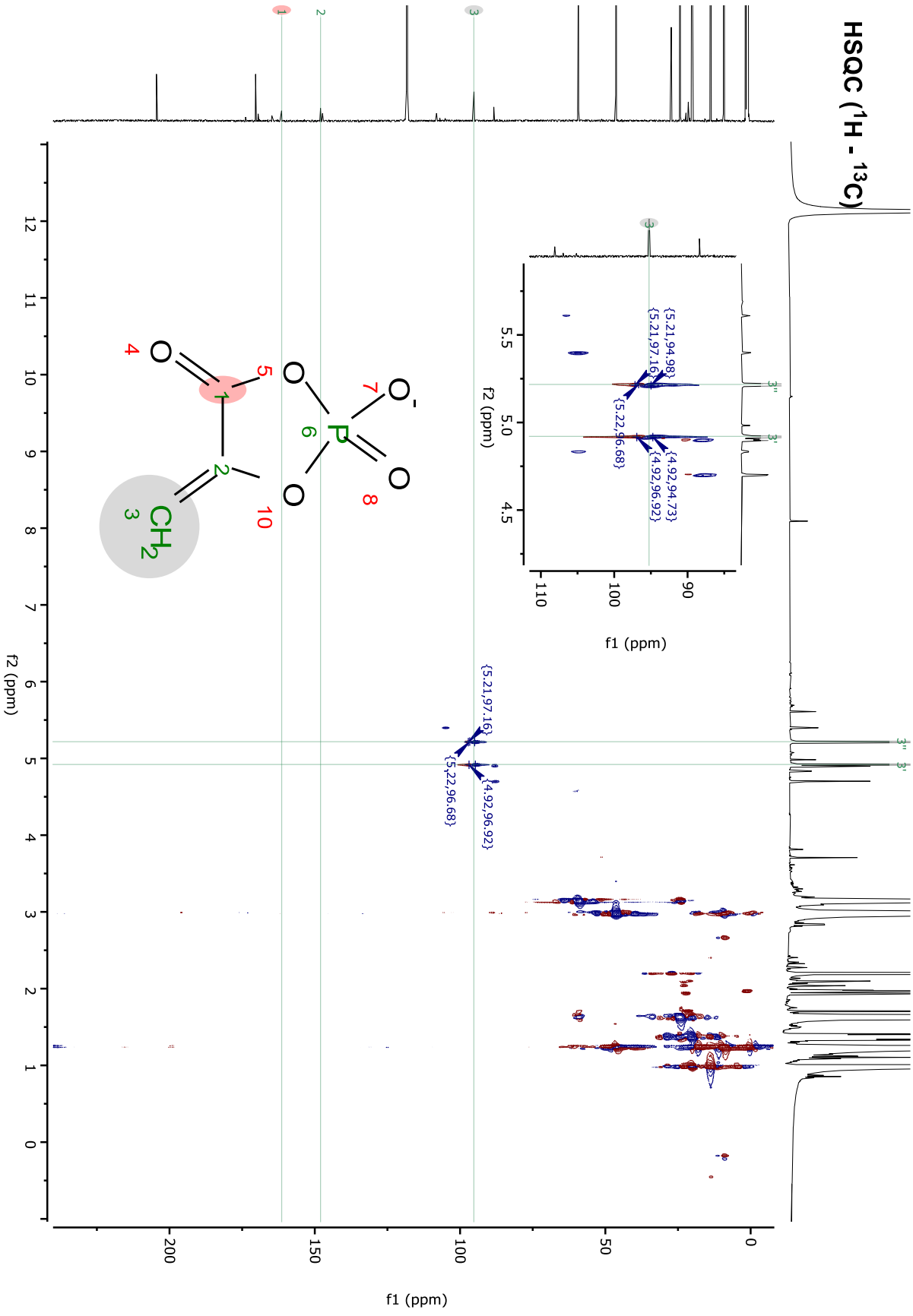
HSQC (^{1}H - ^{13}C)
f1 (ppm)
f2 (ppm)
{5.21,97.16}
{5.22,96.68}
{4.92,96.92}
{5.21,94.98}
{4.92,94.73}
O
O
O
O
P
CH2
1
2
3
4
5
6
7
8
10

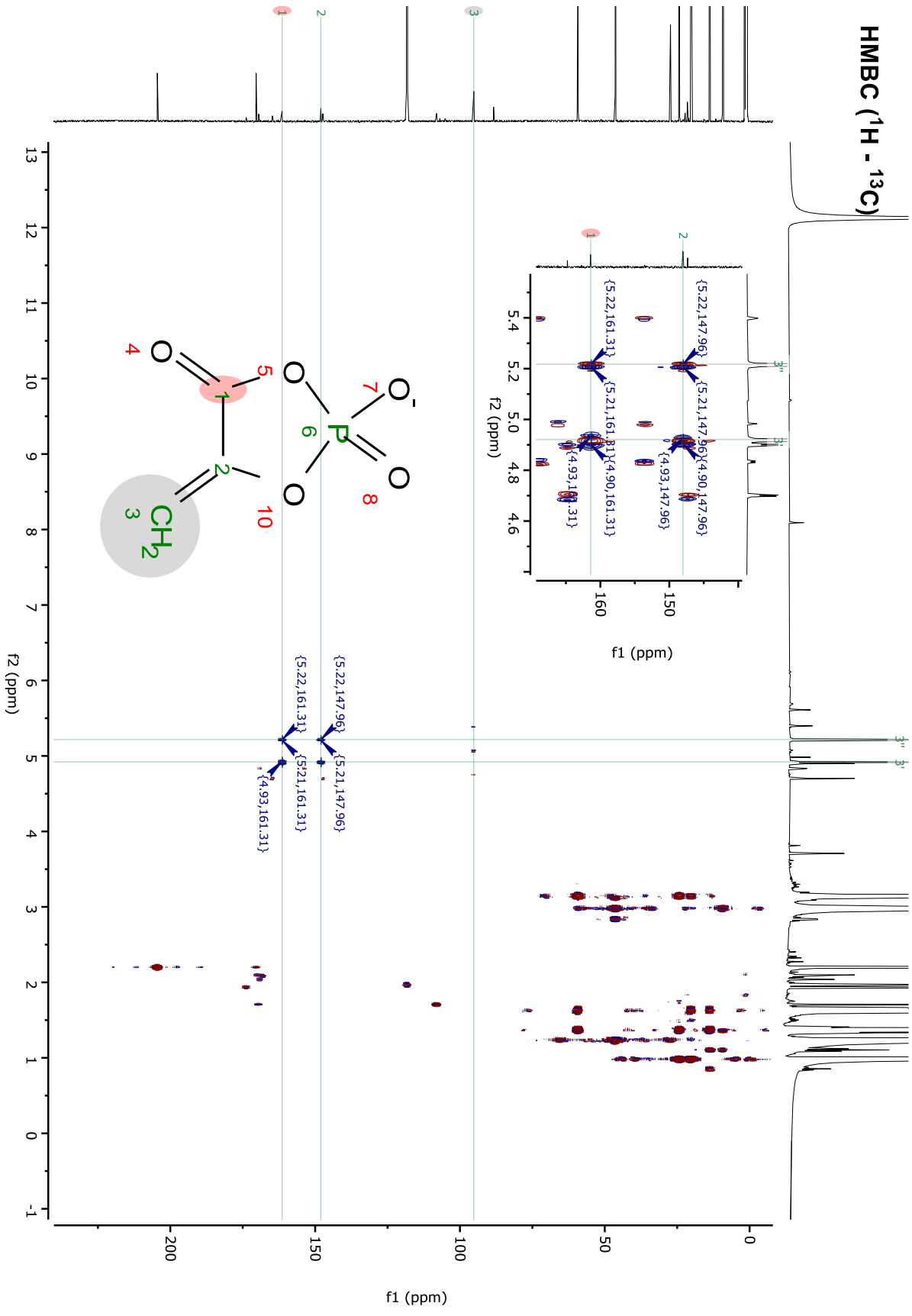
HMBC (^{1}H - ^{13}C)
f2 (ppm)
f1 (ppm)
{5.22,147.96}
{5.21,147.96}
{5.22,161.31}
{5.21,161.31}
{4.93,161.31}
{4.90,147.96}
{4.93,147.96}
{4.90,161.31}
O
O
O
O
P
CH2
1
2
3
4
5
6
7
8
10

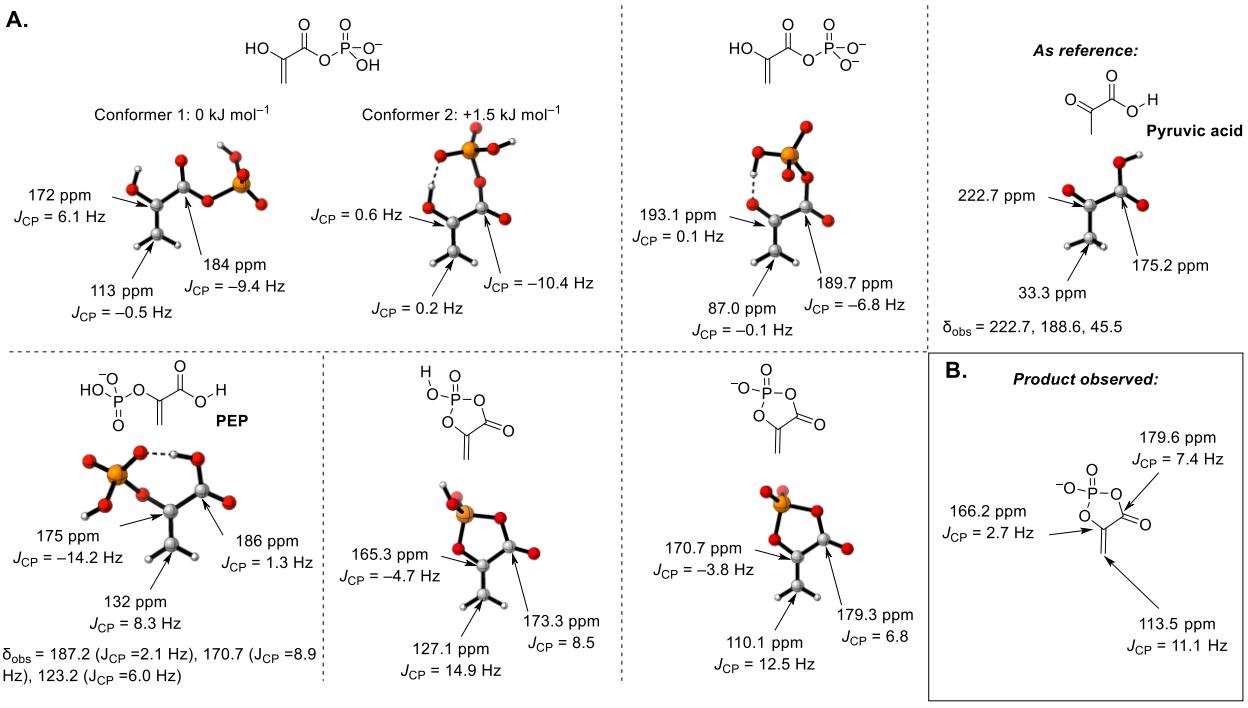

Figure S5. (A). DFT calculations of the ^{13}C chemical shifts and the associated coupling constant of plausible **cPEP** structures. (B) Obtained chemical shifts of the observed product.

The experimental spectra of pyruvic acid, **PEP**, and the observed product (**cPEP**) were calibrated by setting the C-2 chemical shift of pyruvic acid at its calculated value δ = 222.7 ppm. Their chemical shifts are described in Figure S5. An error of 10 ppm was observed. The structure of **cPEP** (Fig. S5B) was assigned according to the observed chemical shifts and the associated coupling constants. For details of the DFT method, see Table S17 + Fig. S9 (section VII. E., p. S147-S148).

B. Magic Angle Spinning (MAS) solid-state NMR for the characterization of the paste

1) $^{31}P\{1H\}$ DP/MAS (Direct Polarization), CP/MAS (Cross Polarization) and ^{1}H-^{31}P FSLG HETCOR NMR

Reactions were set up as described in the general procedure **GP-II**. After 10 min at 60 °C, the reaction was stopped and the paste was inserted in 3.2 diameter OD zirconia rotors closed with vespel caps. Samples were spun at 22.5 kHz in a triple resonance MAS probe (Bruker™) on an AVANCE 500 MHz wide bore spectrometer (Bruker™). All experiments involving ^{31}P detection were done at room temperature on an AVANCE 500 MHz wide bore spectrometer (Bruker™) operating at a frequency of 500.12 MHz for ^{1}H and 202.42 MHz for 31P. Both DP (Direct Polarization) and CP (Cross Polarization) spectra were acquired with a 30.52 Hz/pt resolution, namely 4096 data points in time domain and 62.5 kHz for the spectral width (308.76ppm). A B_1 RF field of 100kHz (P90°pulse=2.5µs) was used 1D 31P{1H} DP/MAS and 32 transients were taken with a 1s recycle delay thus leading to a total acquisition time of 32 s per spectrum. CP/MAS experiments were performed by following the so called APHH-CP (Adiabatic Passage through the Hartmann-Hahn conditions)[7,8] with the modified Hartman & Hahn conditions spin-lock B_1 fields being 73.5 kHz for ^{31}P and 96 kHz for ^{1}H. Contact times of 150 µs and 3 ms were used in order to check proton to phosphorus proximities. Here the recycling delay was set to 3 s and 8192 scans were acquired, thus giving overall acquisition time of ca 7 h. In order to get undistorted lineshapes and flat baselines, a rotation synchronized Hahn echo[9] was inserted prior to FID acquisition for all CP/MAS based experiments (including the bidimensional ^{1}H-^{31}P HETCORS). Also the ^{1}H spectra obtained here at 22.5kHz spinning frequency were acquired directly with this pulse scheme (P_{90}-τ-P_{180}-τ) and the

corresponding echo time set to 4 rotation periods (178µs), allowing probe background signals suppression. For the proton side, the B_1 RF field was set to 121 kHz for hard pulse while decoupling was achieved through the SPINAL-64 decoupling sequence at 90 kHz RF strength[10] for all experiments. The bidimensional ^{1}H-^{31}P heteronuclear correlation (HETCOR) experiments with frequency-switched Lee-Goldburg (FSLG) irradiation during the evolution time[11] were obtained with the following conditions: the duration of the successive FSLG pulses was 5.997 µs, corresponding to an effective ^{1}H-^{1}H decoupling field of 166.8 kHz and the same modified Hartman and Hahn conditions for the CP step (73.5 kHz ^{31}P /96 kHz ^{1}H). Two different contact times were used during the CP step: 150 µs for close contact ^{1}H-^{31}P detection and 3 ms for longer ^{1}H-^{31}P distances sensing. 224 complex data points were acquired in the ^{1}H indirect dimension and for each t1 increment 384 scans were accumulated over 4096 time domain data points with the same recycle time as previously deascribed (3 s). The corresponding spectral widths were 16217 Hz for ^{1}H (32.4329 ppm) and 62.5 kHz for ^{31}P (308.7655 ppm), leading to a frequency resolution of 144.8 Hz and 30.52 Hz respectively. A 90° shifted squared sinebell apodization function was applied in both dimensions prior to the Fourier transform. Chemical shifts are given respective to tetramethysilane (TMS) for ^{1}H NMR using adamantane as a secondary reference; H_3PO_4 (80% saturated solution) was used as the reference for ^{31}P NMR.

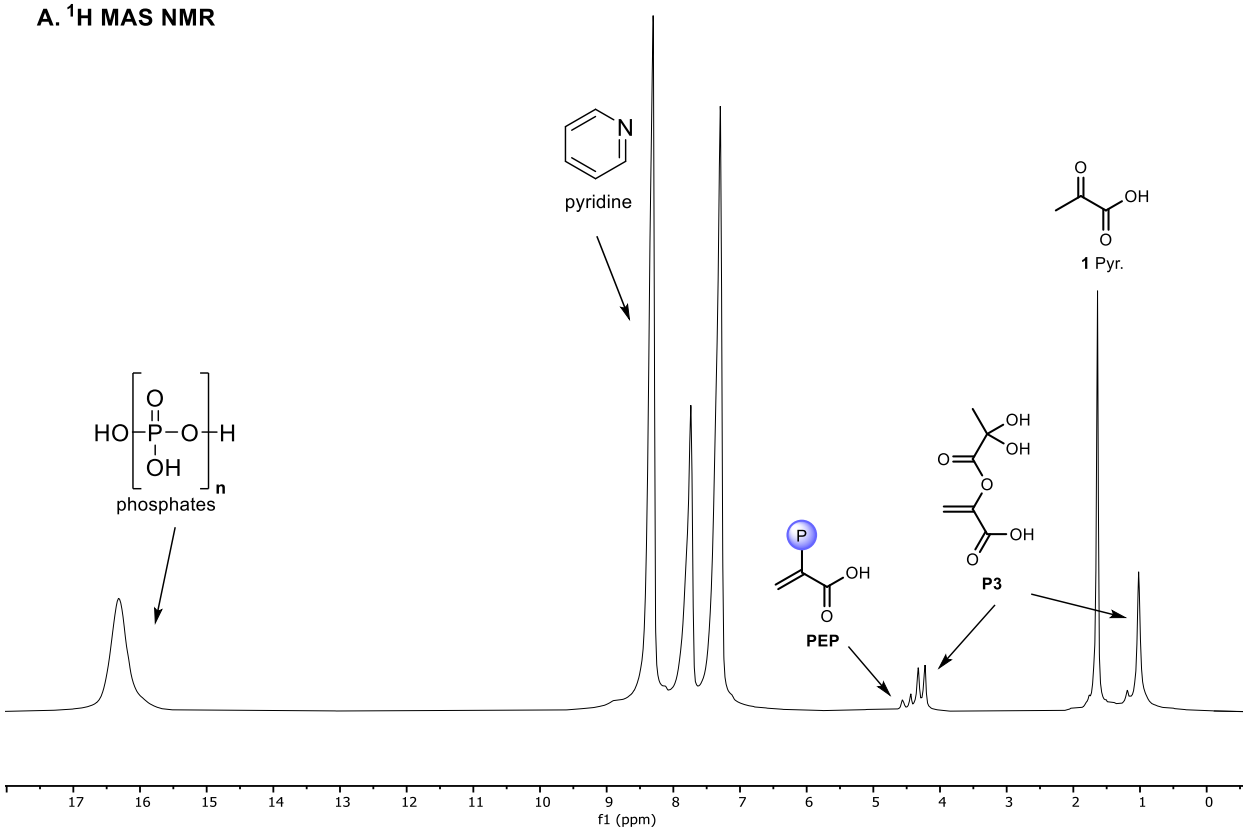

B. ^{31}P DP/MAS NMR

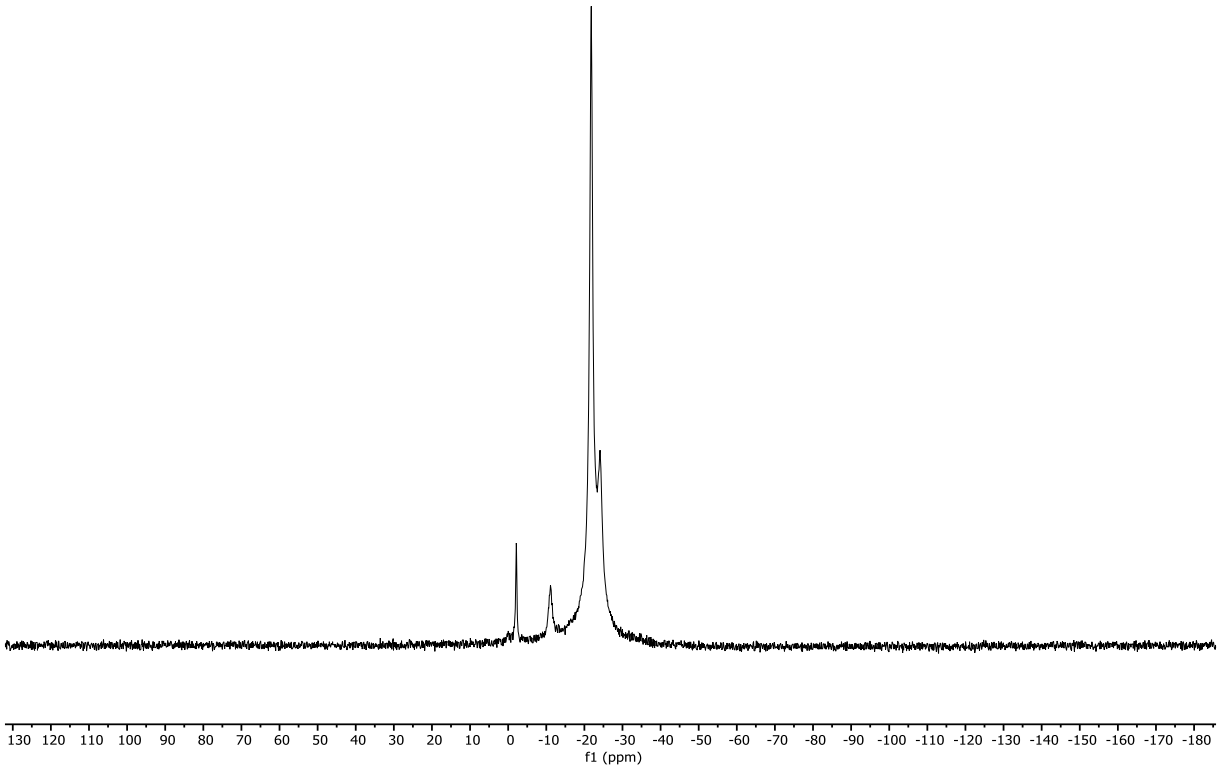

C. ^{31}P CP/MAS NMR

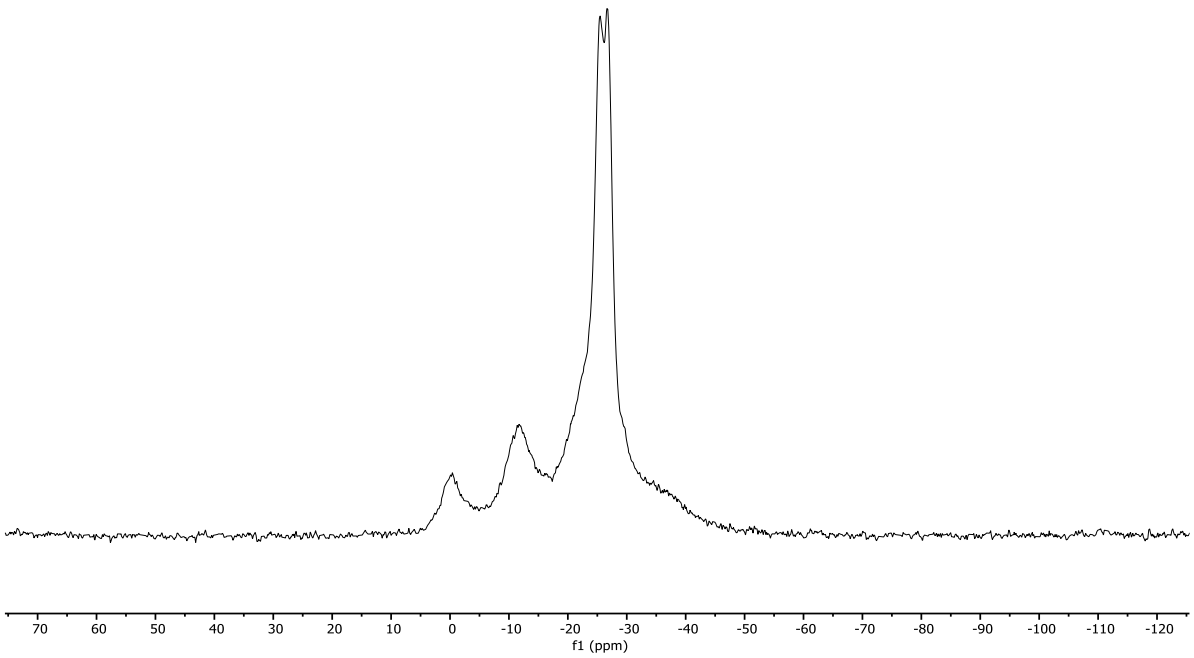

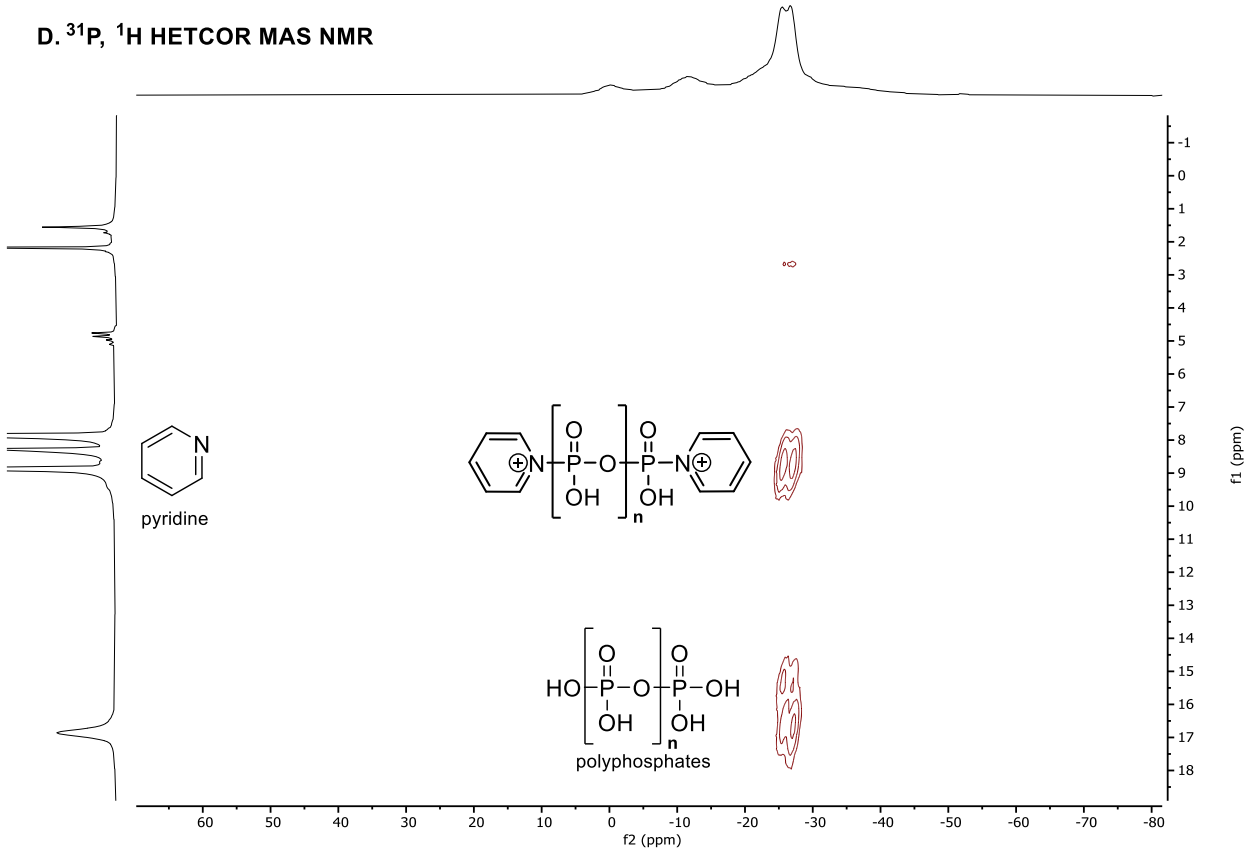

2) High Resolution MAS NMR (HR-MAS NMR)

Reactions were set up as described in the general procedure **GP-II**. 1-Methylimidazole was used as base. After 10 min at 60 °C, the reaction was stopped, and the paste was packed into HRMAS zirconia rotors of 4 mm OD closed with Kel-F caps (sample volume 60 µl) with 5 µl of CD3CN for locking purposes. Data were acquired on an AVANCE HD 500 MHz spectrometer (BrukerTM) operating at a frequency of 500.046 MHz and equipped with a double-resonance HRMAS iProbe (BrukerTM). Samples were spun at 6.5 kHz and 1D data acquired using a MAS rate synchronized Carr-Purcell-Meiboom-Gill (CPMG) pulse sequence (relaxation delay 90°–(τ –180°– τ)$_n$– acquire FID, τ=1/6250Hz=160 µs, n=40). In order to get a flat baseline, the broader signals arising from the probe background were removed and ^{1}H signals coming from rigid parts of the system were filtered out [12,13] 16 transients were accumulated over 16384 time domain points, leading to a 3 Hz/point resolution (Spectral Width = 25000Hz, 49.9 ppm) with a total recycle time of 5.3 s. After a Fourier Transform over 32768 points, an exponential line broadening of 5 Hz was applied. 2D 1H-1H RFDR (Radio Frequency Driven Recoupling) was employed here as residual dipolar interactions (through space) may have a chance to be detected in these systems[14] together with through bond interactions (TOCSY like). Here two experiments were done: synchronous (through bond and through space detection) and asynchronous (only through bond detection, not shown). No difference was observed between the two, meaning that no residual dipolar interactions were detected with the 80 ms mixing time that was used. 512 complex data points were acquired in the indirect dimension and for each t_1 increment 16 scans were accumulated over 1024 time domain data points with a 5 s recycle delay. Corresponding spectral widths were 25 kHz (49.9 ppm) and 7 kHz (14 ppm) giving a frequency resolution of 12.21 Hz and 27.35 Hz in the f_2 and f_1 dimensions. A 90° shifted squared sinebell apodization function was applied in both dimensions prior to the Fourier transform.

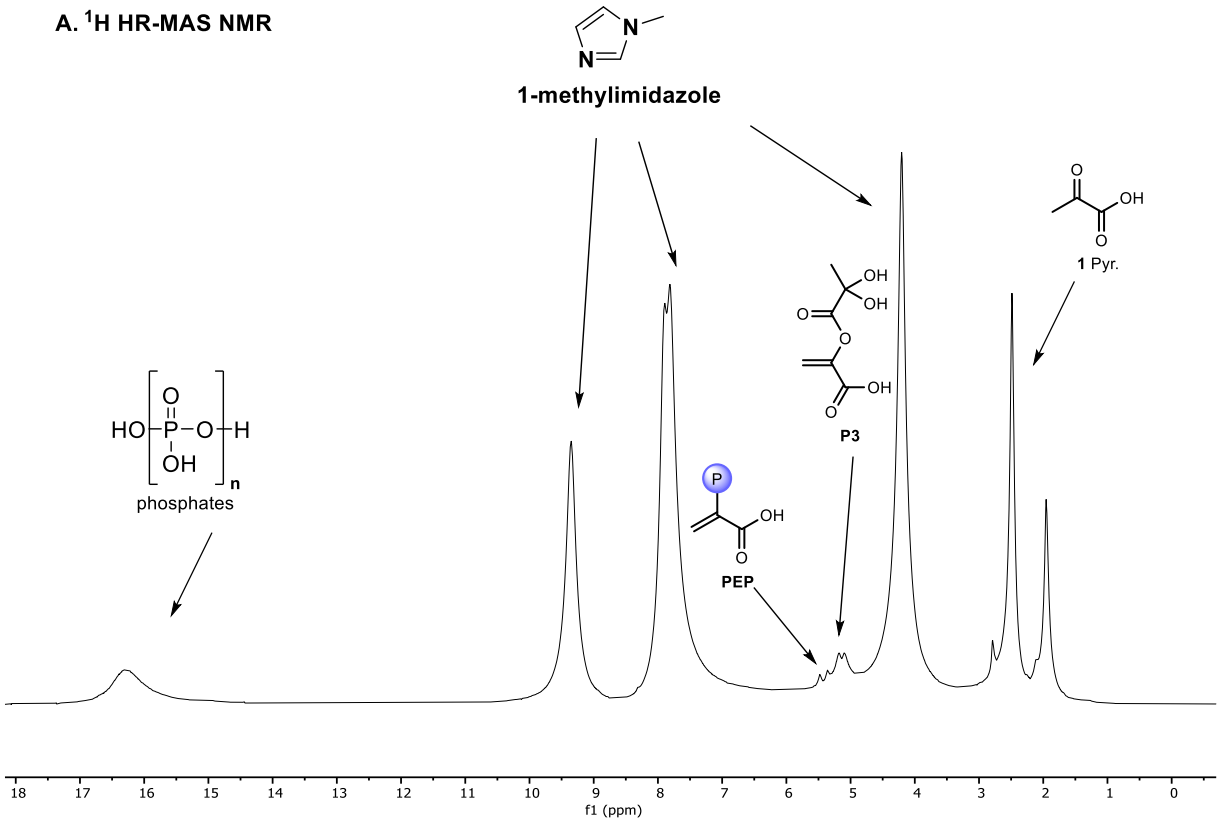
A. 1H HR-MAS NMR
1-methylimidazole
1 Pyr.
P3
PEP
phosphates
f1 (ppm)

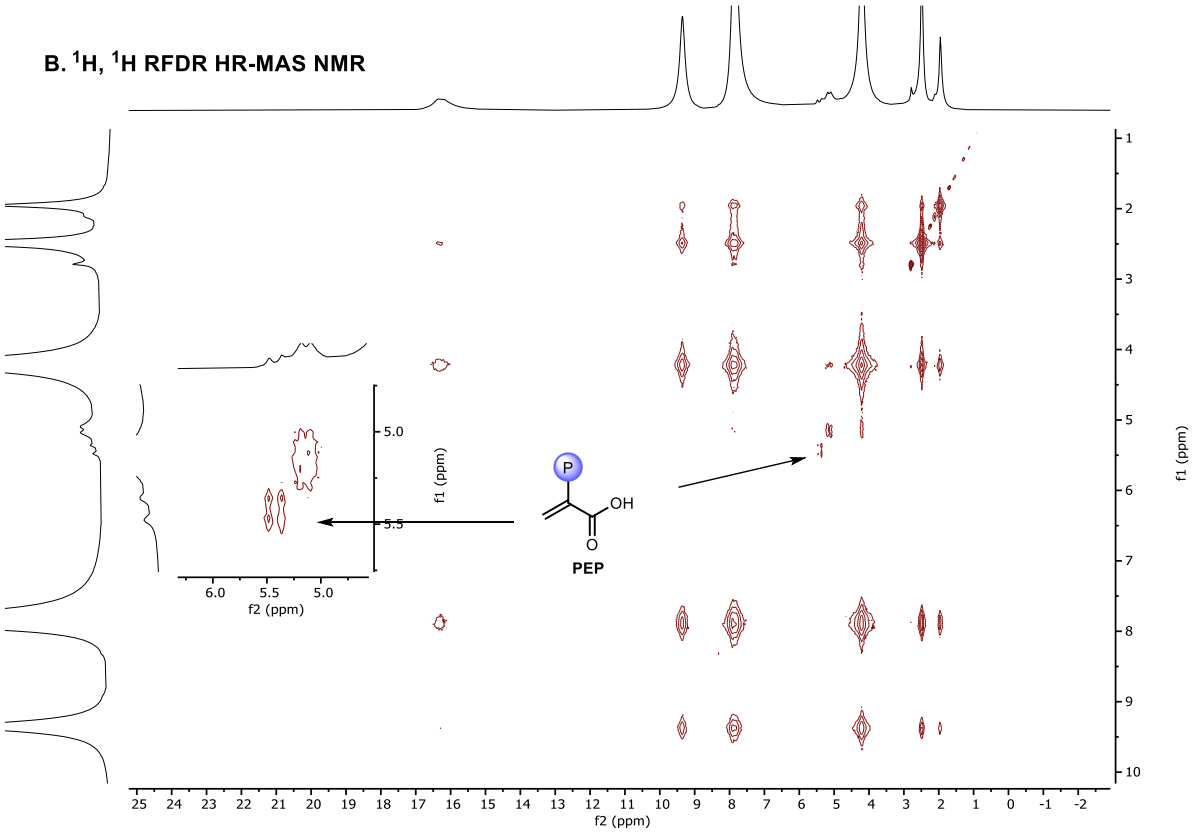
B. 1H, 1H RFDR HR-MAS NMR
PEP
f1 (ppm)
f2 (ppm)

C. Alternative solvents for the characterization of the paste (is PEP formation coming from hydrolysis?)

Reactions were set up as described in the general procedure. To figure out if the two products **PEP** and the acyl phosphate of pyruvate were formed by hydrolysis of the paste when the latter is dissolved in water, alternative solvents were used (see Table S13).

Table S13. Solvent screening table with product identification by ^{1}H and ^{31}P NMR spectroscopy.

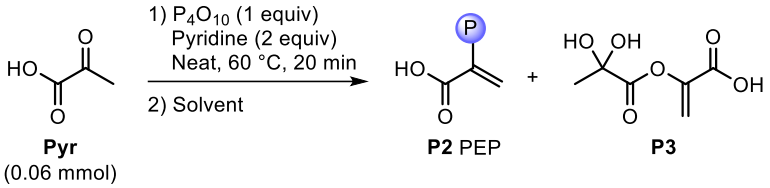

Entry	Solvent	Products	Comment
1	Acetone-d_3	**P3**	Poorly soluble, no signals in ^{31}P NMR
2	Acetonitrile-d_3	**PEP** + **P3**	Poorly soluble
3	Chloroform-d	**P3**	Poorly soluble, no signals in ^{31}P NMR
4	DMSO-d_6	**PEP** + **P3**	Partially soluble

Table S13 Entry 2

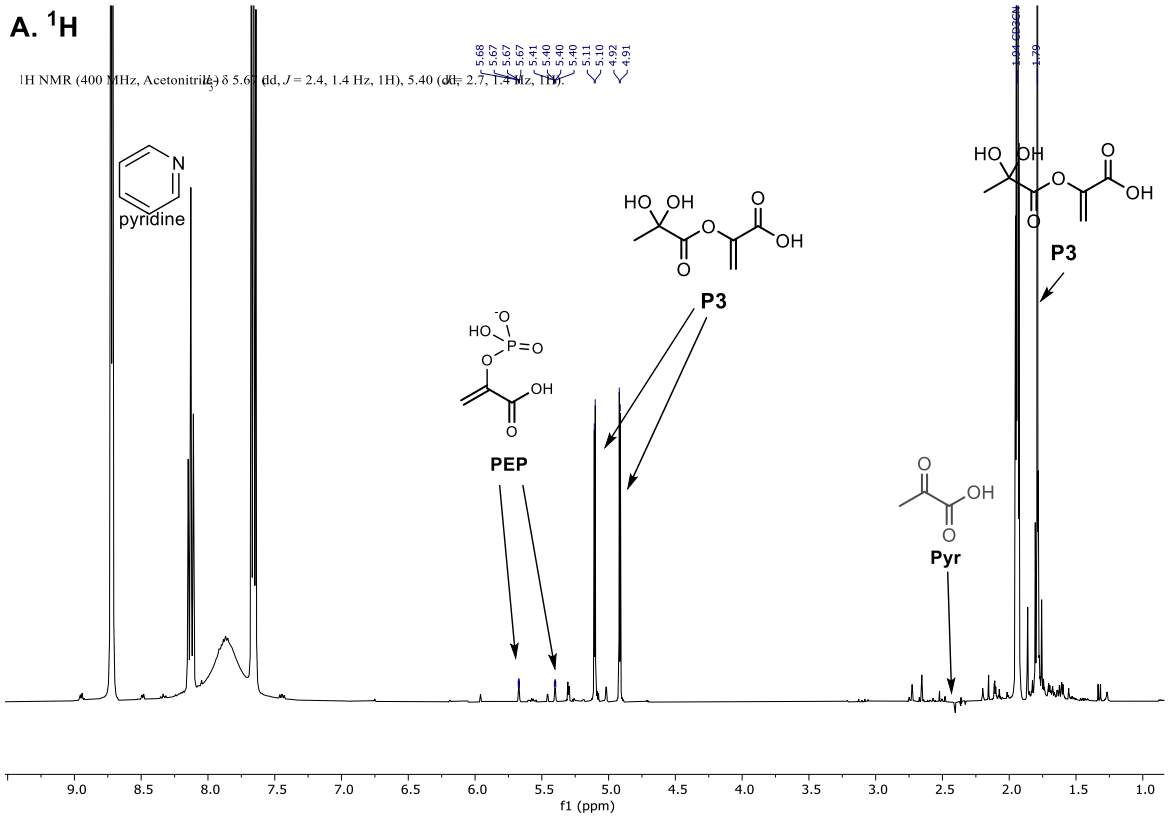

B. ^{31}P (^{1}H decoupled)

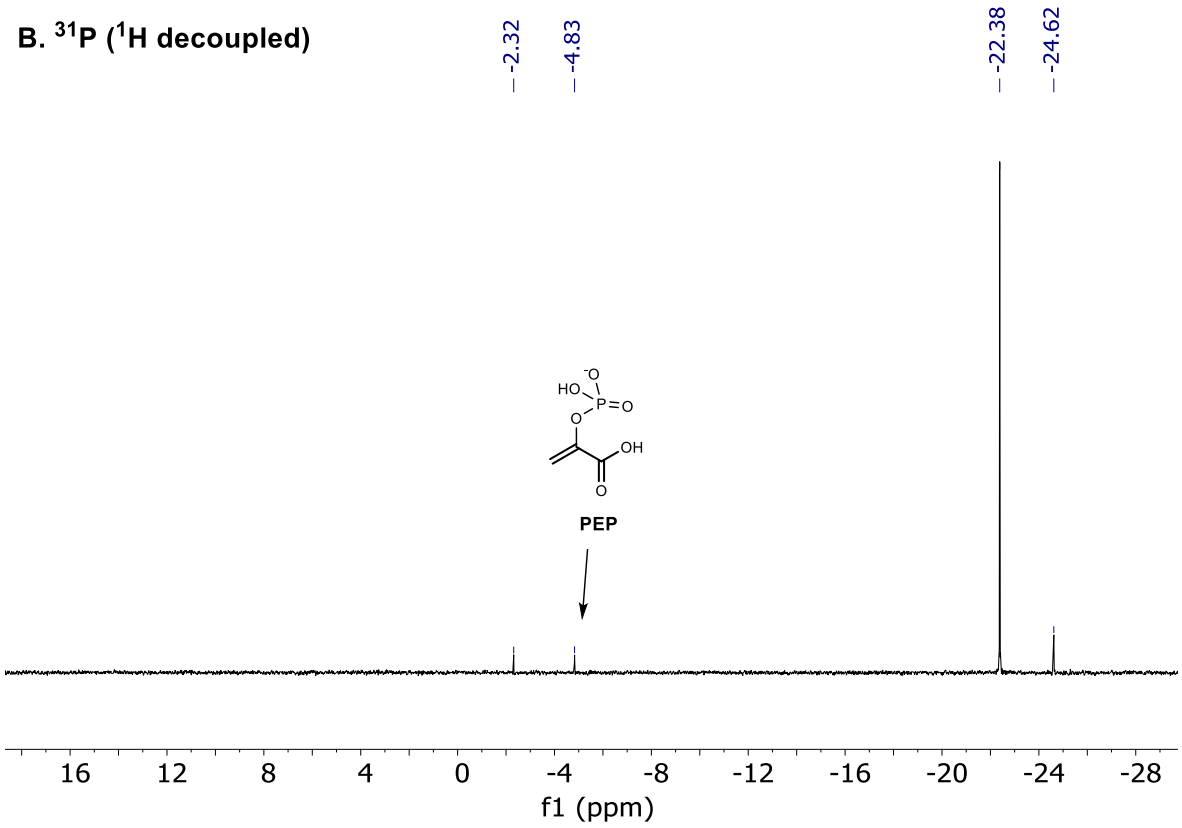

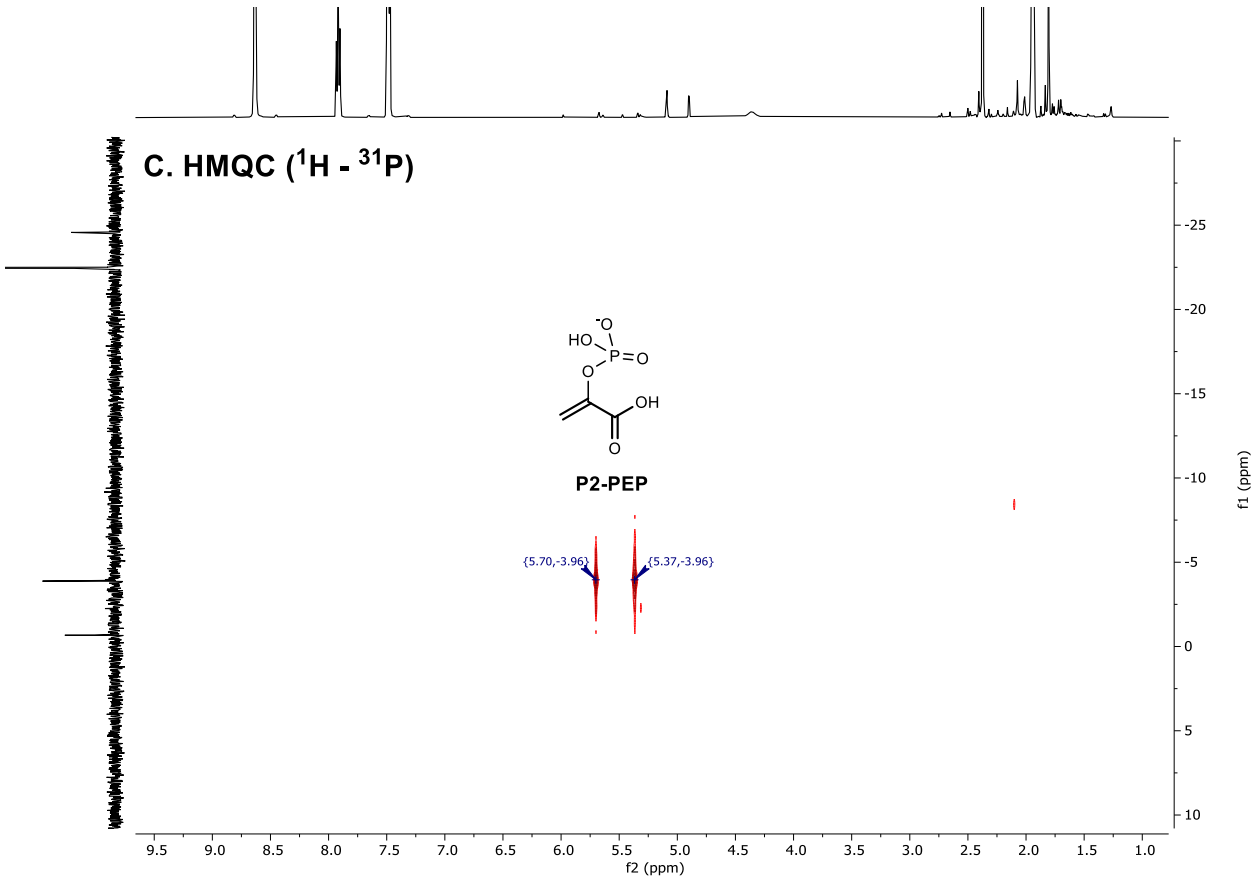
C. HMQC (1H - 31P)
HO
O
P=O
O
OH
O
P2-PEP
{5.70,-3.96}
{5.37,-3.96}
f2 (ppm)
f1 (ppm)

Table S13 Entry 4

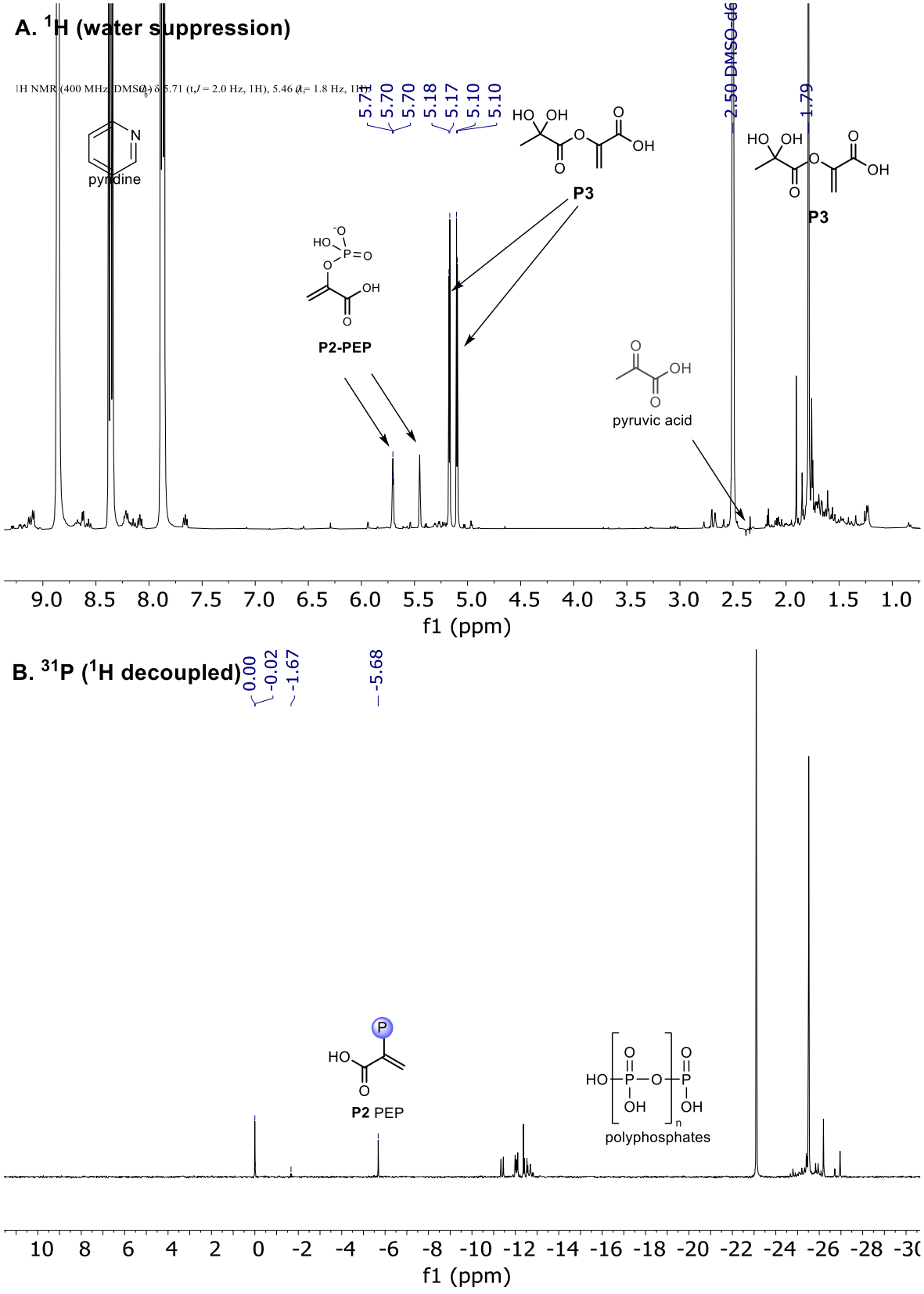

D. Reference spectra of different products

Phospho(enol)pyruvic acid monopotassium salt was suspended in CD_3CN. Different additives were added to solubilize the substrate (Table S14, entries 1-3). Reference spectra of acetylacetone were recorded neat with an insert containing the deuterated solvent (Table S14, entry 4) to observe the keto-enol equilibrium in neat conditions.

Table S14. Reference of different products with ^{1}H and ^{13}C NMR chemical shifts.

Entry	Substrate	Additives	Solvent	Characteristic peaks (^{1}H + ^{13}C)
1	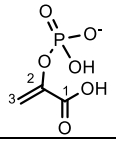	18-crown	CD_3CN	C-1 (166.2), $J_{C\text{-}P}$ = 1.6 Hz C-2 (148.9), $J_{C\text{-}P}$ = 9.4 Hz C-3 (109.5), $J_{C\text{-}P}$ = 6.1 Hz H-3 (dd, 5.56 / 5.12)
2	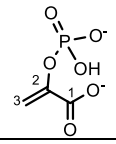	Et_3N	CD_3CN	C-1 (169), $J_{C\text{-}P}$ = 2.1 Hz C-2 (152.5), $J_{C\text{-}P}$ = 8.9 Hz C-3 (105), $J_{C\text{-}P}$ = 6 Hz H-3 (d, 5.4 / 4.9)
3	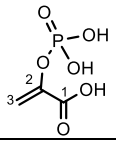	CF_3SO_3H	CD_3CN	C-1 (163.9), $J_{C\text{-}P}$ = 6.9 Hz C-2 (144.7), $J_{C\text{-}P}$ = 7.2 Hz C-3 (110.2), $J_{C\text{-}P}$ = 4.6 Hz H-3 (t, 5.9 / 5.6)
4	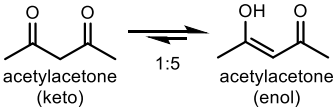	/	neat	Ratio 1 to 5 (keto:enol) See below
5[a]	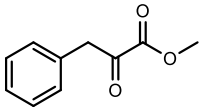	/	$CDCl_3$	See below

[a] Prepared according to a literature procedure.

Table S14 Entry 4

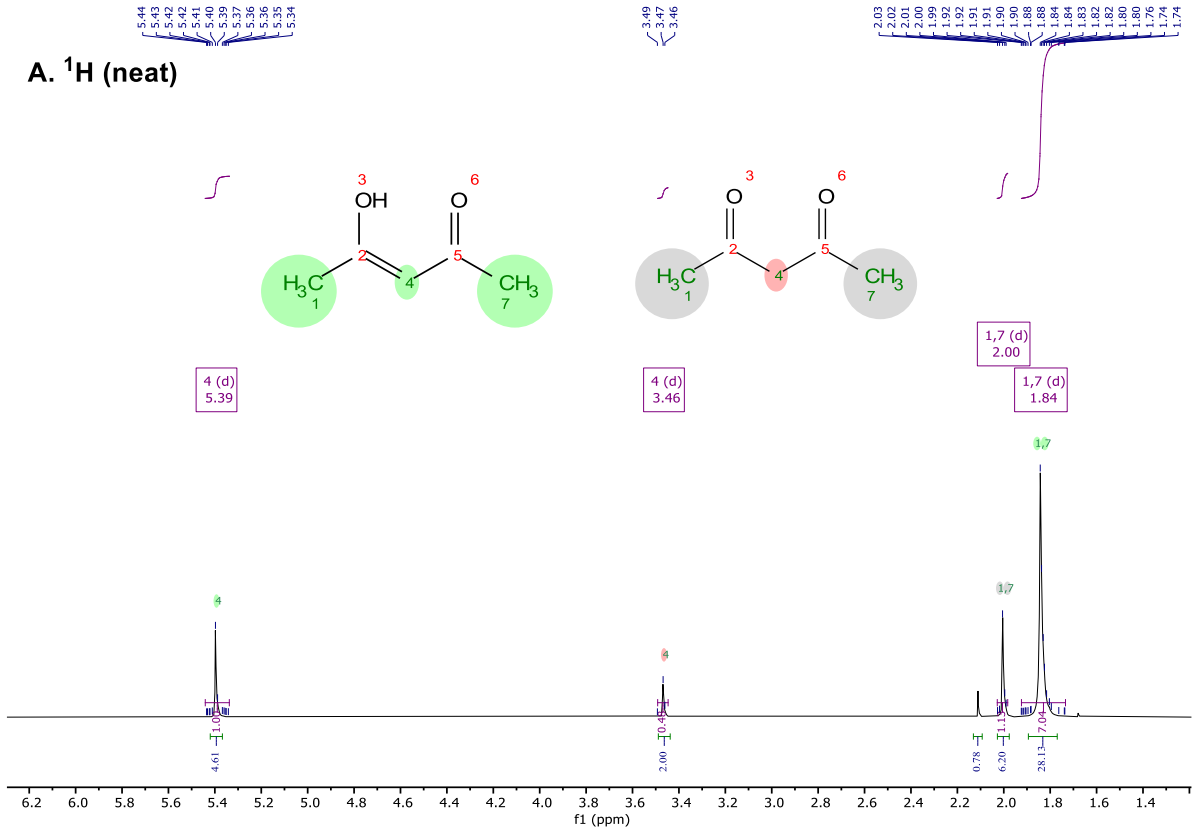

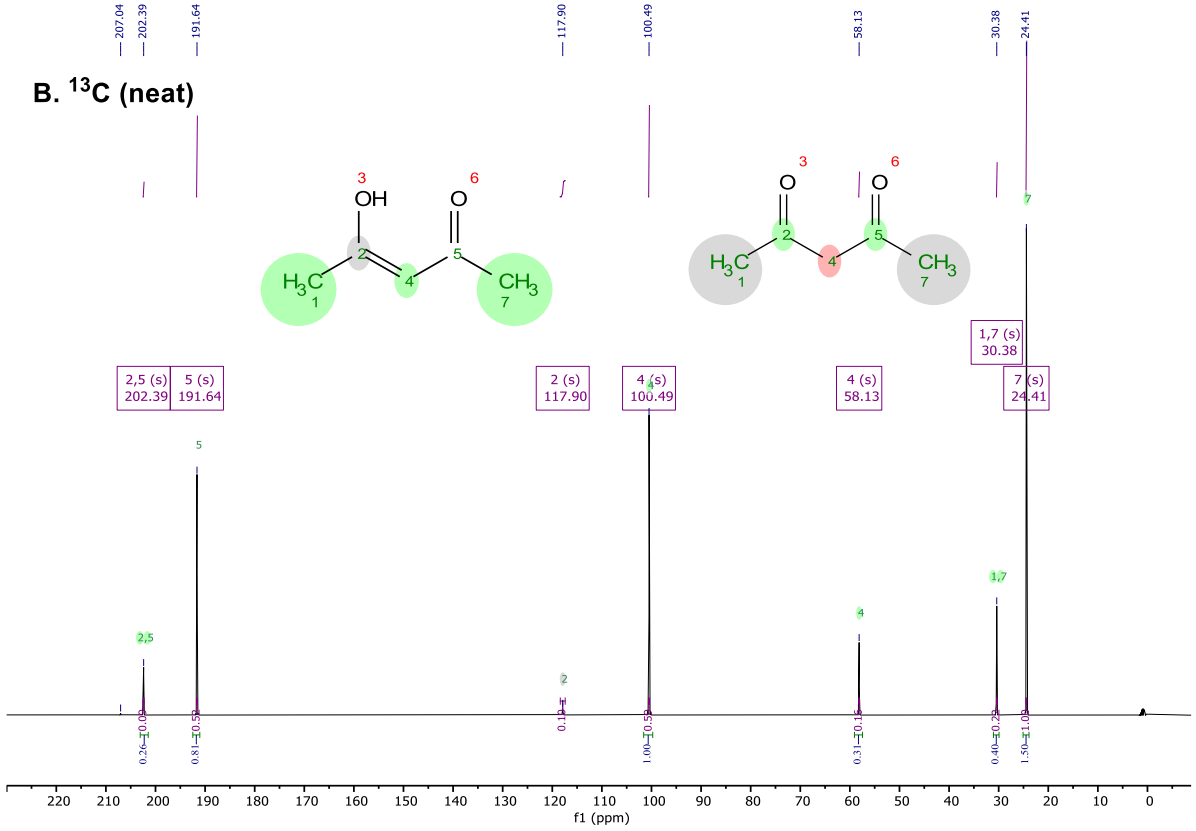

Table S14 Entry 5

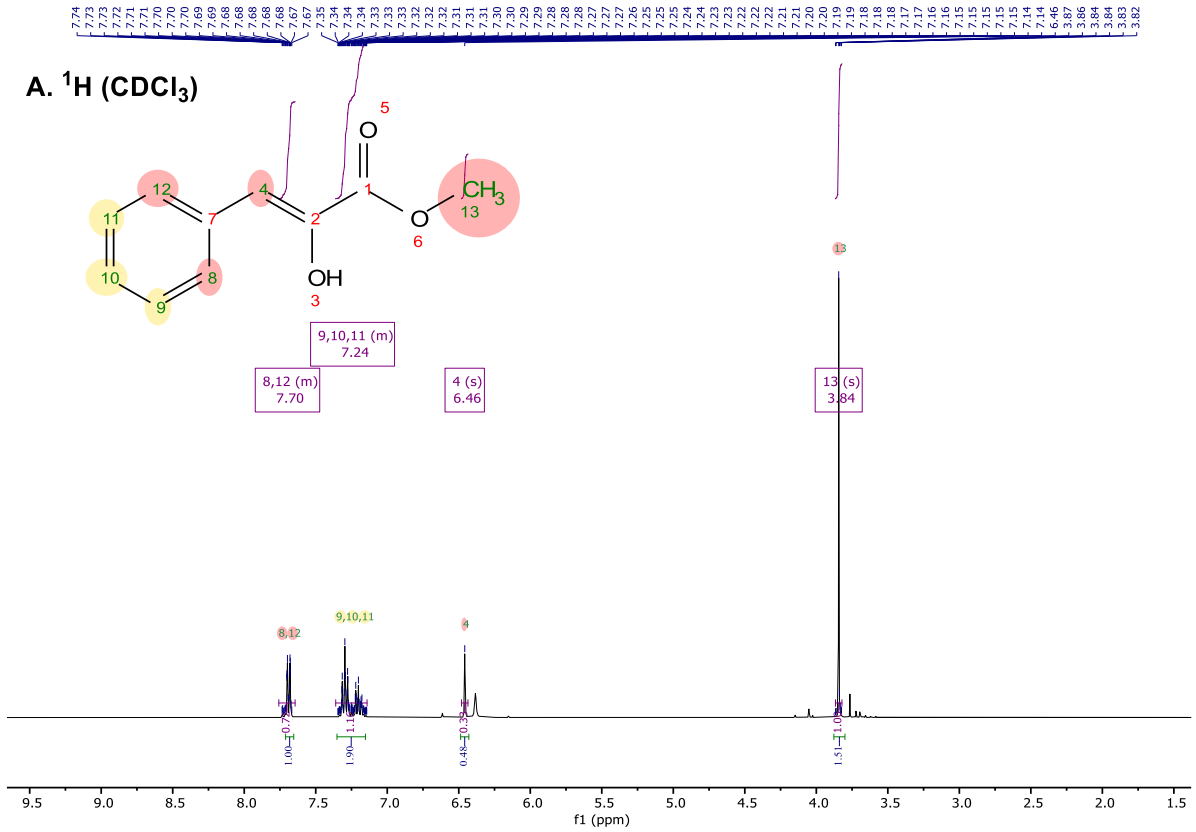

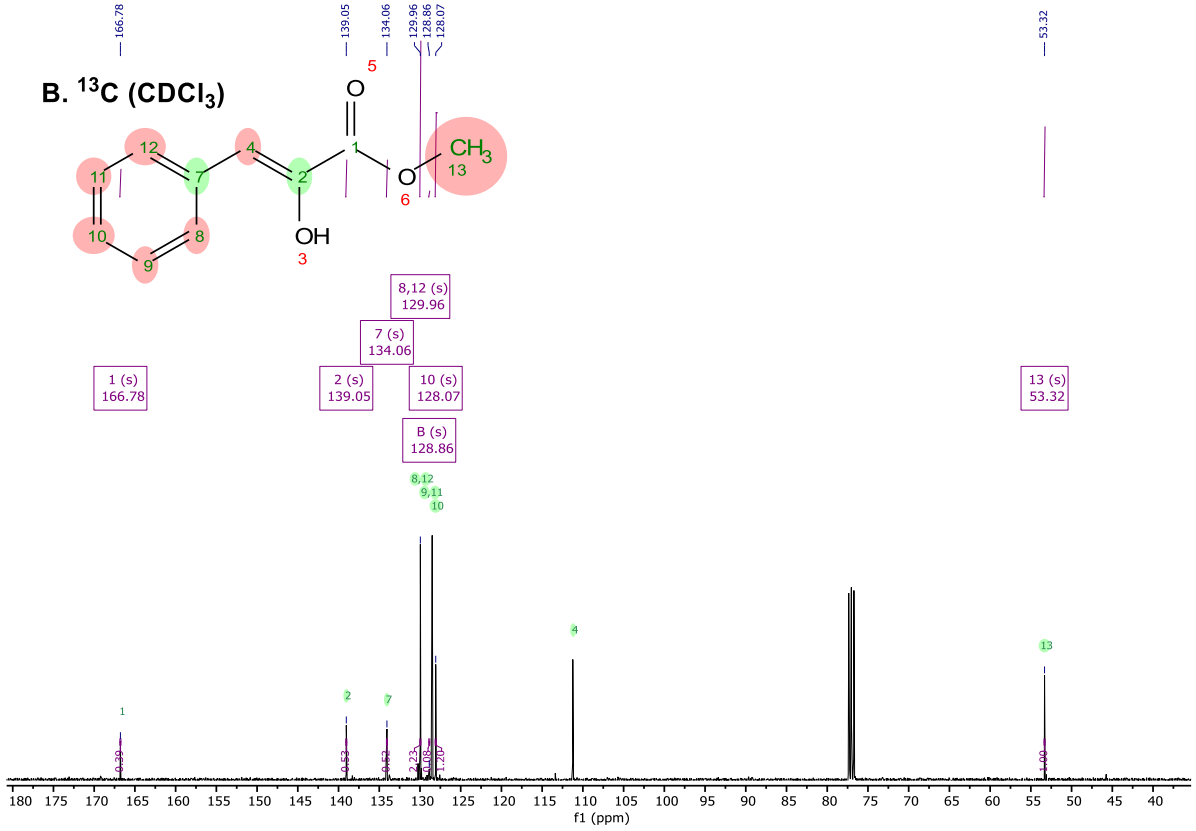

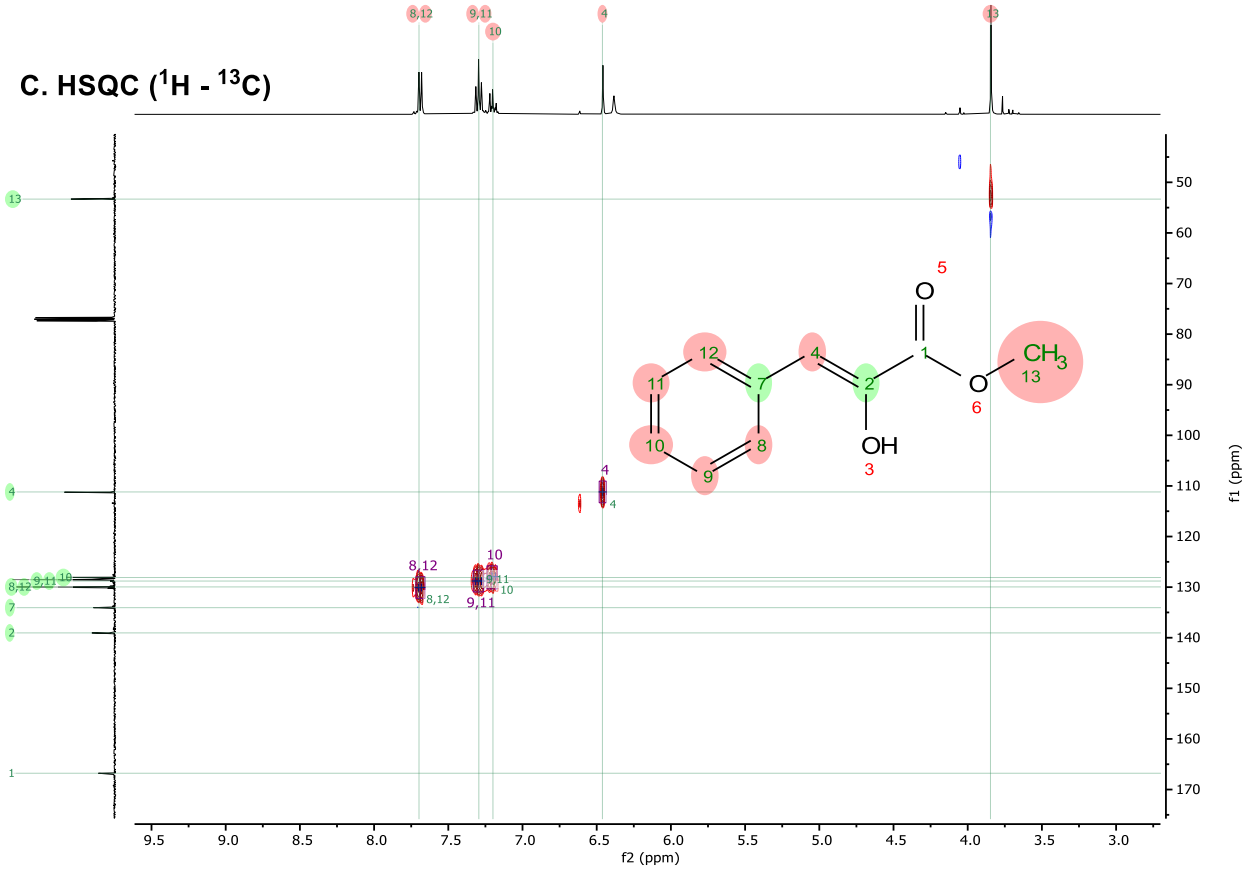
C. HSQC (^{1}H - ^{13}C)
f2 (ppm)
f1 (ppm)
OH
CH3

VII. DFT computations

A. General procedure

Initially, all structures were subjected to a conformational search using the CREST tool from Grimme and coworkers at the GFN2-xTB level and the ALPB solvation model for water.[15] All conformers were subsequently optimized with the Gaussian 16 software package[16] at the SMD(water)[17]/M06-2X[18]/Def2-SVP[19] level of theory. Frequency analyses at the same level considering Grimmes quasi-harmonic corrections were performed to confirm that all structures correspond to minima (or transition states).[20] Transition states were further verified by IRC computations and visual inspection of the imaginary vibration. The thermal corrections were next combined with single-point calculations at the SMD(water)/M06-2X/Def2-TZVPD level. Gibbs energies for unique conformers were Boltzmann weighted and, finally, a free energy change of +7.92 kJ/mol (= $R \cdot 298\ K \cdot \ln(24.47\ L\ mol^{-1}/L\ mol^{-1})$) was applied for their conversion from the gas phase (1 atm) to liquid phase (1 M). Structures were visualized with CYLView.[21]

B. Transition states for phosphoryl transfer

To investigate the relative nucleophilicity of the different sites of pyruvic acid to undergo phosphoryl transfer, we computationally studied the model reaction with pyridinium phosphate $PyPO_3H$. $PyPO_3H$ has been used in multiple experimental and computational studies on phosphoryl transfer and is considered a potentially relevant species also for the conditions of this study.[22,23] The reaction of P_4O_{10} with pyridine was shown to yield adducts of the form $P_2O_5Py_2$, which can further hydrolyze to the zwitterionic pyridinium phosphate $PyPO_3H$. Both $P_2O_5Py_2$ and $PyPO_3H$ are potential phosphorylating agents for pyruvic acid. However, we decided to use $PyPO_3H$ as the model phosphorylating agent for our computations.

Table S15. Raw data from DFT calculations at the SMD(H_2O)/M06-2X/Def2-TZVPD//SMD(H_2O)/M06-2X/Def2-SVP level (in hartree) for the transition states of phosphorylation.

Filename (.xyz)	E^0_l (hartree)[a]	G^0_l (hartree)[b]	E^0_h (hartree)[c]	G^0_h (hartree)[d]	G^0_{rel}
py2_po3h_carboxy_ts1	-1405.394400	-1405.159522	-1406.777718	-1406.542840	0.0
py2_po3h_enol_carboxy_ts1	-1405.381848	-1405.144988	-1406.765655	-1406.528795	36.9
py2_po3h_enol_oa_ts1	-1405.374991	-1405.138317	-1406.756524	-1406.519850	60.4

[a] Electronic energy at the SMD(H_2O)/M06-2X/Def2-SVP level (in hartree).
[b] Gibbs energy at the SMD(H_2O)/M06-2X/Def2-SVP level (in hartree).
[c] Electronic energy at the SMD(H_2O)/M06-2X/Def2-TZVPD//SMD(H_2O)/M06-2X/Def2-SVP level (in hartree).
[d] Gibbs energy at the SMD(H_2O)/M06-2X/Def2-TZVPD//SMD(H_2O)/M06-2X/Def2-SVP level (in hartree) calculated as $G^0_h = E^0_h + (G^0_l - E^0_l)$.

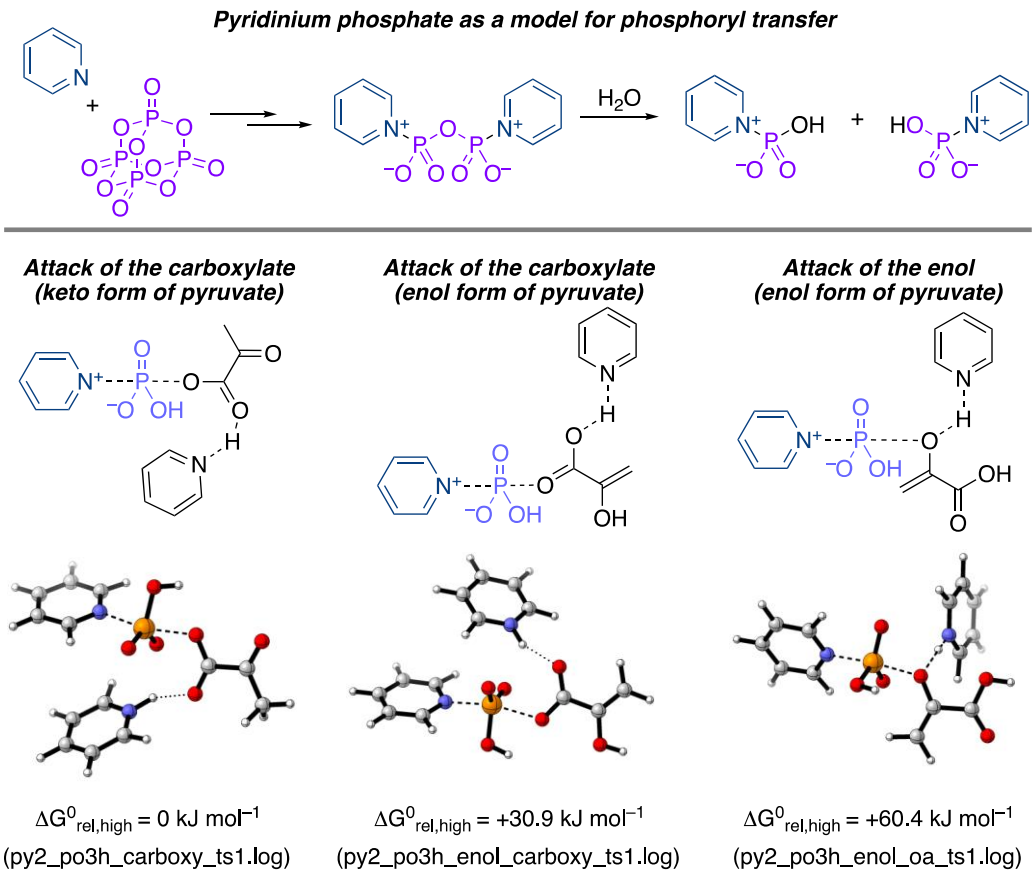

Figure S6. Top: formation of pyridinium phosphate. Bottom: transition states for phosphoryl transfer to pyruvic acid.

C. Thermochemistry of pyruvate phosphorylation in acidic water

Most of the experimental characterization of products was obtained after dissolving the paste in water. Due to the hydrolysis of unreacted P_4O_{10} (or other phosphorylated species), the resulting solution was found to be highly acidic (≈ pH 1). Thus, we decided to model the overall thermochemistry of pyruvate phosphorylation using an aqueous solvation model assuming full protonation of all phosphate sites. Due to the highly approximative nature of the model, the computed thermochemistry should be considered to be only of qualitative nature.
While we additionally computed the activation barriers for intramolecular phosphoryl transfer, these steps experimentally occur under elevated temperature (60 °C) and paste conditions where the reaction is significantly more concentrated. Thus, also these energy barriers should rather illustrate the possibility of a pathway but are by no means accurate representations of the actual reaction.

Table S16. Raw data from DFT calculations at the SMD(H_2O)/M06-2X/Def2-TZVPD//SMD(H_2O)/M06-2X/Def2-SVP level (in hartree) for the thermochemistry in water.

Species	Filename (.xyz)	E^0_l (hartree)[a]	G^0_l (hartree)[b]	E^0_h (hartree)[c]	G^0_h (hartree)[d]	weighting	G^0_{rel}
H_2O	h2o	-76.335434	-76.329424	-76.440954	-76.434944		
H_3O^+	h3o	-76.759817	-76.740884	-76.854743	-76.835810		
H_3PO_4	h3po4_2	-643.707479	-643.685797	-644.245451	-644.223769	1.0000	
				weighted	-644.223769		
Pyr	pyr_1	-342.016867	-341.971856	-342.422477	-342.377466	0.3718	
	pyr_3	-342.017626	-341.972580	-342.423007	-342.377961	0.6282	
				weighted	-342.377777		
H-Pyr	pyr_hyd_1	-418.382081	-418.309840	-418.882132	-418.809891	0.1984	
	pyr_hyd_2	-418.380970	-418.308520	-418.881070	-418.808620	0.0515	
	pyr_hyd_3	-418.382088	-418.309404	-418.882240	-418.809556	0.1390	
	pyr_hyd_4	-418.380293	-418.308319	-418.880976	-418.809002	0.0773	
	pyr_hyd_5	-418.381205	-418.308971	-418.881060	-418.808826	0.0641	
	pyr_hyd_6	-418.378465	-418.306509	-418.879823	-418.807867	0.0232	
	pyr_hyd_7	-418.381977	-418.309328	-418.882481	-418.809832	0.1864	
	pyr_hyd_8	-418.379340	-418.306997	-418.880433	-418.808090	0.0294	
	pyr_hyd_9	-418.378546	-418.306895	-418.879437	-418.807786	0.0213	
	pyr_hyd_10	-418.381429	-418.308436	-418.882085	-418.809092	0.0850	
	pyr_hyd_11	-418.380756	-418.308631	-418.881577	-418.809452	0.1245	
				weighted	-418.809364		8.8
Pyr-Enol	pyr_enol_1	-342.010042	-341.964185	-342.416360	-342.370503	0.7373	
	pyr_enol_2	-342.008043	-341.962360	-342.413833	-342.368150	0.0608	
	pyr_enol_4	-342.007798	-341.961733	-342.413896	-342.367831	0.0434	
	pyr_enol_5	-342.007815	-341.961746	-342.414561	-342.368492	0.0874	
	pyr_enol_6	-342.008009	-341.962074	-342.414232	-342.368297	0.0711	
				weighted	-342.369912		20.7
PEP	pep_h_1	-909.375165	-909.309709	-910.214080	-910.148624	0.3424	
	pep_h_2	-909.375918	-909.310180	-910.214296	-910.148558	0.3192	
	pep_h_3	-909.371493	-909.306319	-910.211603	-910.146429	0.0334	
	pep_h_4	-909.370502	-909.305322	-910.210171	-910.144991	0.0073	
	pep_h_6	-909.372392	-909.307108	-910.211135	-910.145851	0.0181	
	pep_h_7	-909.375184	-909.309597	-910.213860	-910.148273	0.2359	
	pep_h_8	-909.370862	-909.306196	-910.211007	-910.146341	0.0304	
	pep_h_9	-909.369114	-909.304507	-910.209162	-910.144555	0.0046	
	pep_h_10	-909.370528	-909.305764	-910.209915	-910.145151	0.0086	
				weighted	-910.148252		48.2
cyPEP	cypep_1	-833.003274	-832.961401	-833.747019	-833.705146	0.5184	
	cypep_2	-833.002651	-832.960551	-833.747177	-833.705077	0.4816	
				weighted	-833.705113		69.7
AcP-Pyr-Cycl	acp_pyr_cycl_1	-909.381615	-909.313893	-910.218932	-910.151210	0.2736	
	acp_pyr_cycl_2	-909.380948	-909.312497	-910.219131	-910.150680	0.1561	
	acp_pyr_cycl_3	-909.381719	-909.314029	-910.219014	-910.151324	0.3088	
	acp_pyr_cycl_4	-909.381045	-909.312959	-910.219253	-910.151167	0.2614	
				weighted	-910.151151		40.6
Int-B	int_b_1	-909.366406	-909.302652	-910.207511	-910.143757	0.1882	
	int_b_2	-909.364810	-909.300207	-910.205231	-910.140628	0.0068	
	int_b_3	-909.364898	-909.300667	-910.204856	-910.140625	0.0068	
	int_b_4	-909.365469	-909.301380	-910.207090	-910.143001	0.0844	
	int_b_5	-909.360530	-909.296505	-910.199819	-910.135794	0.0000	
	int_b_6	-909.363724	-909.299019	-910.201942	-910.137237	0.0002	
	int_b_7	-909.366789	-909.302597	-910.207246	-910.143054	0.0893	
	int_b_8	-909.365242	-909.300712	-910.206407	-910.141877	0.0256	
	int_b_9	-909.363570	-909.300360	-910.204657	-910.141447	0.0162	
	int_b_10	-909.365134	-909.300765	-910.204997	-910.140628	0.0068	
	int_b_11	-909.363789	-909.299990	-910.204353	-910.140554	0.0063	
	int_b_12	-909.365268	-909.300856	-910.204670	-910.140258	0.0046	
	int_b_13	-909.367522	-909.302887	-910.208030	-910.143395	0.1281	
	int_b_14	-909.364279	-909.299926	-910.201979	-910.137626	0.0003	
	int_b_15	-909.364050	-909.300316	-910.205871	-910.142137	0.0338	

	int_b_16	-909.366024	-909.301777	-910.205506	-910.141259	0.0133	
	int_b_17	-909.365805	-909.301463	-910.205773	-910.141431	0.0160	
	int_b_18	-909.364743	-909.300603	-910.206773	-910.142633	0.0572	
	int_b_19	-909.365568	-909.301341	-910.206192	-910.141965	0.0281	
	int_b_21	-909.365353	-909.301315	-910.206494	-910.142456	0.0474	
	int_b_22	-909.366374	-909.301754	-910.207092	-910.142472	0.0482	
	int_b_23	-909.365929	-909.301146	-910.205673	-910.140890	0.0090	
	int_b_24	-909.363423	-909.299628	-910.204002	-910.140207	0.0044	
	int_b_25	-909.367293	-909.302092	-910.208101	-910.142900	0.0758	
	int_b_26	-909.365783	-909.301796	-910.205927	-910.141940	0.0274	
	int_b_27	-909.363778	-909.299893	-910.203832	-910.139947	0.0033	
	int_b_28	-909.363015	-909.299420	-910.204005	-910.140410	0.0054	
	int_b_29	-909.363352	-909.299432	-910.205578	-910.141658	0.0203	
	int_b_30	-909.366320	-909.301040	-910.207292	-910.142012	0.0296	
	int_b_31	-909.362607	-909.298479	-910.200782	-910.136654	0.0001	
	int_b_32	-909.363997	-909.300140	-910.205355	-910.141498	0.0171	
	int_b_33	-909.358315	-909.294197	-910.197484	-910.133366	0.0000	
				weighted	-910.142711		62.7
Int-C	int_c_1	-985.743819	-985.651895	-986.672840	-986.580916	0.0082	
	int_c_2	-985.739891	-985.648761	-986.670258	-986.579128	0.0012	
	int_c_3	-985.738874	-985.648262	-986.673294	-986.582682	0.0535	
	int_c_4	-985.740103	-985.649439	-986.669959	-986.579295	0.0015	
	int_c_5	-985.737754	-985.648154	-986.672792	-986.583192	0.0920	
	int_c_6	-985.744268	-985.652498	-986.672768	-986.580998	0.0090	
	int_c_7	-985.738211	-985.647818	-986.672540	-986.582147	0.0304	
	int_c_8	-985.735608	-985.644941	-986.666774	-986.576107	0.0001	
	int_c_9	-985.737814	-985.646814	-986.672814	-986.581814	0.0213	
	int_c_10	-985.739230	-985.648348	-986.673188	-986.582306	0.0359	
	int_c_11	-985.733794	-985.643998	-986.665401	-986.575605	0.0000	
	int_c_12	-985.739007	-985.648144	-986.669616	-986.578753	0.0008	
	int_c_14	-985.738563	-985.648485	-986.669045	-986.578967	0.0010	
	int_c_15	-985.737198	-985.646910	-986.672067	-986.581779	0.0206	
	int_c_17	-985.737164	-985.646791	-986.672006	-986.581633	0.0176	
	int_c_18	-985.740268	-985.649749	-986.669636	-986.579117	0.0012	
	int_c_19	-985.738119	-985.647836	-986.672477	-986.582194	0.0319	
	int_c_20	-985.739907	-985.649184	-986.673785	-986.583062	0.0801	
	int_c_21	-985.739440	-985.648423	-986.670150	-986.579133	0.0012	
	int_c_22	-985.738532	-985.647865	-986.672181	-986.581514	0.0155	
	int_c_23	-985.737229	-985.647065	-986.672543	-986.582379	0.0389	
	int_c_24	-985.739866	-985.649683	-986.673729	-986.583546	0.1338	
	int_c_25	-985.736649	-985.645891	-986.672271	-986.581513	0.0155	
	int_c_26	-985.736618	-985.646436	-986.671758	-986.581576	0.0166	
	int_c_27	-985.739005	-985.648128	-986.670043	-986.579166	0.0013	
	int_c_28	-985.737108	-985.646718	-986.672446	-986.582056	0.0276	
	int_c_29	-985.738105	-985.647822	-986.672634	-986.582351	0.0377	
	int_c_30	-985.739291	-985.648584	-986.673040	-986.582333	0.0370	
	int_c_31	-985.731557	-985.641578	-986.663572	-986.573593	0.0000	
	int_c_32	-985.736303	-985.645282	-986.667863	-986.576842	0.0001	
	int_c_33	-985.739248	-985.648378	-986.673043	-986.582173	0.0312	
	int_c_34	-985.736132	-985.644962	-986.666754	-986.575584	0.0000	
	int_c_35	-985.739006	-985.648106	-986.670050	-986.579150	0.0013	
	int_c_36	-985.735471	-985.644643	-986.666913	-986.576085	0.0000	
	int_c_37	-985.735664	-985.645336	-986.670787	-986.580459	0.0051	
	int_c_38	-985.736419	-985.646242	-986.671563	-986.581386	0.0136	
	int_c_39	-985.734793	-985.644301	-986.666981	-986.576489	0.0001	
	int_c_40	-985.733517	-985.643668	-986.665350	-986.575501	0.0000	
	int_c_41	-985.738811	-985.647377	-986.668745	-986.577311	0.0002	
	int_c_42	-985.737722	-985.647490	-986.672304	-986.582072	0.0280	
	int_c_43	-985.738218	-985.646800	-986.669272	-986.577854	0.0003	
	int_c_44	-985.739655	-985.648990	-986.670170	-986.579505	0.0018	
	int_c_45	-985.738639	-985.647497	-986.672785	-986.581643	0.0178	
	int_c_46	-985.731512	-985.641790	-986.663670	-986.573948	0.0000	
	int_c_47	-985.738629	-985.647560	-986.667915	-986.576846	0.0001	
	int_c_48	-985.734063	-985.643363	-986.666104	-986.575404	0.0000	
	int_c_49	-985.736542	-985.645805	-986.671802	-986.581065	0.0096	
	int_c_50	-985.734691	-985.644772	-986.670391	-986.580472	0.0051	
	int_c_51	-985.735432	-985.646111	-986.671208	-986.581887	0.0231	
	int_c_53	-985.736423	-985.645791	-986.671675	-986.581043	0.0094	
	int_c_54	-985.737140	-985.646597	-986.671547	-986.581004	0.0090	
	int_c_55	-985.735353	-985.645228	-986.671109	-986.580984	0.0088	
	int_c_57	-985.739665	-985.648359	-986.673768	-986.582462	0.0424	
	int_c_58	-985.739034	-985.648133	-986.673051	-986.582150	0.0305	
	int_c_59	-985.737806	-985.645329	-986.668564	-986.576087	0.0000	
	int_c_60	-985.734608	-985.643966	-986.664738	-986.574096	0.0000	
	int_c_63	-985.737103	-985.645219	-986.668456	-986.576572	0.0001	
	int_c_64	-985.736718	-985.644500	-986.667500	-986.575282	0.0000	
	int_c_65	-985.731191	-985.641599	-986.663376	-986.573784	0.0000	
	int_c_66	-985.736236	-985.645340	-986.666563	-986.575667	0.0000	
	int_c_67	-985.737540	-985.647144	-986.672216	-986.581820	0.0215	
	int_c_68	-985.734848	-985.644920	-986.670921	-986.580993	0.0089	

				weighted	-986.582358		50.4
AcP-Pyr	acp_pyr_1	-909.373562	-909.310247	-910.211614	-910.148299	0.0109	
	acp_pyr_3	-909.370308	-909.307175	-910.209119	-910.145986	0.0009	
	acp_pyr_4	-909.374180	-909.311076	-910.211651	-910.148547	0.0142	
	acp_pyr_5	-909.374199	-909.310824	-910.211700	-910.148325	0.0112	
	acp_pyr_6	-909.373089	-909.310496	-910.213234	-910.150641	0.1306	
	acp_pyr_7	-909.372433	-909.310044	-910.212438	-910.150049	0.0697	
	acp_pyr_8	-909.372432	-909.309962	-910.212437	-910.149967	0.0639	
	acp_pyr_9	-909.372343	-909.310079	-910.212894	-910.150630	0.1290	
	acp_pyr_15	-909.371582	-909.309929	-910.212023	-910.150370	0.0980	
	acp_pyr_16	-909.372824	-909.310602	-910.212289	-910.150067	0.0710	
	acp_pyr_18	-909.374054	-909.311130	-910.213496	-910.150572	0.1214	
	acp_pyr_19	-909.372676	-909.309384	-910.210469	-910.147177	0.0033	
	acp_pyr_20	-909.374055	-909.311085	-910.213497	-910.150527	0.1157	
	acp_pyr_21	-909.371617	-909.309069	-910.212550	-910.150002	0.0663	
	acp_pyr_23	-909.372221	-909.310080	-910.212243	-910.150102	0.0737	
	acp_pyr_24	-909.370828	-909.308061	-910.211649	-910.148882	0.0202	
	acp_pyr_25	-909.365618	-909.302631	-910.206121	-910.143134	0.0000	
				weighted	-910.150251		42.9
P1-pyr-OH	p1_pyr_oh_1	-985.755833	-985.663401	-986.686010	-986.593578	0.1138	
	p1_pyr_oh_2	-985.752619	-985.660916	-986.684000	-986.592297	0.0292	
	p1_pyr_oh_3	-985.752633	-985.661225	-986.684206	-986.592798	0.0498	
	p1_pyr_oh_4	-985.753068	-985.662007	-986.684343	-986.593282	0.0831	
	p1_pyr_oh_5	-985.752785	-985.661687	-986.684334	-986.593236	0.0792	
	p1_pyr_oh_6	-985.750942	-985.659040	-986.682304	-986.590402	0.0039	
	p1_pyr_oh_7	-985.749821	-985.658625	-986.682528	-986.591332	0.0105	
	p1_pyr_oh_8	-985.754253	-985.662404	-986.684919	-986.593070	0.0664	
	p1_pyr_oh_9	-985.756411	-985.664304	-986.686178	-986.594071	0.1919	
	p1_pyr_oh_10	-985.755140	-985.663176	-986.685070	-986.593106	0.0690	
	p1_pyr_oh_14	-985.750657	-985.659732	-986.682512	-986.591587	0.0138	
	p1_pyr_oh_15	-985.751269	-985.659655	-986.682087	-986.590473	0.0042	
	p1_pyr_oh_16	-985.751057	-985.660157	-986.682982	-986.592082	0.0233	
	p1_pyr_oh_19	-985.747304	-985.656273	-986.679767	-986.588736	0.0007	
	p1_pyr_oh_21	-985.751094	-985.660127	-986.683581	-986.592614	0.0409	
	p1_pyr_oh_22	-985.751217	-985.661152	-986.683827	-986.593762	0.1383	
	p1_pyr_oh_23	-985.751307	-985.659846	-986.683282	-986.591821	0.0177	
	p1_pyr_oh_24	-985.751939	-985.660450	-986.684070	-986.592581	0.0395	
	p1_pyr_oh_27	-985.753028	-985.660631	-986.684540	-986.592143	0.0249	
				weighted	-986.593244		21.8
TSB	ts_b	-1062.468898	-1062.346791	-1063.487488	-1063.365381		146.0
TSC	ts_c	-1138.841622	-1138.692765	-1139.952793	-1139.803936		129.1

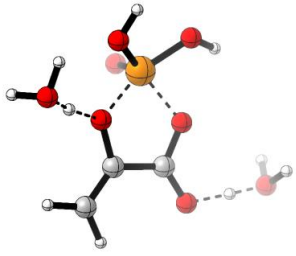

ts_b.log

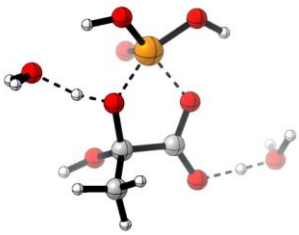

ts_c.log

Pathway with Methylimidazole							
IM	methylimidazole_1	-265.226705	-265.152068	-265.527766	-265.453129	1.0000	
				weighted	-265.453129		
$H_2PO_4^-$	h2po4_1	-643.251152	-643.239080	-643.803324	-643.791252	0.5170	
	h2po4_2	-643.250910	-643.239143	-643.802955	-643.791188	0.4830	
				weighted	-643.791221		
Int-A-Im	int_a_im_9	-1175.079367	-1174.904931	-1176.206879	-1176.032443	0.0000	
	int_a_im_10	-1175.081999	-1174.907667	-1176.208653	-1176.034321	0.0001	
	int_a_im_13	-1175.083688	-1174.908178	-1176.210010	-1176.034500	0.0001	
	int_a_im_17	-1175.083050	-1174.908917	-1176.213173	-1176.039040	0.0166	
	int_a_im_18	-1175.083038	-1174.908915	-1176.213180	-1176.039057	0.0169	
	int_a_im_19	-1175.083039	-1174.908911	-1176.213181	-1176.039053	0.0168	
	int_a_im_20	-1175.083037	-1174.908913	-1176.213181	-1176.039057	0.0169	
	int_a_im_23	-1175.082003	-1174.907445	-1176.208702	-1176.034144	0.0001	
	int_a_im_27	-1175.082914	-1174.909365	-1176.212976	-1176.039427	0.0250	
	int_a_im_28	-1175.082552	-1174.907791	-1176.212059	-1176.037298	0.0026	
	int_a_im_30	-1175.082916	-1174.909369	-1176.212986	-1176.039439	0.0253	
	int_a_im_31	-1175.083207	-1174.909160	-1176.213507	-1176.039460	0.0258	
	int_a_im_32	-1175.082915	-1174.909378	-1176.212978	-1176.039441	0.0253	
	int_a_im_35	-1175.082919	-1174.909471	-1176.212997	-1176.039549	0.0284	
	int_a_im_36	-1175.078888	-1174.905379	-1176.206708	-1176.033199	0.0000	
	int_a_im_39	-1175.081335	-1174.906622	-1176.210519	-1176.035806	0.0005	
	int_a_im_42	-1175.083744	-1174.909233	-1176.213442	-1176.038931	0.0147	

	int_a_im_43	-1175.078928	-1174.904736	-1176.206819	-1176.032627	0.0000	
	int_a_im_50	-1175.083023	-1174.909710	-1176.213252	-1176.039939	0.0430	
	int_a_im_51	-1175.083886	-1174.910136	-1176.213579	-1176.039829	0.0382	
	int_a_im_53	-1175.083022	-1174.909757	-1176.213249	-1176.039984	0.0451	
	int_a_im_54	-1175.083051	-1174.909680	-1176.213324	-1176.039953	0.0436	
	int_a_im_56	-1175.083014	-1174.909789	-1176.213236	-1176.040011	0.0464	
	int_a_im_57	-1175.083603	-1174.909351	-1176.214217	-1176.039965	0.0442	
	int_a_im_59	-1175.083885	-1174.910128	-1176.213579	-1176.039822	0.0380	
	int_a_im_66	-1175.081957	-1174.907820	-1176.210819	-1176.036682	0.0014	
	int_a_im_67	-1175.083166	-1174.909155	-1176.213095	-1176.039084	0.0173	
	int_a_im_68	-1175.082174	-1174.908216	-1176.212631	-1176.038673	0.0112	
	int_a_im_69	-1175.081956	-1174.907779	-1176.210831	-1176.036654	0.0013	
	int_a_im_70	-1175.082195	-1174.908019	-1176.212585	-1176.038409	0.0085	
	int_a_im_74	-1175.082203	-1174.908305	-1176.212592	-1176.038694	0.0115	
	int_a_im_75	-1175.083181	-1174.909157	-1176.213227	-1176.039203	0.0197	
	int_a_im_78	-1175.082211	-1174.909686	-1176.212653	-1176.040128	0.0525	
	int_a_im_80	-1175.082048	-1174.908113	-1176.212250	-1176.038315	0.0077	
	int_a_im_82	-1175.081721	-1174.908141	-1176.211916	-1176.038336	0.0078	
	int_a_im_84	-1175.082212	-1174.909708	-1176.212653	-1176.040149	0.0537	
	int_a_im_85	-1175.082905	-1174.908812	-1176.213052	-1176.038959	0.0152	
	int_a_im_86	-1175.081578	-1174.908169	-1176.211683	-1176.038274	0.0073	
	int_a_im_88	-1175.081678	-1174.907405	-1176.208564	-1176.034291	0.0001	
	int_a_im_89	-1175.082367	-1174.909066	-1176.212912	-1176.039611	0.0304	
	int_a_im_92	-1175.082173	-1174.908221	-1176.212632	-1176.038680	0.0113	
	int_a_im_93	-1175.082226	-1174.909651	-1176.212915	-1176.040340	0.0657	
	int_a_im_95	-1175.082225	-1174.909648	-1176.212916	-1176.040339	0.0656	
	int_a_im_96	-1175.082216	-1174.909886	-1176.212906	-1176.040576	0.0844	
	int_a_im_97	-1175.081824	-1174.907552	-1176.211851	-1176.037579	0.0035	
	int_a_im_98	-1175.081783	-1174.907695	-1176.211618	-1176.037530	0.0033	
	int_a_im_99	-1175.081825	-1174.907426	-1176.211510	-1176.037111	0.0021	
	int_a_im_100	-1175.081899	-1174.907619	-1176.212162	-1176.037882	0.0049	
				weighted	-1176.039729		32.9
P1-pyr-im	p1_pyr_im_1	-1175.092673	-1174.916500	-1176.219236	-1176.043063	0.0057	
	p1_pyr_im_5	-1175.092453	-1174.917106	-1176.218947	-1176.043600	0.0100	
	p1_pyr_im_9	-1175.094242	-1174.919080	-1176.221645	-1176.046483	0.2125	
	p1_pyr_im_10	-1175.094243	-1174.919147	-1176.221640	-1176.046544	0.2269	
	p1_pyr_im_13	-1175.094242	-1174.919298	-1176.221597	-1176.046653	0.2545	
	p1_pyr_im_16	-1175.093339	-1174.916872	-1176.219959	-1176.043492	0.0089	
	p1_pyr_im_20	-1175.093191	-1174.916757	-1176.220361	-1176.043927	0.0141	
	p1_pyr_im_22	-1175.093673	-1174.918406	-1176.220747	-1176.045480	0.0734	
	p1_pyr_im_23	-1175.093682	-1174.918606	-1176.220766	-1176.045690	0.0917	
	p1_pyr_im_25	-1175.093223	-1174.917128	-1176.220693	-1176.044598	0.0288	
	p1_pyr_im_28	-1175.091433	-1174.916754	-1176.218243	-1176.043564	0.0096	
	p1_pyr_im_29	-1175.088602	-1174.913408	-1176.216530	-1176.041336	0.0009	
	p1_pyr_im_33	-1175.093426	-1174.917446	-1176.219767	-1176.043787	0.0122	
	p1_pyr_im_35	-1175.093409	-1174.917367	-1176.221176	-1176.045134	0.0508	
				weighted	-1176.046094		16.2
TSA-im	ts_a_im	-1328.186129	-1327.952050	-1329.492314	-1329.258235		137.2

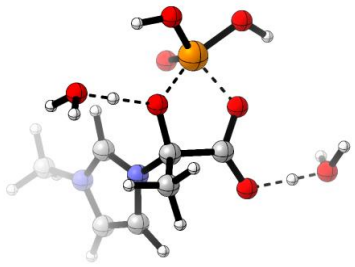

ts_a_im.log

Pathway with Pyridine							
Pyridine	pyridine	-247.994950	-247.929551	-248.273270	-248.207871	1.0000	
				weighted	-248.207871		
Int-A-Py	int_a_py_py_2	-1157.837358	-1157.672045	-1158.943526	-1158.778213	0.0000	
	int_a_py_py_3	-1157.841377	-1157.675680	-1158.949927	-1158.784230	0.0221	
	int_a_py_py_4	-1157.839874	-1157.673827	-1158.945339	-1158.779292	0.0001	
	int_a_py_py_5	-1157.841055	-1157.675056	-1158.945609	-1158.779610	0.0002	
	int_a_py_py_6	-1157.841632	-1157.677338	-1158.949773	-1158.785479	0.0830	
	int_a_py_py_7	-1157.841173	-1157.676077	-1158.949786	-1158.784690	0.0359	
	int_a_py_py_9	-1157.839608	-1157.675149	-1158.948258	-1158.783799	0.0140	
	int_a_py_py_10	-1157.839778	-1157.675199	-1158.948284	-1158.783705	0.0127	
	int_a_py_py_11	-1157.841248	-1157.676303	-1158.948822	-1158.783877	0.0152	
	int_a_py_py_12	-1157.840595	-1157.675558	-1158.949459	-1158.784422	0.0271	
	int_a_py_py_13	-1157.840610	-1157.675708	-1158.949540	-1158.784638	0.0340	
	int_a_py_py_14	-1157.840957	-1157.675814	-1158.949222	-1158.784079	0.0188	
	int_a_py_py_15	-1157.841334	-1157.676108	-1158.949307	-1158.784081	0.0188	

	int_a_py_py_17	-1157.841386	-1157.676626	-1158.949642	-1158.784882	0.0441	
	int_a_py_py_18	-1157.840925	-1157.675938	-1158.949648	-1158.784661	0.0349	
	int_a_py_py_20	-1157.841281	-1157.674962	-1158.945173	-1158.778854	0.0001	
	int_a_py_py_21	-1157.840961	-1157.676291	-1158.949550	-1158.784880	0.0440	
	int_a_py_py_22	-1157.840924	-1157.675960	-1158.949168	-1158.784204	0.0215	
	int_a_py_py_23	-1157.840390	-1157.675446	-1158.949287	-1158.784343	0.0249	
	int_a_py_py_24	-1157.841789	-1157.676449	-1158.949641	-1158.784301	0.0238	
	int_a_py_py_25	-1157.840940	-1157.675626	-1158.949741	-1158.784427	0.0272	
	int_a_py_py_26	-1157.836240	-1157.671124	-1158.942898	-1158.777782	0.0000	
	int_a_py_py_27	-1157.840893	-1157.675716	-1158.949457	-1158.784280	0.0233	
	int_a_py_py_28	-1157.839182	-1157.674177	-1158.948063	-1158.783058	0.0064	
	int_a_py_py_29	-1157.840599	-1157.675708	-1158.949498	-1158.784607	0.0329	
	int_a_py_py_32	-1157.841783	-1157.676751	-1158.949885	-1158.784853	0.0428	
	int_a_py_py_33	-1157.836847	-1157.671155	-1158.942783	-1158.777091	0.0000	
	int_a_py_py_34	-1157.840981	-1157.676010	-1158.949395	-1158.784424	0.0271	
	int_a_py_py_35	-1157.840702	-1157.675839	-1158.949166	-1158.784303	0.0238	
	int_a_py_py_36	-1157.840993	-1157.676359	-1158.949428	-1158.784794	0.0401	
	int_a_py_py_37	-1157.840255	-1157.675038	-1158.948543	-1158.783326	0.0085	
	int_a_py_py_38	-1157.842119	-1157.676710	-1158.949988	-1158.784579	0.0320	
	int_a_py_py_39	-1157.840586	-1157.675482	-1158.949110	-1158.784006	0.0174	
	int_a_py_py_41	-1157.840045	-1157.677338	-1158.949078	-1158.786371	0.2136	
	int_a_py_py_42	-1157.836844	-1157.671097	-1158.942780	-1158.777033	0.0000	
	int_a_py_py_43	-1157.839628	-1157.675153	-1158.948107	-1158.783632	0.0117	
	int_a_py_py_44	-1157.839392	-1157.673702	-1158.948316	-1158.782626	0.0040	
	int_a_py_py_46	-1157.840099	-1157.675259	-1158.948647	-1158.783807	0.0141	
				weighted	-1158.784925		58.0
P1-pyr-py	p1_pyr_py_1	-1157.849000	-1157.682593	-1158.954966	-1158.788559	0.2366	
	p1_pyr_py_2	-1157.847885	-1157.681201	-1158.953525	-1158.786841	0.0383	
	p1_pyr_py_3	-1157.849044	-1157.681623	-1158.954283	-1158.786862	0.0391	
	p1_pyr_py_4	-1157.849902	-1157.683176	-1158.954915	-1158.788189	0.1598	
	p1_pyr_py_5	-1157.850089	-1157.683631	-1158.955636	-1158.789178	0.4559	
	p1_pyr_py_6	-1157.847248	-1157.681046	-1158.953208	-1158.787006	0.0456	
	p1_pyr_py_9	-1157.845233	-1157.679158	-1158.951524	-1158.785449	0.0087	
	p1_pyr_py_10	-1157.844645	-1157.679432	-1158.951226	-1158.786013	0.0159	
				weighted	-1158.788512		48.6
TSA-py	ts_a_py_1	-1310.944362	-1310.718563	-1312.229455	-1312.003656	0.5555	
	ts_a_py_2	-1310.943762	-1310.718574	-1312.228634	-1312.003446	0.4445	
				weighted	-1312.003563		136.8

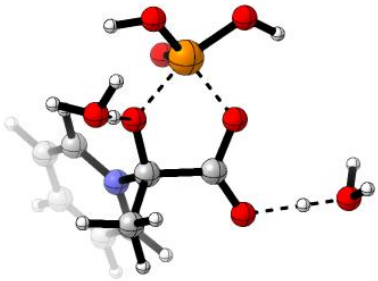

ts_a_py_1.log

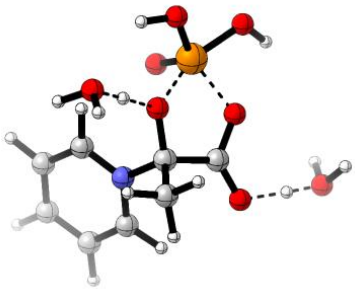

ts_a_py_2.log

[a] Electronic energy at the SMD(H_2O)/M06-2X/Def2-SVP level (in hartree).
[b] Gibbs energy at the SMD(H_2O)/M06-2X/Def2-SVP level (in hartree).
[c] Electronic energy at the SMD(H_2O)/M06-2X/Def2-TZVPD//SMD(H_2O)/M06-2X/Def2-SVP level (in hartree).
[d] Gibbs energy at the SMD(H_2O)/M06-2X/Def2-TZVPD//SMD(H_2O)/M06-2X/Def2-SVP level (in hartree) calculated as $G^0_h = E^0_h + (G^0_l - E^0_l)$.

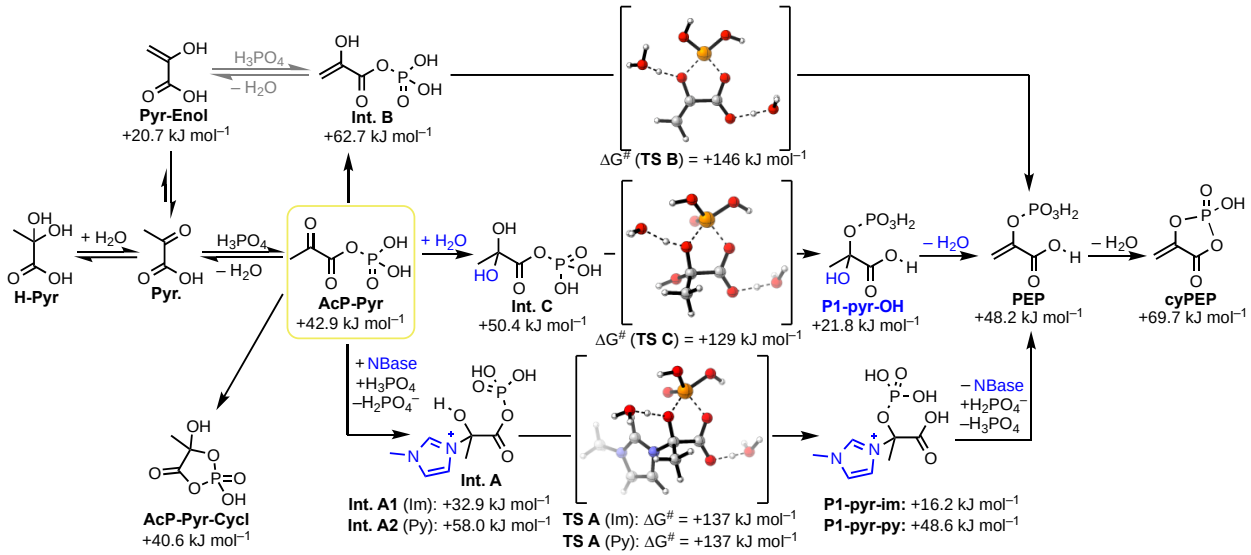

Figure S7. Computational study of the thermochemistry of the key steps and the barriers for intramolecular phosphoryl transfer at the SMD(H_2O)M06-2X/def2-TZVPD//SMD(H_2O)/M06-2X/def2-SVP level of theory.

D. Computations of coupling constants

In ^{1}H NMR spectra, the Karplus relation is typically used for relating the dihedral angle of protons with the experimentally observed coupling constant. To aid the assignment of the experimental NMR spectra and specifically the ^{13}C-^{31}P coupling constants, we computed a Karplus-type relationship for PEP system. NMR properties were calculated using the GIAO method as implemented in Gaussian at SMD(H_2O)M06-2X/def2-TZVPD//SMD(H_2O)/M06-2X/def2-SVP level together with the "spinspin" option to compute the coupling constants.

Whereas the computed coupling constants (Fig. S7) might only be qualitatively accurate, they allow for the key conclusion that the coupling constant between the carboxylate and phosphorous ($J_{P\text{-}C3}$) is highly sensitive on the dihedral angle and is largest for an angle of 180 °.

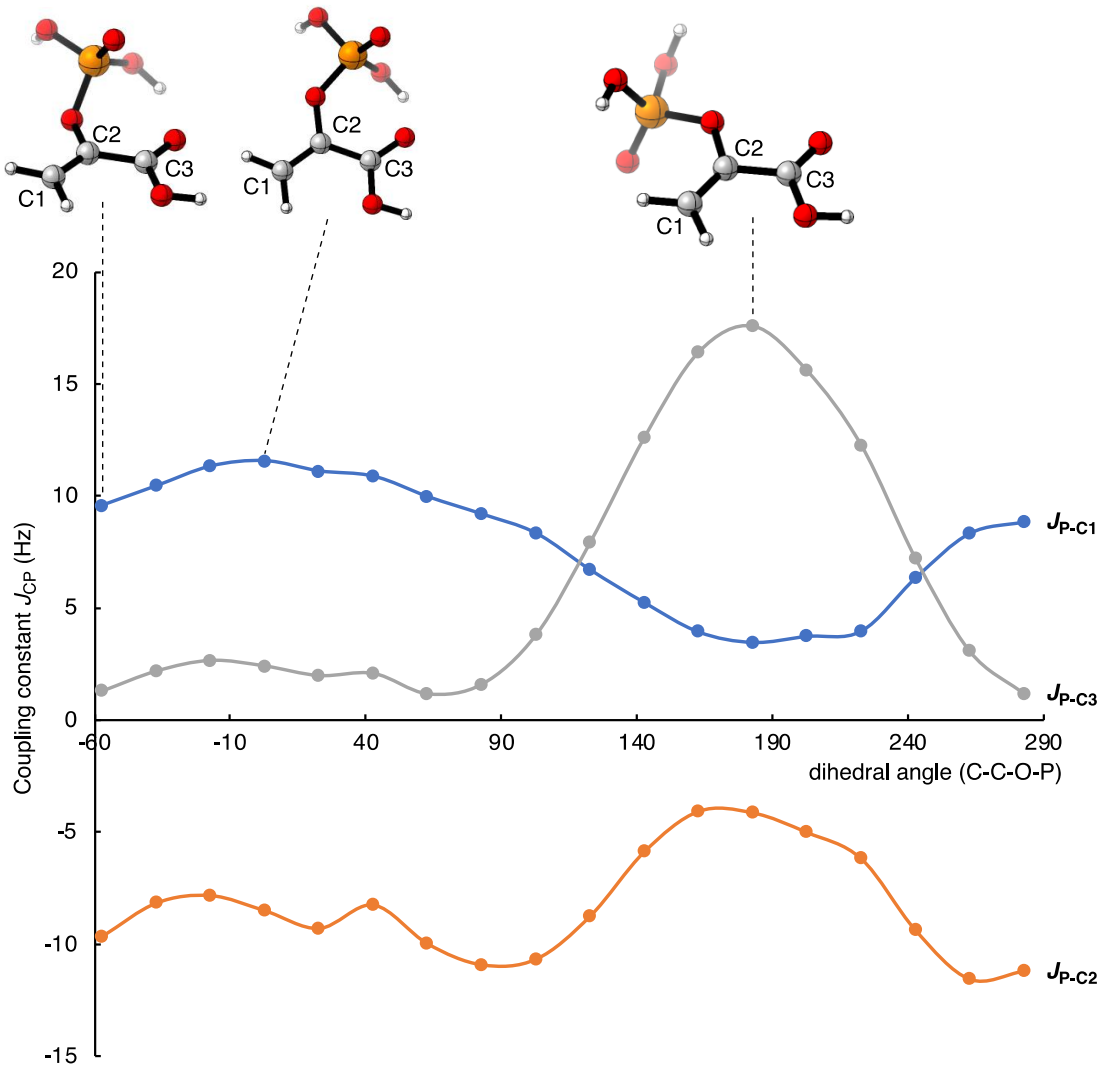

Figure S8. Computed phosphorous-carbon coupling constants as function of the C-C-O-P dihedral angle of PEP at the SMD(H_2O)M06-2X/def2-TZVPD//SMD(H_2O)/M06-2X/def2-SVP level.

E. Reference NMR shifts in acetonitrile

To aid in the assignment of the NMR spectra recorded in acetonitrile, the ^{13}C NMR shifts and J_{CP} coupling constants for various compounds were computed. To resemble the experimental conditions, most phosphates were calculated as the mono-anionic species. For the computations, the same workflow as outlined above for aqueous solutions was applied with acetonitrile as solvent. Thus, structures were initially subjected to a conformational search using the CREST tool at the GFN2-xTB level and the ALPB solvation model for acetonitrile. Subsequently, structures were optimized at the SMD(MeCN)/M06-2X/Def2-SVP level, which were combined with single point computations with SMD(MeCN)/M06-2X/Def2-TZVPD method. Finally, the NMR properties were calculated using the GIAO method at SMD(MeCN)M06-2X/def2-TZVPD//SMD(MeCN)/M06-2X/def2-SVP level together with the "spinspin" option for the major conformers (within 4 kJ mol^{-1}). ^{13}C NMR shifts were calculated subsequently as

$$\delta_{iso} = (\sigma_{iso} - \sigma_{ref})$$

where σ_{ref} is the isotropic shielding tensor of tetramethylsilane optimized and calculated at the same theory level (SI file: tms_opt_sym.log). Thereby obtained NMR shifts were subjected to Boltzmann averaging based on the Gibbs energy values. The coupling constants were reported for the lowest conformer (or multiple ones, as shown below).

Note: As we only used a single reference for the NMR computations (TMS) and neglected potential counterions, a certain error in the computed chemical shifts of approx. 10 ppm is expected.

Table S17. Raw data from DFT calculations at the SMD(MeCN)/M06-2X/Def2-TZVPD//SMD(MeCN)/M06-2X/Def2-SVP level (in hartree) for the calculation of ^{13}C NMR shifts. Note: In the following table, the carboxylic acid site is labeled for all compounds C1, the α-site C2, and the β-site C3.

Species	Filename (.xyz)	E^0_l (hartree)[a]	G^0_l (hartree)[b]	E^0_h (hartree)[c]	G^0_h (hartree)[d]	weighting	^{13}C Shielding (ppm)		
TMS	mecn_tms	-448.860719	-448.743833				186.656300		
							C1	C2	C3
IntB (anion)	pyr_enol_po3h_1	-908.901264	-908.847154	-909.757784	-909.707908	0.1254	77.180000	15.932300	4.451000
	pyr_enol_po3h_15	-908.906939	-908.853088	-909.757954	-909.708761	0.3100	69.418300	10.223800	3.404600
	pyr_enol_po3h_2	-908.905805	-908.850897	-909.760252	-909.709327	0.5646	75.218200	16.354900	1.588200
						shift (ppm):	113.0	172.3	184.1
							C1	C2	C3
IntB (dianion)	pyr_enol_po3_1	-908.411498	-908.369366	-909.277970	-909.235838	1.0000	99.7058	-6.446	-3.001
						shift (ppm):	87.0	193.1	189.7
							C1	C2	C3
PEP (anion)	mecn_pep_h_1	-908.913807	-908.859900	-909.766816	-909.712909	0.2364	54.4433	12.1599	0.2531
	mecn_pep_h_4	-908.914061	-908.859981	-909.766858	-909.712778	0.2057	54.4888	12.2441	0.434
	mecn_pep_h_5	-908.915348	-908.861243	-909.767824	-909.713719	0.5579	54.5065	11.1646	0.3629
						shift (ppm):	132.2	175.0	186.3
							C1	C2	C3
cPEP (anion)	mecn_cPEP_1	-832.554010	-832.523224	-833.310120	-833.279334	1.0000	76.6042	15.973	7.3374
						shift (ppm):	110.1	170.7	179.3
							C1	C2	C3
cPEP (neutral)	mecn_cpep_h_1	-833.003169	-832.961221	-833.748345	-833.706397	0.7205	59.6725	21.2921	13.2993
	mecn_cpep_h_2	-833.001494	-832.959508	-833.747490	-833.705504	0.2795	59.2816	21.5296	13.5089
						shift (ppm):	127.1	165.3	173.3
							C1	C2	C3
AcP-Pyr (anion)	mecn_acp_pyr_18	-908.913215	-908.860149	-909.767456	-909.718775	0.6556	153.9154	-38.7524	8.842
	mecn_acp_pyr_10	-908.908857	-908.856629	-909.765258	-909.717543	0.1777	153.8452	-39.6776	11.1854

	mecn_acp_oyr_14	-908.908793	-908.856562	-909.765179	-909.717483	0.1668	153.8436	-39.6709	11.18
						shift (ppm):	32.8	225.7	177.0
							C1	C2	C3
P1-pyr-OH (anion)	mecn_p1_pyr_oh_18	-985.286446	-985.203116	-986.230677	-986.150936	0.7648	157.6798	83.1955	-15.4454
	mecn_p1_pyr_oh_22	-985.281619	-985.199904	-986.227749	-986.149824	0.2352	156.4183	86.397	-8.0915
						shift (ppm):	29.3	102.7	200.4
							C1	C2	C3
Pyr (acid)	mecn_pyr_1	-342.017354	-341.972410	-342.423438	-342.378494	0.7322	153.8825	-36.2556	10.3798
	mecn_pyr_2	-342.016369	-341.971437	-342.422477	-342.377545	0.2678	151.9695	-35.5623	14.2738
						shift (ppm):	33.3	222.7	175.2

[a] Electronic energy at the SMD(MeCN)/M06-2X/Def2-SVP level (in hartree).
[b] Gibbs energy at the SMD(MeCN)/M06-2X/Def2-SVP level (in hartree).
[c] Electronic energy at the SMD(MeCN)/M06-2X/Def2-TZVPD//SMD(MeCN)/M06-2X/Def2-SVP level (in hartree).
[d] Gibbs energy at the SMD(MeCN)/M06-2X/Def2-TZVPD//SMD(MeCN)/M06-2X/Def2-SVP level (in hartree) calculated as $G^0_h = E^0_h + (G^0_l - E^0_l)$.

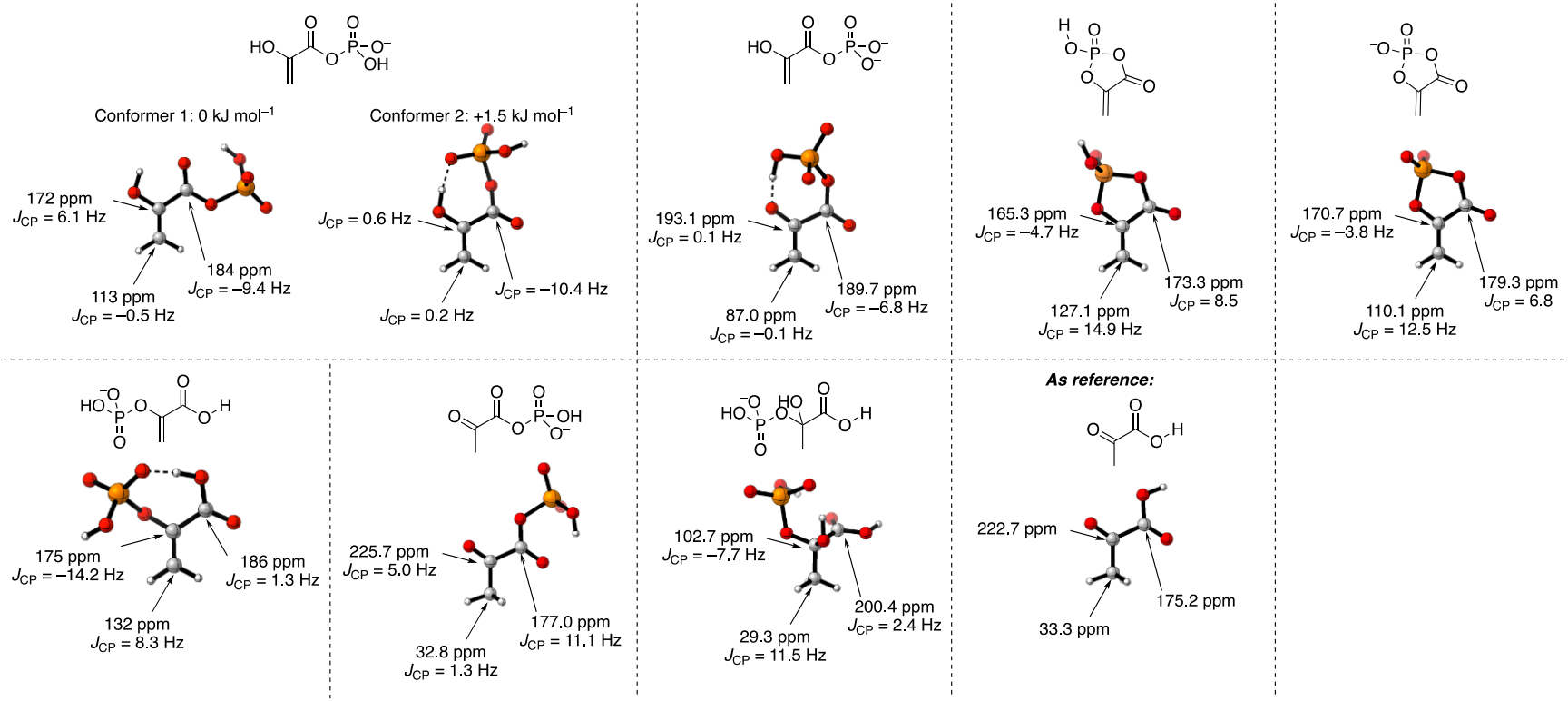

Figure S9. DFT-predicted ^{13}C NMR shifts and J_{CP} coupling constants.

References

[S1] Y. Yamagata, H. Watanabe, M. Saitoh, T. Namba, *Nature* **1991**, *352*, 516–519.
[S2] H. C. J. Ottenheijm, M. W. Tijhuis, *Org. Synth.* **1984**, *61*, 1.
[S2] G. Baccolini, *Phosphorus Sulfur Silicon Relat. Elem.* **2015**, *190*, 2173–2186.
[S4] H. Guo, Y. Zhang, J. Li, T. Mao, E. Shi, *Phosphorus Sulfur Silicon Relat.,* **2023**, *198*, 34-37.
[S5] G. L. Kenyon, J. A. Stubbe, *Biochemistry* **1971**, *10*, 2669–2677.
[S6] W. J. Lees, C. T. Walsh, *J. Am. Chem. Soc.* **1995**, *117*, 7329–7337.
[S7] S. Hediger, B. H. Meier, N. D. Kurur, G. Bodenhausen, R. R. Ernst, *Chem. Phys. Lett.* **1994**, *223*, 283–288.
[S8] J. Raya, B. Perrone, J. Hirschinger, *J. Magn. Reson.* **2013**, *227*, 93–102.
[S9] E. L. Hahn, *Phys. Rev.* **1950**, *80*, 580–59.
[S10] B. M. Fung, A. K. Khitrin, K. J. Ermolaev, *J. Magn. Reson.* **2000**, *142,* 97-101.
[S11] B.-J. Van Rossum, H. Förster, H. J. M. de Groot, *J. Magn. Reson.* **1997**, *124*, 516–519.
[S12] M. Piotto, M. Bourdonneau, J. Furrer, A. Bianco, J. Raya, K. Elbayed, *J. Magn. Reson.* **2001**, *149*,114–118.
[S13] K. Elbayed, B. Dillmann, J. Raya, M. Piotto, F. Engelke, *J. Magn. Reson.* **2005**, *174*, 2–26.
[S14] a) A. E. Bennett, J. H. Ok, S. Vega, R. U. Griffin, *J. Chem. Phys.* **1992**, *96*, 8634. b) D. K. Sodickson, M. H. Levitt, S. Vega, R. G. Griffin, *J. Chem. Phys.*, **1993**, *98*, 6742. c) J. Raya, A. Bianco, J. Furrer, J.-P. Briand, M. Piotto, K. Elbayed, *J. Magn. Reson.* **2002**, *157*, 43–51.
[S15] a) C. Bannwarth, S. Ehlert, S. Grimme, *J. Chem. Theory Comput.* **2019**, *15*, 1652–1671. b) S. Grimme, *J. Chem. Theory Comput.* **2019**, *15*, 2847-2862. c) P. Pracht, F. Bohle, S. Grimme, *Phys. Chem. Chem. Phys.* **2020**, *22*, 7169–7192.
[S16] Gaussian 16, Revision C.01, M. J. Frisch, G. W. Trucks, H. B. Schlegel, G. E. Scuseria, M. A. Robb, J. R. Cheeseman, G. Scalmani, V. Barone, G. A. Petersson, H. Nakatsuji, X. Li, M. Caricato, A. V. Marenich, J. Bloino, B. G. Janesko, R. Gomperts, B. Mennucci, H. P. Hratchian, J. V. Ortiz, A. F. Izmaylov, J. L. Sonnenberg, D. Williams-Young, F. Ding, F. Lipparini, F. Egidi, J. Goings, B. Peng, A. Petrone, T. Henderson, D. Ranasinghe, V. G. Zakrzewski, J. Gao, N. Rega, G. Zheng, W. Liang, M. Hada, M. Ehara, K. Toyota, R. Fukuda, J. Hasegawa, M. Ishida, T. Nakajima, Y. Honda, O. Kitao, H. Nakai, T. Vreven, K. Throssell, J. A. Montgomery, Jr., J. E. Peralta, F. Ogliaro, M. J. Bearpark, J. J. Heyd, E. N. Brothers, K. N. Kudin, V. N. Staroverov, T. A. Keith, R. Kobayashi, J. Normand, K. Raghavachari, A. P. Rendell, J. C. Burant, S. S. Iyengar, J. Tomasi, M. Cossi, J. M. Millam, M. Klene, C. Adamo, R. Cammi, J. W. Ochterski, R. L. Martin, K. Morokuma, O. Farkas, J. B. Foresman, and D. J. Fox, Gaussian, Inc., Wallingford CT, **2016**.
[S17] A. V. Marenich, C. J. Cramer, D. G. Truhlar, *J. Phys. Chem. B* **2009**, *113*, 6378–6396.
[S18] Y. Zhao, D. G. Truhlar, *Theor. Chem. Acc.* **2008**, *120*, 215-241.
[S19] F. Weigend, R. Ahlrichs, *Phys. Chem. Chem. Phys.* **2005**, *7*, 3297–3305.
[S20] S. Grimme, Theory. *Chem. Eur. J.* **2012**, *18*, 9955–9964.
[S21] Visualisation was performed with CYLview20; Legault, C. Y., Université de Sherbrooke, **2020** (http://www.cylview.org).
[S22] K. Qian, S. M. Shepard, T. Xin, G. Park, C. C. Cummins, *J. Am. Chem. Soc.* **2023**, *145*, 6045–6050.
[S23] M. Meisel, H. Bock, B. Solouki, M. Kremer, *Angew. Chem.* **1989**, *101*, 1378–1381.